

Paolo Cannetti

T-11 (c)

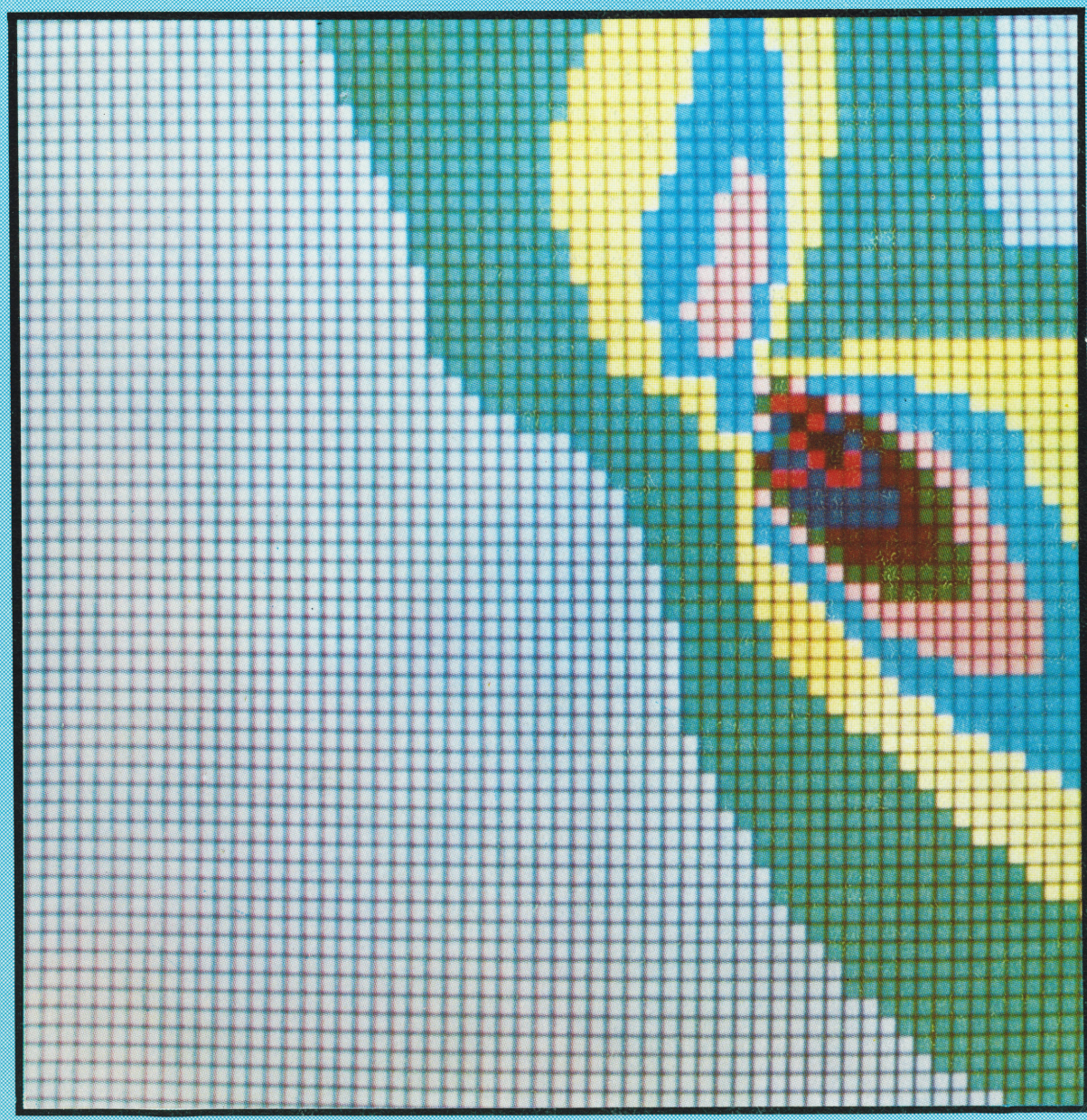


FINAL REPORT

Air pollution dispersion and prediction model for Shuaiba Industrial Area

EES-45

Volume III — Special Studies and Appendices



SUBMITTED TO: SHUAIBA AREA AUTHORITY

KUWAIT INSTITUTE FOR SCIENTIFIC RESEARCH
P. O. BOX 24885 SAFAT
KUWAIT

JULY 1983

The cover picture provides a graphic representation of the ground level NO_x concentration field in the Shuaiba region as simulated by a numerical diffusion computation; darker colors indicate higher concentrations. This picture was produced using the HAZIENDA image processing system at the Kuwait Scientific Center of IBM. We thank Mr. Jesus Rueda of IBM for the preparation and the production of this picture.



KISR 1090 A

8

FINAL REPORT

**AIR POLLUTION DISPERSION AND PREDICTION MODEL
FOR SHUAIBA INDUSTRIAL AREA**

VOLUME III – SPECIAL STUDIES AND APPENDICES

EES-45

P. Zannetti
M. Sudairawi
N. Al-Madani
N. El-Karmi

ENVIRONMENTAL AND EARTH SCIENCES DIVISION

"RESTRICTED"

SUBMITTED TO
SHUAIBA AREA AUTHORITY

**KUWAIT INSTITUTE FOR SCIENTIFIC RESEARCH
P. O. BOX 24885 SAFAT
KUWAIT**

AUGUST 1983

EES-45 PROJECT TEAM

Dr. P. Zannetti, Project Leader

SAA TEAM

Mr. F. Dorgham, Co-Project Leader

Mr. H. Al-Adhad, Supervisor

ENGINEERS

Mr. F. Marei

Mr. M. Pervez

Mr. M. Ghanem

PROGRAMMERS

Ms. S. Emara

TECHNICIANS

Mr. M. Saleem

Mr. A. Zudhi

Mr. H. Batros

Mr. M. Saeed

KISR TEAM

Mr. M. Al-Sudairawi, Leader,
Tasks 1 and 2

Ms. N. Al-Madani, Leader, Task 3

Mr. A. O. El-Karmi, Leader, Task 4

STAFF TASKS 1 AND 2

Mr. M. Abuseil

Mr. D. Wooster

Mr. S. Mohammed

Mr. W. Kittaneh

Ms. S. Homaidan

Mr. S. Khalifa

STAFF TASKS 3 AND 4

Ms. M. Al-Attiah

Ms. M. Kortom

SECRETARIAL SUPPORT

Ms. M. D'Souza

OTHERS

Mr. M. Safar, Climatologist

Preface

This report is Volume III of a five-volume final report to the SAA for the project "Air Pollution Dispersion and Prediction Model for Shuaiba Industrial Area", EES-45. These five volumes contain:

- Volume I : Executive Summary
- Volume II : Technical Report
- Volume III : (the present volume): Special Studies and Appendices
- Volume IV : Software User's Manuals
- Volume V : Data and Program Listings

This Volume contains special studies, program data outputs and appendices that integrate the technical discussion presented in Volume II. Some of these special studies have already been submitted to SAA as appendices to KISR monthly reports. For such cases, only the abstract has been enclosed.

Table of Contents

	Page
SECTION 1 - "A Report on Surface Winds in Kuwait" (Abstract)	1
SECTION 2 - "Meteorological Instruments and Practices at the Meteorological Observation Station of the Kuwait International Airport" (Abstract)	2
SECTION 3 - "The Climate of Kuwait" (Abstract)	3
SECTION 4 - "Preliminary Analysis of Wind and Stability Patterns in Kuwait (Abstract)	4
SECTION 5 - "Stack Sampling : Summary of Instruments and Methods" (Abstract)	6
SECTION 6 - "Meteorological and Air Quality Computer Data Files" (Abstract)	7
SECTION 7 - "A Preliminary Collection of Atmospheric Emission Data in the Shuaiba Industrial Area" (Abstract), and the listing of the emission data used in the modeling simulations.	8
SECTION 8 - "Consultant Report", on Source Sampling and Emission Evaluation (Abstract)	11
SECTION 9 - "Land and Sea Breezes in Kuwait" (Abstract)	20
SECTION 10 - Technical Description of the Industrial Source Complex Models	21
SECTION 11 - "A Description of the Prototype MC-LAGPAR Diffusion Model"	104
SECTION 12 - Data Analysis Tables	109
SECTION 13 - "A Prototype Data Base Management System for Meteorological and Air Quality Data"	187
SECTION 14 - "Tethersonde Measurements in Shuaiba"	203

SECTION 1

Mahmoud I. Safar: A Report on Surface Winds in Kuwait. Report provided to SAA as Appendix A of the EES-45 progress report of December 1, 1981-May 31, 1982, KISR 723.

Abstract

This report is based on hourly observations (each observation represents an average over 10 minutes preceding the end of the hour) from December 1975 to November 1980 taken at Kuwait International Airport. Tables showing the frequency of wind speed and direction were prepared for each month throughout the five years. They were assembled and are presented here on a seasonal basis:

Winter	:	December, January, February.
Spring	:	March, April, May
Summer	:	June, July, August
Autumn	:	September, October, November

and also on an annual basis.

SECTION 2

Mahmoud I. Safar and Mane Al-Sudairawi: Meteorological Instruments and Practices at the Meteorological Observation Station of the Kuwait International Airport. Report provided to SAA as enclosure 1 of the EES-45 monthly report of July 1982, KISR 784.

Abstract

The Kuwait International Airport is located at latitude $29^{\circ} 13'$ and longitude $47^{\circ} 58'$ E. Its mean sea level elevation is 55 m.

The following weather elements are measured at the surface:

- (a) Present weather
- (b) Past weather
- (c) Wind direction and speed
- (d) Temperature
- (e) Humidity
- (f) Clouds: amount, type and height of cloud base
- (g) Visibility
- (h) Atmospheric pressure
- (i) Amount of precipitation
- (j) Vapour pressure
- (k) Dew-point
- (l) Sunshine duration
- (m) Soil temperature
- (n) Solar radiation
- (o) Evaporation

The following upper-air weather elements are measured:

- (a) Atmospheric pressure
- (b) Air temperature
- (c) Humidity
- (d) Wind speed and direction

This report presents the methods and the instruments used for measuring these variables.

SECTION 3

Mahmoud I. Safar: The Climate of Kuwait. Report provided to SAA as Appendix A of the EES-45 monthly report of October 1982, KISR 844.

Abstract

The weather in winter is comfortably cool. The nights may have temperatures below 5° . Monthly mean temperatures do not fall below 10°C , excluding January 1964 when the mean fell to 7.6°C ; cold waves may occur as in January 1964 when the lowest air temperature recorded was 6.0°C below zero at Al-Omariyah on January 21. The second lowest minimum temperature was 5°C below zero recorded at Umm Al-Aish on 13, December, 1963. Still, winter in Kuwait is generally mild. Mean maximum temperatures during the real winter months, December, January and February, are 19.9 , 18.0 and 20.7°C , respectively; mean minimum temperatures are 8.7 , 7.7 and 9.4°C , respectively.

Precipitation is scanty, begins in October and lasts till May. The mean seasonal rainfall is less than 125 mm. (5 inches), but it reached 351.7 mm (13.8 inches) in the winter of 1971/1972 at Ahmadi, and fell to only 20.1 mm (less than one inch) in the winter of 1963/1964 at Umm Al-Aish.

The prevailing winds are from the northwest, but they are sometimes from the southeast.

The outstanding features of summer weather in Kuwait are the heat and the dryness of the air. The mean temperature in July and August is 37°C ; whereas the mean daily maximum is nearly 45°C (absolute maximum, 51°C). It is generally rainless from June to September and the sky is almost cloudless, though not always blue owing to the presence of dust in the atmosphere. The sunshine is strong and continuous throughout the day; the mean monthly sunshine duration is nearly 11 hours during June, July and August, though it might reach 13 hours. Dust is one of the worries of life in the summer in Kuwait, particularly when the strong northwesterly winds blow and raise large amounts of dust and sand. High humidity, though not frequent in summer, occurs generally for a few days and makes the climate very trying.

SECTION 4

Nazik Al-Madani: Preliminary Analysis of Wind and Stability Patterns in Kuwait. Report provided to SAA as Appendix B of the EES-45 monthly report of October 1982, KISR 844.

Abstract

This report presents a preliminary analysis of wind and stability conditions in Kuwait. The hourly averaged meteorological parameters of wind speed, wind direction, and atmospheric stability were used as an input for this analysis. Wind speed and direction were measured at the Kuwait International Airport (KWI) during 1979 through 1981. Hourly atmospheric stability information was obtained from KWI meteorological data using an ad-hoc computer program (CRSTER pre-processor).

Wind roses are commonly used in applied meteorological studies to display the frequency of occurrence of specific categories of wind speed (ranges) and wind direction (sectors). Similarly, stability roses are used to display atmospheric stability (classes) and wind direction (sectors). In this report, both types of roses (wind and stability) were computed using the KWI data and are presented (plots and tabular form) in the following sections.

All such analyses have been performed through computer programming. The KWI meteorological input data were entered into the KISR IBM computer and were analyzed and checked. Computer programs (in APL and FORTRAN languages) were written and tested to perform:

- Computation of the hourly atmospheric stability (using the CRSTER pre-processor, FORTRAN program developed for the U.S. Environmental Protection Agency (EPA); this program, originally written for U.S. data, has been slightly modified and adjusted for handling KWI data).
- Input data preparation into the specific format required by the CRSTER pre-processor (APL programs).

- Computation of the frequencies for each rose and their tabulation (APL programs).
- Computer plotting of each rose (FORTRAN programs).

All these programs are currently available on the KISR IBM 4341 computer. Listings of the programs and user's instructions will be provided in a following report. Results of the analysis of wind and stability patterns in Kuwait are discussed in more detail in the following sections. Results agree with our expectations based on our previous meteorological analyses of the prevailing conditions in Kuwait.

SECTION 5

Mane Al-Sudairawi: Stack Sampling; Summary of Instruments and Methods.

Report provided to SAA as Appendix B of the EES-45 monthly report of December 1982, KISR 866.

Abstract

In stack sampling, special equipment and methods are used to estimate the stack flow rate, temperature, moisture content, pollution concentration, etc. This information is used to control the emission and obtain stack data for air pollution modeling. This report presents the major instruments used to perform such analyses and the procedures to be followed for a proper source parameter evaluation.

SECTION 6

Mane Al-Sudairawi: Meteorological and Air Quality Computer Data Files.

Report provided to SAA as Appendix E of the EES-45 monthly report of ~~Nov~~ember 1982, KISR 866.

Abstract

There are two types of data filed in the KISR computer for Project EES-45 (Air Pollution Dispersion and Prediction Model for Shuaiba Industrial Area): air quality data and meteorological data. Each set of data has been filed in monthly or yearly files depending on the period of observation. Each file has been given a name containing one, two or three letters followed by a number which indicates the observation period. Also, each set of data has been filed with a different format. In the following pages, each file format is presented and discussed together with file characteristics (e.g., measurement location in Universal Transverse Mercator (UTM) system; measurement units, special codes, etc.).

SECTION 7

Daniel Wooster, Sami Mohammed, Wajeeh Kittaneh, and Hussain Al-Adhad: A Preliminary Collection of Atmospheric Emission Data in the Shuaiba Industrial Area. Report provided to SAA as Appendix A of the EES-45 monthly report of February 1983, KISR 977A.

Abstract

The present report is organized in sections.

Section 1 presents some considerations regarding the final review stage of this data collection activity and the major accomplishments of such review of the original (unpublished) report.

Section 2 presents the original report after review and expansion. This report now contains a full set of maps for the accurate location of all emission points.

Section 3 presents the minutes of meetings of the final review activity described in Section 1.

Section 4 gives a brief description of some additional collected data related to this study that have not been discussed in this report.

Finally, Section 5 lists names, addresses and phone numbers of industry representatives whose cooperation was essential for the collection of the emission parameters.

Listing of the emission data used in the modeling simulations presented in
Volume II of this final report

All the information collected on the emission data in Shuaiba has been reviewed and reorganized for modeling input purposes. The following pages show the final emission data used in all modeling simulations.

In each data listing (one for each pollutant) each line (containing 11 data fields) represents one emission source; these are:

- field 1 : emission rate (gr/s)
- field 2 : UTM coordinate (West-East) (m)
- field 3 : UTM coordinate (South-North) (m)
- field 4 : source height above the ground (m)
- field 5 : exit temperature ($^{\circ}$ K)
- field 6 : exit speed (m/s)
- field 7 : exit diameter (m)
- field 8 : company code, number according to Table 7.1
- field 9 : stack number
- field 10 : sub-stack number
- field 11 : emission case (always 1 in this Listing).

TABLE 7.1 List of Facilities and Codes

COMPANY NAME	CODE	#
KUWAIT NATIONAL PETROLEUM COMPANY SHUAIBA REFINERY	KNPS	01
KUWAIT NATIONAL PETROLEUM COMPANY MINA ABDULLA REFINERY	KNPA	02
KUWAIT CEMENT COMPANY	KCCO	03
KUWAIT MELAMINE INDUSTRIES COMPANY	KMIC	04
PETROCHEMICAL INDUSTRIES COMPANY PLANT A	PICA	05
PETROCHEMICAL INDUSTRIES COMPANY PLANT B	PICB	06
SHUAIBA NORTH POWER STATION	SNPS	07
SHUAIBA SOUTH POWER STATION	SSPS	08
LIME PRODUCTS FACTORY	LPF	09
KUWAIT ASBESTOS INDUSTRY	KAI	10
KUWAIT OIL COMPANY	KOC	11

SECTION 8

Richard W. Boubel: Consultant Report. Report provided to SAA as Appendix A of the EES-45 monthly report of March 1983, KISR 1017A.

Abstract

During October and November 1982, Dr. Richard W. Boubel and Mr. Eugene Wellman served as consultants to the Kuwait Institute for Scientific Research (KISR) to determine the emissions to the atmosphere from the Shuaiba and Mina Abdulla Industrial Areas. They also trained local personnel as source testers and performed limited source testing experiments while in Kuwait.

Visits were made to the various industries in the Shuaiba and Mina Abdulla Industrial Areas and conferences were held with both industrial representatives and personnel from the Shuaiba Area Authority (SAA) responsible for air pollution evaluation and control.

Emission evaluations were made for both industrial and fugitive emissions from the area. These emissions were later re-evaluated and updated, based on a revised report from KISR. The industrial emissions were determined to be:

SO ₂	407.223	metric tons per day
NO _x	201.465	metric tons per day
Cement Dust	24.128	metric tons per day
Urea	6.998	metric tons per day
Ammonium Sulfate	0.173	metric tons per day
Lime Dust	0.593	metric tons per day

The particulate, fugitive emissions were determined to be related exponentially to the wind velocity, as follows:

<u>Wind Velocity</u> (m/s)	<u>Fugitive Emissions</u> (t/d)
2	0
4	0
8	0.018
10	0.033
15	189.177
20	8,706.413

Re-entrained emissions from motor vehicle traffic over paved and unpaved roads were calculated at 13.346 metric tons per day.

Suggestions are made for cost-effective future emissions control for the critical sources in the area. The Appendix includes two proposals, which could enable the State of Kuwait and the SAA to obtain the required information and consultation to substantially reduce atmospheric pollution from the industries of the Shuaiba and Mina Abdulla Industrial Areas.

List of SO₂ emissions

11.7	806560	3214980	30.0	533.0	13.5	1.3	4	1	0	1
5.4	806670	3215230	30.5	473.0	12.2	1.5	5	1	0	1
24.6	806640	3215240	51.8	1158.6	1.1	0.3	5	3	0	1
4.5	806650	3215160	16.2	523.0	36.5	1.0	5	6	0	1
4.5	806670	3215160	16.2	523.0	36.5	1.0	5	7	0	1
4.5	806690	3215166	16.2	523.0	36.5	1.0	5	8	0	1
4.5	806710	3215160	16.2	523.0	36.5	1.0	5	9	0	1
4.5	806730	3215160	16.2	523.0	36.5	1.0	5	10	0	1
68.0	806820	3215310	65.5	361.9	5.1	1.2	5	12	0	1
9.2	807280	3215120	25.6	583.0	9.4	2.4	6	16	0	1
9.2	807340	3215150	25.6	583.0	9.4	2.4	6	17	0	1
6.4	807250	3215110	25.6	653.0	9.1	2.0	6	18	0	1
6.4	807310	3215110	25.6	653.0	8.6	2.0	6	19	0	1
6.4	807300	3215160	27.0	653.0	10.3	2.3	6	20	0	1
3.9	807240	3215130	25.6	773.0	6.7	1.8	6	21	0	1
3.9	807310	3215140	25.6	773.0	6.6	1.8	6	22	0	1
4.6	807280	3215050	61.3	1383.0	0.1	0.2	6	25	0	1
191.3	807350	3216060	44.2	533.0	10.1	3.6	7	1	0	1
191.3	807350	3216050	44.2	523.0	10.1	3.6	7	2	0	1
191.3	807350	3216020	44.2	523.0	10.1	3.6	7	3	0	1
252.8	807350	3216000	45.0	523.0	10.1	4.1	7	4	0	1
252.8	807360	3215990	45.0	523.0	10.1	4.1	7	5	0	1
51.4	807340	3215890	38.0	573.0	0.3	3.7	7	6	0	1
51.4	807330	3215860	38.0	573.0	0.3	3.7	7	7	0	1
180.0	807360	3215740	30.5	458.0	13.0	2.8	8	1	1	1
180.0	807370	3215720	30.5	458.0	13.0	2.8	8	1	2	1
180.0	807380	3215700	30.5	458.0	13.0	2.8	8	2	1	1
180.0	807370	3215690	30.5	458.0	13.0	3.8	8	2	2	1
180.0	807370	3215660	30.5	458.0	13.0	2.8	8	3	1	1
180.0	807370	3215650	30.5	458.0	13.0	2.8	8	3	2	1
180.0	807380	3215640	30.5	458.0	13.0	2.8	8	4	1	1
180.0	807380	3215620	30.5	458.0	13.0	2.8	8	4	2	1
180.0	807390	3215600	33.5	458.0	9.5	3.3	8	5	1	1
180.0	807390	3215580	33.5	458.0	9.5	3.3	8	5	2	1
180.0	807400	3215550	33.5	458.0	9.5	3.3	8	6	1	1
180.0	807400	3215540	33.5	458.0	9.5	3.3	8	6	2	1
8.7	806710	3213510	19.8	810.8	8.5	1.5	2	1	1	1
8.7	806710	3213500	19.8	810.8	8.5	1.5	2	1	2	1
8.7	806710	3213490	19.8	810.8	8.5	1.5	2	1	3	1
8.7	806710	3213470	19.8	810.8	8.5	1.5	2	1	4	1
8.7	806710	3213470	9.8	810.8	8.5	1.5	2	10	5	1
8.7	806710	3213450	19.8	810.8	8.5	1.5	2	1	6	1
8.7	806710	3213430	19.8	810.8	8.5	1.5	2	1	7	1
8.7	806710	3213420	19.8	810.8	8.5	1.5	2	1	8	1
8.7	806710	3213410	19.8	810.8	8.5	1.5	2	1	9	1
8.7	806720	3213400	19.8	810.8	8.5	1.5	2	1	10	1
3.2	806700	3213350	19.8	810.8	3.1	2.3	2	2	1	1
3.2	806700	3213340	19.8	810.8	3.1	2.3	2	2	2	1
3.2	806700	3213340	19.8	810.8	3.1	2.3	2	2	3	1
3.2	806720	3213340	19.8	810.0	3.1	2.3	2	2	4	1
7.7	806750	3213360	21.5	810.8	3.0	2.3	2	3	1	1
7.7	806760	3213340	21.3	810.8	3.0	2.3	2	3	2	1
8.0	806810	3213260	43.0	644.1	7.0	2.7	2	4	1	1
8.0	806810	3213250	43.0	644.1	7.0	2.7	2	4	2	1
3.0	806900	3213460	18.3	810.8	6.0	1.8	2	5	1	1

3.0	806910	3213460	18.3	810.8	6.0	1.8	2	5	2	1
3.2	806950	3213320	12.2	727.4	19.0	2.3	2	8	0	1
130.0	806530	3213400	76.2	1643.0	6.7	0.6	2	9	0	1
244.0	806710	3213240	20.1	838.6	1.8	2.0	2	10	0	1
332.1	806830	3215750	67.0	1643.0	7.8	0.9	1	1	0	1
332.1	806830	3215770	67.0	1643.0	7.8	0.9	1	2	0	1
4.3	806340	3215540	52.2	699.7	7.6	3.7	1	4	1	1
4.3	806340	3215540	52.2	699.7	7.6	3.7	1	4	2	1
4.3	806310	3215530	52.2	699.7	7.6	3.7	1	5	1	1
4.3	806310	3215530	52.2	699.7	7.6	3.7	1	5	2	1
4.3	806270	3215530	52.2	699.7	7.6	3.7	1	6	1	1
4.3	806270	3215530	52.2	699.7	7.6	3.7	1	6	2	1
4.3	806160	3215540	33.8	741.3	5.5	1.5	1	7	1	1
4.3	806160	3215540	33.8	741.3	5.5	1.5	1	7	2	1
5.1	806170	3215610	49.1	644.1	5.7	1.8	1	8	1	1
5.1	806170	3215610	49.1	644.1	5.7	1.8	1	8	2	1
2.2	806380	3215520	40.4	826.3	9.6	2.4	1	15	0	1
6.8	806590	3215680	18.3	680.2	16.4	3.0	1	24	0	1
6.8	806590	3215660	18.3	680.2	16.4	3.0	1	25	0	1
6.8	806590	3215640	18.3	680.2	16.4	3.0	1	26	0	1
6.8	806600	3215620	18.3	680.2	16.4	3.0	1	27	0	1
485.1	806820	3215870	61.0	849.7	7.0	2.7	1	34	0	1
2.2	806730	3215640	40.4	960.8	11.0	2.4	1	36	0	1

List of NO_x emission (expressed as NO₂)

82.3	806670	3215230	30.5	473.0	12.2	1.5	5	1	0	1
26.4	806650	3215160	16.2	523.0	36.5	1.0	5	6	0	1
26.4	806670	3215160	16.2	523.0	36.5	1.0	5	7	0	1
26.4	806690	3215166	16.2	523.0	36.5	1.0	5	8	0	1
26.4	806710	3215160	16.2	523.0	36.5	1.0	5	9	0	1
26.4	806730	3215160	16.2	523.0	36.5	1.0	5	10	0	1
25.0	807250	3215110	25.6	653.0	9.1	2.0	6	18	0	1
41.5	807300	3215160	27.0	653.0	10.3	2.3	6	20	0	1
15.2	807240	3215130	25.6	773.0	6.7	1.8	6	21	0	1
15.2	807310	3215140	25.6	773.0	6.6	1.8	6	22	0	1
11.1	807350	3216060	44.2	533.0	10.1	3.6	7	1	0	1
11.1	807350	3216050	44.2	523.0	10.1	3.6	7	2	0	1
11.1	807350	3216020	44.2	523.0	10.1	3.6	7	3	0	1
11.1	807350	3216000	45.0	523.0	10.1	4.1	7	4	0	1
11.1	807360	3215990	45.0	523.0	10.1	4.1	7	5	0	1
15.6	807360	3215740	30.5	458.0	13.0	2.8	8	1	1	1
15.6	807370	3215720	30.5	458.0	13.0	2.8	8	1	2	1
15.6	807380	3215700	30.5	458.0	13.0	2.8	8	2	1	1
15.6	807370	3215690	30.5	458.0	13.0	3.8	8	2	2	1
15.6	807370	3215660	30.5	458.0	13.0	2.8	8	3	1	1
15.6	807370	3215650	30.5	458.0	13.0	2.8	8	3	2	1
15.6	807380	3215640	30.5	458.0	13.0	2.8	8	4	1	1
15.6	807380	3215620	30.5	458.0	13.0	2.8	8	4	2	1
15.6	807390	3215600	33.5	458.0	9.5	3.3	8	5	1	1
15.6	807390	3215580	33.5	458.0	9.5	3.3	8	5	2	1
15.6	807400	3215550	33.5	458.0	9.5	3.3	8	6	1	1
15.6	807400	3215540	33.5	458.0	9.5	3.3	8	6	2	1
21.0	806710	3213510	19.8	810.8	8.5	1.5	2	1	1	1
21.0	806710	3213500	19.8	810.8	8.5	1.5	2	1	2	1
21.0	806710	3213490	19.8	810.8	8.5	1.5	2	1	3	1
21.0	806710	3213480	19.8	810.8	8.5	1.5	2	1	4	1
21.0	806710	3213450	19.8	810.8	8.5	1.5	2	1	6	1
21.0	806710	3213430	19.8	810.8	8.5	1.5	2	1	7	1
21.0	806710	3213420	19.8	810.8	8.5	1.5	2	1	8	1
21.0	806710	3213410	19.8	810.8	8.5	1.5	2	1	9	1
21.3	806720	3213400	19.8	810.8	8.5	1.5	2	1	10	1
7.3	806700	3213350	19.8	810.8	3.1	2.3	2	2	1	1
7.3	806700	3213340	19.8	810.8	3.1	2.3	2	2	2	1
7.3	806700	3213340	19.8	810.8	3.1	2.3	2	2	3	1
7.3	806720	3213340	19.8	810.0	3.1	2.3	2	2	4	1
18.3	806810	3213260	43.0	644.1	7.0	2.7	2	4	1	1
18.3	806810	3213250	43.0	644.1	7.0	2.7	2	4	2	1
6.8	806900	3213460	18.3	810.8	6.0	1.8	2	5	1	1
6.8	806910	3213460	18.3	810.8	6.0	1.8	2	5	2	1
6.8	806950	3213320	12.2	727.4	19.0	2.3	2	8	0	1
56.7	806830	3215750	67.0	273.0	0.0	0.9	1	1	0	1
56.7	806830	3215770	67.0	273.0	0.0	0.9	1	2	0	1
63.9	806340	3215540	52.2	699.7	7.6	3.7	1	4	1	1
63.9	806310	3215530	52.2	699.7	7.6	3.7	1	4	2	1
63.9	806310	3215530	52.2	699.7	7.6	3.7	1	5	1	1
63.9	806270	3215530	52.2	699.7	7.6	3.7	1	5	2	1
63.9	806270	3215530	52.2	699.7	7.6	3.7	1	6	1	1
13.0	806440	3215560	29.0	921.9	10.0	1.8	1	10	1	1
13.0	806440	3215560	29.0	921.9	10.0	3.5	1	10	2	1

13.0	806430	3215570	29.0	921.9	10.0	1.8	1	11	1	1
13.0	806430	3215570	29.0	921.9	10.0	1.8	1	11	1	1
13.0	806430	3215570	29.0	921.9	10.0	1.8	1	11	2	1
26.3	806380	3215520	40.4	826.3	9.6	2.4	1	12	2	1
20.2	806370	3215620	44.2	623.6	7.9	2.0	1	15	0	1
20.2	806370	3215620	44.2	623.6	7.9	2.0	1	16	1	1
22.3	806350	3215680	45.1	697.4	7.9	2.3	1	16	2	1
22.3	806350	3215680	45.1	697.4	7.9	2.3	1	18	1	1
80.8	806590	3215680	18.3	680.2	10.4	3.0	1	18	2	1
80.8	806590	3215660	18.3	680.2	16.4	3.0	1	24	0	1
80.8	806590	3215640	18.3	680.2	16.4	3.0	1	25	0	1
80.8	806600	3215620	18.3	680.2	16.4	3.0	1	26	0	1
12.8	806680	3215550	33.8	1005.2	12.0	1.7	1	27	0	1
14.8	806660	3215650	35.1	1005.2	10.0	2.0	1	28	0	1
10.4	806640	3215520	30.5	902.4	6.1	2.0	1	29	0	1
273.5	806820	3215870	61.0	849.7	7.0	2.7	1	31	0	1
14.5	806580	3215540	24.7	1088.6	9.3	1.8	1	34	0	1
14.5	806580	3215540	24.7	1088.6	9.3	1.5	1	35	1	1
14.5	806580	3215540	24.7	1088.6	9.3	1.5	1	35	2	1
25.7	806730	3215640	40.4	960.8	11.0	2.4	1	35	3	1
10.9	806680	3215560	32.9	839.7	9.2	1.6	1	36	0	1
								38	0	1

List of cement dust emissions

46.0	806560	3216440	36.0	383.0	32.6	0.5	3	1	0	1
46.0	806530	3216450	36.0	383.0	32.6	0.5	3	2	0	1
46.0	806500	3216440	36.0	383.0	32.6	0.5	3	3	0	1
48.7	806580	3216430	29.0	383.0	34.6	0.5	3	4	0	1
0.8	806550	3216300	27.0	325.0	13.8	0.5	3	5	0	1
0.8	806540	3216200	27.0	325.0	13.8	0.5	3	6	0	1
0.8	806500	3216290	27.0	325.0	13.8	0.5	3	7	0	1
0.7	806530	3216320	26.0	325.0	18.9	0.4	3	8	0	1
0.5	806490	3216330	27.0	325.0	13.3	0.4	3	9	0	1
0.5	806490	3216300	27.0	325.0	13.3	0.4	3	10	0	1
0.5	806540	3216430	28.5	325.0	13.3	0.4	3	11	0	1
0.5	806520	3216430	28.5	325.0	13.3	0.4	3	12	0	1
0.5	806650	3216460	10.6	325.0	13.3	0.4	3	13	0	1
0.5	806600	3216440	10.6	325.0	13.3	0.4	3	14	0	1
0.5	806580	3216460	28.5	325.0	13.3	0.4	3	15	0	1
0.6	806510	3216350	29.0	325.0	13.6	0.4	3	16	0	1
0.8	806530	3216350	37.0	325.0	13.8	0.5	3	17	0	1
0.8	806560	3216350	37.2	325.0	13.8	0.5	3	18	0	1

List of urea dust emissions

10.4	806750	3215230	56.7	333.0	16.4	1.8	5	5	1
10.4	806750	3215230	56.7	333.0	16.4	1.8	5	5	2
10.4	806750	3215230	56.7	333.0	16.4	1.8	5	5	3
10.4	806750	3215230	56.7	333.0	16.4	1.8	5	5	4
13.9	807150	3215270	75.0	343.0	9.2	2.6	6	14	1
13.9	807150	3215250	75.0	343.0	9.2	2.6	6	14	2
13.9	807150	3215250	75.0	343.0	9.2	2.6	6	14	3
13.9	807150	3215250	75.0	343.0	9.2	2.6	6	14	4

List of NH₃ emissions

3.8	806660	3215310	56.1	293.0	106.2	0.1	5	2	0	1
82.3	806730	3215230	65.5	373.0	16.1	0.3	5	4	0	1
34.7	807160	3215230	72.2	373.0	2.7	0.5	6	13	0	1
1.0	807240	3215220	10.1	313.0	9.0	0.3	6	15	0	1
0.0	807540	3215250	38.4	273.0	0.0	0.1	6	23	0	1

SECTION 9

Mahmoud I. Safar: Land and Sea Breezes in Kuwait. Report provided to SAA as Appendix B of the EES-45 monthly report of March 1983, KISR 1017A.

Abstract

This report presents an analysis of the wind breeze conditions in Kuwait. Two meteorological stations were chosen for this purpose: Mina Al-Ahmadi, a coastal station and Kuwait International Airport, an inland station.

Kuwait International Airport wind data were analyzed every three hours for a period of five years (December 1975–November 1980); Mina Al-Ahmadi wind data, available only during daytime, were analyzed at 06.00, 09.00, 12.00, 15.00 and 18.00 hours during the entire year of 1980.

In this study, wind directions are divided into 16 sectors. Only those hours with wind speed less or equal to 10 knots were analyzed, since higher winds do not represent breeze conditions.

Data from both stations were divided on a seasonal basis:

Winter: December, January, February

Spring: March, April, May

Summer: June, July, August

Autumn: September, October, November

Wind frequency tables for the Kuwait International Airport and Mina Al-Ahmadi are shown, and wind roses for each season at 00.00 and 15.00 h local time at Kuwait International Airport and Mina Al-Ahmadi are displayed.

SECTION 10

This section contains an excerpt (Chapter 2) of Bowers J.F., J.R. Bjorklund and C.S. Cheney (1979) Industrial Source Complex (ISC) Dispersion Model User's Guide (Volume 1). Technical Report EPA-450/4-79-030. In this excerpt, a technical description of the ISCST and ISCLT dispersion models is presented.

CHAPTER 2
TECHNICAL DESCRIPTION

2.1 GENERAL

The Industrial Source Complex (ISC) Dispersion Model is an advanced Gaussian plume model. The technical discussion contained in this section assumes that the reader is already familiar with the theory and concepts of Gaussian plume models. Readers who lack a fundamental knowledge of the basic concepts of Gaussian plume modeling are referred to Section 2 of the User's Manual for the Single Source (CRSTER) Model (EPA, 1977) or to other references such as Meteorology and Atomic Energy (Slade, 1968) or the Workbook of Atmospheric Dispersion Estimates (Turner, 1970).

2.2 MODEL INPUT DATA

2.2.1 Meteorological Input Data

2.2.1.1 Meteorological Inputs for the ISC Short-Term (ISCST) Model Program

Table 2-1 gives the hourly meteorological inputs required by the ISC Model short-term computer program (ISCST). These inputs include the mean wind speed measured at height z_1 , the direction *toward which the wind is blowing*, the wind-profile exponent, the ambient air temperature, the Pasquill stability category and the vertical potential temperature gradient. In general, these inputs are developed from concurrent surface and upper-air meteorological data by the same preprocessor program as used by the Single Source (CRSTER) Model (see Appendix G). If the pre-processed meteorological data are used, the user may input, for each combination of wind-speed and Pasquill stability categories, site-specific values of the wind-profile exponent and the vertical potential temperature

TABLE 2-1
 HOURLY METEOROLOGICAL INPUTS REQUIRED BY THE ISC
 SHORT-TERM MODEL PROGRAM

Parameter	Definition
\bar{u}_1	Mean wind speed in meters per second (m/sec) at height z_1 (default value for z_1 is 10 meters)
AFVR	Average random flow vector (direction toward which the wind is blowing)
P	Wind-profile exponent (default values assigned on the basis of stability; see Table 2-2)
T_a	Ambient air temperature in degrees Kelvin ($^{\circ}$ K)
H_m	Depth of surface mixing layer (meters), developed from twice-daily mixing height estimates by the meteorological preprocessor program
Stability	Pasquill stability category (1 = A, 2 = B, etc.)
$\frac{\partial \theta}{\partial z}$	Vertical potential temperature gradient in degrees Kelvin per meter (default values assigned on the basis of stability; see Table 2-2)

TABLE 2-2
 DEFAULT VALUES FOR THE WIND-PROFILE EXPONENTS AND VERTICAL
 POTENTIAL TEMPERATURE GRADIENTS

Pasquill Stability Category	Wind-Profile Exponent p	Vertical Potential Temperature Gradient ($^{\circ}$ K/m)
A	0.10	0.000
B	0.15	0.000
C	0.20	0.000
D	0.25	0.000
E	0.30	0.020
F	0.30	0.035

gradient. If the user does not input site-specific wind-profile exponents and vertical potential temperature gradients, the ISC Model uses the default values given in Table 2-2. The inputs listed in Table 2-1 may also be developed by the user from observed hourly meteorological data and input by card deck. In these cases, the direction from which the wind is blowing must be reversed 180 degrees to conform with the average flow vector (the direction toward which the wind is blowing) generated by the meteorological preprocessor program.

It should be noted that concentrations calculated using Gaussian dispersion models are inversely proportional to the mean wind speed and thus the calculated concentrations approach infinity as the mean wind speed approaches zero (calm). Also, there is no basis for estimating wind direction during periods of calm winds. The meteorological preprocessor program arbitrarily sets the wind speed equal to 1 meter per second if the observed wind speed is less than 1 meter per second and, in the case of calm winds, sets the wind direction equal to the value reported for the last non-calm hour. Thus, considerable uncertainties exist in the results of model calculations for hours with calm winds, especially if a series of consecutive calm hours occurs. In this case, the preprocessor program assumes a single persistent wind direction for the duration of the period of calm winds. Concentrations calculated for such periods may significantly overestimate the concentrations that can actually be expected to occur. Consequently, it is recommended that the ISCST user examine the preprocessed meteorological data for the periods with calculated maximum short-term concentrations to ensure that the results are not determined by an arbitrary assumption. Periods of persistent calm winds may be recognized by the combination of a constant wind direction with a wind speed of exactly 1.0 meter per second.

The ISCST program has a rural and two urban options. In the Rural Mode, rural mixing heights and the σ_y and σ_z values for the indicated stability category are used in the calculations. Urban mixing heights are used in both urban modes. In Urban Mode 1, the stable E and

F stability categories are redefined as neutral D stability following current EPA guidance. In Urban Mode 2, the E and F stability categories are combined and the σ_y and σ_z values for the stability category one step more unstable than the indicated category are used in the calculations. For example, the σ_y and σ_z values for C stability are used in calculations for D stability in Urban Mode 2. Table 2-3 gives the dispersion coefficients used in each mode.

The Rural Mode is usually selected for industrial source complexes located in rural areas. However, the urban options may also be considered in modeling an industrial source complex located in a rural area if the source complex is large and contains numerous tall buildings and/or large heat sources (for example, coke ovens). An urban mode is appropriate for these cases in order to account for the enhanced turbulence generated during stable meteorological conditions by the surface roughness elements and/or heat sources. If an urban mode is appropriate, Urban Mode 1 is recommended for most situations. Urban Mode 2 is primarily recommended for area sources in urban areas. Urban Mode 2 should not be used for stack sources in modeling studies for regulatory purposes.

2.2.1.2 Meteorological Inputs for the ISC Long-Term (ISCLT) Model Program

Table 2-4 lists the meteorological inputs required by the ISC Model long-term computer program (ISCLT). Seasonal or annual STAR summaries are the principal meteorological inputs to the ISCLT program. A STAR summary is a tabulation of the joint frequency of occurrence of wind-speed and wind-direction categories, classified according to the Pasquill stability categories. Table 2-5 identifies the combinations of wind-speed and Pasquill stability categories that are possible following the Turner (1964) procedures of using airport surface weather observations to estimate atmospheric stability. The wind-speed categories in Table 2-5 are in knots because the National Weather Service (NWS) reports airport wind speeds to the nearest knot. The default values of the wind

TABLE 2-3

PASQUILL-GIFFORD DISPERSION COEFFICIENTS USED BY THE
ISC MODEL IN THE RURAL AND URBAN MODES

Actual Pasquill Stability Category*	Pasquill Stability Category for the σ_y, σ_z Values Used in ISC Model Calculations		
	Rural Mode	Urban Mode 1	Urban Mode 2
A	A	A	A
B	B	B	A
C	C	C	B
D	D	D	C
E	E	D	D
F	F	D	D

*The ISCST program redefines extremely stable G stability as very stable F stability.

TABLE 2-4

METEOROLOGICAL INPUTS REQUIRED BY
THE ISC LONG-TERM MODEL PROGRAM

Parameter	Definition
$f_{i,j,k,l}$	Frequency of occurrence of the i^{th} wind-speed category and j^{th} wind-direction category by stability category k for the l^{th} season (STAR summary)
\bar{u}_1	Mean wind speed in meters per second (m/sec) at height z_1 for each wind-speed category (default values based on STAR wind-speed categories)
$P_{j;k}$	Wind-profile exponent for each combination of wind-speed and stability categories (default values are assigned on the basis of stability; see Table 2-2)
$T_{a;k,l}$	Ambient air temperature for the k^{th} stability category and l^{th} season in degrees Kelvin ($^{\circ}\text{K}$)
$\frac{\partial \theta}{\partial z}_{i,k}$	Vertical potential temperature gradient in degrees Kelvin per meter ($^{\circ}\text{K}/\text{m}$) for each combination of wind-speed and stability categories (default values are assigned on the basis of stability; see Table 2-2)
$H_{m;i,k,l}$	Mixing height in meters for the i^{th} wind-speed category, k^{th} stability category and l^{th} season

TABLE 2-5
 POSSIBLE COMBINATIONS OF WIND-SPEED AND PASQUILL STABILITY
 CATEGORIES* AND MEAN WIND SPEEDS IN EACH NCC
 STAR SUMMARY WIND-SPEED CATEGORY

Pasquill Stability Category	Wind Speed (kt)					
	0-3	4-6	7-10	11-16	17-21	>21
A	X	X				
B	X	X	X			
C	X	X	X	X	X	X
D	X	X	X	X	X	X
E		X	X			
F	X	X				
ISCLT Wind Speed (m/sec)	0.75	2.50	4.30	6.80	9.50	12.50

*Based on Turner (1964) definitions of the Pasquill stability categories.

speeds in meters per second assigned by ISCLT to each wind-speed category are shown at the bottom of Table 2-5. The sixteen standard 22.5-degree wind-direction sectors used in STAR summaries are shown in Figure 2-1. ISCLT accepts STAR summaries with six stability categories (A through F) or five stability categories (A through E with the E and F categories combined). ISCLT is not designed to use the Climatological Dispersion Model (CDM) STAR summaries which divide the neutral D stability category into day and night D categories. STAR summaries are available for most NWS surface weather stations from the National Climatic Center (NCC).

The ISCLT user must specify ambient air temperatures by stability and season and mixing heights by stability and/or wind-speed and season. It is suggested that the average seasonal maximum daily temperature be assigned to the A, B and C stability categories; the average seasonal minimum daily temperature be assigned to the E and F stability categories; and the average seasonal temperature be assigned to the D stability category. In urban areas, common practice is to assign the mean afternoon mixing height given by Holzworth (1972) to the B and C stability categories, 1.5 times the mean afternoon mixing height to the A stability category, the mean early morning mixing height to the E and F stability categories, and the average of the mean early morning and afternoon mixing heights to the D stability category. In rural areas, the applicability of Holzworth early morning urban mixing heights is questionable. Consequently, ISCLT in the Rural Mode currently assumes that there is no restriction on vertical mixing during hours with E and F stability. It is suggested that Holzworth mean afternoon mixing heights be assigned to the B, C and D stability categories in rural areas and that 1.5 times the mean afternoon mixing height be assigned to the A stability category. If sufficient climatological data are available, wind-profile exponents and vertical potential temperature gradients can be assigned by the user to each combination of wind-speed and stability categories in order to make the long-term model site specific. In the

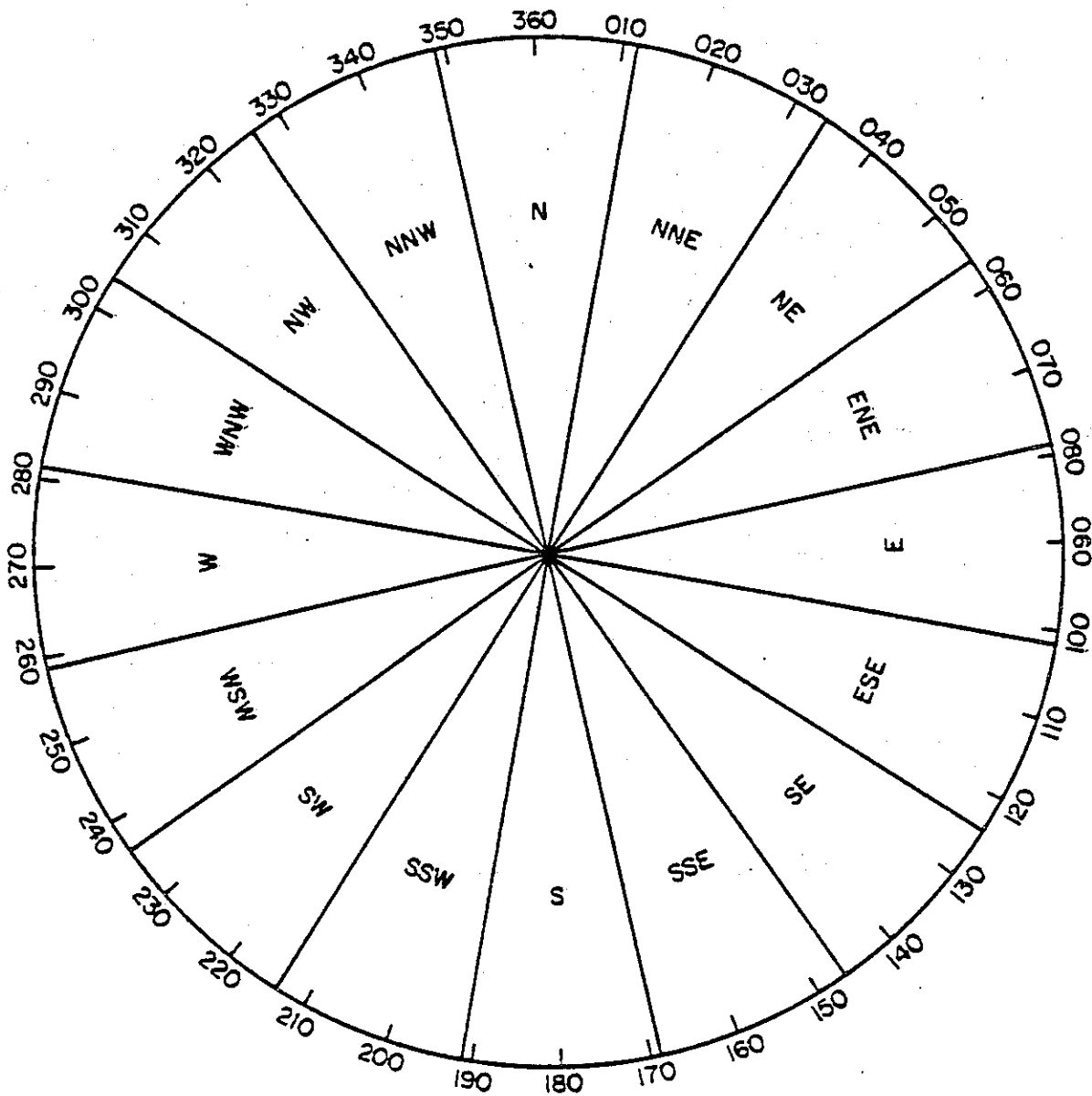


FIGURE 2-1. The sixteen standard 22.5-degree wind-direction sectors used in STAR summaries.

absence of site-specific wind-profile exponents and vertical potential temperature gradients, the default values given in Table 2-2 are automatically used by the ISCLT program.

The ISCLT program contains a rural mode and two urban modes. A discussion of these modes and guidance on their use is given in Section 2.2.1.1.

2.2.2 Source Input Data

Table 2-6 summarizes the source input data requirements of the ISC Dispersion Model computer programs. As shown by the table, there are three source types: stack, volume and area. The volume source option is also used to simulate line sources. Source elevations above mean sea level and source locations with respect to a user-specified origin are required for all sources. If the Universal Transverse Mercator (UTM) coordinate system is used to define receptor locations, UTM coordinates are also used to define source locations. Otherwise, the origin of the receptor array (either polar or Cartesian) is usually placed at the location of the most significant pollutant source within the industrial source complex. The X and Y coordinates of the other sources with respect to this origin are then obtained from a plant layout drawn to scale. The X axis is positive to the east and the Y axis is positive to the north.

The pollutant emission rate is also required for each source. If the pollutant is depleted by any mechanism that can be described by time-dependent exponential decay, the user may enter a decay coefficient ψ . The parameters ϕ_n , V_{sn} and γ_n are only required if concentration or deposition calculations are being made for particulates with appreciable gravitational settling velocities (diameters greater than about 20 micrometers). Particulate emissions from each source can be divided by the user into a maximum of 20 gravitational settling-velocity categories.

TABLE 2-6

SOURCE INPUTS REQUIRED BY THE
ISC MODEL PROGRAMS

Parameter	Definition
<u>Stacks</u>	
Q	Pollutant emission rate for concentration calculations (mass per unit time)
Q_T	Total pollutant emissions during the time period τ for which deposition is calculated (mass)
ψ	Pollutant decay coefficient (seconds ⁻¹)
X, Y	X and Y coordinates of the stack (meters)
Z_s	Elevation of base of stack (meters above mean sea level)
h	Stack height (meters)
V_s	Stack exit velocity (meters per second)
d	Stack inner diameter (meters)
T_s	Stack exit temperature (degrees Kelvin)
ϕ_n	Mass fraction of particulates in the n^{th} settling-velocity category
V_{sn}	Gravitational settling velocity for particulates in the n^{th} settling-velocity category (meters per second)
γ_n	Surface reflection coefficient for particulates in the n^{th} settling-velocity category
h_b	Height of building adjacent to the stack (meters)

TABLE 2-6 (Continued)

Parameter	Definition
W	Width of building adjacent to the stack (meters)
L	Length of building adjacent to the stack (meters)
<u>Volume Source</u>	
<u>(Line Source)</u>	
Q	Same definition as for stacks
Q _T	Same definition as for stacks
ψ	Same definition as for stacks
X, Y	X and Y coordinates of the center of the volume source or of each volume source used to represent a line source (meters)
Z _s	Elevation of the ground surface at the point of the center of each volume source (meters above mean sea level)
H	Height of the center of each volume source above the ground surface (meters)
σ _{yo}	Initial horizontal dimension (meters)
σ _{zo}	Initial vertical dimension (meters)
φ _n	Same definition as for stacks
V _{sn}	Same definition as for stacks
γ _n	Same definition as for stacks
<u>Area Source</u>	
Q _A	Pollutant emission rate for concentration calculations (mass per unit time per unit area)

TABLE 2-6 (Continued)

Parameters	Definition
Q_{AT}	Total pollutant emissions during the time period τ for which deposition is calculated (mass per unit area)
ψ	Same definition as for stacks
X, Y	X and Y coordinates of the southwest corner of the square area source (meters)
Z_s	Elevation of the area source (meters above mean sea level)
H	Effective emission height of the area source (meters)
x_0	Width of the square area source (meters)
ϕ_n	Same definition as for stacks
V_{sn}	Same definition as for stacks
γ_n	Same definition as for stacks

Emission rates used by the short-term model program ISCST may be held constant or may be varied as follows:

- By hour of the day
- By season or month
- By hour of the day and season
- By wind-speed and stability categories (applies to fugitive sources of wind-blown dust)

Emission rates used by the long-term model program ISCLT may be annual average rates or may be varied by season or by wind-speed and stability categories.

Additional source inputs required for stacks include the physical stack height, the stack exit velocity, the stack inner diameter and the stack exit temperature. For an area source or a volume source, the dimensions of the source and the effective emission height are entered in place of these parameters. If a stack is located on or adjacent to a building and the stack height to building height ratio is less than 2.5, the length (L) and width (W) of the building are required as source inputs in order to include aerodynamic wake effects in the model calculations. *The building wake effects option is automatically exercised if building dimensions are entered.*

2.2.3 Receptor Data

The ISC Dispersion Model computer programs allow the user to select either a Cartesian (X, Y) or a polar (r, θ) receptor grid system. In the Cartesian system, the X-axis is positive to the east of a user-specified origin and the Y-axis is positive to the north. In the polar system, r is the radial distance measured from the user-specified origin and the angle θ (azimuth bearing) is measured clockwise from

north. If pollutant emissions are dominated by a single source or by a group of sources in close proximity, a polar coordinate system with its origin at the location of the dominant source or sources is the preferred receptor grid system. However, if the industrial source complex is comprised of multiple sources that are not located at the same point, a Cartesian coordinate system is usually more convenient. Additionally, if the Universal Transverse Mercator (UTM) coordinate system is used to define source locations and/or to extract the elevations of receptor points from USGS topographic maps, the UTM system can also be used in the ISC Model calculations. Discrete (arbitrarily placed) receptor points corresponding to the locations of air quality monitors, elevated terrain features, the property boundaries of the industrial source complex or other points of interest can be used with either coordinate system.

In the polar coordinate system, receptor points are usually spaced at 10-degree intervals on concentric rings. Thus, there are 36 receptors on each ring. The radial distances from the origin to the receptor rings are user selected and are generally set equal to the distances to the expected maximum ground-level concentrations for the major pollutant sources under the most frequent stability and wind-speed combinations. Estimates of these distances can be obtained from the PTMAX computer program (Turner and Busse, 1973) or from preliminary calculations using the ISCST computer program. The maximum number of receptor points is determined by factors such as the number of sources and the desired output (see Equation (3-1) for the short-term model and Equations (4-1), (4-2) and (4-3) for the long-term model). An example of a polar receptor array is shown in Figure 2-2.

In the Cartesian coordinate system, the X and Y coordinates of the receptors are specified by the user. The spacing of grid points is not required to be uniform so that the density of grid points can be greatest in the area of the expected maximum ground-level concentrations.

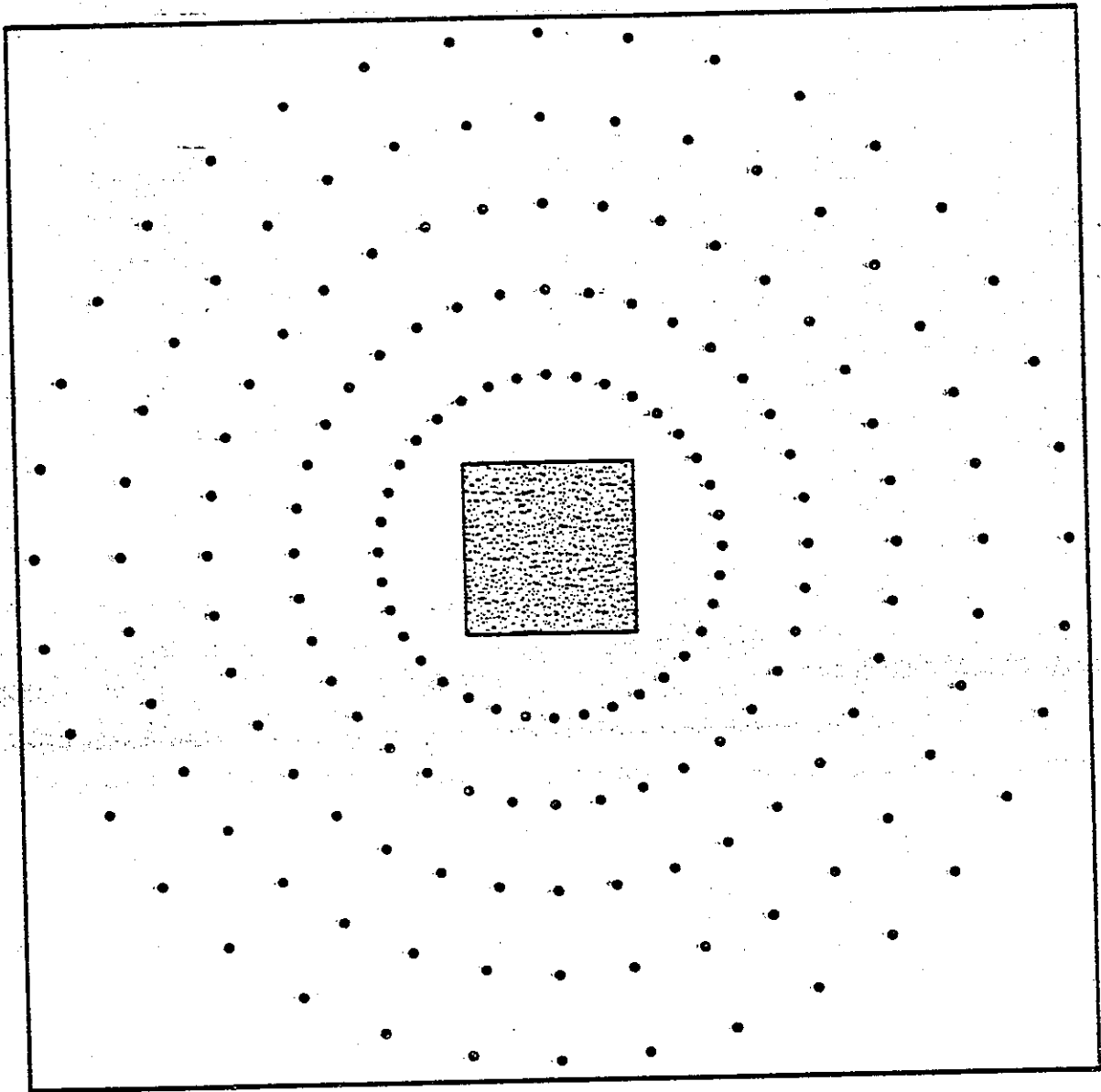


FIGURE 2-2. Example of a polar receptor grid. The stippled area shows the property of a hypothetical industrial source complex.

For example, assume that an industrial source complex is comprised of a number of major sources, contained within a 1-kilometer square, whose maximum ground-level concentrations are expected to occur at downwind distances ranging from 500 to 1000 meters. The Cartesian receptor grid {X and Y = 0, +200, +400, +600, +800, +1,000, +1,200, +1,500, +2,000, +3,000} illustrated in Figure 2-3 provides a dense spacing of grid points in the areas where the highest concentrations are expected to occur. As shown by Figure 2-3, use of the Cartesian system requires that some of the receptor points be located within the property of the source complex. Also, some of the receptors may be located within 100 meters of an individual source. If a receptor is located within 100 meters of a source, a warning message is printed and concentrations are not calculated for the source-receptor combination. The 100-meter restriction, which arises from the fact that the Pasquill-Gifford curves begin at 100 meters, is not a problem in this case because the concentrations of concern are the concentrations calculated at and beyond the property boundaries of the source complex. Comparison of Figures 2-2 and 2-3 shows that, for the hypothetical industrial source complex described above, the Cartesian receptor array is more likely to detect the maximum concentrations produced by the combined emissions from the various sources within the industrial source complex than is the polar receptor array.

As noted above, discrete (arbitrarily spaced) receptor points may be entered using either a polar or a Cartesian coordinate system. In general, discrete receptor points are placed at the locations of air quality monitors, the boundaries of the property of an industrial source complex or at other points of interest. However, discrete receptor points can be used for many purposes. For example, assume that a proposed coal-fired power plant will be located approximately 30 kilometers from a National Park that is a Class I (pristine air quality) area and that it is desired to determine whether the 3-hour and 24-hour Class I Non-Deterioration Increments for SO₂ will be exceeded on more

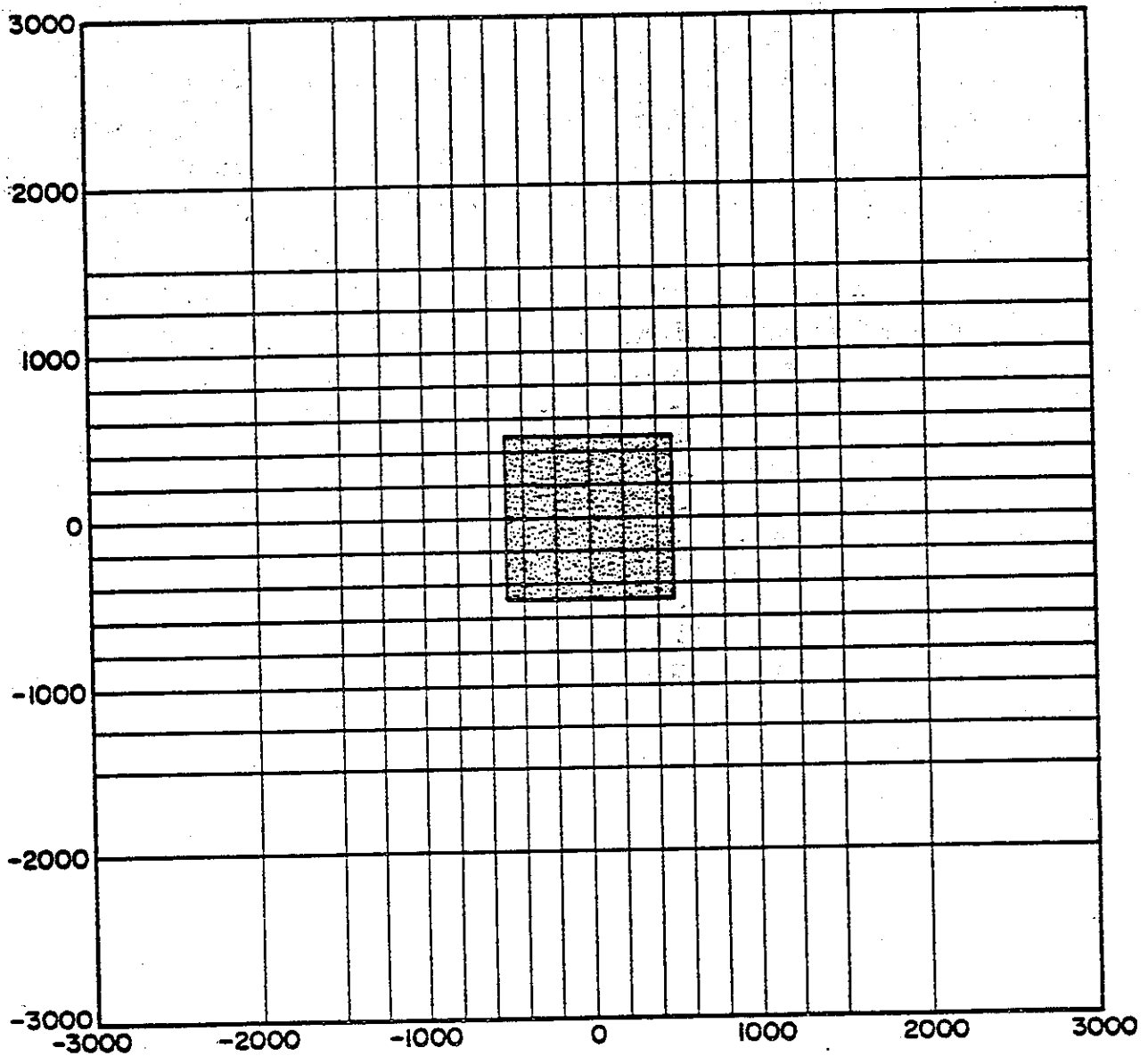


FIGURE 2-3. Example of an irregularly-spaced Cartesian receptor grid. The stippled area shows the property of a hypothetical industrial source complex.

than 18 days per year. The angular dimensions of the areas within which the 3-hour and 24-hour Class I Non-Deterioration Increments for SO₂ are exceeded are usually less than 10 degrees. It follows that a polar coordinate system with a 10-degree angular separation of receptors is not adequate to detect all occurrences of 3-hour and 24-hour SO₂ concentrations above the short-term Class I SO₂ Increments. The user may therefore wish to place discrete receptors at 1-degree intervals along the boundary of and within the Class I area.

If model calculations are to be made for an industrial source complex located in complex terrain, the elevation above mean sea level of each receptor must be input. *If the elevation of any receptor exceeds the height of any stack or the effective emission height of any volume source, an error message is printed and program execution is terminated.*

2.3 PLUME RISE FORMULAS

The effective stack height H of a plume with momentum and/or thermal buoyancy is given by the sum of the physical stack height h and the plume rise Δh . The ISC Model programs use the generalized Briggs (1971, 1975) plume-rise equations. Parameters used in these equations are defined as follows:

$$F_m = \left(T_a / T_s \right) v_s^2 d^2 / 4 \quad (2-1)$$

$$F = \left\{ \begin{array}{l} F' = \frac{g v_s d^2}{4} \left(1 - T_a / T_s \right) ; F' > F_c \\ 0 ; F' \leq F_c \end{array} \right. \quad (2-2a)$$

(2-19)

$$F_c = \left\{ \begin{array}{l} 0.0727 (V_s d)^{4/3} ; F' \leq 55 \text{ m}^4/\text{sec}^3 \\ 0.0141 (V_s d)^{5/3} ; F' > 55 \text{ m}^4/\text{sec}^3 \end{array} \right\} \quad (2-2b)$$

$$\beta_j = \left(1/3 + \frac{\bar{u}\{h\}}{V_s} \right) \quad (2-3)$$

where

F_m = momentum flux term

F = buoyancy flux term

F_c = buoyancy flux below which plume rise is due to momentum only

β_j = jet entrainment coefficient

T_a = ambient air temperature ($^{\circ}\text{K}$)

T_s = stack exit temperature ($^{\circ}\text{K}$); input as zero for a pure momentum source

V_s = stack exit velocity (m/sec), input as zero if no plume rise is to be calculated

d = stack inner diameter (m)

g = acceleration due to gravity ($9.8 \text{ m}/\text{sec}^2$)

$\bar{u}\{h\}$ = mean wind speed (m/sec) at emission height h

If the vertical potential temperature gradient is less than or equal to zero (the default value for the A, B, C and D Pasquill stability categories), plume rise Δh_N due to buoyancy and/or momentum at downwind distance x is given by

$$\Delta h_N\{x\} = \left[\frac{3F_m x'}{S_j^2 \bar{u}\{h\}^2} + \frac{3F x'^2}{2\beta_1^2 \bar{u}\{h\}^3} \right]^{1/3} \quad (2-4)$$

(2-20)

$$x' = \left\{ \begin{array}{l} x \quad ; \quad x < 3.5 x^* \quad \text{and} \quad F > 0 \\ x \quad ; \quad x < \frac{4d (v_s + 3\bar{u}\{h\})^2}{v_s \bar{u}\{h\}} \quad \text{and} \quad F = 0 \\ 3.5 x^* \quad ; \quad x \geq 3.5 x^* \quad \text{and} \quad F > 0 \\ \frac{4d (v_s + 3\bar{u}\{h\})^2}{v_s \bar{u}\{h\}} ; \quad x \geq \frac{4d (v_s + 3\bar{u}\{h\})^2}{v_s \bar{u}\{h\}} \quad \text{and} \quad F = 0 \end{array} \right. \quad (2-5)$$

$$x^* = \left\{ \begin{array}{l} 14 F^{5/8}; \quad F \leq 55 \text{ m}^4/\text{sec}^3 \\ 34 F^{2/5}; \quad F > 55 \text{ m}^4/\text{sec}^3 \end{array} \right. \quad (2-6)$$

where the default value for the adiabatic entrainment coefficient β_1 is 0.6 (Briggs, 1975). It should be noted that Equation (2-4) is a theoretical formulation. At present, sufficient experimental data to determine the validity of the final plume rises yielded by Equation (2-4) for non-buoyant plumes are not available.

If the vertical potential temperature gradient is positive, plume rise Δh_s at downwind distance x is given by

$$\Delta h_s \{x\} = \left[\frac{3F_m}{\beta_j^2 \bar{u}\{h\} s^{1/2}} \sin (s^{1/2} x'/\bar{u}\{h\}) + \frac{3F}{\beta_2^2 \bar{u}\{h\} s} (1 - \cos (s^{1/2} x'/\bar{u}\{h\})) \right]^{1/3} \quad (2-7)$$

(2-21)

$$x' = \left\{ \begin{array}{l} x \quad ; \quad x < \pi \bar{u}\{h\} s^{-1/2} \quad \text{and } F > 0 \\ x \quad ; \quad x < \frac{\pi}{2} \bar{u}\{h\} s^{-1/2} \quad \text{and } F = 0 \\ \pi \bar{u}\{h\} s^{-1/2}; \quad x \geq \pi \bar{u}\{h\} s^{-1/2} \quad \text{and } F > 0 \\ \frac{\pi}{2} \bar{u}\{h\} s^{-1/2}; \quad x \geq \frac{\pi}{2} \bar{u}\{h\} s^{-1/2} \quad \text{and } F = 0 \end{array} \right\} \quad (2-8)$$

$$s = \frac{F}{T_a} \frac{\partial \theta}{\partial z} \quad (2-9)$$

where

s = stability parameter

$\frac{\partial \theta}{\partial z}$ = vertical potential temperature gradient (the default value is 0.020°K/m for E stability and 0.035°K/m for F stability)

The default value for the stable entrainment coefficient β_2 is 0.6 (Briggs, 1975). It should be noted that, if the buoyancy parameter F is equal to zero and $\Delta h_s\{x\}$ is greater than $3V_s d/\bar{u}\{h\}$, the ISC Model programs set $\Delta h_s\{x\}$ equal to $3V_s d/\bar{u}\{h\}$. Equation (2-7) is a theoretical formulation. In the case of non-buoyant plumes, sufficient experimental data to determine the validity of the final plume rises calculated by Equation (2-7) currently are not available.

It is important to note that the calculation of plume rise as a function of downwind distance is an ISC Model option. If the ISC Model

programs are not directed to calculate plume rise as a function of downwind distance, the programs will assume that the final plume rise applies at all downwind distances. The final plume rise with an adiabatic or unstable thermal stratification is given by Equation (2-4) with x' set equal to the maximum value allowed by Equation (2-5). Similarly, the final plume rise with a stable thermal stratification is given by Equation (2-7) with x' set equal to the maximum value allowed by Equation (2-8).

A wind-profile exponent law is used to adjust the mean wind speed \bar{u}_1 from the wind system measurement height z_1 (default value of 10 meters) to the emission height h . This law is of the form

$$\bar{u}\{h\} = \bar{u}_1 \left(\frac{h}{z_1} \right)^p \quad (2-10)$$

where p is the wind-profile exponent. The default values for p are given in Table 2-2.

As an option, the user may direct the ISC Model programs to consider stack-tip downwash for all stacks following the suggestions of Briggs (1973). The physical stack height h is replaced by an adjusted stack height h' , which is defined as

$$h' = \left\{ \begin{array}{ll} h & ; V_s \geq 1.5 \bar{u}\{h\} \\ h + 2 \left[\frac{V_s}{\bar{u}\{h\}} - 1.5 \right] d & ; V_s < 1.5 \bar{u}\{h\} \end{array} \right\} \quad (2-11)$$

The user is cautioned that Equation (2-11) is based on data obtained in an aeronautical wind tunnel without airstream turbulence and without proper Froude number scaling for buoyancy effects (see Halitsky, 1978). Additionally, the published data upon which Equation (2-11) is based (Sherlock and Stalker, 1941) refer to the downward displacement of the lower plume boundary rather than to the downward displacement of the plume centerline.

2.4 THE ISC SHORT-TERM DISPERSION MODEL EQUATIONS

2.4.1 Stack Emissions

The ISC short-term concentration model for stacks uses the steady-state Gaussian plume equation for a continuous elevated source. For each stack and each hour, the origin of the stack's coordinate system is placed at the ground surface at the base of the stack. The x axis is positive in the downwind direction, the y axis is crosswind (normal) to the x axis and the z axis extends vertically. The fixed receptor locations are converted to each stack's coordinate system for each hourly concentration calculation. The hourly concentrations calculated for each stack at each receptor are summed to obtain the total concentration produced at each receptor by the combined stack emissions.

The hourly ground-level concentration at downwind distance x and crosswind distance y is given by

$$\chi(x,y) = \frac{KQ}{\pi \bar{u}\{h\} \sigma_y \sigma_z} \exp \left[-\frac{1}{2} \left(\frac{y}{\sigma_y} \right)^2 \right] \quad (2-12)$$

{Vertical Term} {Decay Term}

where

Q = pollutant emission rate (mass per unit time)

K = a scaling coefficient to convert calculated concentrations to desired units (default value of 1×10^6 for Q in g/sec and concentration in $\mu\text{g}/\text{m}^3$)

σ_y, σ_z = standard deviation of lateral, vertical concentration distribution (m)

$\bar{u}\{h\}$ = mean wind speed (m/sec) at stack height h

Equation (2-12) includes a Vertical Term, a Decay Term, and dispersion coefficients (σ_y and σ_z). The dispersion coefficients and the Vertical Term are discussed below. It should be noted that the Vertical Term includes the effects of source elevation, plume rise, limited mixing in the vertical, and the gravitational settling and dry deposition of larger particulates (particulates with diameters greater than about 20 micrometers).

The Decay Term, which is a simple method of accounting for pollutant removal by physical or chemical processes, is of the form

$$\{\text{Decay Term}\} = \exp \left[-\psi x/\bar{u}\{h\} \right] \quad (2-13)$$

where

ψ = the decay coefficient (sec^{-1})

For example, if $T_{1/2}$ is the pollutant half life in seconds, the user can obtain ψ from the relationship

$$\psi = \frac{0.693}{T_{1/2}} \quad (2-14)$$

(2-25)

The default value for ψ is zero. That is, decay is not considered in the model calculations unless ψ is specified.

In addition to stack emissions, the ISC short-term concentration model considers emissions from area and volume sources. The volume-source option is also used to simulate line sources. These model options are described in Section 2.4.2. Section 2.4.3 gives the optional algorithms for calculating dry deposition for stack, area and volume sources.

2.4.1.1 The Dispersion Coefficients

a. Point Source Dispersion Coefficients. Equations that approximately fit the Pasquill-Gifford curves (Turner, 1970) are used to calculate σ_y and σ_z . The equations used to calculate σ_y are of the form

$$\sigma_y = 465.11628 \times \tan(\text{TH}) \quad (2-15)$$

$$\text{TH} = 0.017453293 (c - d \ln x) \quad (2-16)$$

where the downwind distance x is in kilometers in Equations (2-15) and (2-16); the coefficients c and d are listed in Table 2-7. The equation used to calculate σ_z is of the form

$$\sigma_z = ax^b \quad (2-17)$$

where the downwind distance x is in kilometers in Equation (2-17) and the coefficients a and b are given in Table 2-8.

TABLE 2-7

PARAMETERS USED TO
CALCULATE σ_y

Pasquill Stability Category	$\sigma_y = 465.11628 x(\text{km}) \tan (\text{TH})$	
	$\text{TH} = 0.017453293 (c - d \ln (x(\text{km})))$	
	c	d
A	24.1670	2.5334
B	18.3330	1.8096
C	12.5000	1.0857
D	8.3330	0.72382
E	6.2500	0.54287
F	4.1667	0.36191

(2-27)

TABLE 2-8
PARAMETERS USED TO
CALCULATE σ_z

Pasquill Stability Category	x (km)	$\sigma_z = a x(\text{km})^b$	
		a	b
A*	0.10 - 0.15	158.080	1.05420
	0.16 - 0.20	170.220	1.09320
	0.21 - 0.25	179.520	1.12620
	0.26 - 0.30	217.410	1.26440
	0.31 - 0.40	258.890	1.40940
	0.41 - 0.50	346.750	1.72830
	0.51 - 3.11	453.850	2.11660
	>3.11	**	**
B*	0.10 - 0.20	90.673	0.93198
	0.21 - 0.40	98.483	0.98332
	>0.40	109.300	1.09710
C*	>0.10	61.141	0.91465
D	0.10 - 0.30	34.459	0.86974
	0.31 - 1.00	32.093	0.81066
	1.01 - 3.00	32.093	0.64403
	3.01 - 10.00	33.504	0.60486
	10.01 - 30.00	36.650	0.56589
	>30.00	44.053	0.51179

*If the calculated value of σ_z exceeds 5000 m, σ_z is set to 5000 m.

** σ_z is equal to 5000 m.

TABLE 2-8 (Continued)

Pasquill Stability Category	x (km)	$\sigma_z = a x(\text{km})^b$	
		a	b
E	0.10 - 0.30	23.331	0.81956
	0.31 - 1.00	21.628	0.75660
	1.01 - 2.00	21.628	0.63077
	2.01 - 4.00	22.534	0.57154
	4.01 - 10.00	24.703	0.50527
	10.01 - 20.00	26.970	0.46713
	20.01 - 40.00	35.420	0.37615
	>40.00	47.618	0.29592
F	0.10 - 0.20	15.209	0.81558
	0.21 - 0.70	14.457	0.78407
	0.71 - 1.00	13.953	0.68465
	1.01 - 2.00	13.953	0.63227
	2.01 - 3.00	14.823	0.54503
	3.01 - 7.00	16.187	0.46490
	7.01 - 15.00	17.836	0.41507
	15.01 - 30.00	22.651	0.32681
	30.01 - 60.00	27.074	0.27436
	>60.00	34.219	0.21716

b. Downwind and Crosswind Distances. As noted in Section 2.2.3, the ISC Model uses either a polar or a Cartesian receptor grid as specified by the user. In the polar coordinate system, the radial coordinate of the point (r, θ) is measured from the user-specified origin and angular coordinate θ is measured clockwise from north. In the Cartesian coordinate system, the X axis is positive to the east of the user-specified origin and the Y axis is positive to the north. For either type of receptor grid, the user must define the location of each source with respect to the origin of the grid using Cartesian coordinates. In the polar coordinate system, the X and Y coordinates of a receptor at the point (r, θ) are given by

$$X(R) = r \sin \theta \quad (2-18)$$

$$Y(R) = r \cos \theta \quad (2-19)$$

If the X and Y coordinates of the source are $X(S)$ and $Y(S)$, the downwind distance x to the receptor is given by

$$x = -(X(R) - X(S)) \sin DD - (Y(R) - Y(S)) \cos DD \quad (2-20)$$

where DD is the direction from which the wind is blowing. If any receptor is located within 100 meters of a source, a warning message is printed and no concentrations are calculated for the source-receptor combination. The crosswind distance y to the receptor (see Equation (2-12)) is given by

$$y = -(Y(R) - Y(S)) \sin DD + (X(R) - X(S)) \cos DD \quad (2-21)$$

c. Lateral and Vertical Virtual Distances. Equations (2-15) through (2-17) define the dispersion coefficients for an ideal point source. However, volume sources have initial lateral and vertical dimensions. Also, as discussed below, building wake effects can enhance the initial growth of stack plumes. In these cases, lateral (x_y) and vertical (x_z) virtual distances are added by the ISC Model to the actual downwind distance x for the σ_y and σ_z calculations. The lateral virtual distance in kilometers is given by

$$x_y \text{ (km)} = \left(\frac{\sigma_{y0} \text{ (m)}}{p} \right)^{1/q} \quad (2-22)$$

where the stability-dependent coefficients p and q are given in Table 2-9 and σ_{y0} is the standard deviation of the lateral concentration distribution at the source. Similarly, the vertical virtual distance in kilometers is given by

$$x_z \text{ (km)} = \left(\frac{\sigma_{z0} \text{ (m)}}{a} \right)^{1/b} \quad (2-23)$$

where the coefficients a and b are obtained from Table 2-8 and σ_{z0} is the standard deviation of the vertical concentration distribution at the source. It is important to note that the ISC Model programs check to ensure that the x_z used to calculate $\sigma_z\{x+x_z\}$ is the x_z calculated using the coefficients a and b that correspond to the distance category specified by the quantity $(x + x_z)$.

d. Procedures Used to Account for the Effects of Building Wakes on Effluent Dispersion. The procedures used by the ISC Model to account for the effects of the aerodynamic wakes and eddies produced by plant buildings and structures on plume dispersion follow the suggestions of Huber and Snyder (1976) and Huber (1977). Their suggestions are princi-

TABLE 2-9

COEFFICIENTS USED TO CALCULATE
LATERAL VIRTUAL DISTANCES

Pasquill Stability Category	$x_y = \left(\frac{\sigma_{y0}}{P}\right)^{1/q}$	
	P	q
A	209.14	0.890
B	154.46	0.902
C	103.26	0.917
D	68.26	0.919
E	51.06	0.921
F	33.92	0.919

pally based on the results of wind-tunnel experiments using a model building with a crosswind dimension double that of the building height. The atmospheric turbulence simulated in the wind-tunnel experiments was intermediate between the turbulent intensity associated with the slightly unstable Pasquill C category and the turbulent intensity associated with the neutral D category. Thus, the data reported by Huber and Snyder reflect a specific stability, building shape and building orientation with respect to the mean wind direction. It follows that the ISC Model wake-effects evaluation procedures may not be strictly applicable to all situations. However, the suggestions of Huber and Snyder are based on the best available data and are used by the ISC Model as interim procedures until additional data become available.

The wake-effects evaluation procedures may be applied by the user to any stack on or adjacent to a building. *The distance-dependent plume rise option generally should be used with the building wake effects option. Additionally, because the effects of stack-tip downwash (see Equation (2-11)) are implicitly included in the building wake effects option, the stack-tip downwash option normally should not be used in combination with the building wake effects option.* The first step in the wake-effects evaluation procedures used by the ISC Model programs is to calculate the plume rise due to momentum alone at a distance of two building heights downwind from the stack. Equation (2-4) or Equation (2-7) with the buoyancy parameter F set equal to zero is used to calculate this momentum rise. If the plume height, given by the sum of the stack height and the momentum rise at a downwind distance of two building heights, is greater than either 2.5 building heights ($2.5 h_p$) or the sum of the building height and 1.5 times the building width ($h_b + 1.5 h_w$), the plume is assumed to be unaffected by the building wake. Otherwise, the plume is assumed to be affected by the building wake.

The ISC Model programs account for the effects of building wakes by modifying σ_z for plumes from stacks with plume height to building height ratios greater than 1.2 (but less than 2.5) and by

modifying both σ_y and σ_z for plumes with plume height to building height ratios less than or equal to 1.2. The plume height used in the plume height to stack height ratios is the same plume height used to determine if the plume is affected by the building wake. The ISC Model defines buildings as squat ($h_w \geq h_b$) or tall ($h_w < h_b$). The building width h_w is approximated by the diameter of a circle with an area equal to the horizontal area of the building. The ISC Model includes a general procedure for modifying σ_z and σ_y at distances greater than $3 h_b$ for squat buildings or $3 h_w$ for tall buildings. The air flow in the building cavity region is both highly turbulent and generally recirculating. The ISC Model is not appropriate for estimating concentrations within such regions. The ISC Model assumption that this recirculating cavity region extends to a downwind distance of $3 h_b$ for a squat building or $3 h_w$ for a tall building is most appropriate for a building whose width is not much greater than its height. The ISC Model user is cautioned that, for other types of buildings, receptors located at downwind distances of $3 h_b$ (squat buildings) or $3 h_w$ (tall buildings) may be within the recirculating region. Some guidance and techniques for estimating concentrations very near buildings can be found in Barry (1964), Halitsky (1963) and Vincent (1977). The downwash procedure found in Budney (1977) may also be used to obtain a "worst-case" estimate.

The modified σ_z equation for a squat building is given by

$$\sigma_z' = \left\{ \begin{array}{l} 0.7h_b(m) + 0.067 [x(m) - 3h_b(m)]; \quad 3h_b(m) < x(m) < 10h_b(m) \\ \sigma_z \{ x(km) + x_z(km) \} \quad ; \quad x(m) \geq 10h_b(m) \end{array} \right\} \quad (2-24)$$

where the building height h_b is in meters. For a tall building, Huber (1977) suggests that the width scale h_w replace h_b in Equation (2-24).

The modified σ_z equation for a tall building is then given by

$$\sigma_z' = \left\{ \begin{array}{l} 0.7h_w(m) + 0.067 [x(m) - 3h_w(m)] ; \quad 3h_w < x(m) < 10h_w(m) \\ \sigma_z \{x(\text{km}) + x_z(\text{km})\} \quad ; \quad x(m) \geq 10h_w(m) \end{array} \right\} \quad (2-25)$$

where h_w is in meters. It is important to note that σ_z' is not permitted to be less than the point source value given by Equation (2-17), a condition that may occur with the A and B stability categories.

The vertical virtual distance x_z is added to the actual downwind distance x at downwind distances beyond $10h_b$ (squat buildings) or $10h_w$ (tall buildings) in order to account for the enhanced initial plume growth caused by the building wake. Equations (2-17) and (2-24) can be combined to derive the vertical virtual distance x_z for a squat building. First, it follows from Equation (2-24) that σ_z is equal to $1.2h_b$ at a downwind distance of $10h_b$ in meters or $0.01h_b$ in kilometers. Thus, x_z for a squat building is obtained from Equation (2-17) as follows:

$$\sigma_z \{0.01h_b\} = 1.2h_b = a(0.01h_b + x_z)^b \quad (2-26)$$

$$x_z = \left(\frac{1.2h_b}{a} \right)^{1/b} - 0.01h_b \quad (2-27)$$

where the stability-dependent constants a and b are given in Table 2-8. Similarly, the vertical virtual distance for tall buildings is given by

$$x_z = \left(\frac{1.2h_w}{a} \right)^{1/b} - 0.01h_w \quad (2-28)$$

(2-35)

For a squat building with a building width to building height ratio h_w/h_b less than or equal to 5, the modified σ_y equation is given by

$$\sigma'_y = \left\{ \begin{array}{l} 0.35h_w(m) + 0.067 [x(m) - 3h_b(m)] ; \quad 3h_b < x(m) < 10h_b(m) \\ \sigma_y \{x(km) + x_y(km)\} ; \quad x(m) \geq 10h_b(m) \end{array} \right\} \quad (2-29)$$

with the lateral virtual distance x_y given by

$$x_y = \left(\frac{0.35h_w + 0.5h_b}{p} \right)^{1/q} - 0.01h_b \quad (2-30)$$

The stability-dependent coefficients p and q are given in Table 2-9.

For building width to building height ratios h_w/h_b greater than 5, the presently available data are insufficient to provide general equations for σ_y . For a building that is much wider than it is tall and a stack located toward the center of the building (i.e., away from either end), only the height scale is considered to be significant. The modified σ_y equation for a squat building is then given by

$$\sigma'_y = \left\{ \begin{array}{l} 0.35h_b(m) + 0.067 [x(m) - 3h_b(m)] ; \quad 3h_b < x(m) < 10h_b(m) \\ \sigma_y \{x(km) + x_y(km)\} ; \quad x(m) \geq 10h_b(m) \end{array} \right\} \quad (2-31)$$

with the lateral virtual distance x_y given by

$$x_y = \left(\frac{0.85h_b}{p} \right)^{1/q} - 0.01h_b \quad (2-32)$$

For h_w/h_b greater than 5 and a stack located laterally within about $2.5 h_b$ of the end of the building, lateral plume spread is affected by the flow around the end of the building. With end effects, the enhancement in the initial lateral spread is assumed not to exceed that given by Equation (2-29) with h_w replaced by $5h_b$. The modified σ_y equation is given by

$$\sigma'_y = \begin{cases} 1.75h_b(m) + 0.067 [x(m) - 3h_b(m)] & ; \quad 3h_b < x(m) < 10h_b(m) \\ \sigma_y \{x(m) + x_y(km)\} & ; \quad x(m) \geq 10h_b(m) \end{cases} \quad (2-33)$$

$$x_y = \left(\frac{2.25h_b}{p} \right)^{1/q} - 0.01h_b \quad (2-34)$$

The upper and lower bounds of the concentrations that can be expected to occur near a building are determined respectively by Equations (2-31) and (2-33). The user must specify whether Equation (2-31) or Equation (2-33) is to be used in the model calculations. In the absence of user instructions, the ISC Model uses Equation (2-31) if the building width to building height ratio h_w/h_b exceeds 5.

Although Equation (2-31) provides the highest concentration estimates for squat buildings with building width to building height ratios

(2-37)

h_w/h_b greater than 5, the equation is applicable only to a stack located near the center of the building when the wind direction is perpendicular to the long side of the building (i.e., when the air flow over the portion of the building containing the source is two dimensional). Thus, Equation (2-33) generally is more appropriate than Equation (2-31). It is believed that Equations (2-31) and (2-33) provide reasonable limits on the extent of the lateral enhancement of dispersion and that these equations are adequate until additional data are available to evaluate the flow near very wide buildings.

The modified σ_y equation for a tall building is given by

$$\sigma_y' = \begin{cases} 0.35h_w(m) + 0.067 [x(m) - 3h_w]; & 3h_w < x(m) < 10h_w \\ \sigma_y \{x(km) + x_y(km)\} & ; \quad x(m) \geq 10h_w \end{cases} \quad (2-35)$$

$$x_y = \left(\frac{0.85h_w}{P} \right)^{1/q} - 0.01h_w \quad (2-36)$$

Because the Pasquill-Gifford σ_y and σ_z curves begin at a downwind distance of 100 meters, the ISC Model programs print a warning message and do not calculate concentrations for any source-receptor combination where the source-receptor separation is less than the maximum of 100 meters or $3h_b$ for a squat building or $3h_w$ for a tall building. It should be noted that, for certain combinations of stability and building height and/or width, the vertical and/or lateral plume dimensions indicated for a point source by the Pasquill-Gifford curves at a downwind distance of ten building heights or widths can exceed the values

given by Equation (2-24) or (2-25) and by Equation (2-29), (2-31) or (2-32). Consequently, the ISC Model programs do not permit the virtual distances x_y and x_z to be less than zero.

It is important to note that the use of a single effective building width h_w for all wind directions is a simplification that is required to enable the ISC Model computer programs to operate within the constraints imposed on the programs without sacrificing other desired ISC Model features. The effective building width h_w affects σ_z for tall buildings ($h_w < h_b$) and σ_y for squat buildings ($h_w \geq h_b$) with plume height to building height ratios less than or equal to 1.2. Tall buildings typically have lengths and widths that are equivalent so that the use of one value of h_w for all wind directions does not significantly affect the accuracy of the calculations. However, the use of one value of h_w for squat buildings with plume height to building height ratios less than or equal to 1.2 affects the accuracy of the calculations near the source if the building length is large in comparison with the building width. For example, if the building height and width are approximately the same and the building length is equal to five building widths, the ISC Model at a downwind distance of $10h_b$ underestimates the centerline concentration or deposition by about 40 percent for winds parallel to the building's long side and overestimates the centerline concentration (or deposition) by about 60 percent for winds normal to the building's long side. Thus, the user should exercise caution in interpreting the results of concentration (or deposition) calculations for receptors located near a squat building if the stack height to building height ratio is less than or equal to 1.2.

The recommended procedure for calculating accurate concentration (or deposition) values for receptors located near squat buildings consists of two phases. First, the appropriate ISC Model program is executed using the effective building width h_w derived from the building length and width. Second, the ISC Model calculations are repeated for

the receptors near the source with highest calculated concentration (or deposition) values using receptor-specific values of h_w . For example, assume that the ISCST program is used with a year of sequential hourly data to calculate maximum 24-hour average concentrations and that the highest calculated concentrations occur at Receptor A on Julian Day 18 and at Receptor B on Julian Day 352. The crosswind building width h_w associated with the wind directions required to transport emissions to Receptors A and B may be obtained from a scale drawing of the building. The ISCST program is then executed for Receptor A only on Day 18 only using the appropriate h_w value for Receptor A. Similarly, the ISCST program is executed for Receptor B only on Day 352 only using the appropriate h_w value for Receptor B.

2.4.1.2 The Vertical Term

a. The Vertical Term for Gases and Small Particulates. In general, the effects on ambient concentrations of gravitational settling and dry deposition can be neglected for gaseous pollutants and small particulates (diameters less than about 20 micrometers). The Vertical Term is then given by

$$\begin{aligned} \{\text{Vertical Term}\} = & \left\{ \exp \left[-\frac{1}{2} \left(\frac{H}{\sigma_z} \right)^2 \right] + \sum_{i=1}^{\infty} \left[\exp \left[-\frac{1}{2} \left(\frac{2iH_m - H}{\sigma_z} \right)^2 \right] \right. \right. \\ & \left. \left. + \exp \left[-\frac{1}{2} \left(\frac{2iH_m + H}{\sigma_z} \right)^2 \right] \right] \right\} \end{aligned} \quad (2-37)$$

where

H = effective stack height = sum of actual stack height h (m) and buoyant rise Δh (m)

H_m = mixing height (m)

The infinite series term in Equation (2-37) accounts for the effects of the restriction on vertical plume growth at the top of the surface mixing layer. As shown by Figure 2-4, the method of image sources is used to account for multiple reflections of the plume from the ground surface and at the top of the surface mixing layer. It should be noted that, if the effective stack height H exceeds the mixing height H_m , the plume is assumed to remain elevated and the ground-level concentration is set equal to zero.

Equation (2-37) assumes that the mixing height in rural and urban areas is known for all stability categories. As explained below, the meteorological preprocessor program uses mixing heights derived from twice-daily mixing heights calculated using the Holzworth (1972) procedures. These mixing heights are believed to be representative, at least on the average, of mixing heights in urban areas under all stabilities and of mixing heights in rural areas during periods of unstable or neutral stability. However, because the Holzworth minimum mixing heights are intended to include the heat island effect for urban areas, their applicability to rural areas during periods of stable meteorological conditions (E or F stability) is questionable. Consequently, the ISC Model in the Rural Mode currently deletes the infinite series term in Equation (2-37) for the E and F stability categories.

The Vertical Term defined by Equation (2-37) changes the form of the vertical concentration distribution from Gaussian to rectangular (uniform concentration within the surface mixing layer) at long downwind

(2-41)

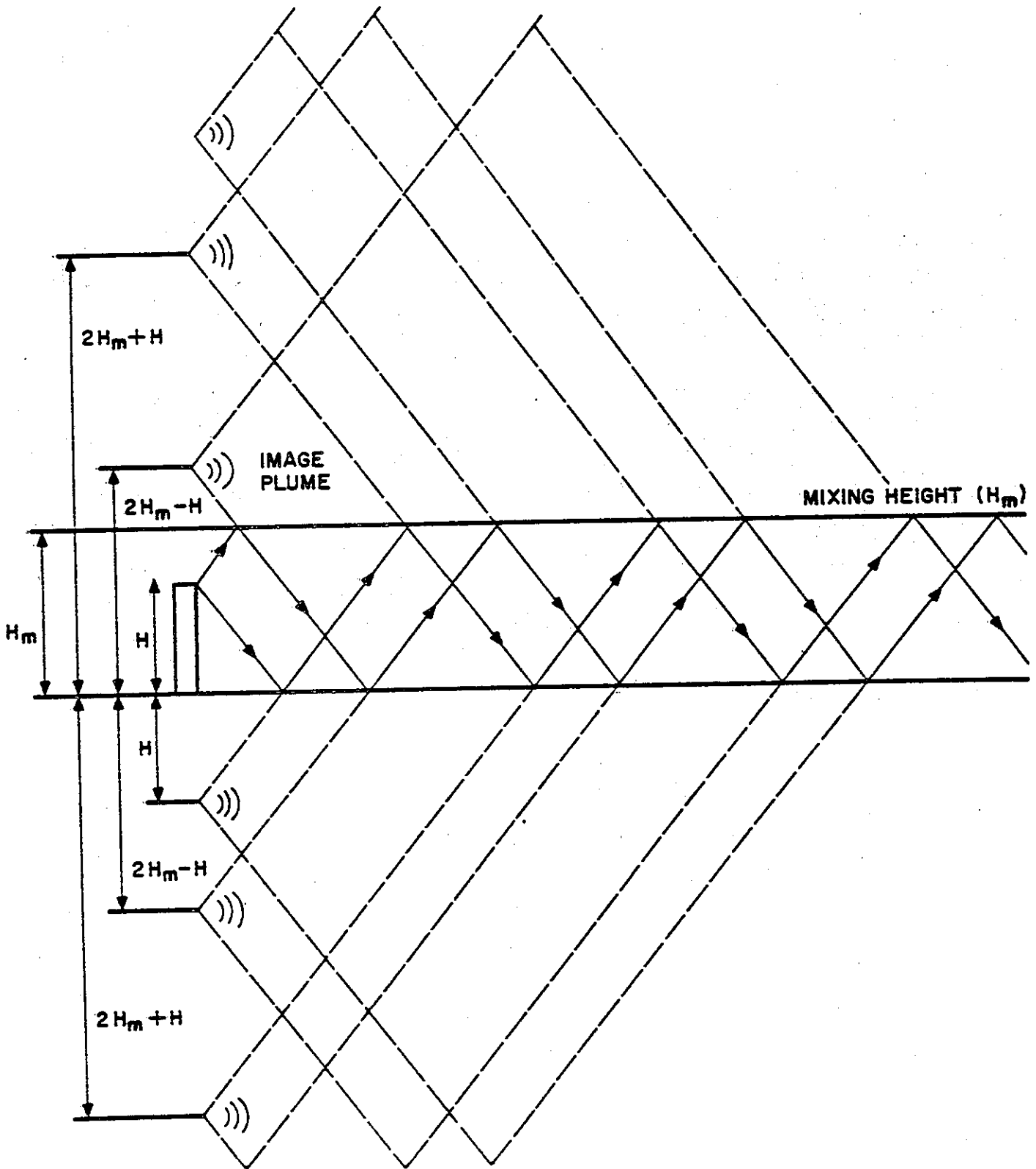


FIGURE 2-4. The method of multiple plume images used to simulate plume reflection in the ISC Model.

(2-42)

distances. Consequently, in order to reduce computational time without a loss of accuracy, Equation (2-12) is changed to the form

$$\chi(x,y) = \frac{KQ}{\sqrt{2\pi} \bar{u}(h) \sigma_y H_m} \exp \left[-\frac{1}{2} \left(\frac{y}{\sigma_y} \right)^2 \right] \{\text{Decay Term}\} \quad (2-38)$$

at downwind distances where the σ_z/H_m ratio is greater than or equal to 1.6.

The meteorological preprocessor program used by the ISC short-term model (see Appendix G) uses an interpolation scheme to assign hourly rural or urban mixing heights on the basis of the early morning and afternoon mixing heights calculated using the Holzworth (1972) procedures. The procedures used to interpolate hourly mixing heights in urban and rural areas are illustrated in Figure 2-5, where

$H_m\{\text{max}\}$ = maximum mixing height on a given day

$H_m\{\text{min}\}$ = minimum mixing height on a given day

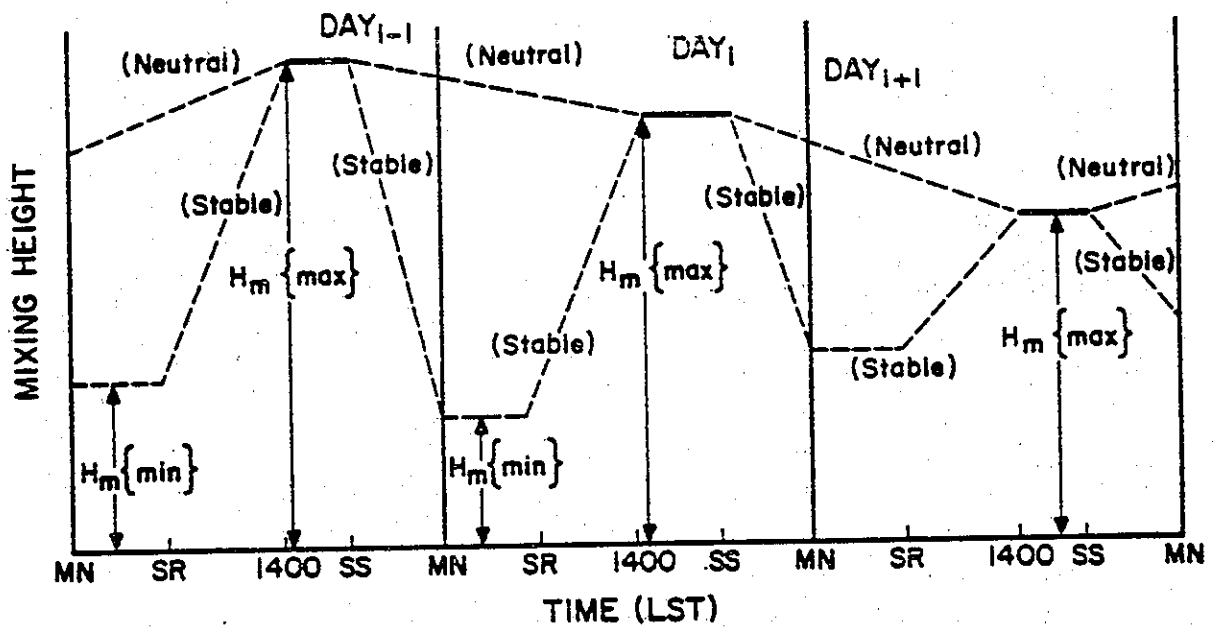
MN = midnight

SR = sunrise

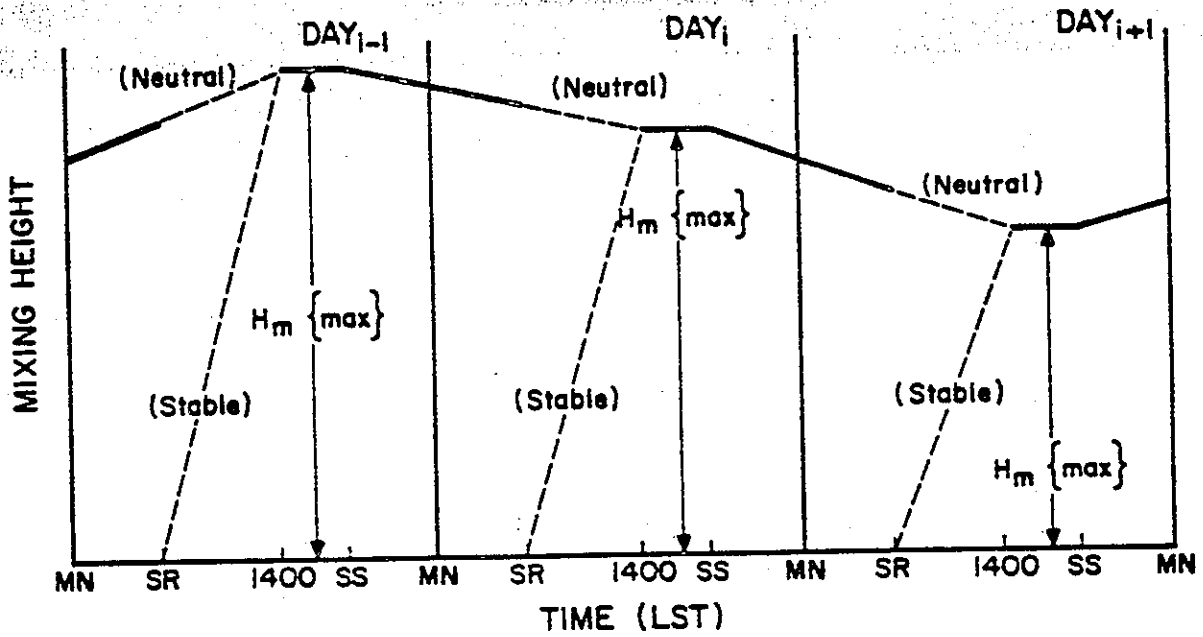
SS = sunset

The interpolation procedures are functions of the stability category for the hour before sunrise. If the hour before sunrise is neutral, the mixing heights that apply are indicated by the dashed lines labeled neutral in Figure 2-5. If the hour before sunset is stable, the mixing heights that apply are indicated by the dashed lines labeled stable. It should be pointed out that there is a discontinuity in the rural mixing

(2-43)



(a) Urban Mixing Heights



(b) Rural Mixing Heights

FIGURE 2-5. Schematic illustration of (a) urban and (b) rural mixing height interpolation procedures.

height at sunrise if the preceding hour is stable. As explained above, because of the uncertainties about the applicability of Holzworth mixing heights to rural areas during periods of E and F stability, the ISC Model in the Rural Mode ignores the interpolated mixing heights for E and F stabilities and effectively sets the mixing height equal to infinity.

b. The Vertical Term in Complex Terrain. The ISC Model makes the following assumption about plume behavior in complex terrain:

- The plume axis remains at the plume stabilization height above mean sea level as it passes over elevated terrain
- The mixing height is terrain following
- The wind speed is a function of height above the surface (see Equation (2-10))

Thus, a modified plume stabilization height H' is substituted for the effective stack height H in the Vertical Term given by Equation (2-37). For example, the effective plume stabilization height at the point (X, Y) is given by

$$H' \{X,Y\} = h + \Delta h + z_s - z \{X,Y\} \quad (2-39)$$

where

z_s = height above mean sea level of the base of the stack

$z \{X,Y\}$ = height above mean sea level of the point (X,Y)

(2-45)

It should be noted that, if the terrain height ($z\{X,Y\} - z_s$) exceeds h for a stack or H for a volume source (See Section 2.4.2), the computer program prints an error message and terminates execution. Also, if the receptor elevation is less than the stack base elevation, the receptor elevation is set equal to the stack base elevation by the computer program. Figure 2-6 illustrates the terrain-adjustment procedures used by the ISC Model.

c. The Vertical Term for Large Particulates. The dispersion of particulates or droplets with significant gravitational settling velocities differs from that of gaseous pollutants and small particulates in that the larger particulates are brought to the surface by the combined processes of atmospheric turbulence and gravitational settling. Additionally, gaseous pollutants and small particulates tend to be reflected from the surface, while larger particulates that come in contact with the surface may be completely or partially retained at the surface. The ISC Model Vertical Term for large particulates includes the effects of both gravitational settling and dry deposition. Gravitational settling is assumed to result in a tilted plume with the plume axis inclined to the horizontal at an angle given by $\arctan(V_s/\bar{u})$ where V_s is the gravitational settling velocity. A user-specified fraction γ of the material that reaches the ground surface by the combined processes of gravitational settling and atmospheric turbulence is assumed to be reflected from the surface. Figure 2-7 illustrates the vertical concentration profiles for complete reflection from the surface (γ equal to unity), 50-percent reflection from the surface (γ equal to 0.5) and complete retention at the surface (γ equal to zero).

For a given particulate source, the user must subdivide the total particulate emissions into N settling-velocity categories (the maximum value of N is 20). The ground-level concentration of particulates with settling velocity V_{sn} is given by Equation (2-12) with the Vertical Term defined as (Dumbauld and Bjorklund, 1975)

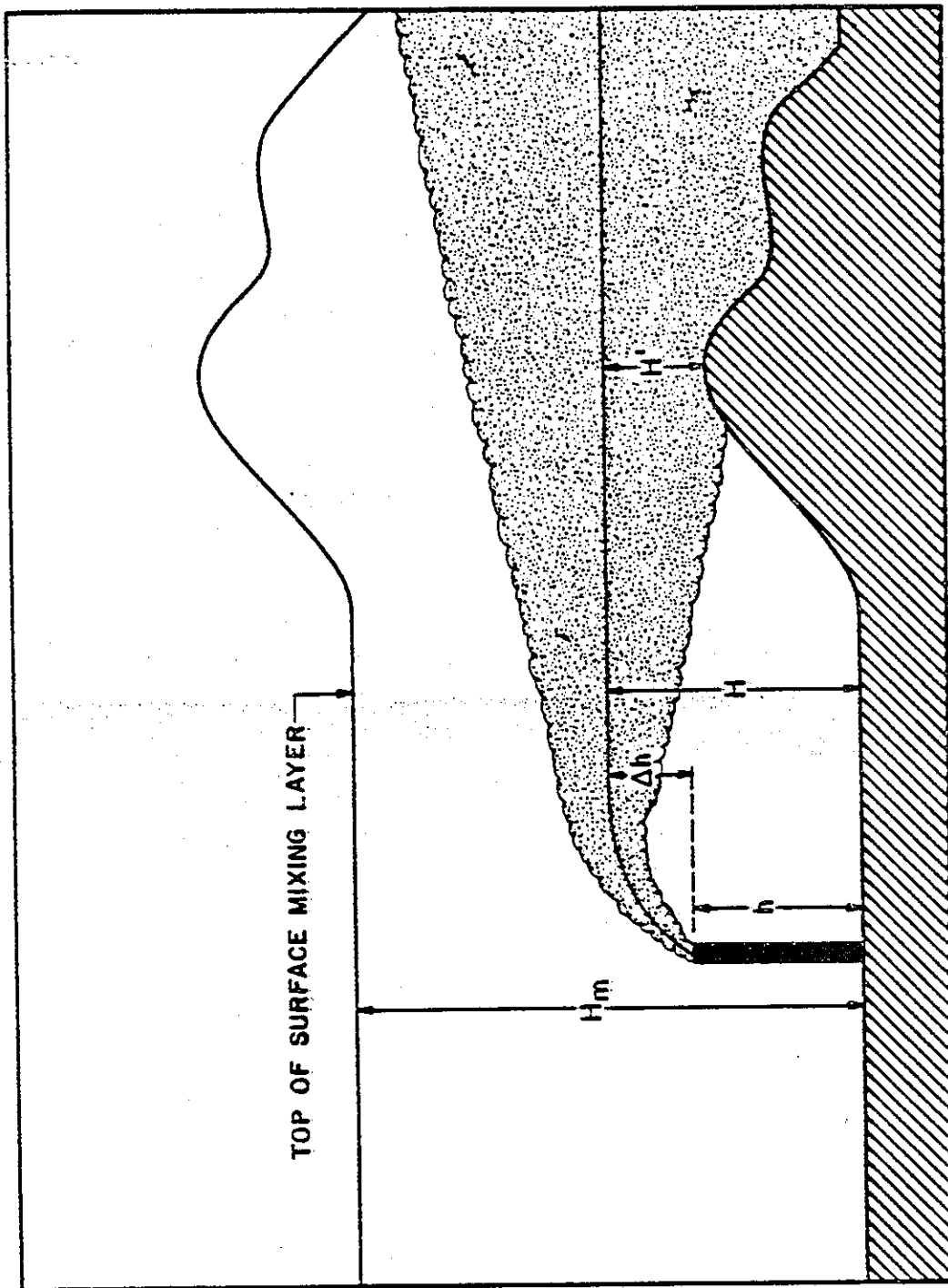


FIGURE 2-6. Illustration of plume behavior in complex terrain assumed by the ISC Model.

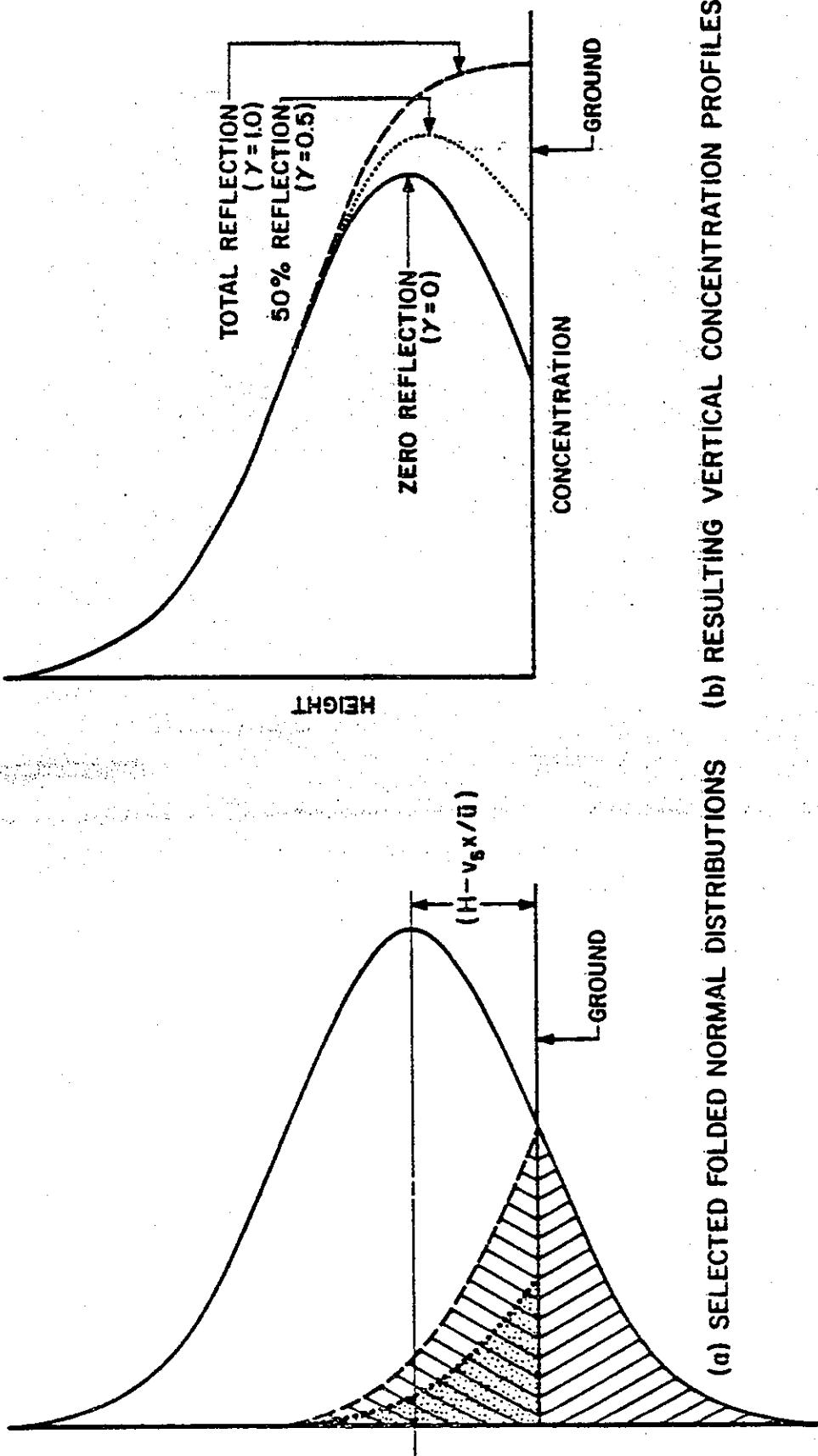


FIGURE 2-7. Illustration of vertical concentration profiles for reflection coefficients of 0, 0.5 and 1.0.

$$\begin{aligned}
\{\text{Vertical Term}\} &= \frac{\phi_n}{2} \left\{ \sum_{i=0}^{\infty} \left[\gamma_n^i \exp \left[-\frac{1}{2} \left(\frac{2iH_m - H + (V_{sn}x/\bar{u}\{h\})}{\sigma_z} \right)^2 \right] \right. \right. \\
&\quad \left. \left. + \gamma_n^{i+1} \exp \left[-\frac{1}{2} \left(\frac{2iH_m + H - (V_{sn}x/\bar{u}\{h\})}{\sigma_z} \right)^2 \right] \right] \right. \\
&\quad \left. + \sum_{i=1}^{\infty} \left[\gamma_n^i \exp \left[-\frac{1}{2} \left(\frac{2iH_m + H - (V_{sn}x/\bar{u}\{h\})}{\sigma_z} \right)^2 \right] \right. \right. \\
&\quad \left. \left. + \gamma_n^{i-1} \exp \left[-\frac{1}{2} \left(\frac{2iH_m - H + (V_{sn}x/\bar{u}\{h\})}{\sigma_z} \right)^2 \right] \right] \right\} \quad (2-40)
\end{aligned}$$

where

- ϕ_n = mass fraction of particulates in the n^{th} settling-velocity category
- γ_n = reflection coefficient for particulates in the n^{th} settling-velocity category (set equal to unity for complete reflection)
- V_{sn} = settling velocity of particulates in the n^{th} settling-velocity category

For convenience, 0^0 is defined to be unity in Equation (2-40). The total concentration is computed by the program by summing over the N settling-velocity categories. The optional algorithm used to calculate dry deposition is discussed in Section 2.4.3.

Use of Equation (2-40) requires a knowledge of both the particulate size distribution and the density of the particulates emitted by each

source. The total particulate emissions for each source are subdivided by the user into a maximum of 20 categories and the gravitational settling velocity is calculated for the mass-mean diameter of each category. The mass-mean diameter is given by

$$\bar{d} = \left[\frac{d_2^3 + d_1^2 d_2 + d_1 d_2^2 + d_1^3}{4} \right]^{1/3} \quad (2-41)$$

where d_1 and d_2 are the lower and upper bounds of the particle-size category. McDonald (1960) gives simple techniques for calculating the gravitational settling velocity for all sizes of particulates. For particulates with a density on the order of 1 gram per cubic centimeter and diameters less than about 80 micrometers, the settling velocity is given by

$$v_s = \frac{2\rho g r^2}{9\mu} \quad (2-42)$$

where

- v_s = settling velocity (cm · sec⁻¹)
- ρ = particle density (gm · cm⁻³)
- g = acceleration due to gravity (980 cm · sec⁻²)
- r = particle radius (cm)
- μ = absolute viscosity of air ($\mu = 1.83 \times 10^{-4}$ gm · cm⁻¹ · sec⁻¹)

It should be noted that the settling velocity calculated using Equation (2-42) must be converted by the user from centimeters per second to meters per second for use in the model calculations.

The reflection coefficient γ_n can be estimated for each particle-size category using Figure 2-8 and the settling velocity calculated for the mass-mean diameter. If it is desired to include the effects of gravitational settling in calculating ambient particulate concentrations while at the same time excluding the effects of deposition, γ_n should be set equal to unity for all settling velocities. On the other hand, if it is desired to calculate maximum possible deposition, γ_n should be set equal to zero for all settling velocities. The effects of dry deposition for gaseous pollutants may be estimated by setting the settling velocity V_{sn} equal to zero and the reflection coefficient γ_n equal to the amount of material assumed to be reflected from the surface. For example, if 20 percent of a gaseous pollutant that reaches the surface is assumed to be retained at the surface by vegetation uptake or other mechanisms, γ_n is equal to 0.8.

The derivation of Equation (2-40) assumes that the terrain is flat or gently rolling. Consequently, the gravitational settling and dry deposition options cannot be used for sources located in complex terrain without violating mass continuity. However, the effects of gravitational settling alone can be estimated for sources located in complex terrain by setting γ_n equal to unity for each settling velocity category. This procedure will tend to overestimate ground-level concentrations, especially at the longer downwind distances, because it neglects the effects of dry deposition.

It should be noted that Equation (2-40) assumes that σ_z is a continuous function of downwind distance. Also, Equation (2-40) does not simplify for σ_z/H_m greater than 1.6 as does Equation (2-37). As shown by Table 2-8, σ_z for the very unstable A stability category attains a maximum value of 5,000 meters at 3.11 kilometers. Because Equation (2-40) requires that σ_z be a continuous function of distance, the coefficients a and b given in Table 2-8 for A stability and the 0.51- to 3.11-kilometer range are used by the ISC Model in calculations beyond 3.11 kilometers. Consequently, this introduces uncertainties in the results of the calculations beyond 3.11 kilometers for A stability.

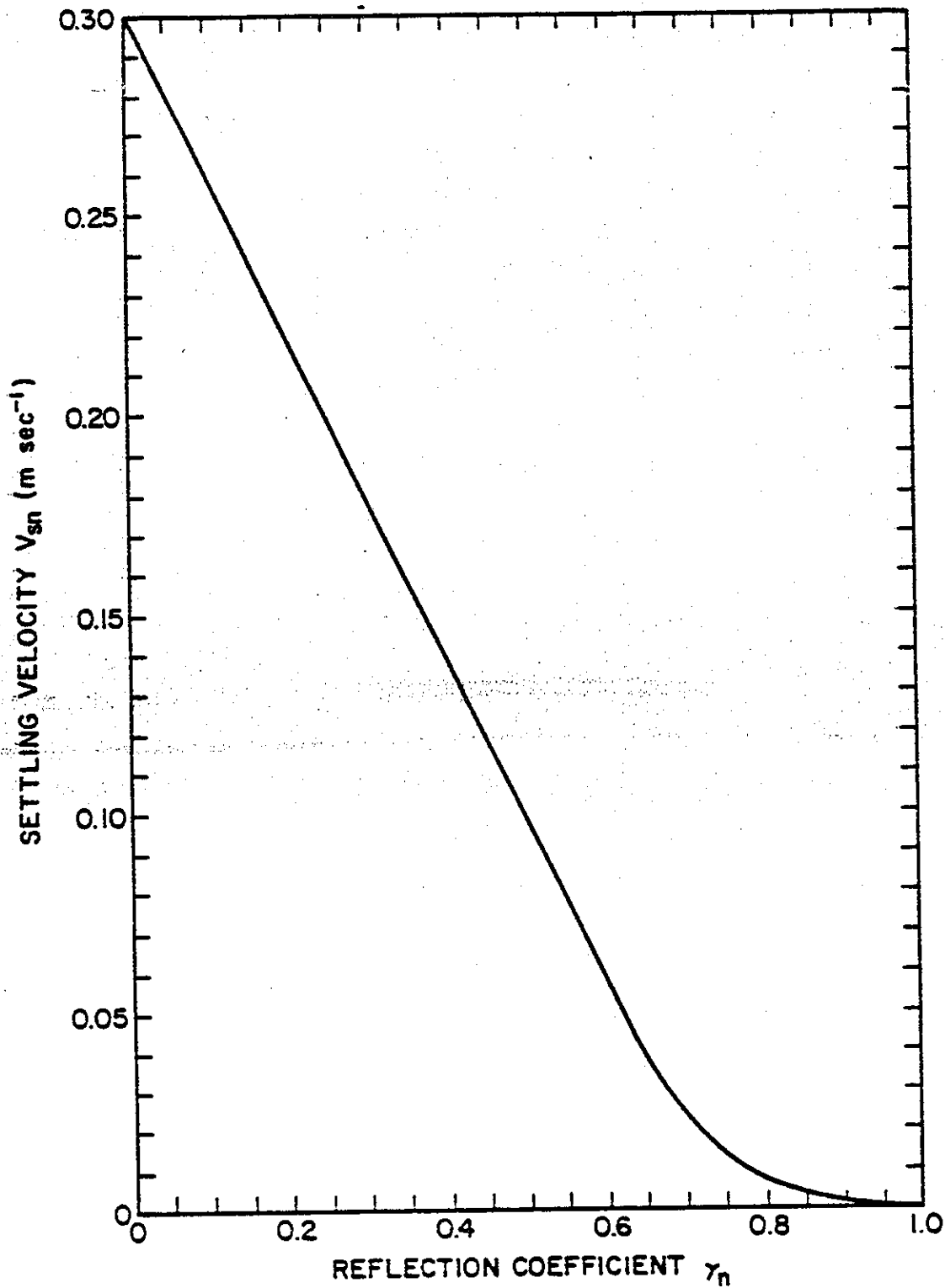


FIGURE 2-8. Relationship between the gravitational settling velocity V_{sn} and the reflection coefficient γ_n suggested by Dumbauld, et al. (1976).

2.4.2 Area, Volume and Line Source Emissions

2.4.2.1 General

The area and volume sources options of the ISC Model are used to simulate the effects of emissions from a wide variety of industrial sources. In general, the ISC area source model is used to simulate the effects of fugitive emissions from sources such as storage piles and slag dumps. The ISC volume source model is used to simulate the effects of emissions from sources such as building roof monitors and line sources (for example, conveyor belts and rail lines).

2.4.2.2 The Short-Term Area Source Model

The ISC area source model is based on the equation for a finite crosswind line source. Individual area sources are required to have the same north-south and east-west dimensions. However, as shown by Figure 2-9, the effects of an area source with an irregular shape can be simulated by dividing the area source into multiple squares that approximate the geometry of the area source. Note that the size of the individual area sources in Figure 2-9 varies; the only requirement is that each area source must be square. The ground-level concentration at downwind distance x (measured from the downwind edge of the area source) and crosswind distance y is given by

$$\chi(x,y) = \frac{KQ_A x_0}{\sqrt{2\pi} \bar{u}(h) \sigma_z} \left\{ \text{Vertical Term} \right\} \left\{ \text{erf} \left(\frac{x_0/2 + y}{\sqrt{2} \sigma_y} \right) \right. \\ \left. + \text{erf} \left(\frac{x_0/2 - y}{\sqrt{2} \sigma_y} \right) \right\} \left\{ \text{Decay Term} \right\} \quad (2-43)$$

(2-53)

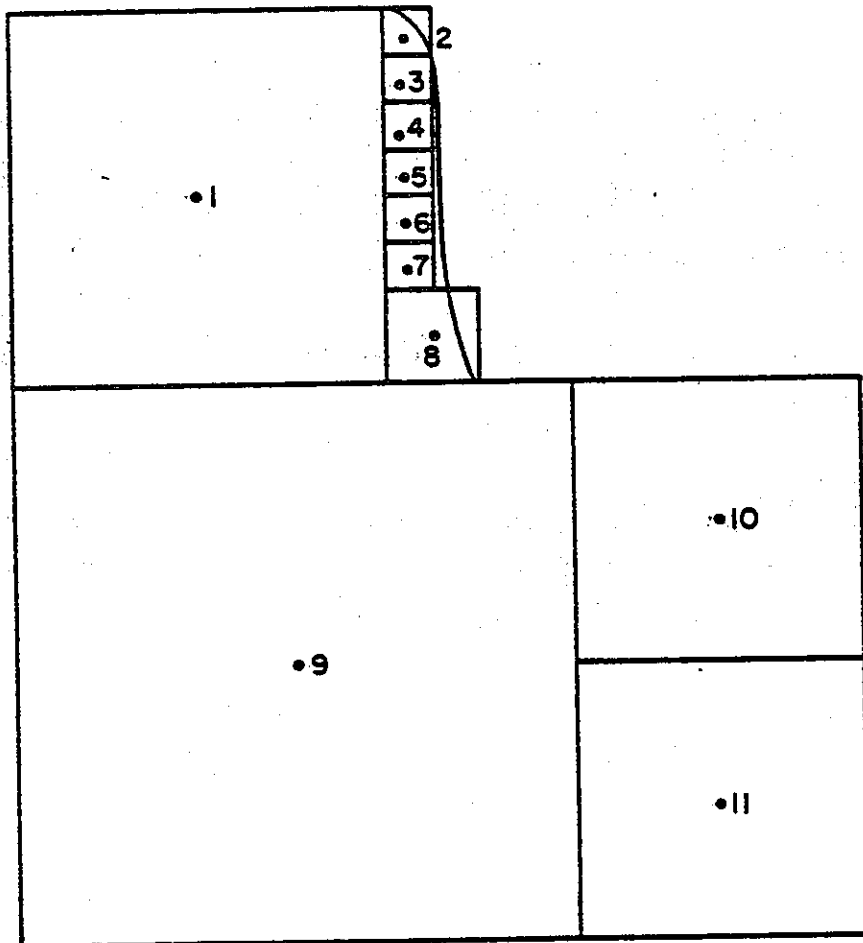


FIGURE 2-9. Representation of an irregularly shaped area source by 11 square area sources.

where

Q_A = area source emission rate (mass per unit area per unit time)

x_0 = length of the side of the area source (m)

x'_0 = effective crosswind width = $2x_0/\sqrt{\pi}$

and the Vertical Term is given by Equation (2-37) or Equation (2-40) with the effective emission height H assigned by the user. In general, H should be set equal to the physical height of the source of fugitive emissions. For example, the emission height H of a slag dump is the physical height of the slag dump. A vertical virtual distance, given by x_0 in kilometers, is added to the actual downwind distance x for the σ_z calculations. If a receptor is located within $x'_0/2$ plus 100 meters of the center of an area source, a warning message is printed and no concentrations are calculated for the source-receptor combination. However, program execution is not terminated.

It is recommended that, if the separation between an area source and a receptor is less than the side of the area source x_0 , the area source be subdivided into smaller area sources. If the source-receptor separation is less than x_0 , the ISC Model tends to overpredict the area source concentration. The degree of overprediction is a function of stability, the orientation of the receptor with respect to the area source and the mean wind direction. However, the degree of overprediction near the area source rarely exceeds about 30 percent.

2.4.2.3 The Short-Term Volume Source Model

Equation (2-12) is also used to calculate ground-level concentrations produced by volume-source emissions. If the volume source is elevated, the user assigns the emission height H . The user also assigns initial lateral (σ_{y0}) and vertical (σ_{z0}) dimensions for the volume source.

Lateral (x_y) and vertical (x_z) virtual distances are added to the actual downwind distance x for the σ_y and σ_z calculations. The lateral virtual distance in kilometers is given by Equation (2-22). Similarly, the vertical virtual distance in kilometers is given by Equation (2-23).

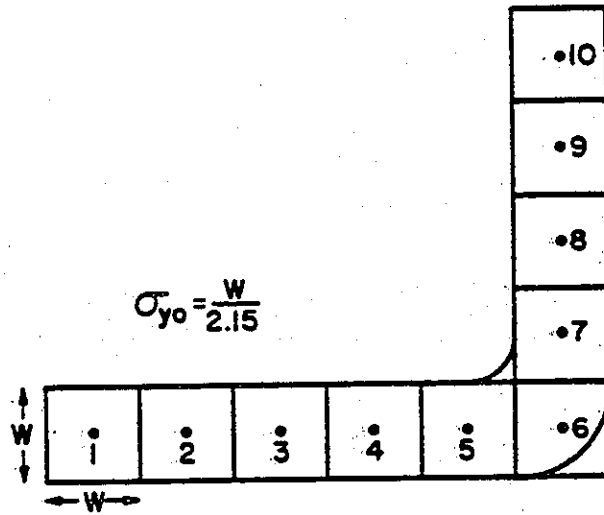
The volume source model is used to simulate the effects of emissions from sources such as building roof monitors and line sources (for example, conveyor belts and rail lines). As with the area source model, the north-south and east-west dimensions of each volume source used in the model must be the same. Table 2-10 summarizes the general procedures suggested for estimating initial lateral (σ_{y0}) and vertical (σ_{z0}) dimensions for single volume sources and for multiple volume sources used to represent a line source. In the case of a long and narrow line source such as a rail line, it may not be practical to divide the source into N volume sources, where N is given by the length of the line source divided by its width. The user can obtain an approximate representation of the line source by placing a smaller number of volume sources at equal intervals along the line source. In general, the spacing between individual volume sources should not be greater than twice the width of the line source. However, a larger spacing can be used if the ratio of the minimum source-receptor separation and the spacing between individual volume sources is greater than about 3. In these cases, concentrations at the nearest receptors may be underestimated by 10 to 15 percent. At longer downwind distances, concentrations calculated using fewer than N volume sources to represent the line source converge to the concentrations calculated using N volume sources to represent the line source as long as sufficient volume sources are used to preserve the horizontal geometry of the line source.

Figure 2-10 illustrates representations of a curved line source by multiple volume sources. Emissions from a line source or narrow volume source represented by multiple volume sources are divided equally

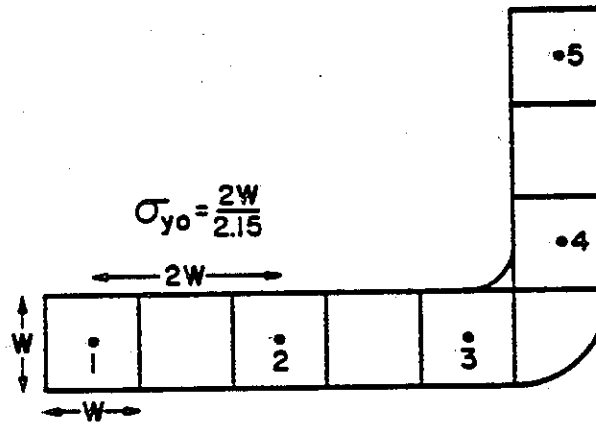
TABLE 2-10

SUMMARY OF SUGGESTED PROCEDURES FOR ESTIMATING
 INITIAL LATERAL DIMENSIONS (σ_{y0}) AND INITIAL
 VERTICAL DIMENSIONS (σ_{z0}) FOR VOLUME
 AND LINE SOURCES

Type of Source	Procedure for Obtaining Initial Dimension
(a) Initial Lateral Dimensions (σ_{y0})	
Single Volume Source	σ_{y0} = length of side divided by 4.3
Line Source Represented by Adjacent Volume Sources (see Figure 2-10(a))	σ_{y0} = length of side divided by 2.15
Line Source Represented by Separated Volume Sources (see Figure 2-10(b))	σ_{y0} = center to center distance divided by 2.15
(b) Initial Vertical Dimensions (σ_{z0})	
Surface-Based Source ($H=0$)	σ_{z0} = vertical dimension of source divided by 2.15
Elevated Source ($H>0$) on or Adjacent to a Building	σ_{z0} = building height divided by 2.15
Elevated Source ($H>0$) not on or Adjacent to a Building	σ_{z0} = vertical dimension of source divided by 4.3



(a) EXACT REPRESENTATION



(b) APPROXIMATE REPRESENTATION

FIGURE 2-10. Exact and approximate representations of a line source by multiple volume sources.

among the individual sources unless there is a known spatial variation in emissions. Setting the initial lateral dimension σ_{y0} equal to $W/2.15$ in Figure 2-10(a) or $2W/2.15$ in Figure 2-10(b) results in overlapping Gaussian distributions for the individual sources. If the wind direction is normal to a straight line source that is represented by multiple volume sources, the initial crosswind concentration distribution is uniform except at the edges of the line source. The doubling of σ_{y0} by the user in the approximate line-source representation in Figure 2-10(b) is offset by the fact that the emission rates for the individual volume sources are also doubled by the user.

There are two types of volume sources: surface-based sources, which may also be modeled as area sources, and elevated sources. An example of a surface-based source is a surface rail line. The effective emission height H for a surface-based source is usually set equal to zero. An example of an elevated source is an elevated rail line with an effective emission height H set equal to the height of the rail line.

2.4.3 The ISC Short-Term Dry Deposition Model

2.4.3.1 General

The Industrial Source Complex short-term dry deposition model is based on the Dumbauld, et al. (1976) deposition model. The Dumbauld, et al. model, which is an advanced version of the Cramer, et al. (1972) deposition model, assumes that a user-specified fraction γ_n of the material that comes into contact with the ground surface by the combined processes of atmospheric turbulence and gravitational settling is reflected from the surface (see Section 2.4.1.2.c). The reflection coefficient γ_n , which is a function of settling velocity and the ground surface for particulates and of the ground surface for gaseous pollutants, is analogous in purpose to the deposition velocity used in other deposition models. The Cramer, et al. (1972) deposition model has closely matched ground-level deposition

patterns for droplets with diameters above about 30 micrometers, while the more generalized Dumbauld, et al. (1976) deposition model has closely matched observed deposition patterns for both large and small droplets.

Section 2.4.1.2.c discusses the selection of the reflection coefficient γ_n as well as the computation of the gravitational settling velocity V_{sn} . The ISC dry deposition model should not be applied to sources located in complex terrain. Also, as noted in Section 2.4.1.2.c, uncertainties in the deposition calculations are likely for the A stability category if deposition calculations are made at downwind distances greater than 3.11 kilometers. Deposition and ambient concentration calculations cannot be made in a single program execution. In an individual computer run, the ISC Model calculates either concentration (including the effects of gravitational settling and dry deposition) or dry deposition.

2.4.3.2 Stack and Volume Source Emissions

Deposition for particulates in the n^{th} settling-velocity category or a gaseous pollutant with zero settling velocity V_{sn} and a reflection coefficient γ_n is given by

$$\begin{aligned}
 \text{DEP}_n\{x,y\} = & \frac{KQ_T (1 - \gamma_n)\phi_n}{2\pi \sigma_y \sigma_z x} \exp \left[-\frac{1}{2} \left(\frac{y}{\sigma_y} \right)^2 \right] \exp \left[-\psi x/\bar{u}\{h\} \right] \\
 & \left\{ \left[\bar{b}H + (1 - \bar{b}) V_{sn} x/\bar{u}\{h\} \right] \exp \left[-\frac{1}{2} \left(\frac{H - V_{sn} x/\bar{u}\{h\}}{\sigma_z} \right)^2 \right] \right. \\
 & \left. + \sum_{i=1}^{\infty} \left[\gamma^{i-1} \left[\bar{b} (2iH_m - H) - (1 - \bar{b}) V_{sn} x/\bar{u}\{h\} \right] \right] \right\} \quad (2-44)
 \end{aligned}$$

(Equation (2-44) continued on following page)

(Equation (2-44) continued)

$$\begin{aligned} & \exp \left[-\frac{1}{2} \left(\frac{2iH_m - H + v_{sn} x / \bar{u}\{h\}}{\sigma_z} \right)^2 \right] \\ & + \gamma^i \left[\bar{b} (2iH_m + H) + (1 - \bar{b}) v_{sn} x / \bar{u}\{h\} \right] \\ & \exp \left[-\frac{1}{2} \left(\frac{2iH_m + H - v_{sn} x / \bar{u}\{h\}}{\sigma_z} \right)^2 \right] \end{aligned} \quad (2-44)$$

The parameter Q_τ is the total amount of material emitted during the time period τ for which the deposition calculation is made. For example, Q_τ is the total amount of material emitted during a 1-hour period if an hourly deposition is calculated. For time periods longer than an hour, the program sums the deposition calculated for each hour to obtain the total deposition. For convenience, Q^0 is defined to be unity in Equation (2-44). The coefficient \bar{b} is the average value of the exponent b for the interval between the source and the downwind distance x (see Table 2-8). In the case of a volume source, the user must specify the effective emission height H and the initial source dimensions σ_{y0} and σ_{z0} .

2.4.3.3. Area Source Emissions

For area source emissions, the first line of Equation (2-44) is changed to the form

(2-61)

$$\begin{aligned}
 \text{DEP}_n \{x,y\} = & \frac{KQ_{AT} x_o (1 - \gamma_n) \phi_n}{\sqrt{2\pi} \sigma_z x} \left\{ \text{erf} \left(\frac{x_o'/2 + y}{\sqrt{2} \sigma_y} \right) \right. \\
 & \left. + \text{erf} \left(\frac{x_o'/2 - y}{\sqrt{2} \sigma_y} \right) \right\} \exp \left[-\psi x/\bar{u}\{h\} \right]
 \end{aligned}
 \tag{2-45}$$

The parameter Q_{AT} is the total mass per unit area emitted over the time period τ for which deposition is calculated.

2.5 THE ISC LONG-TERM DISPERSION MODEL EQUATIONS

2.5.1 Stack Emissions

The ISC long-term concentration model makes the same basic assumptions as the short-term model. In the long-term model, the area surrounding a continuous source of pollutants is divided into sectors of equal angular width corresponding to the sectors of the seasonal and annual frequency distributions of wind direction (see Figure 2-1). Seasonal or annual emissions from the source are partitioned among the sectors according to the frequencies of wind blowing toward the sectors. The ground-level concentration fields calculated for each source are translated to a common coordinate system (either polar or Cartesian as specified by the user) and summed to obtain the total due to all sources.

For a single stack, the mean seasonal concentration at a point ($r > 100$ m, θ) with respect to the stack is given by

$$X_2(r, \theta) = \frac{2K}{\sqrt{2\pi} r \Delta\theta'} \sum_{i,j,k} \left[\frac{Q_{i,k,l} f_{i,j,k,l}}{\bar{u}_{i,k}(h) \sigma_{z;k}} s(\theta) V_{i,k,l} \right] \exp \left[-\psi r / \bar{u}_{i,k}(h) \right] \quad (2-45)$$

where

$Q_{i,k,l}$ = pollutant emission rate (mass per unit time), for the i^{th} wind-speed category, k^{th} stability category and l^{th} season

$f_{i,j,k,l}$ = frequency of occurrence of the i^{th} wind-speed category, j^{th} wind-direction category and k^{th} stability category for the l^{th} season

$\Delta\theta'$ = the sector width in radians

$s(\theta)$ = a smoothing function similar to that of the AQDM (see Section 2.5.1.3)

$\bar{u}_{i,k}(h)$ = mean wind speed (m/sec) at stack height h for the i^{th} wind-speed category and k^{th} stability category

$\sigma_{z;k}$ = standard deviation of the vertical concentration distribution (m) for the k^{th} stability category

$V_{i,k,l}$ = the Vertical Term for the i^{th} wind-speed category, k^{th} stability category and l^{th} season

ψ = the decay coefficient (sec^{-1})

The mean annual concentration at the point (r, θ) is calculated from the seasonal concentrations using the expression

(2-63)

$$\chi_a\{r,\theta\} = \frac{1}{4} \sum_{\ell=1}^4 \chi_{\ell}\{r,\theta\} \quad (2-47)$$

The terms in Equation (2-46) correspond to the terms discussed in Section 2.4.1 for the short-term model except that the *i* subscript refers to wind-speed categories, the *j* subscript refers to wind-direction categories, the *k* subscript refers to stability categories, and the *l* subscript refers to the season. The various terms are briefly discussed in the following subsections. In addition to stack emissions, the ISC long-term concentration model considers emissions from area and volume sources. These model options are discussed in Section 2.5.2. The optional algorithms for calculating dry deposition are discussed in Section 2.5.3.

2.5.1.1 The Dispersion Coefficients

a. Point Source Dispersion Coefficients. See Section 2.4.1.1.a for a discussion of the procedures used to calculate the standard deviation of the vertical concentration distribution σ_z for point sources (sources without initial dimensions).

b. Downwind and Crosswind Distances. See the discussion given in Section 2.4.1.1.b.

c. Vertical Virtual Distances. See Section 2.4.1.1.c for a discussion of the procedures used to calculate vertical virtual distances. The lateral virtual distance is given by

$$x_y = r_o \cot (\Delta\theta'/2) \quad (2-48)$$

where r_o is the effective source radius. For volume sources (see Section 2.5.2), the program sets r_o equal to $2.15 \sigma_{y0}$, where σ_{y0} is

the initial lateral dimension. For area sources (see Section 2.5.2), the program sets r_0 equal to $x_0/\sqrt{\pi}$ where x_0 is the side of the area source. For plumes affected by building wakes (see Section 2.4.1.1.d), the program sets r_0 equal to $2.15 \sigma'_y$ where σ'_y is given for squat buildings by Equation (2-29), (2-31) or (2-33) for downwind distances between 3 and 10 building heights and for tall buildings by Equation (2-35) for downwind distances between 3 and 10 building widths. At downwind distances greater than 10 building heights for Equation (2-29), (2-31) or (2-33), σ'_y is held constant at the value of σ'_y calculated at a downwind distance of 10 building heights. Similarly, at downwind distances greater than 10 building widths for Equation (2-35), σ'_y is held constant at the value of σ'_y calculated at a downwind distance of 10 building widths.

d. Procedures Used to Account for the Effects of Building Wakes on Effluent Dispersion. With the exception of the equations used to calculate the lateral virtual distance, the procedures used to account for the effects of building wake effects on effluent dispersion are the same as those outlined in Section 2.4.1.1.d for the short-term model. The calculation of lateral virtual distances by the long-term model is discussed in Section 2.5.1.1.c above.

2.5.1.2 The Vertical Term

a. The Vertical Term for Gases and Small Particulates. The Vertical Term for gases and small particulates is given by

$$V_{i,k,l} = \exp \left[-\frac{1}{2} \left(\frac{R_{i,k,l}}{\sigma_{z;k}} \right)^2 \right] \quad (2-49)$$

(Equation (2-49) continued on following page.)

(2-65)

(Equation 2-48) continued.)

$$\begin{aligned}
 & + \sum_{n=1}^{\infty} \left\{ \exp \left[-\frac{1}{2} \left(\frac{2nH_{m;i,k,l} - H_{i,k,l}}{\sigma_{z;k}} \right)^2 \right] \right. \\
 & \left. + \exp \left[-\frac{1}{2} \left(\frac{2nH_{m;i,k,l} + H_{i,k,l}}{\sigma_{z;k}} \right)^2 \right] \right\}
 \end{aligned} \tag{2-49}$$

Except for the use of subscripts to indicate wind-speed and stability categories and season, the parameters in Equation (2-49) correspond to those discussed in Section 2.4.1.2. As shown by Equation (2-49), the user may assign a separate mixing height H_m to each combination of wind-speed and stability categories for each season.

As with the short-term model, the Vertical Term given by Equation (2-48) is changed to the form

$$V_{i,k,l} = \frac{\sqrt{2\pi} \sigma_{z;k}}{2H_{m;i,k,l}} \tag{2-50}$$

at downwind distances where the $\sigma_{z;k}/H_{m;i,k,l}$ ratio is greater than or equal to 1.6. Additionally, the ground-level concentration is set equal to zero if the effective stack height H exceeds the mixing height H_m . As explained in Section 2.2.1.2, ISCLT in the Rural Mode currently sets the mixing height equal to infinity for the E and F stability categories.

b. The Vertical Term in Complex Terrain. See Section 2.4.1.2.b.

c. The Vertical Term for Large Particulates. Section 2.4.1.2.c discusses the differences in the dispersion of large particulates and the dispersion of gases and small particulates. The Vertical Term for large particulates is given by

$$\begin{aligned}
V_{i,k,l} = & \frac{\phi_n}{2} \left\{ \sum_{a=0}^{\infty} \left[\gamma_n^a \exp \left[-\frac{1}{2} \left(\frac{2aH_{m;i,k,l} - H_{i,k,l} + V_{sn} r / \bar{u}(h)}{\sigma_{z;k}} \right)^2 \right] \right. \right. \\
& + \gamma_n^{a+1} \exp \left[-\frac{1}{2} \left(\frac{2aH_{m;i,k,l} + H_{i,k,l} - V_{sn} r / \bar{u}_{i,k}(h)}{\sigma_{z;k}} \right)^2 \right] \left. \right] \\
& + \sum_{a=1}^{\infty} \left[\gamma_n^a \exp \left[-\frac{1}{2} \left(\frac{2aH_{m;i,k,l} + H_{i,k,l} - V_{sn} r / \bar{u}_{i,k}(h)}{\sigma_{z;k}} \right)^2 \right] \right. \\
& \left. \left. + \gamma_n^{a-1} \exp \left[-\frac{1}{2} \left(\frac{2aH_{m;i,k,l} - H_{i,k,l} + V_{sn} r / \bar{u}_{i,k}(h)}{\sigma_{z;k}} \right)^2 \right] \right] \right\}
\end{aligned} \tag{2-51}$$

where ϕ_n is the mass fraction of particulates with settling velocity V_{sn} , γ_n is the surface reflection coefficient and 0^0 is defined as unity. See Section 2.4.1.2.c for a discussion of the parameters in Equation (2-51) and guidance on the use of this model option.

2.5.1.3 The Smoothing Function

As shown by Equation (2-46), the rectangular concentration distribution within a given angular sector is modified by the function $S\{\theta\}$ which smoothes discontinuities in the concentration at the boundaries of adjacent sectors. The centerline concentration in each sector is unaffected by contributions from adjacent sectors. At points off the sector centerline, the concentration is a weighted function of the concentration at the centerline and the concentration at the centerline of the nearest adjoining sector. The smoothing function is given by

$$s\{\theta\} = \left\{ \begin{array}{ll} \frac{\Delta\theta' - |\theta'_j - \theta'|}{\Delta\theta'} ; & |\theta'_j - \theta'| \leq \Delta\theta' \\ 0 & ; |\theta'_j - \theta'| > \Delta\theta' \end{array} \right\} \quad (2-52)$$

where

θ'_j = the angle measured in radians from north to the centerline of the j^{th} wind-direction sector

θ' = the angle measured in radians from north to the point (r, θ)

2.5.2 Area, Volume and Line Source Emissions

2.5.2.1 General

As explained in Section 2.4.2.1, the ISC Model area and volume sources are used to simulate the effects of emissions from a wide variety of industrial sources. Section 2.4.2.2 provides guidance on the use of the area source model and Section 2.4.2.3 provides guidance on the use of the volume source model. The volume source model is also used to simulate line sources. The following subsections give the area and volume source equations used by the long-term model.

2.5.2.2 The Long-Term Area Source Model

The seasonal average ground-level concentration at the point (r, θ) with respect to the center of an area source is given by the expression

$$X_{g\{r' > r_0, \theta\}} = \frac{2K x_0^2}{\sqrt{2\pi} R \Delta\theta'} \left\{ \sum_{i,j,k} \left[\frac{Q_{A;i,k,l}^f}{\bar{u}_{i,k} \sigma_{z;k}} s\{\theta\} v_{i,k,l} \right] \right\} \quad (2-53)$$

(Equation (2-53) continued on following page.)

(Equation (2-53) continued.)

$$\exp \left[-\psi (r' - r_0) / \bar{u}_{i,k}(h) \right] \quad (2-53)$$

where

- R = radial distance from the lateral virtual point source to the receptor
- $$= \left((r' + x_y)^2 + y^2 \right)^{1/2}$$
- r' = distance from source center to receptor, measured along the plume axis
- r₀ = effective source radius = x₀/√π
- y = lateral distance from the cloud axis to the receptor
- x_y = lateral virtual distance (see Equation (2-48))

The Vertical Term $V_{i,k,l}$ for gaseous pollutants and small particulates is given by Equation (2-49) or Equation (2-50) with the emission height H defined by the user. If the user selects the gravitational settling and dry deposition option, the Vertical Term is given by Equation (2-51).

2.5.2.3 The Long-Term Volume Source Model

Equation (2-46) is also used to calculate seasonal average ground-level concentrations for volume sources. The user must assign initial lateral (σ_{y0}) and vertical (σ_{z0}) dimensions and the effective emission height H. A discussion of the application of the volume source model is given in Section 2.4.2.3.

2.5.3 The ISC Long-Term Dry Deposition Model

2.5.3.1 General

The concepts upon which the ISC long-term dry deposition model are based are discussed in Sections 2.4.1.2.c and 2.4.3.1.

2.5.3.2 Stack and Volume Source Emissions

The seasonal deposition at the point (r, θ) with respect to the base of a stack or the center of a volume source for particulates in the n^{th} settling-velocity category or a gaseous pollutant with zero settling velocity V_{sn} and a reflection coefficient γ_n is given by

$$\begin{aligned}
 \text{DEP}_{\ell, n}(r, \theta) &= \frac{K (1 - \gamma_n) \phi_n}{\sqrt{2\pi} r^2 \Delta\theta'} \sum_{i, j, k} \left[\frac{Q_{r; i, k, \ell} f_{i, j, k, \ell}}{\sigma_{z; k}} \right. \\
 &\quad \exp \left[-\psi r / \bar{u}_{i, k} \{h\} \right] s\{\theta\} \\
 &\quad \left. \left\{ \bar{b}_k H_{i, k, \ell} + (1 - \bar{b}_k) V_{sn} r / \bar{u}_{i, k} \{h\} \right\} \right. \\
 &\quad \left. \exp \left[-\frac{1}{2} \left(\frac{H_{i, k, \ell} - V_{sn} r / \bar{u}_{i, k} \{h\}}{\sigma_{z; k}} \right)^2 \right] \right. \\
 &\quad \left. + \sum_{a=1}^{\infty} \left[\gamma^{a-1} \left[\bar{b}_k (2aH_{m; i, k, \ell} - H_{i, k, \ell}) \right] \right] \right.
 \end{aligned} \tag{2-54}$$

(Equation (2-54) continued on following page.)

(Equation (2-54) continued.)

$$\begin{aligned}
 & - (1 - \bar{b}_k) v_{sn} r / \bar{u}_{i,k} \{h\}] \\
 & \exp \left[-\frac{1}{2} \left(\frac{2aH_{m;i,k,l} - H_{i,k,l} + v_{sn} r / \bar{u}_{i,k} \{h\}}{\sigma_{z;k}} \right)^2 \right] \\
 & + \gamma^a \left[\bar{b}_k (2aH_{m;i,k,l} + H_{i,k,l}) + (1 - \bar{b}_k) v_{sn} r / \bar{u}_{i,k} \{h\} \right] \\
 & \exp \left[-\frac{1}{2} \left(\frac{2aH_{m;i,k,l} + H_{i,k,l} - v_{sn} r / \bar{u}_{i,k} \{h\}}{\sigma_{z;k}} \right)^2 \right] \Bigg] \Bigg\}
 \end{aligned} \tag{2-54}$$

where $Q_{T;i,k,l}$ is the product of the total time during the l^{th} season and the seasonal emission rate $Q_{i,k,l}$ for the i^{th} wind-speed category and k^{th} stability category. For example, if the emission rate is in grams per second and there are 92 days in the summer season (June, July and August), $Q_{T;i,k,l=3}$ is given by $7.95 \times 10^6 Q_{i,k,l=3}$. It should be noted that the user need not vary the emission rate by season or by wind speed and stability. If an annual average emission rate is assumed, Q_T is equal to $3.15 \times 10^7 Q$ for a 365-day year. For convenience, Q^0 is defined as unity in Equation (2-54). For a plume comprised of N settling velocity categories, the total seasonal deposition is obtained by summing Equation (2-54) over the N settling-velocity categories. The program also sums the seasonal deposition values to obtain the annual deposition.

2.5.3.3 Area Source Emissions

With slight modifications, Equation (2-54) is applied to area source emissions. The user assigns the effective emission height H and

(2-71)

the first line of Equation (2-54) is changed to

$$\text{DEP}_{\ell,n}^Q(r,\theta) = \frac{K (1 - \gamma_n) \phi_n x_o^2}{\sqrt{2\pi} R^2 \Delta\theta} \sum_{i,j,k} \left[\frac{Q_{AT;i,k,\ell}^f \sigma_{z;k}}{\sigma_{z;k}} \exp \left[-\psi r/u_{i,k}\{h\} \right] s(\theta) \dots \right] \quad (2-55)$$

where

$Q_{AT;i,k,\ell}^Q$ = the product of the total time during the ℓ^{th} season and the emission rate per unit area for the i^{th} wind-speed category and k^{th} stability category

2.6 EXAMPLE PROBLEM

2.6.1 Description of a Hypothetical Potash Processing Plant

Figure 2-11(a) shows the plant layout and Figure 2-11(b) shows a side view of a hypothetical potash processing plant. Sylvinite ore is brought to the surface from an underground mine by a hoist and dumped on the ore storage pile. The ore then travels along an inclined conveyor belt to the ore processing building where the ore is crushed and screened. Fugitive particulate emissions resulting from the crushing and screening processes are discharged horizontally at ambient temperature from a roof monitor extending the length of the ore processing building. The ore is then refined by froth flotation and sent to the dryers. Particulate emissions produced by the drying process are discharged from a 50-meter stack, located adjacent to the ore processing building, which has a height of 25 meters.

2.6.2 Example ISCST Problem

Table 2-11 gives the emissions data for the hypothetical potash processing plant shown in Figure 2-11. The sylvinite mine and hoist are assumed to operate during the period 0800 to 1600 LST. Fugitive emissions

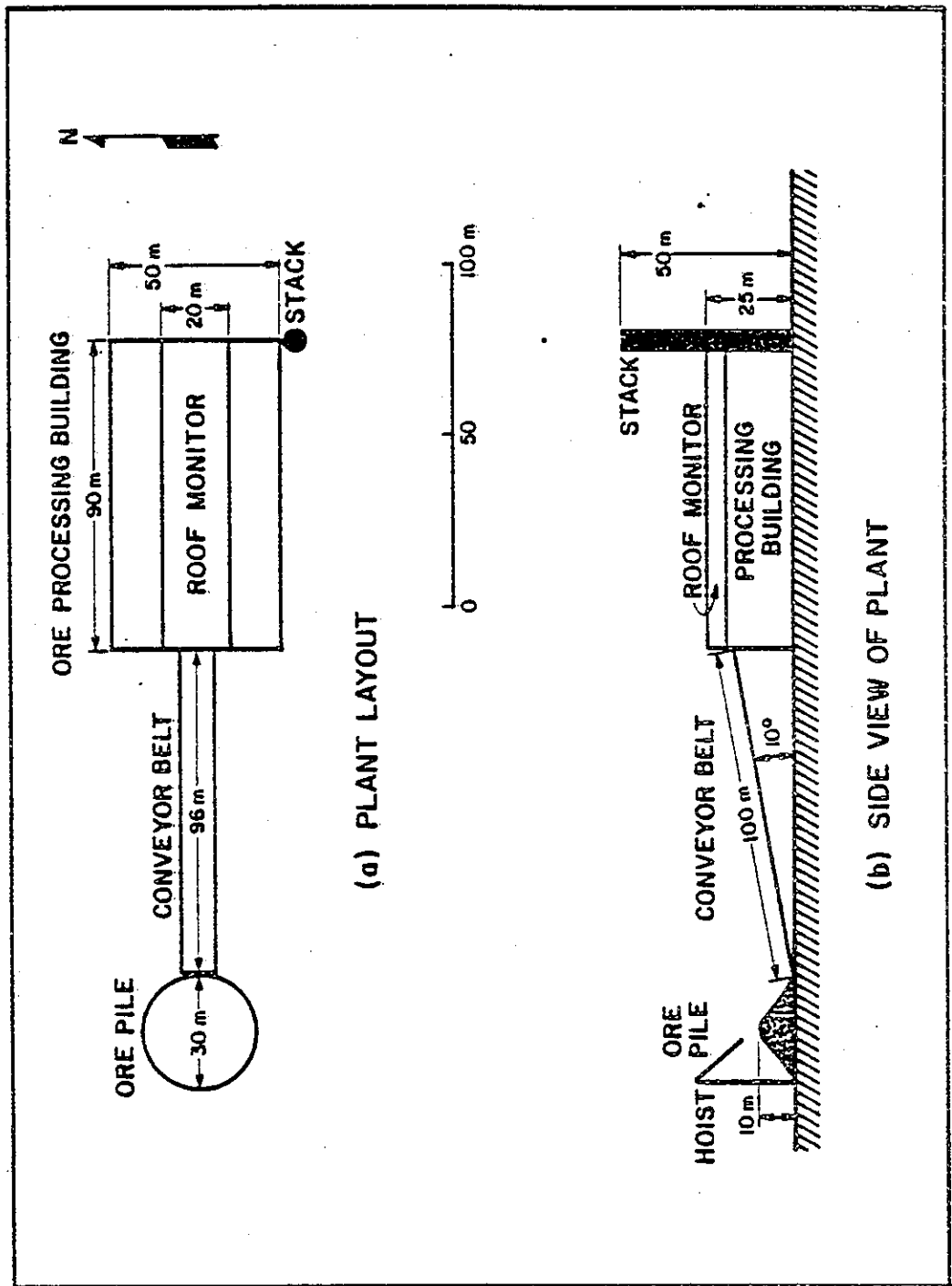


FIGURE 2-11. Plant layout and side view of a hypothetical potash processing plant.

TABLE 2-11

EMISSIONS DATA FOR A HYPOTHETICAL
POTASH PROCESSING PLANT

Source	Source			
	Ore Pile	Conveyor Belt	Roof Monitor	Main Stack
Particulate emission rate (g/sec)	353.4*	1.3	10.5	5
Emission height (m)	--	--	--	50
Exit velocity (m/sec)	--	--	--	8
Diameter (m)	--	--	--	1.0
Exit temperature (°K)	--	--	--	340

*Emission rate during the period 0800 to 1600 LST. The emission rate during the period 1600 to 0800 LST is 70.7 grams per second.

TABLE 2-12

PARTICLE-SIZE DISTRIBUTION, GRAVITATIONAL SETTLING VELOCITIES
AND SURFACE REFLECTION COEFFICIENTS FOR PARTICULATE
EMISSIONS FROM THE ORE PILE AND CONVEYOR BELT

Particle Size Category (μ)	Mass Mean Diameter (μ)	Mass Fraction ϕ_n	Settling Velocity V_{sn} (m/sec)	Reflection Coefficient γ_n
0 - 10	6.30	0.10	0.001	1.00
10 - 20	15.54	0.40	0.007	0.82
20 - 30	25.33	0.28	0.019	0.72
30 - 40	35.24	0.12	0.037	0.65
40 - 50	45.18	0.06	0.061	0.59
50 - 65	17.82	0.04	0.099	0.50

(2-74)

from the ore pile during the period 0800 to 1600 LST are higher than during the period 1600 to 0800 LST because the hoist is continuously dumping sylvinite ore onto the ore pile. A significant fraction of the fugitive emissions from the ore pile and the conveyor belt consists of large particulates. The particle-size distribution, gravitational settling velocities and surface reflection coefficients for particulate emissions from the ore pile and conveyor belt are given in Table 2-12. The settling velocities in Table 2-12 were calculated using Equations (2-41) and (2-42) with the particulate density assumed to be 1 gram per cubic centimeter; the reflection coefficients were obtained from Figure 2-8. The remainder of the particulate emissions from the hypothetical plant are assumed to be submicron particulates so that the effects of gravitational settling and dry deposition need not be included in the model calculations. The purpose of this example problem is to use ISCST to calculate 24-hour average particulate concentrations produced by emissions from the hypothetical potash plant. Additionally, estimates of the dry deposition of fugitive emissions from the ore pile and the conveyor belt are required for each 24-hour period.

The ore pile is modeled as an area source with the effective side x_0 of the circular storage pile given by

$$x_0 = \frac{\sqrt{\pi}}{2} D \quad (2-56)$$

where D is the diameter of the base of the storage pile. The emission height H is set equal to the height of the ore pile (10 meters). The emission rate in grams per second is divided by the horizontal area of the storage pile (706.9 square meters) to obtain the area source emission rate in grams per second per square meter.

The conveyor belt is 10 meters wide and 100 meters long and is inclined at an angle of 10 degrees. Thus, the conveyor belt is modeled as ten 10-meter square volume sources. The initial lateral dimension of each source is obtained by dividing the width (10 meters) by 2.15. The initial

(2-75)

vertical dimension σ_{z0} is arbitrarily set equal to 1 meter to account for the effects of local plant roughness elements. The emission height H_i for the i^{th} source is given by

$$H_i = L_i \sin \theta \quad (2-57)$$

where

- H_i = the effective emission height for the i^{th} volume source
- L_i = the length, measured from the beginning of the conveyor belt, to the center of the i^{th} volume source
- θ = the angle of inclination (10 degrees)

The volume source model is also used to model the 90-meter by 20-meter roof monitor. The roof monitor is approximated by four 20-meter square volume sources with the centers of the volume sources spaced at 23.3-meter intervals. The initial lateral dimension σ_{y0} of each of the four volume sources is obtained by dividing 23.3 meters by 2.15. Because the opening of the roof monitors extends from 20 to 25 meters above plant grade, the emission height H is set equal to 22.5 meters. In order to account for the effects of the aerodynamic wake of the processing building on the initial dispersion of emissions from the roof monitor, the initial vertical dimension σ_{z0} is obtained by dividing the building height (25 meters) by 2.15.

In summary, the effects of emissions from the hypothetical potash processing plant shown in Figure 2-11 can be simulated by 16 sources. A single area source represents the ore pile, ten volume sources simulate the inclined conveyor belt, four volume sources represent the roof monitor, and there is one stack. It should be noted that the stack height to build-

ing height ratio is less than 2.5 so that the ISC Model procedures for evaluating wake effects are applied to the stack emissions. The emissions data for the hypothetical plant given in Table 2-11 are converted to the form required for input to ISCST in Tables 2-13 and 2-14. The information given in Table 2-12 is also required for the ore pile and the conveyor belt. Because the plant is located in open terrain, all source elevations are set equal to zero. The X and Y coordinates assume that the origin of the coordinate system is located at the center of the ore pile. Source combinations that are of interest in analyzing the results of the calculations are as follows:

- Source 1 -- Ore Pile
- Sources 2-11 -- Conveyor Belt
- Sources 12-12 -- Roof Monitor
- Source 16 -- Stack
- Sources 1-16 -- Plant as a Whole

Example ISCST runs that use the inputs given in Tables 2-12 through 2-14 and the receptor grid shown in Figure 2-3 to calculate concentrations and deposition are given in Appendix C. The hypothetical potash plant is assumed to be located in a rural area. Also, the plant does not contain large surface roughness elements or heat sources. Consequently, the Rural Mode is used in the ISCST calculations.

2.6.3 Example ISCLT Problem

The purpose of this example problem is to use ISCLT to calculate, for the receptor grid shown in Figure 2-3, annual average ground-level particulate concentrations produced by emissions from the hypothetical potash processing plant shown in Figure 2-11 as well as the annual deposition produced by fugitive emissions from the ore pile and conveyor belt. Annual

TABLE 2-13

EMISSIONS INVENTORY IN FORM FOR INPUT
TO THE ISC DISPERSION MODEL.

Source Number	Source Type*	X (m)	Y (m)	Z (m)	h (m)	V_e (m/sec) - Type 0 σ_{y0} (m) - Type 1 σ_{z0} (m) - Type 2	d (m) - Type 0 σ_{z0} (m) - Type 1	T_a (°K) Type 0	H_b (m) Type 0	Q (g/sec) - Type 0 & 1 g/(sec · m ²) - Type 2
1	2	-133	-133	0	10.0	26.6	--	--	--	5.00×10^{-1}
2	1	20	0	0	0.9	4.7	1.0	--	--	1.30×10^{-1}
3	1	30	0	0	2.6	4.7	1.0	--	--	1.30×10^{-1}
4	1	40	0	0	4.3	4.7	1.0	--	--	1.30×10^{-1}
5	1	49	0	0	6.1	4.7	1.0	--	--	1.30×10^{-1}
6	1	59	0	0	7.8	4.7	1.0	--	--	1.30×10^{-1}
7	1	69	0	0	9.6	4.7	1.0	--	--	1.30×10^{-1}
8	1	79	0	0	11.3	4.7	1.0	--	--	1.30×10^{-1}
9	1	89	0	0	13.0	4.7	1.0	--	--	1.30×10^{-1}
10	1	99	0	0	14.8	4.7	1.0	--	--	1.30×10^{-1}
11	1	109	0	0	16.5	4.7	1.0	--	--	1.30×10^{-1}
12	1	121	0	0	22.5	10.8	11.6	--	--	2.63
13	1	144	0	0	22.5	10.8	11.6	--	--	2.63
14	1	167	0	0	22.5	10.8	11.6	--	--	2.63
15	1	190	0	0	22.5	10.8	11.6	--	--	2.63
16**	0	201	30	0	50.0	8.0	1.0	340	25	5.00

*Source Type 0 = Stack, Source Type 1 = Volume and Source Type 2 = Area.

**Building width is 50 meters and building length is 90 meters (see Figure 2-11).

TABLE 2-14

PARTICULATE EMISSION RATES
FOR THE ORE PILE

Hour (LST)	Emission Rate Q_A (g/(sec·m ²))	Total Hourly Emission Q_{AT}^* (g/m ²)
0100	0.1	360
0200	0.1	360
0300	0.1	360
0400	0.1	360
0500	0.1	360
0600	0.1	360
0700	0.1	360
0800	0.5	1,800
0900	0.5	1,800
1000	0.5	1,800
1100	0.5	1,800
1200	0.5	1,800
1300	0.5	1,800
1400	0.5	1,800
1500	0.5	1,800
1600	0.1	360
1700	0.1	360
1800	0.1	360
1900	0.1	360
2000	0.1	360
2100	0.1	360
2200	0.1	360
2300	0.1	360
2400	0.1	360

*The amount of material emitted during each hour is required for the deposition calculations.

concentration and deposition estimates are also required for an air quality monitoring station located 2,108 meters from the center of the ore pile at a bearing of 014 degrees. With the exception of emissions from the ore pile and the conveyor belt, the emissions data for the plant are assumed to be identical to the data given in Tables 2-13 and 2-14. Fugitive emission rates for the ore pile and conveyor belt are given in Table 2-15 as functions of the wind-speed and Pasquill stability categories. The corresponding annual particulate emissions required for the annual deposition calculations are given in Table 2-16. Example ISCLT runs that calculate annual average concentration and total annual deposition values for this problem are presented in Appendix D.

TABLE 2-15

PARTICULATE EMISSION RATES FOR THE ORE PILE AND CONVEYOR
BELT AS FUNCTIONS OF WIND SPEED
AND STABILITY

Pasquill Stability Category	Emission Rate for Wind Speeds (m/sec) of					
	0-1.5	1.6-3.1	3.2-5.1	5.2-8.2	8.3-10.8	>10.8
(a) Ore Pile $Q_{A;i,k}$ (g/(sec.m ²))						
A	0.40	0.50	—	—	—	—
B	0.30	0.40	0.50	—	—	—
C	0.20	0.30	0.40	0.50	0.70	1.00
D	0.10	0.25	0.50	0.50	0.70	1.00
E	—	0.20	0.25	—	—	—
F	0.05	0.10	—	—	—	—
(b) Individual Volume Sources $Q_{i,k}$ (g/sec) Used to Represent the Conveyor Belt						
A	0.13	0.16	—	—	—	—
B	0.10	0.13	0.16	—	—	—
C	0.08	0.12	0.14	0.16	0.19	0.22
D	0.04	0.10	0.13	0.16	0.19	0.22
E	—	0.08	0.10	—	—	—
F	0.02	0.05	—	—	—	—

TABLE 2-16

ANNUAL PARTICULATE EMISSIONS FOR THE ORE PILE AND CONVEYOR BELT AS FUNCTIONS OF WIND SPEED AND STABILITY

Pasquill Stability Category	Annual Emissions for Wind Speeds (m/sec) of					
	0-1.5	1.6-3.1	3.2-5.1	5.2-8.2	8.3-10.8	>10.8
(a) Ore Pile $Q_{AT;1,k}^*$						
A	1.26×10^7	1.58×10^7	--	--	--	--
B	9.46×10^6	1.26×10^7	1.58×10^7	--	--	--
C	6.31×10^6	9.46×10^6	1.26×10^7	1.58×10^7	2.21×10^7	3.15×10^7
D	3.15×10^7	7.88×10^6	1.26×10^7	1.58×10^7	2.21×10^7	3.15×10^7
E	--	6.31×10^6	9.46×10^6	--	--	--
F	1.58×10^6	3.15×10^6	--	--	--	--
(b) Individual Volume Sources $Q_{T;1,k}^{**}$ (g) Used to Represent the Conveyor Belt						
A	4.10×10^6	5.05×10^6	--	--	--	--
B	3.15×10^6	4.10×10^6	5.05×10^6	--	--	--
C	2.52×10^6	3.78×10^6	4.42×10^6	5.05×10^6	5.99×10^6	6.94×10^6
D	1.26×10^6	3.15×10^6	4.10×10^6	5.05×10^6	5.99×10^6	6.94×10^6
E	--	2.52×10^6	3.15×10^6	--	--	--
F	6.31×10^5	1.58×10^6	--	--	--	--

* $Q_{AT;1,k}$ (g/m²) = $Q_{A;1,k}$ (g/(sec·m²)) × (3600 sec/hr) × (24 hr/day) × (365 day/yr) = $3.1536 \times 10^7 Q_{A;1,k}$

**Similarly, $Q_{T;1,k}$ (g) = $3.1536 \times 10^7 Q_{1,k}$ (g/sec)

SECTION 11

A Description of the Prototype MC-LAGPAR Diffusion Model

An APL prototype diffusion model, (MC-LAGPAR) which can simulate short-term releases (e.g., a puff) of air pollutants in extremely complex diffusion conditions, has been developed. This technique uses the Lagrangian particle modeling approach, with Monte-Carlo random statistical generation of the diffusivity velocity u'_e (see Section 5.1.2 of Volume II of this final report for an introductory description of the fundamentals of such technique).

This section briefly discusses the structure and characteristics of the MC-LAGPAR code, and the software instructions (user's manual) for running this computer code have been included in Volume IV of this final report.

The flow-chart of MC-LAGPAR is shown in Fig. 11-1 and presents all the major features of the program. In this preliminary version, flat terrain conditions are assumed (which is the case in Kuwait) and meteorological variables are allowed to vary only with the altitude (horizontal homogeneity).

The program allows an initial release of non-reactive pollutants. The size of this initial release can also be specified and, therefore, MC-LAGPAR is able to simulate both a puff (instantaneous release) and an elongated plume segment (continuous release).

At least a few thousand particles should be used to allow enough resolution. Each particle is moved at each time step to properly simulate transport and diffusion phenomena. Moreover, particles are only partially reflected at the ground to simulate dry deposition. Non-reflected particles are deleted, together with those that travel outside the computational domain. Other particles are deleted to properly simulate chemical decay.

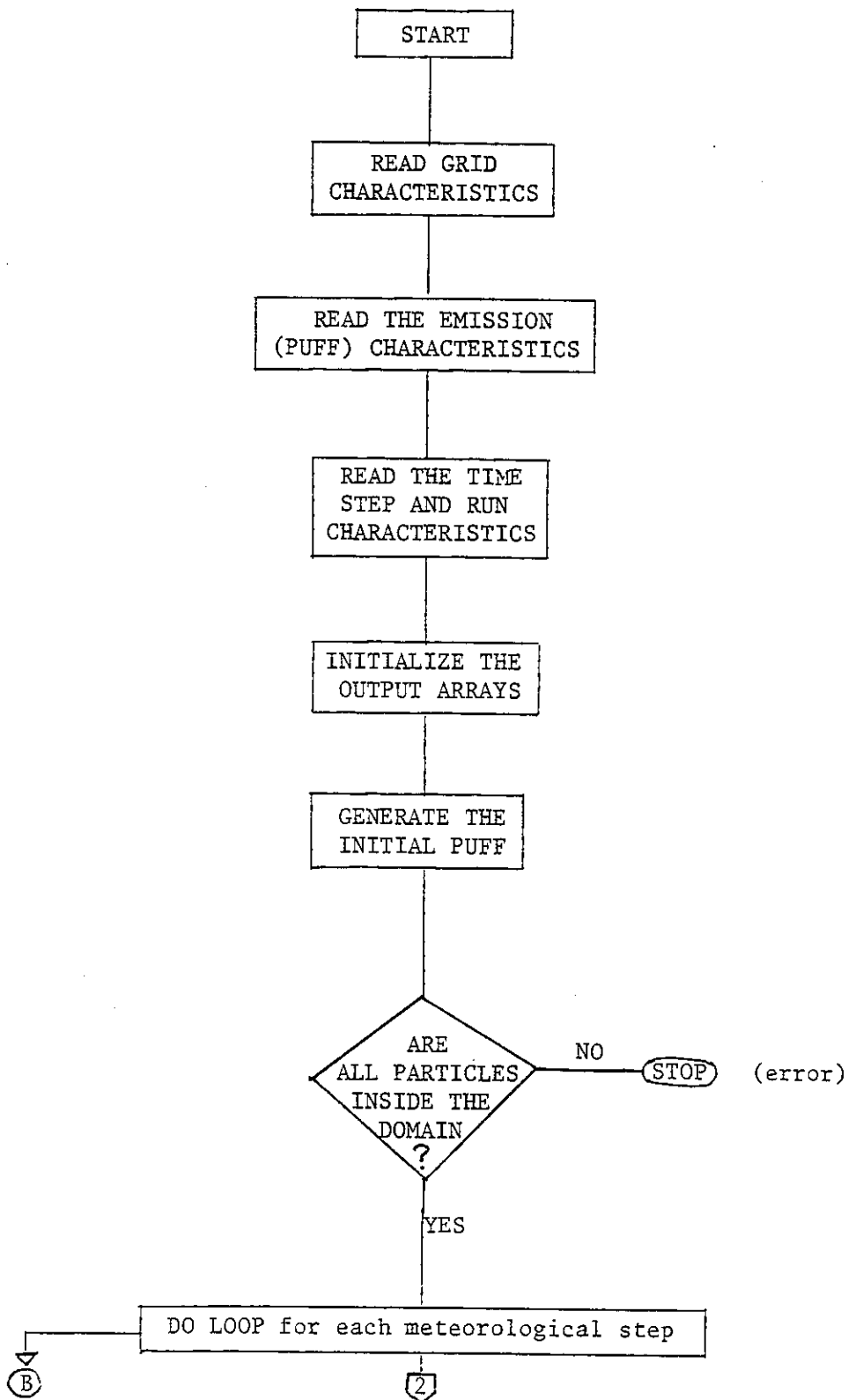


Fig. 11-1. Flow-chart of MC-LAGPAR

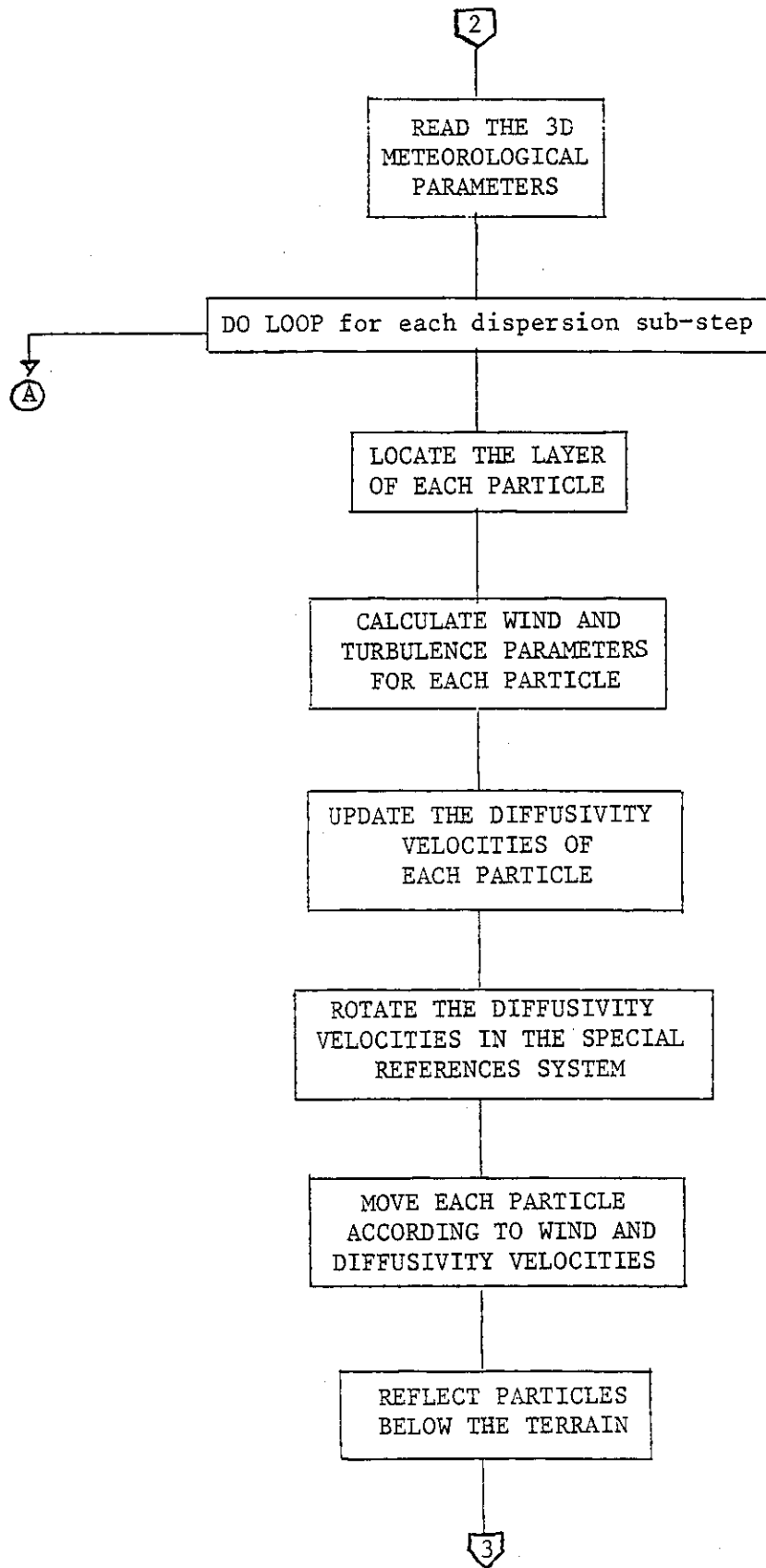


Fig. 11-1 (Cont'd)

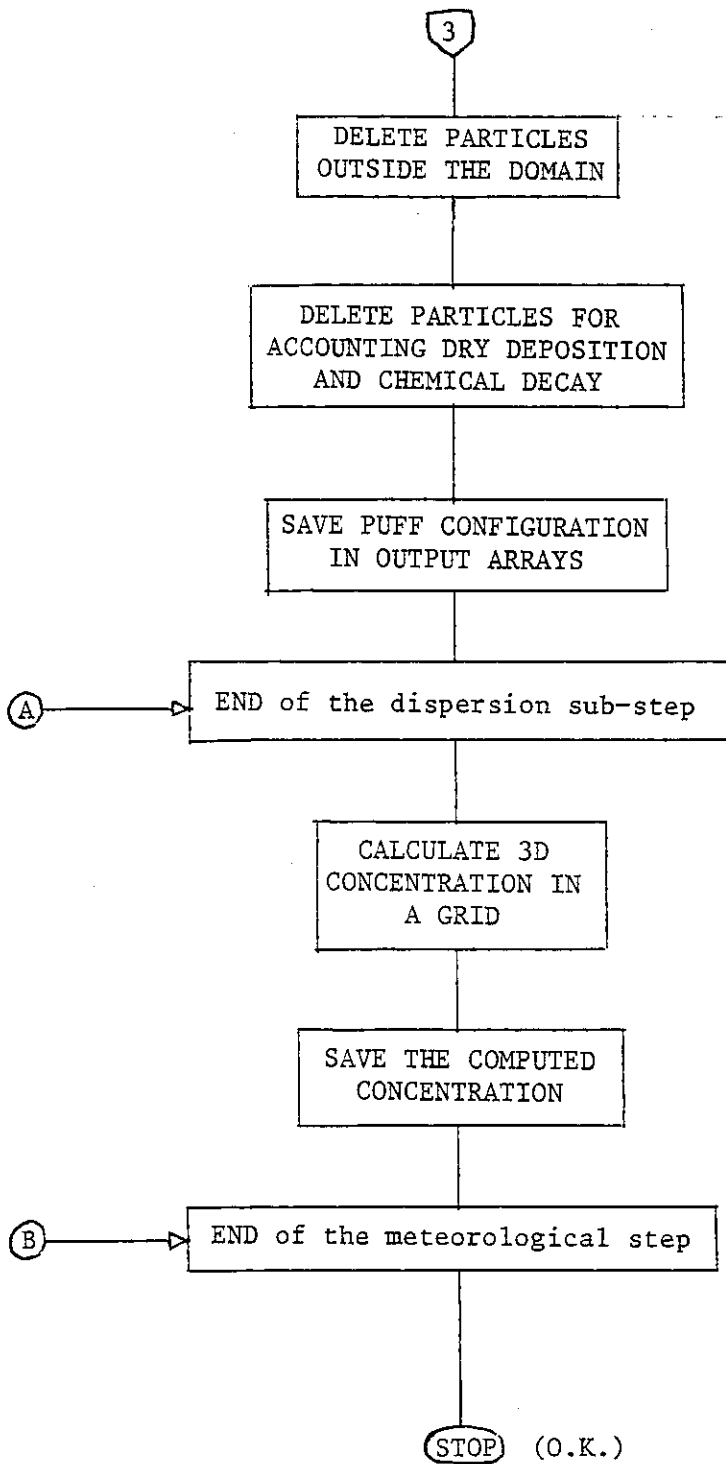


Fig. 11-1 (Cont'd)

Each particle motion is a function of the meteorological readings (wind and turbulence parameters) at different specified elevations. Such readings are interpolated at each particle's elevation to allow their smooth variation with height. Particle motion at each step is the sum of two vectors. The first is the average wind vector, containing deterministic information on the average transport pattern in the computational domain. The second is a diffusivity velocity vector, which simulates the total effect (on a particle ensemble basis) of the atmospheric turbulent diffusion in that step.

MC-LAGPAR is a fully Lagrangian, grid-free, three-dimensional, time-varying diffusion model. At the present stage, it requires meteorological input parameters (turbulence intensities and wind fluctuation auto-correlations) not generally available. Therefore, MC-LAGPAR future operation applications require either the installation in Kuwait of special ad-hoc instrumentation, or a semi-empirical study providing a relation between standard available meteorological measurements and the required special meteorological input. Future tracer studies in the SIA should strongly help in determining this semi-empirical relation.

In spite of some difficulties in the practical application of MC-LAGPAR, its potential capability in fully representing extremely complex conditions is outstanding, as displayed in Section 5.5.2 of Volume II of this final report, where shear effects and vertical stratifications (inversions) are uniquely simulated by the computer code.

SECTION 12

Data Analysis Tables

Figures were presented in Section 6 of Volume II which summarize the outputs of a special statistical analysis of meteorological data. This analysis was performed using the Statistical Analysis System (SAS) package. The full computer output of some of these analyses is enclosed in this section.

The following pages contain SAS outputs for the analysis of temperature, pressure and relative humidity during 1977-87-79-80-81-82. Each analysis contains:

- a monthly analysis (month, frequency, mean, standard deviation, minimum value, day of the minimum value, hour of the minimum value, maximum value, day of the maximum value, hour of the maximum value, range, percentage of missing values)
- a similar yearly analysis
- a similar seasonal analysis
- a daily cycle analysis, for each season and each hour of the day (frequency, mean, standard deviation, minimum value, maximum value, range, percentage of missing data)

MONTHLY ANALYSIS OF TEMPERATURE (DEG. C.) OF YEAR 1978

MONTH	_FREQ_	MEAN	STD	MIN	MINDAY	MINHR	MAX	MAXDAY	MAXHR	RANGE	MISSING
1	744	13.4265	3.90570	2.6	17	2	26.3	20	11	23.7	0
2	672	15.8616	4.01321	6.5	57	3	25.8	47	9	19.3	0
3	744	19.7663	4.18671	9.7	60	1	31.3	89	11	21.6	0
4	720	25.7782	4.48835	13.6	92	2	36.7	54	8	23.1	0
5	744	31.9423	5.78817	17.0	132	3	43.6	146	10	26.6	0
5	744	31.9423	5.78817	17.0	132	3	43.6	149	10	26.6	0
6	720	35.0686	5.59426	23.1	153	2	48.2	160	11	25.1	0
7	744	36.8302	4.81844	27.6	184	2	49.0	203	10	21.4	0
7	744	36.8302	4.81844	27.6	205	1	49.0	203	11	21.4	0
8	744	35.9798	4.91654	25.6	241	2	45.6	222	12	20.0	0
8	744	35.9798	4.91654	25.6	241	2	45.6	223	10	20.0	0
8	744	35.9798	4.91654	25.6	241	2	45.6	224	11	20.0	0
9	720	33.4151	5.35240	22.4	272	2	45.0	244	10	22.6	0
9	720	33.4151	5.35240	22.4	273	2	45.0	244	10	22.6	0
10	744	27.6165	5.15015	18.6	288	3	38.8	292	9	20.2	0
11	720	17.0883	4.53734	6.7	328	1	28.5	305	10	21.8	0
11	720	17.0883	4.53734	6.7	328	3	28.5	305	10	21.8	0
12	744	16.5036	3.92004	8.0	354	3	29.4	343	9	21.4	0

YEARLY ANALYSIS OF TEMPERATURE (DEG. C.) OF YEAR 1978

FREQ	MEAN	STD	MIN	MINMONTH	MINDAY	MINHR	MAX	MAXMONTH	MAXDAY	MAXHR	RANGE	MISSING
8760	25.8336	9.71488	2.6	1	17	2	49	7	203	10	46.4	0
8760	25.8336	9.71488	2.6	1	17	2	49	7	203	11	46.4	0

SEASONAL ANALYSIS OF TEMPERATURE (DEG. C.) FOR 1977-1978

SEASON	_FREQ_	MEAN	STD	MIN	MINMONTH	MINDAY	MINHR	MAX	MAXMONTH	MAXDAY	MAXHR	RANGE	MISSING
WINTER	2166	14.9544	4.20746	2.6	1	17	2	28.6	12	338	11	26.0	0
SPRING	2208	25.8362	6.97550	9.7	3	60	1	43.6	5	146	10	33.9	0
SPRING	2208	25.8362	6.97550	9.7	3	60	1	43.6	5	149	10	33.9	0
SUMMER	2206	35.9692	5.16374	23.1	6	153	2	49.0	7	203	10	25.9	0
SUMMER	2208	35.9692	5.16374	23.1	6	153	2	49.0	7	203	11	25.9	0
AUTUMN	2164	26.0573	8.39405	6.7	11	328	1	45.0	9	244	10	38.3	0
AUTUMN	2164	26.0573	8.39405	6.7	11	328	3	45.0	9	244	10	38.3	0

SEASONAL DAILY CYCLE OF TEMPERATURE (DEG. C.) OF YEAR 77-78

SEASON	HOUR	_FREQ_	MEAN	STD	MIN	MAX	RANGE	MISSING
WINTER	1	90	11.5744	3.62409	3.4	19.4	16.0	0
WINTER	2	90	11.3756	3.76734	2.6	19.7	17.1	0
WINTER	3	90	11.1589	3.77959	3.2	20.0	16.8	0
WINTER	4	90	12.1667	3.47498	4.6	21.0	16.4	0
WINTER	5	90	14.0878	3.15077	7.6	22.4	14.8	0
WINTER	6	90	15.8189	3.07688	9.4	24.2	14.8	0
WINTER	7	90	17.1789	3.15073	10.6	26.3	15.7	0
WINTER	8	90	18.3300	3.26663	11.6	27.0	15.4	0
WINTER	9	90	19.0511	3.40229	12.4	28.1	15.7	0
WINTER	10	90	19.3211	3.32327	13.1	28.4	15.3	0
WINTER	11	90	19.2611	3.15105	13.6	28.6	15.0	0
WINTER	12	90	18.7789	2.92308	13.4	28.0	14.6	0
WINTER	13	90	17.8933	2.74410	12.5	25.8	13.3	0
WINTER	14	90	16.7844	2.56072	11.1	22.9	11.8	0
WINTER	15	90	15.9733	2.55157	9.7	22.1	12.4	0
WINTER	16	90	15.4133	2.65657	9.0	22.3	13.3	0
WINTER	17	90	14.8356	2.75503	7.8	21.8	14.0	0
WINTER	18	90	14.1811	2.89439	7.2	22.0	14.8	0
WINTER	19	90	13.5744	3.02972	6.4	22.0	15.6	0
WINTER	20	90	13.1400	3.21551	5.8	21.5	15.7	0
WINTER	21	90	12.7233	3.32262	4.9	21.4	16.5	0
WINTER	22	90	12.3689	3.44718	4.2	20.9	16.7	0
WINTER	23	90	12.1111	3.53049	4.2	20.6	16.4	0
WINTER	24	90	11.7644	3.48610	3.7	20.0	16.3	0
SPRING	1	92	20.2696	5.12176	9.7	33.0	23.3	0
SPRING	2	92	20.1190	5.32810	10.0	33.5	23.5	0
SPRING	3	92	21.0913	5.81243	10.0	34.4	24.4	0
SPRING	4	92	23.8446	6.10297	12.6	35.7	23.1	0
SPRING	5	92	26.2567	6.25538	15.4	38.4	23.0	0
SPRING	6	92	28.2815	6.20669	17.3	40.0	22.7	0
SPRING	7	92	29.5891	6.35899	17.7	42.4	24.7	0
SPRING	8	92	30.4685	6.49109	17.2	43.3	26.1	0
SPRING	9	92	31.1717	6.39923	17.8	43.0	25.2	0
SPRING	10	92	31.4815	6.38742	18.7	43.6	24.9	0
SPRING	11	92	31.4228	6.26208	19.7	43.0	23.3	0
SPRING	12	92	30.9902	6.22406	20.4	42.8	22.4	0
SPRING	13	92	30.0196	6.18743	20.0	42.3	22.3	0
SPRING	14	92	28.7120	6.24529	19.0	41.3	22.3	0
SPRING	15	92	27.1783	6.02757	17.2	41.3	24.1	0
SPRING	16	92	26.3663	5.64889	16.6	37.1	20.5	0
SPRING	17	92	25.4696	5.61600	16.3	36.3	20.0	0
SPRING	18	92	24.6207	5.37517	14.7	35.4	20.7	0
SPRING	19	92	23.6946	5.25747	14.5	34.4	19.9	0
SPRING	20	92	23.0228	5.26559	13.8	33.3	19.5	0
SPRING	21	92	22.2837	5.08696	13.4	32.6	19.2	0
SPRING	22	92	21.7611	5.02864	12.8	31.6	18.8	0
SPRING	23	92	21.2130	4.97751	12.2	31.0	18.8	0
SPRING	24	92	20.7609	4.93654	11.4	32.0	20.6	0
SUMMER	1	92	29.3033	2.44771	23.3	35.3	12.0	0
SUMMER	2	92	29.2446	2.45300	23.1	35.0	11.9	0
SUMMER	3	92	31.0554	2.13585	25.0	35.5	10.9	0
SUMMER	4	92	33.7380	2.37893	27.6	39.6	12.0	0

SEASONAL DAILY CYCLE OF TEMPERATURE (DEG. C.) OF YEAR 77-78

SEASON	HOUR	_FREQ_	MEAN	STD	MIN	MAX	RANGE	MISSING
SUMMER	5	92	36.2120	2.42966	29.6	42.2	12.6	0
SUMMER	6	92	38.2402	2.67693	28.7	43.7	15.0	0
SUMMER	7	92	39.9011	2.72939	33.1	46.3	13.2	0
SUMMER	8	92	41.0648	2.86933	33.5	47.4	13.9	0
SUMMER	9	92	41.7891	2.83310	34.3	48.7	14.4	0
SUMMER	10	92	42.2707	2.86512	34.4	49.0	14.6	0
SUMMER	11	92	42.2500	2.87259	34.4	49.0	14.6	0
SUMMER	12	92	41.8543	2.94400	33.5	48.7	15.2	0
SUMMER	13	92	41.0630	2.97512	32.4	48.4	16.0	0
SUMMER	14	92	39.6676	2.82560	31.4	46.1	14.7	0
SUMMER	15	92	37.9826	2.71352	30.0	44.4	14.4	0
SUMMER	16	92	36.7967	2.65191	29.3	43.8	14.5	0
SUMMER	17	92	35.7761	2.41399	28.8	41.9	13.1	0
SUMMER	18	92	34.7502	2.39895	27.3	40.7	13.4	0
SUMMER	19	92	33.8250	2.44017	26.3	39.9	13.6	0
SUMMER	20	92	32.9109	2.42403	26.1	38.1	12.0	0
SUMMER	21	92	32.0609	2.41774	25.6	37.4	11.8	0
SUMMER	22	92	31.1674	2.46073	24.5	36.8	12.3	0
SUMMER	23	92	30.4880	2.50559	23.8	36.2	12.4	0
SUMMER	24	92	29.8500	2.46521	24.1	35.9	11.8	0
AUTUMN	1	91	20.6033	6.05439	6.7	30.5	23.8	0
AUTUMN	2	91	20.1956	6.00627	6.8	30.4	23.6	0
AUTUMN	3	91	20.5527	6.41378	6.7	32.0	25.3	0
AUTUMN	4	91	22.9198	6.81133	9.7	34.8	25.1	0
AUTUMN	5	91	25.6440	7.30334	12.0	37.1	25.1	0
AUTUMN	6	91	28.1484	7.76709	12.6	40.5	27.9	0
AUTUMN	7	91	30.1637	8.18962	13.0	42.6	29.6	0
AUTUMN	8	91	31.4655	8.47395	13.6	44.4	30.8	0
AUTUMN	9	91	32.3418	8.68594	13.0	44.7	31.7	0
AUTUMN	10	91	32.6231	8.57263	14.1	45.0	30.9	0
AUTUMN	11	91	32.4637	8.46365	13.6	44.7	31.1	0
AUTUMN	12	91	31.8275	8.29984	14.2	44.0	29.8	0
AUTUMN	13	91	30.3824	8.08544	13.9	43.4	29.5	0
AUTUMN	14	91	28.6352	7.68459	13.4	41.6	28.2	0
AUTUMN	15	91	27.3582	7.30904	13.5	39.5	26.0	0
AUTUMN	16	91	26.4692	7.09389	13.3	38.7	25.4	0
AUTUMN	17	91	25.5747	6.93853	11.4	37.5	26.1	0
AUTUMN	18	91	24.6571	6.80159	10.5	36.0	25.5	0
AUTUMN	19	91	23.7648	6.70226	9.6	34.5	24.9	0
AUTUMN	20	91	23.0198	6.51544	9.3	34.0	24.7	0
AUTUMN	21	91	22.3725	6.41606	8.8	33.5	24.7	0
AUTUMN	22	91	21.8505	6.34617	8.2	33.0	24.8	0
AUTUMN	23	91	21.4110	6.23391	7.8	32.4	24.6	0
AUTUMN	24	91	20.9308	6.06787	7.7	31.0	23.3	0

MONTHLY ANALYSIS OF TEMPERATURE (DEG. C.) OF YEAR 1979

MUNTH	_FREQ_	MEAN	STD	MIN	MINDAY	MINHR	MAX	MAXDAY	MAXHR	RANGE	MISSING
1	744	14.3745	3.73963	6.0	7	2	25.2	4	9	19.2	0
1	744	14.3745	3.73963	6.0	7	3	25.2	4	9	19.2	0
2	672	17.7720	4.01062	7.3	36	3	29.5	51	10	22.2	0
3	744	19.9880	4.82588	8.9	65	2	33.5	84	11	24.6	0
4	720	26.8124	4.57696	16.2	91	1	43.8	112	9	27.6	0
4	720	26.8124	4.57696	16.2	91	1	43.8	112	10	27.6	0
4	720	26.8124	4.57696	16.2	91	1	43.8	112	11	27.6	0
5	744	31.4551	5.55410	17.0	121	1	49.8	134	12	32.8	0
6	720	36.8550	4.56543	28.2	165	1	48.5	164	10	20.3	0
7	744	37.5243	4.52798	27.6	185	1	48.9	206	10	21.3	0
8	744	36.2040	4.76369	27.0	227	2	46.3	215	10	19.3	0
9	720	34.1139	5.24800	23.9	265	2	46.5	256	9	22.6	0
9	720	34.1139	5.24800	23.9	266	3	46.5	256	9	22.6	0
10	744	28.7138	4.93488	19.0	304	22	41.4	276	10	22.4	0
10	744	28.7138	4.93488	19.0	304	23	41.4	276	10	22.4	0
10	744	28.7138	4.93488	19.0	304	24	41.4	276	10	22.4	0
11	720	21.5174	4.84066	11.6	330	2	32.5	317	9	20.9	0
12	744	13.8239	3.63579	3.6	365	3	23.9	340	10	20.3	0

YEARLY ANALYSIS OF TEMPERATURE (DEG. C.) OF YEAR 1979

FREQ	MEAN	STD	MIN	MINMONTH	MINDAY	MINHR	MAX	MAXMONTH	MAXDAY	MAXHR	RANGE	MISSING
8760	26.6663	9.65255	3.6	12	365	3	49.8	5	134	12	46.2	0

SEASONAL ANALYSIS OF TEMPERATURE (DEG. C.) FOR 1978-1979

SEASON	_FREQ_	MEAN	STD	MIN	MINMONTH	MINDAY	MINHR	MAX	MAXMONTH	MAXDAY	MAXHR	RANGE	MISSING
WINTER	2160	16.1580	4.13472	6.0	1	7	2	29.5	2	51	10	23.5	0
WINTER	2160	16.1580	4.13472	6.0	1	7	3	29.5	2	51	10	23.5	0
SPRING	2208	26.0773	6.89026	8.9	3	45	2	49.8	5	134	12	40.9	0
SUMMER	2208	36.8614	4.65036	27.0	8	227	2	48.9	7	206	10	21.9	0
AUTUMN	2184	28.2535	7.05113	11.6	11	330	2	46.5	9	256	9	34.9	0

SEASONAL DAILY CYCLE OF TEMPERATURE (DEG. C.) OF YEAR 78-79

SEASON	HOUR	_FREQ_	MEAN	STD	MIN	MAX	RANGE	MISSING
WINTER	1	90	12.7411	3.32930	6.5	21.8	15.3	0
WINTER	2	90	12.4511	3.36416	6.0	21.1	15.1	0
WINTER	3	90	12.1500	3.35509	6.0	19.9	13.9	0
WINTER	4	90	13.1444	3.16800	6.8	19.5	12.7	0
WINTER	5	90	14.8589	2.95741	8.5	20.5	12.0	0
WINTER	6	90	16.8544	2.57235	10.2	22.6	12.4	0
WINTER	7	90	18.4400	3.11718	10.8	27.6	16.8	0
WINTER	8	90	19.6422	3.27754	10.8	28.3	17.5	0
WINTER	9	90	20.4533	3.49819	11.3	29.4	18.1	0
WINTER	10	90	20.6667	3.29463	11.7	29.5	17.8	0
WINTER	11	90	20.5011	3.06042	12.2	27.5	15.3	0
WINTER	12	90	20.0433	2.97805	12.5	27.7	15.2	0
WINTER	13	90	19.1122	2.79200	12.6	27.5	14.9	0
WINTER	14	90	17.5278	2.54422	11.8	24.4	12.6	0
WINTER	15	89	17.1865	2.52259	11.1	22.9	11.8	0
WINTER	16	91	16.6473	2.52628	10.8	22.4	11.6	0
WINTER	17	90	16.0033	2.64067	9.9	21.8	11.9	0
WINTER	18	90	15.4222	2.74884	9.4	21.9	12.5	0
WINTER	19	90	14.9522	2.52629	8.2	21.8	13.6	0
WINTER	20	90	14.4489	3.03438	8.2	21.4	13.2	0
WINTER	21	90	14.0156	3.14489	8.0	21.5	13.5	0
WINTER	22	90	13.6544	3.24443	7.6	21.7	14.1	0
WINTER	23	90	13.4044	3.21034	7.2	21.7	14.5	0
WINTER	24	90	13.0356	3.27463	7.0	21.7	14.7	0
SPRING	1	92	20.5489	5.82719	9.7	33.4	23.7	0
SPRING	2	92	20.7446	6.08701	8.9	33.6	24.7	0
SPRING	3	92	21.5859	6.46433	9.4	35.6	26.2	0
SPRING	4	92	23.9304	6.55829	10.8	38.4	27.6	0
SPRING	5	92	26.4337	6.40194	12.9	40.2	27.3	0
SPRING	6	92	28.6630	6.41049	15.0	41.6	26.6	0
SPRING	7	92	30.0467	6.36107	16.8	44.8	28.0	0
SPRING	8	92	30.8554	6.36661	18.7	42.8	24.1	0
SPRING	9	92	31.2935	6.16067	18.5	43.8	25.3	0
SPRING	10	92	31.2000	5.92619	19.1	43.8	24.7	0
SPRING	11	92	31.0011	5.87486	19.1	43.8	24.7	0
SPRING	12	92	30.4511	5.97630	18.7	49.8	31.1	0
SPRING	13	92	29.4500	5.46297	18.4	41.0	22.6	0
SPRING	14	92	28.2522	5.66319	17.9	42.4	24.5	0
SPRING	15	92	27.0098	5.48721	17.0	39.5	22.5	0
SPRING	16	92	26.3620	5.41755	16.1	41.4	25.3	0
SPRING	17	92	25.7587	5.37998	15.8	39.1	23.3	0
SPRING	18	92	25.0130	5.41104	15.1	36.4	21.3	0
SPRING	19	92	24.2935	5.41881	13.7	35.6	21.9	0
SPRING	20	92	23.5587	5.52575	12.9	35.4	22.5	0
SPRING	21	92	22.9750	5.65570	12.0	36.6	24.6	0
SPRING	22	92	22.4337	5.83267	11.3	36.2	24.9	0
SPRING	23	92	22.0620	6.05353	10.9	37.9	27.0	0
SPRING	24	92	21.5315	5.86818	10.0	34.0	24.0	0
SUMMER	1	92	30.8685	1.83656	27.5	35.5	8.0	0
SUMMER	2	92	30.8033	1.72693	27.0	34.7	7.7	0
SUMMER	3	92	32.1185	1.70757	27.6	36.6	9.0	0
SUMMER	4	92	34.5630	1.65182	30.7	38.4	7.7	0

SEASONAL DAILY CYCLE OF TEMPERATURE (DEG. C.) OF YEAR 78-79

SEASON	HOUR	_FREQ_	MEAN	STD	MIN	MAX	RANGE	MISSING
SUMMER	5	92	36.8674	1.68302	33.0	40.8	7.8	0
SUMMER	6	92	38.5652	2.01688	34.5	43.0	8.5	0
SUMMER	7	92	40.5402	2.21970	35.5	46.0	10.5	0
SUMMER	8	92	41.6326	2.54339	35.7	48.0	12.3	0
SUMMER	9	92	42.2185	2.71597	35.7	48.6	12.9	0
SUMMER	10	92	42.5370	2.96562	33.6	48.9	15.3	0
SUMMER	11	92	42.4522	2.87927	34.1	48.4	14.3	0
SUMMER	12	92	41.9609	3.06286	33.1	48.2	15.1	0
SUMMER	13	92	41.2196	3.12369	33.1	47.2	14.1	0
SUMMER	14	92	40.0557	3.10751	32.1	45.8	13.7	0
SUMMER	15	92	38.6728	2.93793	31.6	44.4	12.8	0
SUMMER	16	92	37.6043	2.66973	30.7	42.6	11.9	0
SUMMER	17	92	36.7457	2.39718	31.0	41.3	10.3	0
SUMMER	18	92	35.9185	2.28439	30.5	40.4	9.9	0
SUMMER	19	92	35.6772	2.18416	30.0	40.0	10.0	0
SUMMER	20	92	34.2685	2.10023	29.7	38.8	9.1	0
SUMMER	21	92	33.4859	1.96343	29.1	38.2	9.1	0
SUMMER	22	92	32.6750	1.91608	28.9	37.0	8.1	0
SUMMER	23	92	31.9946	1.85392	28.2	36.5	8.3	0
SUMMER	24	92	31.3880	1.83596	28.0	36.2	8.2	0
AUTUMN	1	91	22.7501	5.03903	12.0	30.3	18.3	0
AUTUMN	2	91	22.5011	5.04961	11.6	32.4	20.8	0
AUTUMN	3	91	22.8901	5.26063	11.8	32.2	20.4	0
AUTUMN	4	91	25.0659	5.80156	13.2	34.4	21.2	0
AUTUMN	5	91	27.9121	6.17077	15.6	37.8	22.2	0
AUTUMN	6	91	30.7725	6.31397	17.6	42.4	24.8	0
AUTUMN	7	91	32.7571	6.34282	19.0	44.9	25.9	0
AUTUMN	8	91	34.0681	6.35022	20.4	46.0	25.6	0
AUTUMN	9	91	34.7802	6.25277	21.3	46.5	25.2	0
AUTUMN	10	91	34.8429	6.10767	21.7	45.4	23.7	0
AUTUMN	11	91	34.4110	6.06825	21.8	44.6	22.8	0
AUTUMN	12	91	33.6099	6.09446	21.5	44.2	22.7	0
AUTUMN	13	91	32.1365	6.02181	20.5	43.0	22.5	0
AUTUMN	14	91	30.5571	5.74310	19.4	41.4	22.0	0
AUTUMN	15	91	29.3714	5.48011	18.1	39.5	21.4	0
AUTUMN	16	91	28.4670	5.36590	17.6	37.8	20.2	0
AUTUMN	17	91	27.7578	5.25993	16.4	37.0	21.4	0
AUTUMN	18	91	26.8495	5.21778	15.6	36.3	20.7	0
AUTUMN	19	91	25.9593	5.30947	14.9	35.2	20.3	0
AUTUMN	20	91	25.2220	5.24408	14.1	34.2	20.1	0
AUTUMN	21	91	24.5567	5.25070	13.2	33.0	19.8	0
AUTUMN	22	91	24.0451	5.24562	13.0	32.5	19.5	0
AUTUMN	23	91	23.5791	5.17961	12.9	31.4	18.5	0
AUTUMN	24	91	23.0989	5.15813	12.0	31.0	19.0	0

MONTHLY ANALYSIS OF TEMPERATURE (DEG. C.) OF YEAR 1980

MONTH	_FREQ_	MEAN	STD	MIN	MINDAY	MINHR	MAX	MAYDAY	MAXHR	RANGE	HISSING
1	744	12.6519	3.81456	2.7	17	3	23.9	29	10	21.2	0
2	696	14.3566	3.80352	2.7	33	3	24.4	60	11	21.7	0
3	744	19.9792	5.15039	7.0	65	2	31.8	90	9	24.8	0
3	744	19.9792	5.15039	7.0	65	2	31.8	90	10	24.8	0
4	720	26.3592	4.82658	13.6	109	2	42.4	113	8	28.8	0
5	744	31.6540	5.24340	18.8	123	2	44.6	143	12	25.8	0
6	720	37.2036	5.18991	26.4	171	1	47.9	182	10	21.5	0
7	744	38.9531	4.70075	28.2	189	24	48.9	199	10	20.7	0
8	744	36.5962	4.83573	26.0	244	2	45.7	217	12	19.7	0
9	720	32.0403	6.56979	16.2	268	2	45.5	247	10	29.3	0
9	720	32.0403	6.56979	16.2	268	2	45.5	247	11	29.3	0
9	720	32.0403	6.56979	16.2	268	2	45.5	249	10	29.3	0
10	744	26.9598	6.33430	11.0	305	1	42.6	276	10	31.6	0
10	744	26.9598	6.33430	11.0	305	2	42.6	276	10	31.6	0
11	720	20.7625	5.30428	7.0	331	2	34.0	327	9	27.0	0
12	744	13.2661	4.75353	2.9	348	3	26.0	342	10	23.1	0
12	744	13.2661	4.75353	2.9	349	3	26.0	342	10	23.1	0

YEARLY ANALYSIS OF TEMPERATURE (DEG. C.) OF YEAR 1980

__FREQ__	MEAN	STD	MIN	MINMONTH	MINDAY	MINHR	MAX	MAXMONTH	HAYDAY	HAYHR	RANGE	HISSING
8784	25.9267	10.523	2.7	1	17	3	48.9	7	199	10	46.2	0
8784	25.9267	10.523	2.7	2	33	3	48.9	7	199	10	46.2	0

SEASONAL ANALYSIS OF TEMPERATURE (DEG. C.) FOR 1979-1980

SEASON	_FREQ_	MEAN	STD	MIN	MINMONTH	MIDDAY	MINHR	MAX	MAXMONTH	MAXDAY	MAXHR	RNGR	MISSING
WINTER	2184	13.5856	3.82435	2.7	1	17	3	24.4	2	60	11	21.7	0
WINTER	2184	13.5856	3.82435	2.7	2	33	3	24.4	2	60	11	21.7	0
SPRING	2208	25.9935	6.98674	7.0	3	65	2	44.6	5	143	12	31.6	0
SUMMER	2208	37.5885	5.00944	26.0	8	244	2	48.9	7	199	10	22.9	0
AUTUMN	2184	26.5916	7.62783	7.0	11	331	2	45.5	9	247	10	38.5	0
AUTUMN	2184	26.5916	7.62783	7.0	11	331	2	45.5	9	247	11	38.5	0
AUTUMN	2184	26.5916	7.62783	7.0	11	331	2	45.5	9	249	10	38.5	0

SEASONAL DAILY CYCLE OF TEMPERATURE (DEG. C.) OF YEAR 79-80

SEASON	HOUR	_FREQ_	MEAN	STD	MIN	MAX	RANGE	MISSING
WINTER	1	92	10.5250	3.65705	3.0	22.5	19.5	0
WINTER	2	91	10.1527	3.49699	3.1	18.5	15.4	0
WINTER	3	91	10.0330	3.50736	2.7	18.0	15.3	0
WINTER	4	91	10.8747	3.32123	4.0	17.4	13.4	0
WINTER	5	91	12.3747	3.10632	5.0	19.0	14.0	0
WINTER	6	91	14.1791	3.07186	6.6	20.4	13.8	0
WINTER	7	91	15.5099	2.97351	8.4	22.0	13.6	0
WINTER	8	91	16.5374	2.98525	9.2	23.6	14.4	0
WINTER	9	90	16.9656	2.80522	9.8	23.7	13.9	0
WINTER	10	91	17.3418	2.72731	10.4	24.0	13.6	0
WINTER	11	91	17.3308	2.58297	10.4	24.4	14.0	0
WINTER	12	91	17.1681	2.42853	10.5	23.7	13.2	0
WINTER	13	91	16.4198	2.35246	9.6	22.5	12.9	0
WINTER	14	91	15.3593	2.31910	9.1	21.5	12.4	0
WINTER	15	91	14.6495	2.35138	8.7	21.6	12.9	0
WINTER	16	91	14.1418	2.42107	8.4	21.3	12.9	0
WINTER	17	91	13.6824	2.51695	7.5	21.7	14.2	0
WINTER	18	91	13.1319	2.66933	7.1	20.7	13.6	0
WINTER	19	91	12.6429	2.66701	6.7	17.9	11.2	0
WINTER	20	91	12.1978	2.97601	5.2	18.0	12.8	0
WINTER	21	91	11.7505	3.05445	4.6	17.8	13.2	0
WINTER	22	91	11.3747	3.16725	4.4	18.0	13.6	0
WINTER	23	91	11.0055	3.28594	3.4	18.1	14.7	0
WINTER	24	91	10.7758	3.36767	3.4	18.5	15.1	0
SPRING	1	92	21.1239	5.25130	7.9	30.6	22.7	0
SPRING	2	92	20.9185	5.25691	7.0	30.0	23.0	0
SPRING	3	92	21.9554	5.85940	7.2	32.2	25.0	0
SPRING	4	92	24.1076	6.27990	8.5	34.1	25.6	0
SPRING	5	92	26.0728	6.42916	9.5	38.5	29.0	0
SPRING	6	92	28.0685	6.63565	10.8	40.6	29.8	0
SPRING	7	92	29.3750	6.84007	12.5	41.6	29.1	0
SPRING	8	92	30.4043	6.82878	12.8	43.2	30.4	0
SPRING	9	92	30.8761	6.70542	14.4	43.6	29.2	0
SPRING	10	92	31.0098	6.82450	14.5	43.5	29.0	0
SPRING	11	92	30.7446	6.96526	14.0	44.0	30.0	0
SPRING	12	92	30.1152	6.90550	13.5	44.6	31.1	0
SPRING	13	92	29.6054	6.86092	14.7	43.5	28.8	0
SPRING	14	92	28.3011	6.63034	14.4	41.0	26.6	0
SPRING	15	92	27.0685	6.24514	13.4	39.1	25.7	0
SPRING	16	92	26.3641	6.04568	13.4	37.4	24.0	0
SPRING	17	92	25.7304	5.81156	12.5	36.0	23.5	0
SPRING	18	92	25.1326	5.83259	11.6	39.5	27.9	0
SPRING	19	92	24.3033	5.53454	10.8	33.5	22.7	0
SPRING	20	92	23.5413	5.31335	10.4	32.2	21.8	0
SPRING	21	92	22.9717	5.31526	9.1	31.6	22.5	0
SPRING	22	92	22.3957	5.26416	8.9	31.6	22.7	0
SPRING	23	92	22.0152	5.41384	9.1	31.0	21.9	0
SPRING	24	92	21.6435	5.24734	8.6	30.9	22.3	0
SUMMER	1	92	30.6391	2.22261	26.4	38.0	11.6	0
SUMMER	2	92	30.5304	2.23905	26.0	37.6	11.6	0
SUMMER	3	92	32.2065	2.11040	28.3	38.2	9.9	0
SUMMER	4	92	34.8152	1.85904	31.3	39.1	7.8	0

SEASONAL DAILY CYCLE OF TEMPERATURE (DEG. C.) OF YEAR 79-80

SEASON	HOUR	_FREQ_	MEAN	STD	MIN	MAX	RANGE	MISSING
SUMMER	5	92	37.3326	1.75688	34.0	41.0	7.0	0
SUMMER	6	92	39.7424	1.80550	35.4	45.4	10.0	0
SUMMER	7	92	41.5261	1.84837	37.6	46.0	8.4	0
SUMMER	8	92	42.7946	1.95624	38.2	48.0	9.8	0
SUMMER	9	92	43.5511	1.93643	38.2	48.0	9.8	0
SUMMER	10	92	43.8391	1.81647	38.5	48.9	10.4	0
SUMMER	11	92	43.9478	1.84101	39.0	47.9	8.9	0
SUMMER	12	92	43.7011	1.84102	38.9	47.8	8.9	0
SUMMER	13	92	42.9261	1.93748	37.0	47.5	10.5	0
SUMMER	14	92	41.8000	2.01069	35.4	46.5	11.1	0
SUMMER	15	92	40.0326	1.89517	33.6	43.8	10.2	0
SUMMER	16	92	38.6804	1.75169	33.4	42.0	8.6	0
SUMMER	17	92	37.6630	1.84496	31.7	42.2	10.5	0
SUMMER	18	92	36.4717	1.78093	30.4	39.7	9.3	0
SUMMER	19	92	35.5815	1.94314	29.6	39.8	10.2	0
SUMMER	20	92	34.4609	2.00488	29.0	38.6	9.6	0
SUMMER	21	92	33.6815	2.04552	29.2	39.0	9.8	0
SUMMER	22	92	32.7804	2.18316	28.4	38.6	10.2	0
SUMMER	23	92	32.0424	2.09265	27.5	38.4	10.9	0
SUMMER	24	92	31.3761	2.20526	26.9	38.8	11.9	0
AUTUMN	1	91	20.2286	4.72460	7.8	29.7	21.9	0
AUTUMN	2	91	19.8308	4.65999	7.0	29.1	22.1	0
AUTUMN	3	91	20.7736	5.17206	7.6	30.0	22.4	0
AUTUMN	4	91	23.9308	5.55039	10.0	34.0	24.0	0
AUTUMN	5	91	26.8912	5.89012	13.0	37.6	24.6	0
AUTUMN	6	91	29.5890	6.22039	15.4	40.0	24.6	0
AUTUMN	7	91	31.5176	6.53117	15.8	42.2	26.4	0
AUTUMN	8	91	32.9231	6.76619	16.2	44.1	27.9	0
AUTUMN	9	91	33.8264	6.85277	18.5	45.4	26.9	0
AUTUMN	10	91	34.1945	6.89709	16.4	45.5	29.1	0
AUTUMN	11	91	33.9022	6.81174	15.5	45.5	30.0	0
AUTUMN	12	91	33.0956	6.86001	15.8	45.1	29.3	0
AUTUMN	13	91	31.7253	6.76365	16.0	44.0	28.0	0
AUTUMN	14	91	29.6571	6.32837	15.7	41.5	25.8	0
AUTUMN	15	91	27.9769	5.85548	15.3	38.6	23.3	0
AUTUMN	16	91	26.7615	5.60259	13.8	36.0	22.2	0
AUTUMN	17	91	25.5044	5.34420	12.4	36.4	23.7	0
AUTUMN	18	91	24.3516	5.19885	11.4	33.7	22.3	0
AUTUMN	19	91	23.5000	5.29215	10.4	34.5	24.1	0
AUTUMN	20	91	22.7209	5.32302	9.5	34.6	25.1	0
AUTUMN	21	91	22.1505	5.23599	9.0	33.5	24.5	0
AUTUMN	22	91	21.4879	5.12798	8.8	33.0	24.2	0
AUTUMN	23	91	21.0451	5.00516	8.4	31.6	23.2	0
AUTUMN	24	91	20.6143	4.90260	7.6	31.0	23.4	0

MONTHLY ANALYSIS OF TEMPERATURE (DEG. C.) OF YEAR 1981

MONTH	_FREQ_	MEAN	STD	MIN	MINDAY	MINHR	MAX	MAXDAY	MAXHR	RATUBERGE	MISSING
1	744	13.7528	4.13114	2.8	16	3	24.7	24	10	21.9	0
2	672	15.0868	4.13906	3.2	35	3	25.1	39	9	21.9	0
3	744	20.0030	4.99447	7.9	63	1	33.0	79	10	25.1	0
4	744	20.0030	4.99447	7.9	63	1	33.0	90	14	25.1	0
5	720	25.1946	6.33460	7.3	93	2	38.9	115	8	31.6	0
6	744	30.9173	5.81577	15.5	123	2	43.2	146	11	27.7	0
7	720	35.4267	6.00808	22.8	161	1	48.5	154	10	25.7	0
8	720	35.4267	6.00808	22.8	164	24	48.5	181	11	25.7	0
9	744	37.8040	5.59611	25.0	185	1	47.5	198	12	22.5	0
10	744	37.3270	5.88156	24.5	236	2	50.3	221	10	25.8	0
11	720	32.9700	6.62974	19.4	272	1	45.6	246	10	26.2	0
12	720	32.9700	6.62974	19.4	272	1	45.6	246	11	26.2	0
13	744	26.4867	6.26997	13.2	294	2	40.2	274	10	27.0	0
14	720	19.6192	5.76641	4.9	329	23	35.5	306	9	30.6	0
15	744	15.7457	4.46335	7.3	336	1	27.7	359	11	20.4	0

YEARLY ANALYSIS OF TEMPERATURE (DEG. C.) OF YEAR 1981

FREQ	MEAN	STD	MIN	MINMONTH	MINDAY	MINHR	MAX	MAXMONTH	MAXDAY	MAXHR	RATUENCE	MISSING
8760	25.9229	10.2137	2.8	1	16	3	50.3	8	221	10	47.5	0

SEASONAL ANALYSIS OF TEMPERATURE (DEG. C.) FOR 1980-1981

SEASON	FREQ.	MEAN	STD	MIN	MINMONTH	MINDAY	MINHR	MAX	MAXMONTH	MAXDAY	MAXHR	RA TURENCE	MISSIN
WINTER	2160	13.9977	4.42281	2.8	1	16	3	26.0	12	342	10	23.2	0
SPRING	2208	25.3736	7.27679	7.3	4	93	2	43.2	5	146	11	35.9	0
SUMMER	2208	36.8681	5.91545	22.8	6	161	1	50.3	8	221	10	27.5	0
SUMMER	2208	36.8681	5.91545	22.8	6	164	24	50.3	8	221	10	27.5	0
AUTUMN	2184	26.3600	8.25903	4.9	11	329	23	45.6	9	246	10	40.7	0
AUTUMN	2184	26.3600	8.25903	4.9	11	329	23	45.6	9	246	11	40.7	0

SEASONAL DAILY CYCLE OF TEMPERATURE (DEG. C.) OF YEAR 80-81

SEASON	HOOR	_FREQ_	MEAN	STD	MIN	MAX	RATRENGE	MISSING
WINTER	1	90	10.0911	3.84292	3.0	18.5	15.5	0
WINTER	2	90	9.8833	3.89798	3.1	18.6	15.5	0
WINTER	3	90	9.6667	4.02819	2.8	18.5	15.7	0
WINTER	4	90	11.1878	3.42233	4.7	19.4	14.7	0
WINTER	5	90	13.2322	2.87335	8.0	19.0	11.0	0
WINTER	6	90	15.1744	2.54318	10.6	21.7	11.1	0
WINTER	7	90	16.8689	2.64845	11.7	23.5	11.8	0
WINTER	8	90	17.9811	2.79469	11.4	25.0	13.6	0
WINTER	9	90	18.6722	2.84004	10.7	25.5	14.8	0
WINTER	10	90	19.0322	2.82177	11.0	26.0	15.0	0
WINTER	11	90	19.0056	2.65890	11.0	25.3	14.3	0
WINTER	12	90	18.4622	2.46698	11.0	23.3	12.3	0
WINTER	13	90	17.4100	2.29616	10.7	22.3	11.6	0
WINTER	14	90	16.1656	2.29769	10.1	21.0	10.9	0
WINTER	15	90	15.0856	2.37442	9.7	19.2	9.5	0
WINTER	16	90	14.2056	2.53024	9.6	19.7	10.1	0
WINTER	17	90	12.7567	2.80063	7.7	19.6	11.9	0
WINTER	18	90	12.1644	3.20951	6.5	19.5	13.0	0
WINTER	19	90	11.7311	3.20732	6.0	19.3	13.3	0
WINTER	20	90	11.4000	3.32512	4.8	19.0	14.2	0
WINTER	21	90	11.1344	3.45397	4.0	19.0	15.0	0
WINTER	22	90	10.7622	3.67719	4.0	18.8	14.8	0
WINTER	23	90	10.4322	3.85419	3.5	19.0	15.5	0
WINTER	24	90	19.3239	5.70223	7.4	31.5	24.1	0
SPRING	1	92	19.1935	5.82284	7.3	31.0	23.7	0
SPRING	2	92	20.8761	6.02074	8.2	32.1	23.9	0
SPRING	3	92	23.5707	5.92587	11.8	34.8	23.0	0
SPRING	4	92	26.0207	6.05705	14.0	36.6	22.6	0
SPRING	5	92	27.9576	6.24490	15.6	39.5	23.9	0
SPRING	6	92	29.3152	6.39304	16.2	40.9	24.7	0
SPRING	7	92	30.4946	6.32557	18.2	42.0	23.8	0
SPRING	8	92	31.3565	6.29258	19.0	42.9	23.9	0
SPRING	9	92	31.6402	6.26476	19.5	42.6	23.1	0
SPRING	10	92	31.5413	6.23852	19.5	43.2	23.7	0
SPRING	11	92	30.9174	6.13390	19.3	42.7	23.4	0
SPRING	12	92	30.0413	6.09129	18.6	41.9	23.3	0
SPRING	13	92	28.6598	6.08591	17.5	40.1	22.6	0
SPRING	14	92	26.7935	5.84396	16.4	37.5	21.1	0
SPRING	15	92	25.6402	5.67886	15.3	36.4	21.1	0
SPRING	16	92	24.6924	5.63908	13.6	35.4	21.8	0
SPRING	17	92	23.6902	5.62856	12.8	35.1	22.3	0
SPRING	18	92	22.7391	5.50903	11.6	34.5	22.9	0
SPRING	19	92	22.0152	5.45084	11.1	33.6	22.5	0
SPRING	20	92	21.4043	5.47989	10.7	32.3	21.6	0
SPRING	21	92	20.7717	5.64864	8.6	34.1	25.5	0
SPRING	22	92	20.3630	5.78812	8.4	32.0	23.6	0
SPRING	23	92	19.9467	5.61148	8.3	31.7	23.4	0
SPRING	24	92	28.6500	2.77479	22.8	36.0	13.2	0
SUMMER	1	92	28.9935	2.47896	23.8	35.8	12.0	0
SUMMER	2	92	32.1674	1.90581	27.7	37.0	9.3	0
SUMMER	3	92	35.4728	1.83902	31.0	39.7	8.7	0
SUMMER	4	92						

SEASONAL DAILY CYCLE OF TEMPERATURE (DEG. C.) OF YEAR 80-81

SEASON	HOUR	_ FREQ_	MEAN	STD	MIN	MAX	RATRENGE	MISSING
SUMMER	5	92	38.0109	2.05947	32.0	42.8	10.8	0
SUMMER	6	92	40.3728	2.26760	34.0	44.9	10.9	0
SUMMER	7	92	41.9511	2.30153	35.0	47.1	12.1	0
SUMMER	8	92	43.1065	2.39944	36.1	48.3	12.2	0
SUMMER	9	92	43.8880	2.32983	37.5	49.0	11.5	0
SUMMER	10	92	44.2652	2.32334	38.5	50.3	11.8	0
SUMMER	11	92	44.2152	2.33096	38.4	50.0	11.6	0
SUMMER	12	92	43.7370	2.46196	38.2	49.7	11.5	0
SUMMER	13	92	42.8880	2.58699	37.0	49.5	12.5	0
SUMMER	14	92	41.4380	2.48533	35.5	47.5	12.0	0
SUMMER	15	92	39.4446	2.28157	34.2	44.5	10.3	0
SUMMER	16	92	37.3728	2.54477	24.6	43.7	19.1	0
SUMMER	17	92	36.0761	2.27390	31.4	41.6	10.2	0
SUMMER	18	92	34.8087	2.31970	29.8	40.4	10.6	0
SUMMER	19	92	33.5924	2.44182	27.5	39.5	12.0	0
SUMMER	20	92	32.6054	2.50245	26.2	38.2	12.0	0
SUMMER	21	92	31.6272	2.64480	25.4	39.4	14.0	0
SUMMER	22	92	30.7870	2.62026	25.4	38.6	13.2	0
SUMMER	23	92	30.0522	2.64959	24.2	37.3	13.1	0
SUMMER	24	92	29.3109	2.49441	22.8	35.7	12.9	0
AUTUMN	1	91	19.6264	5.51873	6.0	29.9	23.9	0
AUTUMN	2	91	19.1253	5.52340	6.0	29.8	23.8	0
AUTUMN	3	91	20.3703	6.10836	6.5	30.9	24.4	0
AUTUMN	4	91	23.7143	6.40591	9.2	33.6	24.4	0
AUTUMN	5	91	26.9066	6.65627	11.9	36.8	24.9	0
AUTUMN	6	91	29.8341	7.08788	14.1	40.6	26.5	0
AUTUMN	7	91	31.9220	7.35838	15.2	42.6	27.4	0
AUTUMN	8	91	33.1890	7.36589	16.0	43.7	27.7	0
AUTUMN	9	91	34.0879	7.34152	16.6	44.9	28.3	0
AUTUMN	10	91	34.2868	7.28477	17.2	45.6	28.4	0
AUTUMN	11	91	34.0011	7.30366	17.5	45.6	28.1	0
AUTUMN	12	91	33.1549	7.21768	16.9	45.2	28.3	0
AUTUMN	13	91	31.5462	7.06710	15.9	43.5	27.6	0
AUTUMN	14	91	29.4330	6.62343	14.7	41.0	26.3	0
AUTUMN	15	91	27.6681	6.15911	12.7	39.3	26.6	0
AUTUMN	16	91	26.3967	5.99684	11.8	38.2	26.4	0
AUTUMN	17	91	25.1813	6.01705	10.9	37.0	26.1	0
AUTUMN	18	91	23.9802	5.76322	9.0	35.4	26.4	0
AUTUMN	19	91	23.1198	5.81764	7.9	35.2	27.3	0
AUTUMN	20	91	22.3505	5.89400	7.0	34.0	27.0	0
AUTUMN	21	91	21.4934	5.71141	6.5	33.7	27.2	0
AUTUMN	22	91	21.0088	5.63567	6.6	32.2	25.6	0
AUTUMN	23	91	20.3407	5.60208	4.9	30.7	25.8	0
AUTUMN	24	91	19.9033	5.61337	5.8	31.4	25.6	0

MONTHLY ANALYSIS OF TEMPERATURE IN DEG. C. J OF YEAR 1982

MONTH	MEAN	STD	MIN	MINDAY	MINHR	MAX	MAXDAY	MAXHR	RANGE	MISSING
1	12.5788	4.30213	1.6	21	3	22.5	31	10	20.9	0
1	12.5789	4.30213	1.6	21	3	22.5	31	11	20.9	0
2	12.0323	3.90373	2.9	50	3	23.4	59	9	20.5	0
3	17.1465	4.52865	6.0	68	2	31.6	83	12	25.6	0
4	26.0217	5.42946	10.5	52	1	39.3	116	11	28.8	0
4	26.0217	5.42946	10.5	52	2	39.3	116	11	28.8	0
5	32.3658	4.92596	22.4	146	1	44.1	151	10	21.7	0
6	36.3589	5.63873	23.7	174	1	47.3	158	11	23.6	0
7	37.4504	5.76642	26.0	191	1	49.0	200	9	23.0	0
7	37.4504	5.76642	26.0	157	2	49.0	200	9	23.0	0
8	36.5341	5.34615	23.7	239	2	47.0	232	10	23.3	0
9	33.5341	5.34615	23.7	238	2	47.0	232	11	23.3	0
9	33.8618	6.21322	22.2	272	2	47.0	249	10	24.8	0
10	27.1586	4.85977	14.6	303	2	40.6	278	11	26.0	0
11	16.3987	5.35800	1.4	325	20	30.5	313	10	25.1	0
12	11.2561	4.42886	1.9	346	1	22.5	363	10	20.6	0

YEARLY ANALYSIS OF TEMPERATURE (DEG. C.) OF YEAR 1982

12

PREC	MEAN	STD	MIN	MINMONTH	MINDAY	MINR	MAX	MAXMONTH	MAXDAY	MAXHR	RANGE	MISSING
9/83	25.0625	11.2225	1.4	11	325	20	45	7	200	9	47.6	0

SEASONAL ANALYSIS OF TEMPERATURE (DEG. C.) FOR 1981-1982

SEASON	FREQ	MEAN	STD	MIN	MINMONTH	MINDAY	MINHR	MAX	MAXMONTH	MAXDAY	MAXHR	RANGE	MISSING
WINTER	2160	13.4972	4.54798	1.6	1	21	3	27.7	12	359	11	26.1	0
SPRING	2208	22.1762	6.00564	6.0	3	88	2	44.1	5	151	10	38.1	0
SUMMER	2208	36.7988	5.60300	23.7	6	174	1	49.0	7	200	9	25.3	0
SUMMER	2208	36.7988	5.60300	23.7	8	238	2	49.0	7	200	9	25.3	0
AUTUMN	2184	25.0015	5.01329	1.4	11	325	20	47.0	9	249	10	45.6	0

SEASONAL DAILY CYCLE OF TEMPERATURE (DEG. C.) OF YEAR 81-82

SEASON	HOURL	_FREQ_	MEAN	STD	MIN	MAX	RANGE	MISSING
WINTER	1	50	9.3000	3.43767	2.2	18.4	16.2	0
WINTER	2	50	9.1722	3.48828	2.0	18.0	16.0	0
WINTER	3	50	8.9156	3.5325	1.6	18.0	16.4	0
WINTER	4	50	10.3289	3.21320	3.2	19.0	15.8	0
WINTER	5	50	12.4444	2.94642	6.5	20.6	14.1	0
WINTER	6	50	14.6444	3.02808	8.5	21.5	13.0	0
WINTER	7	50	16.2376	3.38943	8.5	23.0	14.5	0
WINTER	8	50	17.5544	3.43256	10.9	24.5	13.6	0
WINTER	9	50	18.3522	3.46855	11.4	25.1	13.7	0
WINTER	10	50	19.0911	3.49528	11.2	27.0	15.8	0
WINTER	11	50	18.7211	3.35953	11.4	27.7	16.3	0
WINTER	12	50	18.1622	3.07365	11.5	27.2	15.7	0
WINTER	13	50	17.6667	2.63167	10.8	23.8	13.0	0
WINTER	14	50	15.7378	2.44092	10.0	21.5	11.5	0
WINTER	15	50	14.7850	2.47207	9.1	20.0	10.9	0
WINTER	16	50	13.5578	2.55446	8.5	19.0	10.5	0
WINTER	17	50	13.1526	2.65872	7.5	18.7	11.2	0
WINTER	18	50	12.4290	2.83262	6.7	18.4	11.7	0
WINTER	19	50	11.7633	2.93171	5.5	18.0	12.5	0
WINTER	20	50	11.2333	3.06176	5.1	18.1	13.0	0
WINTER	21	50	10.7578	3.09998	4.4	17.6	13.2	0
WINTER	22	50	10.3533	3.13910	3.6	18.1	14.5	0
WINTER	23	50	10.0800	3.17459	3.4	18.3	14.9	0
WINTER	24	50	9.6750	3.29403	3.4	18.0	14.6	0
SPRING	1	52	19.7429	6.68567	6.2	32.3	26.1	0
SPRING	2	52	19.6898	6.81727	6.0	32.1	26.1	0
SPRING	3	52	21.0391	7.35711	8.5	34.0	25.5	0
SPRING	4	52	23.4674	7.19125	11.6	37.0	25.4	0
SPRING	5	52	25.7633	7.31214	13.3	40.0	26.7	0
SPRING	6	52	27.4428	7.32620	13.8	40.8	27.0	0
SPRING	7	52	28.7676	7.46800	13.5	42.0	28.5	0
SPRING	8	52	29.6311	7.48930	14.0	42.5	28.5	0
SPRING	9	52	30.4326	7.42238	15.0	43.1	28.1	0
SPRING	10	52	30.6239	7.51531	16.5	44.1	27.6	0
SPRING	11	52	30.6428	7.40334	16.8	43.1	26.3	0
SPRING	12	52	30.1567	7.30940	16.6	43.0	26.4	0
SPRING	13	52	29.3989	7.19216	15.4	42.5	27.1	0
SPRING	14	52	28.8767	7.16614	15.1	41.2	26.1	0
SPRING	15	52	28.6467	7.02053	14.9	39.4	24.5	0
SPRING	16	52	29.4533	6.82316	14.3	37.1	22.8	0
SPRING	17	52	24.3956	6.78611	13.0	36.8	23.8	0
SPRING	18	52	23.7376	6.76690	12.0	36.0	24.0	0
SPRING	19	52	22.9267	6.67061	11.2	35.0	23.8	0
SPRING	20	52	22.1524	6.76436	9.7	34.4	24.7	0
SPRING	21	52	21.5513	6.68899	8.6	34.0	25.4	0
SPRING	22	52	21.0228	6.73180	7.2	33.4	26.2	0
SPRING	23	52	20.6169	6.78278	7.4	33.2	25.8	0
SPRING	24	52	20.2174	6.72877	7.1	33.0	25.9	0
SUMMER	1	52	28.6169	6.49476	23.7	35.0	11.3	0
SUMMER	2	52	28.7913	6.33815	23.7	34.7	11.0	0
SUMMER	3	52	31.3533	1.78353	26.2	35.5	9.3	0
SUMMER	4	52	34.5876	1.56873	29.8	38.0	8.2	0

SEASONAL DAILY CYCLE OF TEMPERATURE (DEG. C.) OF YEAR 81-82

STATION	HOUR	_FREQ_	MEAN	STD	MIN	MAX	RANGE	MISSING
SUMNER	5	92	37.1603	1.67406	32.5	41.4	8.9	0
SUMNER	6	92	39.2429	1.62764	35.0	44.5	9.5	0
SUMNER	7	92	41.4058	1.94750	36.8	47.0	10.2	0
SUMNER	8	92	42.7250	1.95429	37.2	47.8	10.6	0
SUMNER	9	92	43.5272	1.97990	37.6	49.0	11.4	0
SUMNER	10	92	43.8527	1.92485	38.0	48.5	10.5	0
SUMNER	11	92	43.6663	1.98662	38.0	48.5	10.5	0
SUMNER	12	92	43.4253	1.98503	37.1	48.0	10.9	0
SUMNER	13	92	42.6476	2.04904	36.4	47.6	11.2	0
SUMNER	14	92	41.2370	2.03209	34.4	45.6	11.2	0
SUMNER	15	92	39.3707	1.83666	33.3	44.0	10.7	0
SUMNER	16	92	37.0227	1.76755	32.5	42.0	9.5	0
SUMNER	17	92	36.8605	2.06957	30.5	41.8	11.3	0
SUMNER	18	92	35.5213	2.22659	29.5	40.2	10.7	0
SUMNER	19	92	34.3576	2.39350	28.9	39.5	10.6	0
SUMNER	20	92	33.1641	2.43827	28.0	38.8	10.8	0
SUMNER	21	92	32.6239	2.35523	27.3	38.0	10.7	0
SUMNER	22	92	31.1109	2.40203	25.7	36.7	11.0	0
SUMNER	23	92	30.3726	2.41375	25.4	36.6	11.2	0
SUMNER	24	92	29.4004	2.57090	24.4	36.2	11.8	0
AUTUMN	1	91	20.2600	6.88126	6.4	30.2	23.8	0
AUTUMN	2	91	19.8648	6.90664	5.9	30.2	24.3	0
AUTUMN	3	91	20.6297	7.43751	5.7	32.2	26.5	0
AUTUMN	4	91	23.6999	7.86119	8.0	34.8	26.8	0
AUTUMN	5	91	26.4121	8.25076	10.0	39.7	29.7	0
AUTUMN	6	91	28.6163	8.61166	12.3	43.2	30.9	0
AUTUMN	7	91	30.5233	8.84849	13.6	45.0	31.4	0
AUTUMN	8	91	31.5286	8.59189	14.7	46.1	31.4	0
AUTUMN	9	91	32.1622	8.86141	15.6	46.4	30.8	0
AUTUMN	10	91	32.2596	8.80380	16.3	47.0	30.7	0
AUTUMN	11	91	32.6677	8.68146	16.2	46.5	30.3	0
AUTUMN	12	91	31.2912	8.65020	15.7	46.7	31.0	0
AUTUMN	13	91	30.6676	8.54748	14.7	45.6	30.9	0
AUTUMN	14	91	29.5176	8.26901	13.4	43.8	30.4	0
AUTUMN	15	91	27.6626	8.00726	10.8	41.6	30.8	0
AUTUMN	16	91	26.6319	7.88665	9.0	39.8	30.8	0
AUTUMN	17	91	25.1691	7.64546	7.8	37.5	29.7	0
AUTUMN	18	91	24.6371	7.40316	7.2	35.6	28.4	0
AUTUMN	19	91	23.6667	7.29638	6.6	33.9	27.3	0
AUTUMN	20	91	22.1509	7.41035	1.4	33.5	32.1	0
AUTUMN	21	91	21.6646	7.02276	5.6	32.0	26.4	0
AUTUMN	22	91	21.2629	7.02979	5.0	31.4	26.4	0
AUTUMN	23	91	20.6714	6.99160	4.5	30.2	25.7	0
AUTUMN	24	91	20.2661	6.92904	4.5	30.0	25.5	0

MONTHLY ANALYSIS OF PRESSURE (M BAR) OF YEAR 1978

MONTH	FREQ_	MEAN	STD	MIN	MINDAY	MINHR	MAX	MAXDAY	MAXHR	RANGE	MISSING
1	744	1014.92	3.50406	1005.0	25	17	1023.2	12	6	18.2	0
2	672	1012.38	3.29053	1004.2	40	11	1019.3	32	6	15.1	0
3	744	1008.61	3.85745	997.9	71	12	1016.6	74	7	18.7	0
4	720	1005.21	3.56859	996.1	114	12	1012.8	97	5	16.7	0
4	720	1005.21	3.56859	996.1	114	13	1012.8	97	5	16.7	0
5	744	1000.50	3.97562	992.8	149	14	1011.0	122	5	18.2	0
6	720	994.84	3.97446	988.2	165	13	1007.2	155	24	19.0	0
7	744	991.49	1.97722	980.1	210	9	999.6	210	15	19.5	0
8	744	994.30	2.21235	989.4	222	13	999.7	233	4	10.3	0
8	744	994.30	2.21235	989.4	222	13	999.7	233	6	10.3	0
9	720	1000.07	2.28281	993.4	245	13	1005.9	273	5	12.5	0
10	744	1007.02	2.30341	1000.9	275	11	1012.0	297	5	11.1	0
10	744	1007.02	2.30341	1000.9	275	12	1012.0	298	5	11.1	0
10	744	1007.02	2.30341	1000.9	275	12	1012.0	298	6	11.1	0
11	720	1014.02	3.66219	1004.7	313	10	1021.7	330	6	17.0	0
12	744	1013.67	2.82493	1004.5	336	22	1018.4	354	6	13.9	0

YEARLY ANALYSIS OF PRESSURE (M BAR) OF YEAR 1978

FREQ_	MEAN	STD	MIN	MINMONTH	MINDAY	MINHR	MAX	-MAXMONTH	MAXDAY	MAXHR	RANGE	MISSING
8760	1004.74	8.62224	980.1	7	210	9	1023.2	1	12	6	43.1	0

SEASONAL ANALYSIS OF PRESSURE (M BAR) FOR 1977-1978

SEASON	_FREQ_	MEAN	STD	MIN	MINMONTH	MINDAY	MINHR	MAX	MAXMONTH	MAXDAY	MAXHR	RANGE	MISSING
WINTER	2160	1003.45	100.333	12.9	12	345	21	1023.2	1	12	6	1010.3	0
SPRING	2208	1004.91	4.953	992.8	5	149	14	1016.6	3	74	7	23.8	0
SUMMER	2208	993.53	3.204	980.1	7	210	9	1007.2	6	155	24	27.1	0
AUTUMN	2184	1007.04	6.326	993.4	9	245	13	1021.7	11	330	6	28.3	0

SEASONAL DAILY CYCLE OF PRESSURE (M BAR) OF YEAR 77-78

SEASON	HOUR	_FREQ_	MEAN	STD	MIN	MAX	RANGE	MISSING
WINTER	1	90	1002.19	105.148	16.3	1021.6	1005.3	0
WINTER	2	90	1002.62	105.141	16.8	1022.0	1005.2	0
WINTER	3	90	1003.03	105.133	17.3	1022.6	1005.3	0
WINTER	4	90	1003.62	105.153	17.7	1022.8	1005.1	0
WINTER	5	90	1004.06	105.149	18.2	1022.9	1004.7	0
WINTER	6	90	1004.24	105.177	18.1	1023.2	1005.1	0
WINTER	7	90	1003.75	105.164	17.7	1022.8	1005.1	0
WINTER	8	90	1002.84	105.153	16.9	1022.2	1005.3	0
WINTER	9	90	1001.86	105.211	15.4	1021.4	1006.0	0
WINTER	10	90	1001.40	105.236	14.7	1021.2	1006.5	0
WINTER	11	90	1001.28	105.243	14.5	1021.5	1007.0	0
WINTER	12	90	1001.42	105.290	14.2	1021.8	1007.6	0
WINTER	13	90	1001.62	105.322	14.1	1022.0	1007.9	0
WINTER	14	90	1001.91	105.376	13.9	1022.4	1008.5	0
WINTER	15	90	1002.27	105.391	14.1	1022.7	1008.6	0
WINTER	16	90	1002.58	105.413	14.2	1023.1	1008.9	0
WINTER	17	90	1002.70	105.481	13.7	1023.0	1009.4	0
WINTER	18	90	1002.84	105.456	14.0	1023.0	1009.0	0
WINTER	19	90	1002.69	105.507	13.4	1022.8	1009.4	0
WINTER	20	90	1002.54	105.521	13.1	1022.4	1009.3	0
WINTER	21	90	1002.44	105.534	12.9	1022.7	1009.8	0
WINTER	22	90	1002.33	105.471	13.4	1022.7	1009.3	0
WINTER	23	90	1013.34	3.454	1005.3	1022.3	17.0	0
WINTER	24	90	1013.20	3.508	1005.1	1021.8	16.7	0
SPRING	1	92	1004.68	4.897	994.3	1014.8	20.5	0
SPRING	2	92	1005.23	4.526	995.7	1015.3	19.6	0
SPRING	3	92	1005.71	4.559	996.4	1015.7	19.3	0
SPRING	4	92	1006.22	4.548	996.9	1016.0	19.1	0
SPRING	5	92	1006.56	4.587	997.0	1016.2	19.2	0
SPRING	6	92	1006.58	4.558	996.5	1016.3	19.8	0
SPRING	7	92	1006.35	4.561	996.2	1016.6	20.4	0
SPRING	8	92	1005.75	4.872	995.4	1016.3	20.9	0
SPRING	9	92	1005.01	4.795	994.8	1015.7	20.9	0
SPRING	10	92	1004.36	4.761	993.7	1015.0	21.3	0
SPRING	11	92	1003.88	4.743	993.3	1014.7	21.4	0
SPRING	12	92	1003.64	4.778	993.1	1014.4	21.3	0
SPRING	13	92	1003.63	4.880	993.0	1014.8	21.8	0
SPRING	14	92	1003.78	4.528	992.8	1014.8	22.0	0
SPRING	15	92	1004.08	4.528	993.1	1015.0	21.9	0
SPRING	16	92	1004.56	4.541	994.2	1015.3	21.1	0
SPRING	17	92	1005.06	4.879	994.7	1015.7	21.0	0
SPRING	18	92	1005.21	4.826	994.9	1015.8	20.9	0
SPRING	19	92	1005.18	4.863	994.9	1015.7	20.8	0
SPRING	20	92	1004.94	4.529	995.0	1015.5	20.5	0
SPRING	21	92	1004.64	4.588	994.6	1015.4	20.8	0
SPRING	22	92	1004.33	5.017	994.3	1014.9	20.6	0
SPRING	23	92	1004.16	4.896	994.2	1014.6	20.4	0
SPRING	24	92	1004.21	4.866	994.2	1014.6	20.4	0
SUMMER	1	92	993.67	3.013	986.5	1005.0	18.1	0
SUMMER	2	92	994.08	3.055	987.4	1005.6	18.2	0
SUMMER	3	92	994.48	3.089	987.7	1005.9	18.2	0
SUMMER	4	92	994.73	3.162	987.8	1006.2	18.4	0

SEASONAL DAILY CYCLE OF PRESSURE (M BAR) OF YEAR 77-78

SEASON	HOUR	_FREQ_	MEAN	STD	MIN	MAX	RANGE	MISSING
SUMMER	5	92	994.75	3.15714	988.0	1006.2	18.2	0
SUMMER	6	92	994.82	3.20206	988.1	1006.3	18.2	0
SUMMER	7	92	994.58	3.18608	988.1	1006.0	17.9	0
SUMMER	8	92	994.13	3.15151	988.0	1005.3	17.3	0
SUMMER	9	92	993.48	3.41708	980.1	1004.7	24.6	0
SUMMER	10	92	993.04	3.12207	987.6	1004.0	16.4	0
SUMMER	11	92	992.58	3.11765	987.3	1003.4	16.1	0
SUMMER	12	92	992.23	3.10877	986.8	1002.7	15.9	0
SUMMER	13	92	992.11	3.13264	986.1	1002.7	16.6	0
SUMMER	14	92	992.26	3.13068	985.7	1002.9	17.2	0
SUMMER	15	92	992.79	3.18509	986.1	1003.3	17.2	0
SUMMER	16	92	993.21	3.10906	987.0	1004.0	17.0	0
SUMMER	17	92	993.64	3.13011	987.0	1004.4	17.4	0
SUMMER	18	92	993.87	3.11860	987.2	1004.7	17.5	0
SUMMER	19	92	993.77	3.08777	986.9	1004.7	17.8	0
SUMMER	20	92	993.56	3.03088	986.4	1004.4	18.0	0
SUMMER	21	92	993.25	3.00327	986.0	1004.0	18.0	0
SUMMER	22	92	993.13	2.98467	986.0	1004.0	18.0	0
SUMMER	23	92	993.13	2.55517	986.3	1004.2	17.9	0
SUMMER	24	92	993.38	3.18216	986.5	1007.2	20.7	0
AUTUMN	1	91	1006.91	6.25662	994.2	1019.5	25.3	0
AUTUMN	2	91	1007.38	6.28898	994.5	1019.7	25.2	0
AUTUMN	3	91	1007.93	6.36144	995.1	1020.4	25.3	0
AUTUMN	4	91	1008.42	6.38506	995.6	1020.9	25.3	0
AUTUMN	5	91	1008.65	6.41139	996.0	1021.6	25.6	0
AUTUMN	6	91	1008.56	6.36612	996.9	1021.7	24.8	0
AUTUMN	7	91	1008.05	6.31508	995.7	1021.0	25.3	0
AUTUMN	8	91	1007.34	6.28445	995.5	1020.3	24.8	0
AUTUMN	9	91	1006.57	6.21364	995.1	1020.0	24.9	0
AUTUMN	10	91	1005.98	6.20649	994.8	1018.7	23.9	0
AUTUMN	11	91	1005.76	6.34669	994.1	1018.7	24.6	0
AUTUMN	12	91	1005.64	6.40011	993.6	1018.5	24.9	0
AUTUMN	13	91	1005.77	6.43237	993.4	1018.8	25.4	0
AUTUMN	14	91	1006.07	6.45134	993.7	1019.0	25.3	0
AUTUMN	15	91	1006.54	6.46253	994.2	1019.3	25.1	0
AUTUMN	16	91	1007.00	6.30357	994.7	1019.7	25.0	0
AUTUMN	17	91	1007.36	6.15267	995.1	1020.0	24.9	0
AUTUMN	18	91	1007.32	6.21031	994.8	1019.8	25.0	0
AUTUMN	19	91	1007.25	6.23015	994.3	1019.8	25.5	0
AUTUMN	20	91	1007.16	6.21023	994.2	1019.3	25.1	0
AUTUMN	21	91	1006.97	6.26166	993.9	1019.2	25.3	0
AUTUMN	22	91	1006.85	6.24563	993.7	1019.3	25.6	0
AUTUMN	23	91	1006.78	6.25053	993.5	1019.0	25.5	0
AUTUMN	24	91	1006.84	6.17591	994.0	1019.2	25.2	0

MONTHLY ANALYSIS OF PRESSURE (M BAR) OF YEAR 1979

MONTH	FREQ	MEAN	STD	MIN	MINDAY	MINHR	MAX	MAXDAY	MAXHR	RANGE	MISSING
1	744	1014.25	3.59369	1001.9	9	8	1024.6	25	6	22.7	0
2	672	1010.12	3.32648	999.3	41	12	1017.5	36	6	18.2	0
3	744	1008.50	4.32752	992.8	85	13	1018.1	65	6	25.3	0
4	720	1005.89	3.56145	996.7	112	11	1014.2	116	6	17.5	0
5	744	1003.25	2.29484	997.2	142	13	1010.8	139	4	13.6	0
6	720	997.54	2.94197	991.5	181	22	1003.7	156	5	12.2	0
6	720	997.54	2.94197	991.5	181	22	1003.7	161	18	12.2	0
7	744	993.65	2.41357	988.2	211	12	1001.0	190	5	12.8	0
8	744	994.28	3.29396	986.6	217	13	1001.5	243	5	14.9	0
9	720	999.60	2.10724	993.0	248	13	1007.2	256	18	14.2	0
10	744	1006.80	2.78895	1000.4	277	11	1013.4	303	5	13.0	0
11	720	1010.00	3.26265	1000.4	332	23	1018.0	329	5	17.6	0
11	720	1010.00	3.26265	1000.4	332	24	1018.0	329	5	17.6	0
12	744	1012.95	3.85538	1002.0	349	2	1022.0	336	6	20.0	0

YEARLY ANALYSIS OF PRESSURE (M BAR) OF YEAR 1979

FREQ	MEAN	STD	MIN	MINMONTH	MINDAY	MINHR	MAX	MAXMONTH	MAXDAY	MAXHR	RANGE	MISSING
8760	1004.71	7.50012	986.6	8	217	13	1024.6	1	25	6	38	0

SEASONAL ANALYSIS OF PRESSURE (H BAR) FOR 1978-1979

14

SEASON	FREQ.	MEAN	STD	MIN	MINMONTH	MINDAY	MINHR	MAX	MAXMONTH	MAXDAY	MAXHR	RANGE	MISSING
WINTER	2160	1012.77	3.71975	999.3	2	41	12	1024.6	1	25	6	25.3	0
SPRING	2208	1005.88	4.10632	992.8	3	85	13	1018.1	3	65	6	23.3	0
SUMMER	2208	995.13	3.36237	986.6	8	217	13	1003.7	6	156	5	17.1	0
SUMMER	2208	995.13	3.36237	986.6	8	217	13	1003.7	6	161	18	17.1	0
AUTUMN	2184	1005.48	5.13414	993.0	9	240	13	1018.0	11	329	5	25.0	0

SEASONAL DAILY CYCLE OF PRESSURE (K BAR) OF YEAR 78-79

SEASON	HOUR	_FREQ_	MEAN	STD	MIN	MAX	RANGE	MISSING
WINTER	1	90	1012.41	3.73746	1001.8	1020.8	19.0	0
WINTER	2	90	1012.92	3.69433	1003.1	1021.5	18.4	0
WINTER	3	90	1013.38	3.68858	1003.7	1022.2	18.5	0
WINTER	4	90	1013.82	3.68246	1004.1	1023.0	18.9	0
WINTER	5	90	1014.32	3.70148	1004.2	1024.1	19.9	0
WINTER	6	90	1014.38	3.80301	1003.8	1024.6	20.8	0
WINTER	7	90	1013.89	3.77313	1003.1	1024.1	21.0	0
WINTER	8	90	1013.04	3.81134	1001.9	1023.3	21.4	0
WINTER	9	90	1012.15	3.74422	1001.1	1022.0	20.9	0
WINTER	10	90	1011.66	3.76389	999.9	1021.3	21.4	0
WINTER	11	90	1011.51	3.70742	999.4	1020.9	21.5	0
WINTER	12	90	1011.54	3.75397	999.3	1021.0	21.7	0
WINTER	13	90	1011.81	3.69452	1000.1	1021.3	21.2	0
WINTER	14	90	1012.17	3.63961	1001.4	1021.3	19.9	0
WINTER	15	89	1012.54	3.60928	1003.2	1021.4	18.2	0
WINTER	16	91	1012.92	3.48961	1003.5	1021.4	17.9	0
WINTER	17	90	1013.05	3.43175	1004.1	1021.4	17.3	0
WINTER	18	90	1013.13	3.39715	1004.4	1021.2	16.8	0
WINTER	19	90	1013.03	3.49705	1004.5	1021.2	16.7	0
WINTER	20	90	1012.78	3.55226	1004.8	1020.9	16.1	0
WINTER	21	90	1012.70	3.53825	1004.9	1020.8	15.9	0
WINTER	22	90	1012.57	3.63930	1004.5	1020.9	16.4	0
WINTER	23	90	1012.46	3.62963	1004.0	1020.8	16.8	0
WINTER	24	90	1012.33	3.72728	1002.2	1020.6	18.4	0
SPRING	1	92	1005.76	4.03565	997.4	1015.5	18.1	0
SPRING	2	92	1006.25	4.01419	998.4	1015.8	17.4	0
SPRING	3	92	1006.73	3.97944	998.8	1016.4	17.6	0
SPRING	4	92	1007.23	4.06349	999.7	1017.7	18.0	0
SPRING	5	92	1007.48	4.14838	998.8	1018.0	19.2	0
SPRING	6	92	1007.44	4.15171	998.3	1018.1	19.8	0
SPRING	7	92	1007.12	4.15542	997.8	1017.6	19.8	0
SPRING	8	92	1006.58	4.08684	998.0	1017.3	19.3	0
SPRING	9	92	1005.95	4.04305	997.2	1016.6	19.4	0
SPRING	10	92	1005.26	4.03637	995.7	1015.8	20.1	0
SPRING	11	92	1004.78	4.07883	994.3	1015.7	21.4	0
SPRING	12	92	1004.50	4.04325	993.9	1015.4	21.5	0
SPRING	13	92	1004.53	4.06494	992.8	1015.1	22.3	0
SPRING	14	92	1004.70	4.02940	993.3	1015.1	21.8	0
SPRING	15	92	1005.04	4.08056	993.5	1015.0	21.5	0
SPRING	16	92	1005.52	4.10042	994.4	1015.1	20.7	0
SPRING	17	92	1005.92	4.05800	994.1	1015.8	21.7	0
SPRING	18	92	1006.17	3.92311	995.8	1016.1	20.3	0
SPRING	19	92	1006.16	3.87872	997.7	1015.8	18.1	0
SPRING	20	92	1006.01	3.92842	998.3	1015.9	17.6	0
SPRING	21	92	1005.77	3.99121	997.3	1015.9	18.6	0
SPRING	22	92	1005.50	3.99221	997.2	1015.9	18.7	0
SPRING	23	92	1005.33	3.96650	996.8	1015.7	18.9	0
SPRING	24	92	1005.39	3.95300	997.0	1015.4	18.4	0
SUMMER	1	92	995.30	3.21049	988.5	1002.6	14.1	0
SUMMER	2	92	995.72	3.21048	989.2	1003.2	14.0	0
SUMMER	3	92	996.12	3.22963	989.5	1003.3	13.8	0
SUMMER	4	92	996.34	3.24034	989.8	1003.5	13.7	0

SEASONAL DAILY CYCLE OF PRESSURE (M BAR) OF YEAR 78-79

SEASON	HOUR	_FREQ_	MEAN	STD	MIN	MAX	RANGE	MISSING
SUMMER	5	92	996.45	3.25757	989.7	1003.7	14.0	0
SUMMER	6	92	996.41	3.25204	989.4	1003.5	14.1	0
SUMMER	7	92	996.21	3.29733	989.1	1003.4	14.3	0
SUMMER	8	92	995.74	3.30597	988.6	1003.3	14.7	0
SUMMER	9	92	995.20	3.33134	988.2	1002.9	14.7	0
SUMMER	10	92	994.64	3.32380	987.6	1002.0	14.4	0
SUMMER	11	92	994.18	3.31801	987.1	1001.9	14.8	0
SUMMER	12	92	993.87	3.33582	986.8	1001.6	14.8	0
SUMMER	13	92	993.74	3.33984	986.6	1001.7	15.1	0
SUMMER	14	92	993.86	3.33681	986.7	1002.1	15.4	0
SUMMER	15	92	994.25	3.37494	987.1	1002.4	15.3	0
SUMMER	16	92	994.72	3.33753	987.7	1002.9	15.2	0
SUMMER	17	92	995.14	3.35024	988.4	1003.2	14.8	0
SUMMER	18	92	995.38	3.32790	988.6	1003.7	15.1	0
SUMMER	19	92	995.30	3.30343	988.7	1003.4	14.7	0
SUMMER	20	92	995.13	3.29200	988.5	1003.3	14.8	0
SUMMER	21	92	994.89	3.19638	988.5	1003.0	14.5	0
SUMMER	22	92	994.77	3.20817	988.4	1002.7	14.3	0
SUMMER	23	92	994.78	3.19616	988.2	1002.6	14.4	0
SUMMER	24	92	994.98	3.19616	988.3	1002.5	14.2	0
AUTUMN	1	91	1005.45	5.01326	994.3	1016.0	21.7	0
AUTUMN	2	91	1005.86	5.06572	994.8	1016.7	21.9	0
AUTUMN	3	91	1006.35	5.11408	995.2	1017.1	21.9	0
AUTUMN	4	91	1006.78	5.13266	995.3	1017.4	22.1	0
AUTUMN	5	91	1007.08	5.18799	995.4	1018.0	22.6	0
AUTUMN	6	91	1007.01	5.15032	995.4	1017.8	22.4	0
AUTUMN	7	91	1006.52	5.09109	995.0	1017.3	22.3	0
AUTUMN	8	91	1005.80	4.98100	994.5	1016.4	21.9	0
AUTUMN	9	91	1005.05	4.91310	993.8	1015.5	21.7	0
AUTUMN	10	91	1004.54	4.94070	993.4	1014.9	21.5	0
AUTUMN	11	91	1004.27	5.01714	993.1	1015.0	21.9	0
AUTUMN	12	91	1004.23	5.08112	993.1	1015.3	22.2	0
AUTUMN	13	91	1004.34	5.15526	993.0	1015.2	22.2	0
AUTUMN	14	91	1004.55	5.22207	993.1	1015.7	22.6	0
AUTUMN	15	91	1004.99	5.26885	993.3	1015.7	22.4	0
AUTUMN	16	91	1005.42	5.18084	993.8	1016.0	22.2	0
AUTUMN	17	91	1005.64	5.06444	994.7	1016.0	21.3	0
AUTUMN	18	91	1005.78	4.97766	995.0	1016.0	21.0	0
AUTUMN	19	91	1005.56	5.08005	994.8	1015.9	21.1	0
AUTUMN	20	91	1005.39	5.08076	994.4	1015.7	21.3	0
AUTUMN	21	91	1005.29	5.13985	993.8	1015.7	21.9	0
AUTUMN	22	91	1005.18	5.17484	993.5	1015.4	21.9	0
AUTUMN	23	91	1005.15	5.15722	993.2	1015.4	22.2	0
AUTUMN	24	91	1005.30	5.12887	993.6	1015.6	22.0	0

MONTHLY ANALYSIS OF PRESSURE (M BAR) OF YEAR 1980

MONTH	FREQ	MEAN	STD	MIN	MINDAY	MINHR	MAX	MAXDAY	MAXHR	RANGE	MISSING
1	744	1013.45	3.64800	1003.1	23	12	1020.3	8	6	17.2	0
2	696	1009.66	5.03237	992.9	55	14	1018.6	53	4	25.7	0
3	744	1007.10	4.50667	994.2	78	12	1019.8	64	18	25.6	0
4	720	1004.45	4.40194	995.5	104	12	1014.8	108	6	19.3	0
5	744	1001.13	2.74516	995.8	134	24	1009.1	136	6	13.3	0
5	744	1001.13	2.74516	995.8	134	24	1009.1	136	18	13.3	0
6	720	994.04	2.90119	987.1	182	12	1002.1	162	5	15.0	0
6	720	994.04	2.90119	987.1	182	13	1002.1	162	5	15.0	0
6	720	994.04	2.90119	987.1	182	14	1002.1	162	5	15.0	0
7	744	991.52	1.64371	987.4	204	13	997.8	185	12	10.4	0
8	744	993.90	2.02470	988.5	220	13	999.5	244	5	11.0	0
8	744	993.90	2.02470	988.5	220	13	999.5	244	6	11.0	0
9	720	1000.38	3.35194	993.3	247	12	1008.1	269	5	14.8	0
9	720	1000.38	3.35194	993.3	247	13	1008.1	269	5	14.8	0
10	744	1005.80	2.77260	999.2	275	13	1011.5	305	22	12.3	0
10	744	1005.80	2.77260	999.2	275	22	1011.5	305	22	12.3	0
10	744	1005.80	2.77260	999.2	275	23	1011.5	305	22	12.3	0
11	720	1011.06	2.81309	1004.5	325	10	1017.1	334	5	12.6	0
12	744	1012.40	3.19539	999.0	346	4	1018.6	339	5	19.6	0
12	744	1012.40	3.19539	999.0	346	7	1018.6	339	6	19.6	0

YEARLY ANALYSIS OF PRESSURE (M BAR) OF YEAR 1980

14

FREQ	MEAN	STD	MIN	MINMONTH	MINDAY	MINHR	MAX	MAXMONTH	MAXDAY	MAXHR	RANGE	MISSING
8784	1003.72	8.02316	987.1	6	182	12	1020.3	1	8	6	33.2	0
8784	1003.72	8.02316	987.1	6	182	13	1020.3	1	8	6	33.2	0
8784	1003.72	8.02316	987.1	6	182	14	1020.3	1	8	6	33.2	0

SEASONAL ANALYSIS OF PRESSURE (N BAR) FOR 1979-1980

SEASON	_FREQ_	MEAN	STD	MIN	MINMONTH	MINDAY	MINHR	MAX	MAXMONTH	MAXDAY	MAXHR	RANGE	HISSING
WINTER	2184	1012.08	4.52099	992.9	2	55	14	1022.0	12	336	6	29.1	0
SPRING	2208	1004.23	4.66047	994.2	3	78	12	1019.8	3	64	18	25.6	0
SUMMER	2208	993.14	2.52489	987.1	6	182	12	1002.1	6	162	5	15.0	0
SUMMER	2208	993.14	2.52489	987.1	6	182	13	1002.1	6	162	5	15.0	0
SUMMER	2208	993.14	2.52489	987.1	6	182	14	1002.1	6	162	5	15.0	0
AUTUMN	2184	1005.74	5.26612	993.3	9	247	12	1017.1	11	334	5	23.8	0
AUTUMN	2184	1005.74	5.26612	993.3	9	247	13	1017.1	11	334	5	23.8	0

SEASONAL DAILY CYCLE OF PRESSURE (H BAR) OF YEAR 79-80

SEASON	HOURLY	_FREQ_	MEAN	STD	MIN	MAX	RANGE	MISSING
WINTER	1	92	1011.71	4.34642	999.8	1019.9	20.1	0
WINTER	2	91	1012.22	4.31805	1000.3	1020.2	19.9	0
WINTER	3	91	1012.71	4.37950	1000.5	1020.9	20.4	0
WINTER	4	91	1013.23	4.42345	1000.1	1021.5	21.4	0
WINTER	5	91	1013.62	4.48932	999.7	1021.9	22.2	0
WINTER	6	91	1013.68	4.55527	999.3	1022.0	22.7	0
WINTER	7	91	1013.30	4.53181	998.5	1021.2	22.7	0
WINTER	8	91	1012.38	4.46694	998.0	1020.3	22.3	0
WINTER	9	90	1011.60	4.36442	998.3	1019.6	21.3	0
WINTER	10	91	1011.00	4.45364	997.4	1019.3	21.9	0
WINTER	11	91	1010.82	4.51657	995.1	1019.1	24.0	0
WINTER	12	91	1010.86	4.58466	994.2	1019.4	25.2	0
WINTER	13	91	1011.09	4.57967	993.8	1019.8	26.0	0
WINTER	14	91	1011.37	4.59927	992.9	1020.1	27.2	0
WINTER	15	91	1011.84	4.52268	995.0	1020.7	25.7	0
WINTER	16	91	1012.22	4.41994	995.5	1021.1	25.6	0
WINTER	17	91	1012.31	4.41692	996.9	1021.1	24.2	0
WINTER	18	91	1012.42	4.50909	995.4	1021.0	25.6	0
WINTER	19	91	1012.32	4.46806	996.6	1020.4	23.8	0
WINTER	20	91	1012.07	4.43414	997.0	1020.2	23.2	0
WINTER	21	91	1011.91	4.50604	997.9	1020.1	22.2	0
WINTER	22	91	1011.85	4.47299	998.8	1020.3	21.5	0
WINTER	23	91	1011.72	4.48854	999.0	1020.2	21.2	0
WINTER	24	91	1011.58	4.52048	998.6	1020.0	21.4	0
SPRING	1	92	1004.13	4.52554	996.0	1018.5	22.5	0
SPRING	2	92	1004.60	4.60483	996.7	1018.8	22.1	0
SPRING	3	92	1005.10	4.54764	997.0	1018.8	21.8	0
SPRING	4	92	1005.48	4.61479	997.7	1019.1	21.4	0
SPRING	5	92	1005.73	4.74690	997.4	1019.4	22.0	0
SPRING	6	92	1005.77	4.73333	998.0	1019.6	21.6	0
SPRING	7	92	1005.47	4.71005	997.7	1019.5	21.8	0
SPRING	8	92	1004.88	4.66049	997.5	1019.3	21.8	0
SPRING	9	92	1004.25	4.59616	997.0	1018.7	21.7	0
SPRING	10	92	1003.53	4.48299	995.9	1018.2	22.3	0
SPRING	11	92	1003.14	4.54795	995.3	1018.0	22.7	0
SPRING	12	92	1002.87	4.64976	994.2	1018.1	23.9	0
SPRING	13	92	1002.89	4.70453	994.4	1018.5	24.1	0
SPRING	14	92	1003.05	4.67296	994.8	1018.6	23.8	0
SPRING	15	92	1003.37	4.64179	995.8	1018.7	22.9	0
SPRING	16	92	1003.89	4.58310	996.5	1019.3	22.8	0
SPRING	17	92	1004.31	4.56963	996.9	1019.7	22.8	0
SPRING	18	92	1004.61	4.48665	997.2	1019.8	22.6	0
SPRING	19	92	1004.57	4.47999	997.2	1019.5	22.3	0
SPRING	20	92	1004.33	4.58031	997.0	1019.3	22.3	0
SPRING	21	92	1004.07	4.59661	996.6	1018.7	22.1	0
SPRING	22	92	1003.93	4.65955	996.0	1018.2	22.2	0
SPRING	23	92	1003.69	4.59605	996.0	1018.0	22.0	0
SPRING	24	92	1003.78	4.52422	995.8	1018.0	22.2	0
SUMMER	1	92	993.21	2.38564	988.4	1000.2	11.8	0
SUMMER	2	92	993.58	2.39231	988.5	1000.7	12.2	0
SUMMER	3	92	993.97	2.43720	988.5	1001.3	12.8	0
SUMMER	4	92	994.21	2.43656	989.5	1001.7	12.2	0

SEASONAL DAILY CYCLE OF PRESSURE (M BAR) OF YEAR 79-80

SEASON	HOURLY	FREQ	MEAN	STD	MIN	MAX	RANGE	MISSING
SUMMER	5	92	994.35	2.46106	989.7	1002.1	12.4	0
SUMMER	6	92	994.38	2.45112	989.7	1002.0	12.3	0
SUMMER	7	92	994.17	2.47345	989.4	1001.7	12.3	0
SUMMER	8	92	993.76	2.45720	988.8	1001.2	12.4	0
SUMMER	9	92	993.26	2.45609	988.3	1000.5	12.2	0
SUMMER	10	92	992.69	2.43472	987.9	999.6	11.7	0
SUMMER	11	92	992.25	2.41895	987.4	998.8	11.4	0
SUMMER	12	92	992.11	2.52599	987.1	998.4	11.3	0
SUMMER	13	92	991.74	2.44933	987.1	998.1	11.0	0
SUMMER	14	92	991.89	2.42011	987.1	998.3	11.2	0
SUMMER	15	92	992.28	2.41563	987.5	998.7	11.2	0
SUMMER	16	92	992.77	2.40857	987.8	999.1	11.3	0
SUMMER	17	92	993.23	2.37112	988.2	998.8	10.6	0
SUMMER	18	92	993.58	2.37721	988.6	1000.4	11.8	0
SUMMER	19	92	993.48	2.37334	988.5	1000.2	11.7	0
SUMMER	20	92	993.18	2.39333	988.5	1000.1	11.6	0
SUMMER	21	92	992.89	2.37206	988.3	999.9	11.6	0
SUMMER	22	92	992.73	2.40512	988.0	999.7	11.7	0
SUMMER	23	92	992.74	2.41207	988.0	999.6	11.6	0
SUMMER	24	92	992.91	2.38798	988.2	1000.0	11.8	0
AUTUMN	1	91	1005.61	5.18501	995.3	1015.2	19.9	0
AUTUMN	2	91	1006.00	5.22397	995.9	1015.9	20.0	0
AUTUMN	3	91	1006.55	5.22848	996.0	1016.2	20.2	0
AUTUMN	4	91	1007.05	5.23485	996.4	1016.5	20.1	0
AUTUMN	5	91	1007.38	5.27859	996.4	1017.1	20.7	0
AUTUMN	6	91	1007.28	5.28297	996.2	1016.7	20.5	0
AUTUMN	7	91	1006.70	5.23257	995.8	1016.1	20.3	0
AUTUMN	8	91	1006.12	5.13872	995.0	1015.2	20.2	0
AUTUMN	9	91	1005.34	5.02801	994.7	1014.5	19.8	0
AUTUMN	10	91	1004.82	5.06971	994.2	1014.1	19.9	0
AUTUMN	11	91	1004.54	5.19978	993.6	1013.9	20.3	0
AUTUMN	12	91	1004.50	5.27125	993.3	1013.9	20.6	0
AUTUMN	13	91	1004.62	5.32903	993.3	1013.9	20.6	0
AUTUMN	14	91	1004.85	5.39371	993.4	1014.4	21.0	0
AUTUMN	15	91	1005.27	5.42209	994.0	1015.0	21.0	0
AUTUMN	16	91	1005.73	5.28080	994.8	1015.4	20.6	0
AUTUMN	17	91	1005.98	5.16215	995.1	1015.3	20.2	0
AUTUMN	18	91	1005.99	5.19062	995.2	1015.5	20.3	0
AUTUMN	19	91	1005.87	5.22002	994.8	1015.3	20.5	0
AUTUMN	20	91	1005.70	5.22680	994.4	1015.2	20.8	0
AUTUMN	21	91	1005.60	5.23008	994.6	1015.0	20.4	0
AUTUMN	22	91	1005.48	5.26831	994.7	1014.9	20.2	0
AUTUMN	23	91	1005.37	5.25376	994.8	1014.9	20.1	0
AUTUMN	24	91	1005.49	5.22133	994.9	1015.2	20.3	0

MONTHLY ANALYSIS OF pressure (m bar) OF YEAR 1981

MCNTH	_FREQ_	MEAN	STD	MIN	MINDAY	MINHR	MAX	MAXDAY	MAXHR	RANGE	MISSING
1	744	1012.26	3.90905	1000.2	11	8	1020.5	14	6	20.3	0
2	672	1010.96	3.34624	1002.0	55	11	1018.1	35	6	16.1	0
3	744	1007.42	5.15492	997.2	86	10	1020.3	64	5	23.1	0
4	720	1004.14	4.70289	991.4	120	12	1013.7	92	7	22.3	0
5	744	1002.09	2.65315	995.5	128	22	1010.1	123	6	14.6	0
6	720	995.98	3.30143	987.8	172	12	1002.5	160	6	14.7	0
6	720	995.98	3.30143	987.8	172	13	1002.5	160	6	14.7	0
6	720	995.98	3.30143	987.8	172	14	1002.5	160	6	14.7	0
7	744	991.26	1.65648	986.2	197	13	995.5	209	5	9.3	0
8	744	993.51	2.03803	988.4	213	13	999.0	239	5	10.6	0
8	744	993.51	2.03803	988.4	213	14	999.0	239	6	10.6	0
9	720	1000.23	2.36844	993.4	246	13	1006.3	270	6	12.9	0
9	720	1000.23	2.36844	993.4	246	14	1006.3	270	6	12.9	0
9	720	1000.23	2.36844	993.4	246	22	1006.3	270	6	12.9	0
10	744	1007.03	3.29689	1000.0	281	10	1019.9	297	12	19.9	0
10	744	1007.03	3.29689	1000.0	281	11	1019.9	297	12	19.9	0
10	744	1007.03	3.29689	1000.0	297	9	1019.9	297	12	19.9	0
11	720	1010.86	4.03041	1000.1	306	5	1019.0	334	19	18.9	0
12	744	1013.40	2.43090	1003.2	359	12	1019.3	335	6	16.1	0

YEARLY ANALYSIS OF PRESSURE (H BAR) OF YEAR 1981

	MEAN	STD	MIN	MINMONTH	MINDAY	MINHR	MAX	MAXMONTH	MAXDAY	MAXHR	RANGE	MISSING
8760	1004.05	8.00509	986.2	7	197	13	1020.5	1	14	6	34.3	0

SEASONAL ANALYSIS OF PRESSURE (M BAR) FOR 1980-1981

SEASON	FREQ.	MEAN	STD	MIN	MINMONTH	MINDAY	MINHR	MAX.	MAXMONTH	MAXDAY	MAXHR	RANGE	MISSING
WINTER	2160	1011.91	3.55760	999.0	12	346	4	1020.5	1	14	6	21.5	0
WINTER	2160	1011.91	3.55760	999.0	12	346	7	1020.5	1	14	6	21.5	0
SPRING	2208	1004.55	4.83600	991.4	4	120	12	1020.3	3	64	5	28.9	0
SUMMER	2208	993.56	3.09167	986.2	7	197	13	1002.5	6	160	6	16.3	0
AUTUMN	2184	1006.05	5.47843	993.4	9	246	13	1019.9	10	297	12	26.5	0
AUTUMN	2184	1006.05	5.47843	993.4	9	246	14	1019.9	10	297	12	26.5	0
AUTUMN	2184	1006.05	5.47843	993.4	9	246	22	1019.9	10	297	12	26.5	0

SEASONAL DAILY CYCLE OF PRESSURE (H BAR) OF YEAR 80-81

SEASON	HOUR	FREQ	MEAN	STD	MIN	MAX	RANGE	MISSING
WINTER	1	90	1011.66	3.45368	1000.2	1018.5	18.3	0
WINTER	2	90	1012.07	3.52540	999.9	1019.0	19.1	0
WINTER	3	90	1012.52	3.56492	999.4	1019.2	19.8	0
WINTER	4	90	1013.17	3.59382	999.0	1020.0	21.0	0
WINTER	5	90	1013.53	3.50188	999.2	1020.2	21.0	0
WINTER	6	90	1013.59	3.56754	999.1	1020.5	21.4	0
WINTER	7	90	1013.16	3.61277	999.0	1020.2	21.2	0
WINTER	8	90	1012.14	3.73446	999.1	1018.8	19.7	0
WINTER	9	90	1011.35	3.49195	999.3	1018.0	18.7	0
WINTER	10	90	1010.86	3.44026	999.2	1017.1	17.9	0
WINTER	11	90	1010.71	3.32651	1001.5	1017.1	15.6	0
WINTER	12	90	1010.73	3.31849	1002.2	1017.2	15.0	0
WINTER	13	90	1010.91	3.31241	1002.3	1017.4	15.1	0
WINTER	14	90	1011.21	3.36709	1002.6	1018.2	15.6	0
WINTER	15	90	1011.64	3.41294	1003.3	1018.8	15.5	0
WINTER	16	90	1011.96	3.36055	1003.7	1019.0	15.3	0
WINTER	17	90	1012.05	3.44228	1004.1	1019.2	15.1	0
WINTER	18	90	1012.18	3.43128	1004.4	1019.5	15.1	0
WINTER	19	90	1012.06	3.45623	1004.0	1019.1	15.1	0
WINTER	20	90	1011.88	3.46680	1003.4	1018.7	15.3	0
WINTER	21	90	1011.83	3.39135	1003.5	1018.3	14.8	0
WINTER	22	90	1011.63	3.58060	1002.8	1018.3	15.5	0
WINTER	23	90	1011.55	3.59835	1001.8	1018.5	16.7	0
WINTER	24	90	1011.39	3.62726	1000.9	1018.7	17.8	0
SPRING	1	92	1004.41	4.78504	994.5	1018.1	23.6	0
SPRING	2	92	1004.91	4.76966	994.9	1018.6	23.7	0
SPRING	3	92	1005.55	4.68524	995.7	1019.1	23.4	0
SPRING	4	92	1005.87	4.85150	995.7	1020.0	24.3	0
SPRING	5	92	1005.97	4.90931	995.5	1020.3	24.8	0
SPRING	6	92	1006.10	4.94440	994.5	1020.1	25.6	0
SPRING	7	92	1005.88	4.92724	994.0	1019.7	25.7	0
SPRING	8	92	1005.29	4.93604	993.6	1019.9	26.3	0
SPRING	9	92	1004.56	4.85005	992.9	1018.0	25.1	0
SPRING	10	92	1003.89	4.80665	992.3	1017.3	25.0	0
SPRING	11	92	1003.39	4.77547	991.8	1017.0	25.2	0
SPRING	12	92	1003.17	4.75936	991.4	1016.8	25.4	0
SPRING	13	92	1003.18	4.76330	991.8	1017.0	25.2	0
SPRING	14	92	1003.39	4.74734	992.6	1017.5	24.9	0
SPRING	15	92	1003.79	4.66395	993.4	1017.7	24.3	0
SPRING	16	92	1004.30	4.66856	994.1	1018.0	23.9	0
SPRING	17	92	1004.73	4.69864	994.8	1018.0	23.2	0
SPRING	18	92	1004.86	4.70040	995.4	1018.3	22.9	0
SPRING	19	92	1004.83	4.63677	995.5	1018.3	22.8	0
SPRING	20	92	1004.64	4.70824	995.5	1018.3	22.8	0
SPRING	21	92	1004.38	4.74170	995.5	1018.7	23.2	0
SPRING	22	92	1004.08	4.76895	994.7	1018.1	23.4	0
SPRING	23	92	1003.98	4.85797	994.3	1017.6	23.3	0
SPRING	24	92	1004.09	4.79135	994.5	1018.0	23.5	0
SUMMER	1	92	993.68	2.98068	987.8	1001.4	13.6	0
SUMMER	2	92	994.09	2.96822	988.1	1001.8	13.7	0
SUMMER	3	92	994.45	3.01729	988.3	1002.2	13.9	0
SUMMER	4	92	994.68	3.04554	988.7	1002.4	13.7	0

SEASONAL DAILY CYCLE OF PRESSURE (H BAR) OF YEAR 80-81

SEASON	HOUR	_FREQ_	MEAN	STD	MIN	MAX	RANGE	MISSING
SUMMER	5	92	994.78	3.05902	989.0	1002.3	13.3	0
SUMMER	6	92	994.80	3.07607	989.0	1002.5	13.5	0
SUMMER	7	92	994.58	3.06441	989.0	1002.3	13.3	0
SUMMER	8	92	994.18	3.04578	988.3	1002.0	13.7	0
SUMMER	9	92	993.64	3.03225	987.7	1001.5	13.8	0
SUMMER	10	92	993.11	3.01191	987.2	1001.1	13.9	0
SUMMER	11	92	992.68	3.01814	986.7	1000.7	14.0	0
SUMMER	12	92	992.36	3.03611	986.5	1000.4	13.9	0
SUMMER	13	92	992.21	3.06333	986.2	1000.0	13.8	0
SUMMER	14	92	992.32	3.04968	986.4	1000.2	13.8	0
SUMMER	15	92	992.70	3.04580	986.8	1000.8	14.0	0
SUMMER	16	92	993.24	3.01603	987.3	1001.3	14.0	0
SUMMER	17	92	993.67	2.99742	987.6	1001.9	14.3	0
SUMMER	18	92	993.89	2.98386	987.8	1002.2	14.4	0
SUMMER	19	92	993.79	3.00294	987.7	1002.2	14.5	0
SUMMER	20	92	993.57	2.98022	987.5	1001.8	14.3	0
SUMMER	21	92	993.30	2.95716	987.4	1001.5	14.1	0
SUMMER	22	92	993.11	2.95506	987.2	1001.5	14.3	0
SUMMER	23	92	993.14	2.93707	987.4	1001.4	14.0	0
SUMMER	24	92	993.35	2.91594	987.8	1001.3	13.5	0
AUTUMN	1	91	1005.95	5.37854	994.6	1016.6	22.0	0
AUTUMN	2	91	1006.38	5.37838	995.0	1017.1	22.1	0
AUTUMN	3	91	1006.86	5.37938	995.3	1017.7	22.4	0
AUTUMN	4	91	1007.34	5.46734	995.4	1018.4	23.0	0
AUTUMN	5	91	1007.53	5.59974	995.6	1018.8	23.2	0
AUTUMN	6	91	1007.59	5.54788	995.5	1018.8	23.3	0
AUTUMN	7	91	1007.12	5.46044	995.3	1018.4	23.1	0
AUTUMN	8	91	1006.44	5.35777	995.2	1017.7	22.5	0
AUTUMN	9	91	1005.58	5.26775	994.5	1017.2	22.7	0
AUTUMN	10	91	1005.15	5.28411	994.0	1017.0	23.0	0
AUTUMN	11	91	1004.91	5.33771	993.9	1016.7	22.8	0
AUTUMN	12	91	1004.96	5.61941	993.7	1019.9	26.2	0
AUTUMN	13	91	1004.92	5.48560	993.4	1017.5	24.1	0
AUTUMN	14	91	1005.15	5.52794	993.4	1017.8	24.4	0
AUTUMN	15	91	1005.57	5.55138	993.8	1018.2	24.4	0
AUTUMN	16	91	1005.92	5.46086	994.1	1018.1	24.0	0
AUTUMN	17	91	1006.08	5.39478	994.1	1018.4	24.3	0
AUTUMN	18	91	1006.21	5.42374	994.2	1018.8	24.6	0
AUTUMN	19	91	1006.14	5.46105	993.9	1019.0	25.1	0
AUTUMN	20	91	1006.02	5.45693	993.7	1018.3	24.6	0
AUTUMN	21	91	1005.96	5.51088	993.5	1018.2	24.7	0
AUTUMN	22	91	1005.82	5.53837	993.4	1018.3	24.9	0
AUTUMN	23	91	1005.77	5.51535	993.5	1018.0	24.5	0
AUTUMN	24	91	1005.88	5.41124	994.4	1018.2	23.8	0

MONTHLY ANALYSIS OF PRESSURE (M BAR) OF YEAR 1982

MONTH	INDEX	MEAN	STD	MIN	WINDAY	MINHK	MAX	MAXDAY	MAXHR	RANGE	MISSING
1	794	1012.74	3.44408	1000.7	31	11	1020.4	21	6	15.7	0
2	672	1011.62	3.97811	998.5	44	14	1020.2	41	5	21.9	0
3	743	1008.52	4.76304	998.0	84	1	1019.9	90	6	21.9	0
4	725	1005.15	3.47388	997.6	108	13	1015.5	91	4	17.7	0
5	799	1003.67	2.52321	990.0	151	14	1008.4	130	6	18.4	0
6	723	996.71	2.56372	991.4	179	11	1003.5	152	5	12.1	0
7	729	996.71	2.56372	991.4	179	12	1003.5	152	6	12.1	0
8	727	993.50	2.49306	987.8	202	14	1000.7	188	8	12.5	0
9	721	993.50	2.49306	987.8	202	15	1000.7	188	8	12.5	0
10	721	993.63	1.98378	985.8	224	13	1000.9	239	5	11.1	0
11	729	1001.11	2.64777	995.6	250	13	1008.1	268	5	12.5	0
12	729	1001.11	2.64777	995.6	250	14	1008.1	268	6	12.5	0
13	729	1006.75	2.65127	1000.5	281	13	1013.8	287	6	13.3	0
14	729	1011.81	4.53253	1000.0	313	10	1022.8	323	5	22.8	0
15	729	1014.22	3.03625	1005.0	323	12	1021.8	344	5	16.8	0
16	729	1014.22	3.03625	1005.0	323	12	1021.8	344	6	16.8	0

YEARLY ANALYSIS OF PRESSURE (M BAR) OF YEAR 1982

LINE#	BLAN	STD	MIN	MINMONTH	MINDAY	MINHR	MAX	MAXMONTH	MAXDAY	MAXHR	RANGE	MISSIN
8700	1004.93	7.85400	587.8	7	202	14	1022.8	11	323	5	35	0
8700	1004.93	7.05400	587.8	7	202	15	1022.8	11	323	5	35	0

SEASONAL ANALYSIS OF PRESSURE (M BAR) FOR 1981-1982

SLASLN	-FREQ-	PCAN	STD	MIN	MINMONTH	MINDAY	MINHR	MAX	MAXMONTH	MAXDAY	MAXHR	RANGE	MISSING
WINTER	2100	1012.02	3.35727	998.3	2	44	14	1020.4	1	21	6	22.1	0
SPRING	2200	1009.74	4.42585	990.0	5	151	14	1019.5	3	50	6	29.9	0
SUMMER	2300	994.95	2.78228	987.8	7	202	14	1003.5	6	152	5	15.7	0
SUMMER	2400	994.95	2.78228	987.8	7	202	15	1003.5	6	152	6	15.7	0
AUTUMN	2104	1006.90	5.51888	995.6	9	256	13	1022.8	11	323	5	27.2	0
AUTUMN	2104	1006.90	5.51888	995.6	9	256	14	1022.8	11	323	5	27.2	0

SEASONAL DAILY CYCLE OF PRESSURE (M. BAR) CF YEAR 81-82

SEASON	HOUR	-FREQ-	MEAN	STD	MIN	MAX	RANGE	MISSING
WINTER	1	90	1012.35	3.30557	1004.0	1018.3	14.3	0
WINTER	2	90	1012.81	3.26404	1003.5	1015.0	15.5	0
WINTER	3	90	1013.44	3.21948	1003.7	1015.4	15.7	0
WINTER	4	90	1013.57	3.25058	1004.2	1020.1	15.9	0
WINTER	5	90	1014.38	3.25846	1004.5	1020.2	15.7	0
WINTER	6	90	1014.40	3.35274	1004.0	1020.4	16.4	0
WINTER	7	90	1013.54	3.45385	1002.4	1019.8	17.4	0
WINTER	8	90	1012.92	3.44418	1001.4	1019.0	17.6	0
WINTER	9	90	1012.12	3.52053	1000.4	1019.6	19.2	0
WINTER	10	90	1011.44	3.51154	999.0	1017.6	18.6	0
WINTER	11	90	1011.25	3.47113	998.9	1017.5	18.6	0
WINTER	12	50	1011.33	3.45755	999.4	1017.3	17.9	0
WINTER	13	90	1011.55	3.46473	999.7	1017.4	16.7	0
WINTER	14	90	1011.90	3.43836	998.3	1017.8	19.5	0
WINTER	15	90	1012.36	3.33541	999.5	1018.5	19.0	0
WINTER	16	90	1012.42	3.17880	1001.2	1018.3	17.1	0
WINTER	17	50	1012.75	3.11121	1002.6	1018.7	16.1	0
WINTER	18	50	1012.82	3.16525	1002.2	1019.0	16.8	0
WINTER	19	90	1012.77	3.17871	1003.0	1018.9	15.9	0
WINTER	20	90	1012.52	3.13647	1003.7	1018.8	15.1	0
WINTER	21	90	1012.42	3.08792	1004.1	1018.5	14.4	0
WINTER	22	90	1012.35	3.15948	1004.0	1018.6	14.6	0
WINTER	23	90	1012.24	3.13657	1003.9	1018.5	14.6	0
WINTER	24	90	1012.15	3.22888	1003.8	1018.4	14.6	0
SPRING	1	92	1005.75	4.25079	996.8	1017.9	21.1	0
SPRING	2	92	1006.12	4.30374	997.7	1018.5	20.8	0
SPRING	3	92	1006.58	4.31041	998.3	1018.8	20.5	0
SPRING	4	92	1007.00	4.44574	999.2	1019.6	20.4	0
SPRING	5	92	1007.17	4.45773	999.9	1019.8	19.9	0
SPRING	6	92	1007.22	4.48743	1000.0	1019.9	19.9	0
SPRING	7	92	1006.87	4.40450	999.9	1015.8	19.9	0
SPRING	8	92	1006.55	4.54330	999.1	1015.0	19.9	0
SPRING	9	92	1005.76	4.32054	998.2	1018.2	20.0	0
SPRING	10	92	1005.14	4.25539	997.4	1017.7	20.3	0
SPRING	11	92	1004.68	4.22639	996.3	1017.0	20.7	0
SPRING	12	92	1004.41	4.26469	994.7	1016.2	21.5	0
SPRING	13	92	1004.44	4.31612	993.3	1016.5	23.2	0
SPRING	14	92	1004.50	4.58225	990.0	1017.0	27.0	0
SPRING	15	92	1004.54	4.35116	993.7	1017.2	23.5	0
SPRING	16	92	1005.43	4.35683	994.4	1017.5	23.1	0
SPRING	17	92	1005.84	4.40487	994.6	1018.0	23.4	0
SPRING	18	92	1006.05	4.41365	995.0	1018.0	23.0	0
SPRING	19	92	1005.97	4.41280	995.0	1017.4	22.4	0
SPRING	20	92	1005.82	4.35553	994.7	1017.5	22.8	0
SPRING	21	92	1005.56	4.48685	994.4	1017.7	23.3	0
SPRING	22	92	1005.36	4.45577	994.5	1017.7	23.2	0
SPRING	23	92	1005.22	4.35320	995.4	1017.7	22.3	0
SPRING	24	92	1005.40	4.26756	996.1	1017.7	21.6	0
SUMMER	1	92	999.07	2.80018	988.9	1001.9	13.0	0
SUMMER	2	92	999.05	2.66225	989.3	1002.6	13.3	0
SUMMER	3	92	995.46	2.63578	990.2	1002.9	12.7	0
SUMMER	4	92	995.76	2.60557	990.5	1003.0	12.5	0

SEASONAL DAILY CYCLE OF PRESSURE (M BAR) OF YEAR 81-82

SEASON	HOUR	_FREQ_	MEAN	STD	MIN	MAX	RANGE	MISSING
SUMMER	5	92	955.87	2.63023	990.9	1003.5	12.6	0
SUMMER	6	92	955.87	2.60303	991.0	1003.5	12.5	0
SUMMER	7	92	955.66	2.64548	990.5	1003.0	12.1	0
SUMMER	8	92	955.20	2.71299	990.5	1002.5	12.0	0
SUMMER	9	92	954.62	2.72731	990.1	1002.0	11.9	0
SUMMER	10	92	954.12	2.75344	989.4	1001.4	12.0	0
SUMMER	11	92	953.68	2.76104	988.7	1001.1	12.4	0
SUMMER	12	92	953.38	2.77056	987.9	1000.8	12.9	0
SUMMER	13	92	953.37	2.77118	989.3	1000.8	11.5	0
SUMMER	14	92	953.39	2.79490	987.8	1001.0	13.2	0
SUMMER	15	92	953.78	2.75780	987.8	1001.4	13.6	0
SUMMER	16	92	954.28	2.73541	988.1	1002.0	13.9	0
SUMMER	17	92	954.72	2.71566	988.4	1002.8	14.4	0
SUMMER	18	92	954.53	2.71452	988.8	1002.7	13.9	0
SUMMER	19	92	954.84	2.66600	988.7	1002.4	13.7	0
SUMMER	20	92	954.60	2.67399	988.5	1002.0	13.5	0
SUMMER	21	92	954.34	2.64691	988.5	1001.4	12.9	0
SUMMER	22	92	954.17	2.64226	988.3	1000.7	12.4	0
SUMMER	23	92	954.17	2.60335	988.3	1000.8	12.5	0
SUMMER	24	92	954.34	2.55014	988.6	1001.2	12.6	0
AUTUMN	1	91	1006.27	5.40215	996.7	1021.0	24.3	0
AUTUMN	2	91	1006.75	5.38705	997.5	1021.4	23.9	0
AUTUMN	3	91	1007.25	5.35438	998.3	1021.8	23.5	0
AUTUMN	4	91	1007.62	5.40336	998.7	1022.6	23.9	0
AUTUMN	5	91	1008.16	5.45938	999.0	1022.8	23.8	0
AUTUMN	6	91	1008.12	5.52471	999.0	1022.7	23.7	0
AUTUMN	7	91	1007.70	5.41024	998.7	1022.0	23.3	0
AUTUMN	8	91	1007.02	5.33607	997.8	1021.5	23.7	0
AUTUMN	9	91	1006.26	5.30321	996.8	1020.9	24.1	0
AUTUMN	10	91	1005.73	5.34240	996.3	1020.4	24.1	0
AUTUMN	11	91	1005.53	5.42584	995.9	1020.5	24.6	0
AUTUMN	12	91	1005.48	5.52379	995.7	1020.6	24.9	0
AUTUMN	13	91	1005.56	5.54545	995.6	1020.9	25.3	0
AUTUMN	14	91	1005.77	5.61929	995.6	1020.7	25.1	0
AUTUMN	15	91	1006.15	5.67183	995.8	1021.3	25.5	0
AUTUMN	16	91	1006.49	5.62040	996.3	1021.5	25.2	0
AUTUMN	17	91	1006.72	5.50474	996.8	1021.6	24.8	0
AUTUMN	18	91	1006.72	5.51558	996.5	1021.5	25.0	0
AUTUMN	19	91	1006.59	5.57144	996.3	1021.3	25.0	0
AUTUMN	20	91	1006.43	5.54838	996.2	1021.1	24.9	0
AUTUMN	21	91	1006.31	5.56638	996.2	1020.8	24.6	0
AUTUMN	22	91	1006.20	5.61774	996.0	1021.0	25.0	0
AUTUMN	23	91	1006.10	5.55294	996.4	1020.9	24.5	0
AUTUMN	24	91	1006.26	5.55626	996.4	1020.7	24.3	0

MONTHLY ANALYSIS OF RELATIVE HUMIDITY (%) OF YEAR 1978

MONTH	_FREQ_	MEAN	STD	MIN	MINDAY	MINHR	MAX	MAXDAY	MAXHR	RANGE	MISSING
1	744	67.4384	19.0125	25	27	11	100	3	4	75	0.67204
1	744	67.4384	19.0125	25	27	11	100	3	5	75	0.67204
1	744	67.4384	19.0125	25	27	11	100	4	4	75	0.67204
2	672	57.8015	21.5597	16	46	12	98	40	24	82	0.29762
2	672	57.8015	21.5597	16	54	12	98	40	24	82	0.29762
3	744	46.7540	21.4091	9	82	10	56	64	22	87	0.00000
3	744	46.7540	21.4091	9	83	4	96	66	1	87	0.00000
4	720	28.0486	13.8236	3	106	11	81	112	2	78	0.00000
4	720	28.0486	13.8236	3	106	12	81	112	2	78	0.00000
5	744	15.7876	12.8166	2	136	11	74	121	20	72	0.00000
5	744	19.7876	12.8166	2	136	12	74	121	20	72	0.00000
6	720	17.5941	13.4808	3	159	10	98	166	23	95	0.41667
6	720	17.5941	13.4808	3	159	11	98	166	23	95	0.41667
6	720	17.5941	13.4808	3	159	12	98	166	23	95	0.41667
6	720	17.5941	13.4808	3	164	9	98	166	23	95	0.41667
6	720	17.5941	13.4808	3	164	10	98	166	23	95	0.41667
6	720	17.5941	13.4808	3	164	15	98	166	23	95	0.41667
6	720	17.5941	13.4808	3	169	10	98	166	23	95	0.41667
6	720	17.5941	13.4808	3	165	11	98	166	23	95	0.41667
6	720	17.5941	13.4808	3	177	11	98	166	23	95	0.41667
6	720	17.5941	13.4808	3	177	12	98	166	23	95	0.41667
6	720	17.5941	13.4808	3	180	13	98	166	23	95	0.41667
7	744	26.7366	20.7481	4	184	11	56	198	2	92	0.00000
7	744	26.7366	20.7481	4	185	13	96	198	2	92	0.00000
7	744	26.7366	20.7481	4	210	10	96	198	2	92	0.00000
7	744	26.7366	20.7481	4	212	10	96	198	2	92	0.00000
8	744	16.4892	6.9968	4	234	11	41	227	22	92	0.00000
9	720	25.1003	18.0979	2	255	10	100	261	22	98	0.27778
10	744	44.3057	25.6152	5	298	21	100	279	1	95	1.07527
10	744	44.3057	25.6152	5	298	21	100	279	2	95	1.07527
10	744	44.3057	25.6152	5	298	21	100	279	3	95	1.07527
10	744	44.3057	25.6152	5	298	21	100	280	1	95	1.07527
10	744	44.3057	25.6152	5	298	21	100	280	3	95	1.07527
10	744	44.3057	25.6152	5	298	21	100	280	4	95	1.07527
10	744	44.3057	25.6152	5	298	21	100	280	5	95	1.07527
10	744	44.3057	25.6152	5	298	21	100	288	1	95	1.07527
10	744	44.3057	25.6152	5	298	21	100	288	2	95	1.07527
10	744	44.3057	25.6152	5	298	21	100	295	22	95	1.07527
10	744	44.3057	25.6152	5	298	21	100	296	1	95	1.07527
10	744	44.3057	25.6152	5	298	21	100	296	2	95	1.07527
10	744	44.3057	25.6152	5	298	21	100	296	3	95	1.07527
10	744	44.3057	25.6152	5	298	21	100	296	4	95	1.07527
10	744	44.3057	25.6152	5	298	21	100	296	22	95	1.07527
10	744	44.3057	25.6152	5	298	21	100	296	23	95	1.07527
10	744	44.3057	25.6152	5	298	21	100	296	24	95	1.07527
11	720	45.3467	22.0695	8	310	10	98	331	2	90	0.41667
11	720	45.3467	22.0695	8	328	11	98	334	14	90	0.41667
12	744	71.1797	19.1846	14	352	11	100	336	2	86	0.53763
12	744	71.1797	19.1846	14	352	11	100	336	1	86	0.53763
12	744	71.1797	19.1846	14	352	11	100	336	2	86	0.53763
12	744	71.1797	19.1846	14	352	11	100	336	3	86	0.53763
12	744	71.1797	19.1846	14	352	11	100	340	2	86	0.53763

MONTHLY ANALYSIS OF RELATIVE HUMIDITY (%) OF YEAR 1978

MONTH	FREQ.	MEAN	STD	MIN	MINDAY	MINHR	MAX	MAXDAY	MAXHR	RANGE	MISSING
12	744	71.1797	19.1846	14	352	11	100	340	3	86	0.537634
12	744	71.1797	19.1846	14	352	11	100	340	4	86	0.537634
12	744	71.1797	19.1846	14	352	11	100	343	3	86	0.537634
12	744	71.1797	19.1846	14	352	11	100	358	17	86	0.537634
12	744	71.1797	19.1846	14	352	11	100	358	18	86	0.537634
12	744	71.1797	19.1846	14	352	11	100	358	19	86	0.537634
12	744	71.1797	19.1846	14	352	11	100	358	20	86	0.537634
12	744	71.1797	19.1846	14	352	11	100	358	21	86	0.537634
12	744	71.1797	19.1846	14	352	11	100	358	22	86	0.537634
12	744	71.1797	19.1846	14	352	11	100	358	23	86	0.537634
12	744	71.1797	19.1846	14	352	11	100	358	24	86	0.537634
12	744	71.1797	19.1846	14	352	11	100	359	1	86	0.537634
12	744	71.1797	19.1846	14	352	11	100	359	2	86	0.537634
12	744	71.1797	19.1846	14	352	11	100	359	3	86	0.537634
12	744	71.1797	19.1846	14	352	11	100	359	4	86	0.537634
12	744	71.1797	19.1846	14	352	11	100	359	5	86	0.537634

YEARLY ANALYSIS OF RELATIVE HUMIDITY (%) OF YEAR 1978

FREQ	MEAN	STD	MIN	MINMONTH	MINDAY	MINHR	MAX	MAXMONTH	MAXDAY	MAXHR	RANGE	MISSING
8760	38.8022	26.2433	2	5	136	11	100	1	3	4	98	0.308219
8760	38.8022	26.2433	2	5	136	12	100	1	3	5	98	0.308219
8760	38.8022	26.2433	2	9	255	10	100	1	4	4	98	0.308219
8760	38.8022	26.2433	2	9	255	10	100	9	261	22	98	0.308219
8760	38.8022	26.2433	2	9	255	10	100	10	279	1	98	0.308219
8760	38.8022	26.2433	2	9	255	10	100	10	279	2	98	0.308219
8760	38.8022	26.2433	2	9	255	10	100	10	279	3	98	0.308219
8760	38.8022	26.2433	2	9	255	10	100	10	280	1	98	0.308219
8760	38.8022	26.2433	2	9	255	10	100	10	280	3	98	0.308219
8760	38.8022	26.2433	2	9	255	10	100	10	280	4	98	0.308219
8760	38.8022	26.2433	2	9	255	10	100	10	280	5	98	0.308219
8760	38.8022	26.2433	2	9	255	10	100	10	288	1	98	0.308219
8760	38.8022	26.2433	2	9	255	10	100	10	288	2	98	0.308219
8760	38.8022	26.2433	2	9	255	10	100	10	255	22	98	0.308219
8760	38.8022	26.2433	2	9	255	10	100	10	296	1	98	0.308219
8760	38.8022	26.2433	2	9	255	10	100	10	296	2	98	0.308219
8760	38.8022	26.2433	2	9	255	10	100	10	296	3	98	0.308219
8760	38.8022	26.2433	2	9	255	10	100	10	296	4	98	0.308219
8760	38.8022	26.2433	2	9	255	10	100	10	296	22	98	0.308219
8760	38.8022	26.2433	2	9	255	10	100	10	256	23	98	0.308219
8760	38.8022	26.2433	2	9	255	10	100	10	296	24	98	0.308219
8760	38.8022	26.2433	2	9	255	10	100	10	297	2	98	0.308219
8760	38.8022	26.2433	2	9	255	10	100	12	336	1	98	0.308219
8760	38.8022	26.2433	2	9	255	10	100	12	336	2	98	0.308219
8760	38.8022	26.2433	2	9	255	10	100	12	336	3	98	0.308219
8760	38.8022	26.2433	2	9	255	10	100	12	340	2	98	0.308219
8760	38.8022	26.2433	2	9	255	10	100	12	340	2	98	0.308219
8760	38.8022	26.2433	2	9	255	10	100	12	340	3	98	0.308219
8760	38.8022	26.2433	2	9	255	10	100	12	340	4	98	0.308219
8760	38.8022	26.2433	2	9	255	10	100	12	343	3	98	0.308219
8760	38.8022	26.2433	2	9	255	10	100	12	358	17	98	0.308219
8760	38.8022	26.2433	2	9	255	10	100	12	358	18	98	0.308219
8760	38.8022	26.2433	2	9	255	10	100	12	358	19	98	0.308219
8760	38.8022	26.2433	2	9	255	10	100	12	358	20	98	0.308219
8760	38.8022	26.2433	2	9	255	10	100	12	358	21	98	0.308219
8760	38.8022	26.2433	2	9	255	10	100	12	358	22	98	0.308219
8760	38.8022	26.2433	2	9	255	10	100	12	358	23	98	0.308219
8760	38.8022	26.2433	2	9	255	10	100	12	358	24	98	0.308219
8760	38.8022	26.2433	2	9	255	10	100	12	359	1	98	0.308219
8760	38.8022	26.2433	2	9	255	10	100	12	359	2	98	0.308219
8760	38.8022	26.2433	2	9	255	10	100	12	359	3	98	0.308219
8760	38.8022	26.2433	2	9	255	10	100	12	359	4	98	0.308219
8760	38.8022	26.2433	2	9	255	10	100	12	359	5	98	0.308219

SEASONAL ANALYSIS OF RELATIVE HUMIDITY (%) FOR 1977-1978

SEASON	_FREQ_	MEAN	STD	MIN	MINMONTH	MINDAY	MINHR	MAX	MAXMONTH	MAXDAY	MAXHR	RANGE	MISSING
WINTER	2160	65.3553	20.7486	16	12	338	8	100	12	351	2	84	0.324074
WINTER	2160	65.3553	20.7486	16	2	46	12	100	12	351	3	84	0.324074
WINTER	2160	65.3553	20.7486	16	2	54	12	100	1	3	4	84	0.324074
WINTER	2160	65.3553	20.7486	16	2	54	12	100	1	3	5	84	0.324074
SPRING	2208	31.5679	20.0107	2	5	54	12	100	1	4	4	84	0.324074
SPRING	2208	31.5679	20.0107	2	5	136	11	56	3	64	22	94	0.000000
SUMMER	2208	20.3061	15.5542	3	6	136	12	56	3	66	1	94	0.000000
SUMMER	2208	20.3061	15.5542	3	6	159	10	58	6	166	23	95	0.135870
SUMMER	2208	20.3061	15.5542	3	6	159	11	98	6	166	23	95	0.135870
SUMMER	2208	20.3061	15.5542	3	6	159	12	58	6	166	23	95	0.135870
SUMMER	2208	20.3061	15.5542	3	6	164	9	98	6	166	23	95	0.135870
SUMMER	2208	20.3061	15.5542	3	6	164	10	98	6	166	23	95	0.135870
SUMMER	2208	20.3061	15.5542	3	6	164	15	98	6	166	23	95	0.135870
SUMMER	2208	20.3061	15.5542	3	6	169	10	98	6	166	23	95	0.135870
SUMMER	2208	20.3061	15.5542	3	6	169	11	58	6	166	23	95	0.135870
SUMMER	2208	20.3061	15.5542	3	6	177	11	58	6	166	23	95	0.135870
SUMMER	2208	20.3061	15.5542	3	6	177	12	98	6	166	23	95	0.135870
SUMMER	2208	20.3061	15.5542	3	6	180	13	98	6	166	23	95	0.135870
AUTUMN	2184	38.2985	24.0306	2	9	255	10	100	9	261	22	98	0.595238
AUTUMN	2184	38.2985	24.0306	2	9	255	10	100	10	279	1	98	0.595238
AUTUMN	2184	38.2985	24.0306	2	9	255	10	100	10	279	2	98	0.595238
AUTUMN	2184	38.2985	24.0306	2	9	255	10	100	10	279	3	98	0.595238
AUTUMN	2184	38.2985	24.0306	2	9	255	10	100	10	280	1	98	0.595238
AUTUMN	2184	38.2985	24.0306	2	9	255	10	100	10	280	3	98	0.595238
AUTUMN	2184	38.2985	24.0306	2	9	255	10	100	10	280	4	98	0.595238
AUTUMN	2184	38.2985	24.0306	2	9	255	10	100	10	280	5	98	0.595238
AUTUMN	2184	38.2985	24.0306	2	9	255	10	100	10	288	1	98	0.595238
AUTUMN	2184	38.2985	24.0306	2	9	255	10	100	10	288	2	98	0.595238
AUTUMN	2184	38.2985	24.0306	2	9	255	10	100	10	288	2	98	0.595238
AUTUMN	2184	38.2985	24.0306	2	9	255	10	100	10	295	22	98	0.595238
AUTUMN	2184	38.2985	24.0306	2	9	255	10	100	10	296	1	98	0.595238
AUTUMN	2184	38.2985	24.0306	2	9	255	10	100	10	296	2	98	0.595238
AUTUMN	2184	38.2985	24.0306	2	9	255	10	100	10	296	3	98	0.595238
AUTUMN	2184	38.2985	24.0306	2	9	255	10	100	10	296	4	98	0.595238
AUTUMN	2184	38.2985	24.0306	2	9	255	10	100	10	296	22	58	0.595238
AUTUMN	2184	38.2985	24.0306	2	9	255	10	100	10	296	23	98	0.595238
AUTUMN	2184	38.2985	24.0306	2	9	255	10	100	10	296	24	98	0.595238
AUTUMN	2184	38.2985	24.0306	2	9	255	10	100	10	297	2	98	0.595238

SEASONAL DAILY CYCLE OF RELATIVE HUMIDITY (%) OF YEAR 77-78

SEASON	HOUR	_FREQ_	MEAN	STD	MIN	MAX	RANGE	MISSING
WINTER	1	90	78.2184	13.5873	40	97	57	3.33333
WINTER	2	90	78.6477	13.2466	35	100	61	2.22222
WINTER	3	90	78.3371	13.1347	39	100	61	1.11111
WINTER	4	90	74.8111	14.8202	33	100	67	0.00000
WINTER	5	90	67.4667	16.5205	30	100	70	0.00000
WINTER	6	90	60.1444	17.6543	21	98	77	0.00000
WINTER	7	90	54.5556	19.0730	19	98	79	0.00000
WINTER	8	90	49.5556	19.8195	16	96	80	0.00000
WINTER	9	90	45.5778	19.4572	17	91	74	0.00000
WINTER	10	90	44.9444	20.1184	18	92	74	0.00000
WINTER	11	90	45.1222	20.3618	17	94	77	0.00000
WINTER	12	90	47.0111	20.7481	16	94	78	0.00000
WINTER	13	90	51.6111	20.3374	18	95	77	0.00000
WINTER	14	90	58.4556	18.8478	27	95	68	0.00000
WINTER	15	90	63.5667	16.9904	37	95	58	0.00000
WINTER	16	90	66.9111	16.9007	35	98	63	0.00000
WINTER	17	90	65.6667	15.8168	36	95	59	0.00000
WINTER	18	90	72.8000	14.9728	35	96	57	0.00000
WINTER	19	90	75.4556	14.0818	43	96	53	0.00000
WINTER	20	90	76.7444	13.7380	36	97	61	0.00000
WINTER	21	90	76.6222	13.9345	31	98	67	0.00000
WINTER	22	90	77.2889	14.3364	30	98	68	0.00000
WINTER	23	90	77.3708	14.3720	29	97	68	0.00000
WINTER	24	90	78.0444	14.2505	27	98	71	1.11111
SPRING	1	92	43.2935	20.5467	9	96	87	0.00000
SPRING	2	92	43.5578	20.8733	10	54	84	0.00000
SPRING	3	92	41.1630	20.3455	8	88	80	0.00000
SPRING	4	92	34.6413	18.2664	8	88	80	0.00000
SPRING	5	92	29.1087	16.3690	6	81	75	0.00000
SPRING	6	92	24.4674	14.4614	3	75	72	0.00000
SPRING	7	92	21.4457	13.7780	4	75	71	0.00000
SPRING	8	92	19.4457	13.8876	3	74	71	0.00000
SPRING	9	92	18.2174	13.9684	4	84	80	0.00000
SPRING	10	92	17.1413	13.2022	3	68	65	0.00000
SPRING	11	92	17.1687	12.5981	2	66	64	0.00000
SPRING	12	92	18.0761	12.3335	2	66	64	0.00000
SPRING	13	92	20.9130	14.3264	4	70	66	0.00000
SPRING	14	92	24.3804	15.5449	6	73	67	0.00000
SPRING	15	92	29.0435	17.6043	6	76	70	0.00000
SPRING	16	92	31.3261	17.9988	8	79	71	0.00000
SPRING	17	92	34.4022	19.0211	9	90	81	0.00000
SPRING	18	92	37.6670	19.1045	9	92	83	0.00000
SPRING	19	92	40.6435	19.8239	13	92	79	0.00000
SPRING	20	92	41.6848	20.3561	11	95	84	0.00000
SPRING	21	92	42.7500	19.9133	13	95	82	0.00000
SPRING	22	92	43.0652	19.5722	12	96	84	0.00000
SPRING	23	92	42.5891	20.1976	10	91	81	0.00000
SPRING	24	92	42.2391	19.6157	9	94	85	0.00000
SUMMER	1	92	29.6220	17.9282	10	94	84	1.08656
SUMMER	2	92	28.8681	17.9754	9	96	87	1.08696
SUMMER	3	92	26.6630	17.8364	11	92	81	0.00000
SUMMER	4	92	22.0217	15.0377	8	77	69	0.00000

SEASONAL DAILY CYCLE OF RELATIVE HUMIDITY (%) OF YEAR 77-78

SEASON	HOUR	_FREQ_	MEAN	STD	MIN	MAX	RANGE	MISSING
SUMMER	5	92	17.6630	11.1476	7	58	51	0.00000
SUMMER	6	92	15.2065	10.2545	6	60	54	0.00000
SUMMER	7	92	13.4348	10.6825	5	61	56	0.00000
SUMMER	8	92	12.0000	9.9912	4	56	52	0.00000
SUMMER	9	92	11.4348	10.1009	3	54	51	0.00000
SUMMER	10	92	10.7609	9.2741	3	49	46	0.00000
SUMMER	11	92	11.3043	9.8592	3	52	49	0.00000
SUMMER	12	92	11.8913	10.2662	3	53	50	0.00000
SUMMER	13	92	13.0543	10.4979	3	56	53	0.00000
SUMMER	14	92	15.8913	12.0242	5	63	58	0.00000
SUMMER	15	92	18.7391	13.4523	3	70	67	0.00000
SUMMER	16	92	21.0578	14.9181	5	73	68	0.00000
SUMMER	17	92	22.5326	14.1945	8	71	63	0.00000
SUMMER	18	92	23.4348	15.2685	8	78	70	0.00000
SUMMER	19	92	24.6739	16.0556	6	84	78	0.00000
SUMMER	20	92	26.5000	16.5453	9	82	73	0.00000
SUMMER	21	92	26.6413	16.1344	8	83	75	0.00000
SUMMER	22	92	28.0000	17.7064	10	97	87	0.00000
SUMMER	23	92	28.4022	17.6716	8	98	90	0.00000
SUMMER	24	92	28.3846	16.9232	9	90	81	1.08656
AUTUMN	1	91	48.4382	23.3778	16	100	84	2.19780
AUTUMN	2	91	47.5730	23.3729	16	100	84	2.19780
AUTUMN	3	91	47.1578	24.2360	9	100	91	0.00000
AUTUMN	4	91	41.4667	22.7429	14	100	86	1.09890
AUTUMN	5	91	36.5275	21.2939	10	100	90	0.00000
AUTUMN	6	91	30.0989	19.1248	8	92	84	0.00000
AUTUMN	7	91	25.1868	17.1035	5	93	88	0.00000
AUTUMN	8	91	22.9451	16.9183	4	93	89	0.00000
AUTUMN	9	91	21.8242	17.3132	4	96	92	0.00000
AUTUMN	10	91	21.8462	17.4222	2	91	89	0.00000
AUTUMN	11	91	22.5385	17.5396	3	90	87	0.00000
AUTUMN	12	91	24.1868	18.3539	4	96	92	0.00000
AUTUMN	13	91	29.4615	19.6516	4	97	93	0.00000
AUTUMN	14	91	36.3626	21.1495	9	98	89	0.00000
AUTUMN	15	91	40.5670	22.6173	5	97	88	0.00000
AUTUMN	16	91	42.5275	23.1720	13	97	84	0.00000
AUTUMN	17	91	44.3736	23.6937	13	95	82	0.00000
AUTUMN	18	91	46.1209	23.8154	11	95	84	0.00000
AUTUMN	19	91	47.6703	24.1799	13	96	83	0.00000
AUTUMN	20	91	48.6703	24.2153	14	98	84	0.00000
AUTUMN	21	91	48.3034	24.7604	5	96	91	2.19780
AUTUMN	22	91	49.6667	24.9795	13	100	87	1.09890
AUTUMN	23	91	48.2500	23.6445	13	100	87	3.29670
AUTUMN	24	91	48.3146	24.0571	15	100	85	2.19780

MONTHLY ANALYSIS OF RELATIVE HUMIDITY (%) OF YEAR 1979

MONTH	-- FREQ --	MEAN	STD	MIN	MINDAY	MINHR	MAX	MAXDAY	MAXHR	RANGE	MISSING
1	744	68.6872	18.2034	25	6	10	100	19	23	75	1-61290
1	744	68.6872	18.2034	25	6	10	100	19	24	75	1-61290
1	744	68.6872	18.2034	25	6	10	100	20	19	75	1-61290
1	744	68.6872	18.2034	25	6	10	100	20	20	75	1-61290
1	744	68.6872	18.2034	25	6	10	100	20	21	75	1-61290
1	744	68.6872	18.2034	25	6	10	100	20	22	75	1-61290
1	744	68.6872	18.2034	25	6	10	100	21	1	75	1-61290
1	744	68.6872	18.2034	25	6	10	100	21	3	75	1-61290
1	744	68.6872	18.2034	25	6	10	100	21	4	75	1-61290
1	744	68.6872	18.2034	25	6	10	100	21	5	75	1-61290
2	672	50.6860	20.0545	11	54	10	96	46	23	85	0-00000
3	744	39.6089	18.1507	4	63	11	90	73	2	86	0-00000
4	720	29.6208	13.4076	3	112	5	80	99	2	77	0-00000
4	720	29.6208	13.4076	3	112	6	80	99	2	77	0-00000
4	720	29.6208	13.4076	3	112	7	80	99	2	77	0-00000
4	720	29.6208	13.4076	3	112	8	80	99	2	77	0-00000
5	744	30.6949	18.2276	6	149	8	94	122	1	88	0-00000
6	720	19.5264	12.9764	2	163	8	75	156	1	73	0-00000
6	720	19.5264	12.9764	2	163	9	75	156	1	73	0-00000
6	720	19.5264	12.9764	2	163	10	75	156	1	73	0-00000
7	744	16.0444	9.9016	4	196	10	82	202	20	78	0-00000
7	744	16.0444	9.9016	4	199	11	82	202	20	78	0-00000
7	744	16.0444	9.9016	4	200	10	82	202	20	78	0-00000
7	744	16.0444	9.9016	4	200	11	82	202	20	78	0-00000
7	744	16.0444	9.9016	4	200	12	82	202	20	78	0-00000
7	744	16.0444	9.9016	4	200	13	82	202	20	78	0-00000
7	744	16.0444	9.9016	4	200	14	82	202	20	78	0-00000
7	744	16.0444	9.9016	4	201	9	82	202	20	78	0-00000
7	744	16.0444	9.9016	4	205	10	82	202	20	78	0-00000
7	744	16.0444	9.9016	4	205	11	82	202	20	78	0-00000
7	744	16.0444	9.9016	4	205	12	82	202	20	78	0-00000
8	744	25.8965	23.0460	2	213	12	97	243	24	95	0-00000
9	720	33.3528	22.1146	5	258	9	97	244	2	92	0-00000
9	720	33.3528	22.1146	5	258	10	97	244	3	92	0-00000
9	720	33.3528	22.1146	5	258	11	97	244	3	92	0-00000
9	720	33.3528	22.1146	5	264	12	97	244	3	92	0-00000
9	720	33.3528	22.1146	5	264	13	97	244	3	92	0-00000
10	744	43.1425	23.5564	0	302	21	94	286	24	94	0-00000
10	744	43.1425	23.5564	0	302	22	94	287	1	94	0-00000
11	720	48.6592	20.7629	8	315	9	100	321	4	92	1-38889
11	744	66.6976	18.3093	15	315	9	100	321	20	92	1-38889
12	744	66.6976	18.3093	15	340	8	97	346	8	82	0-00000
12	744	66.6976	18.3093	15	340	8	97	346	10	82	0-00000
12	744	66.6976	18.3093	15	340	8	97	346	11	82	0-00000
12	744	66.6976	18.3093	15	340	8	97	346	12	82	0-00000
12	744	66.6976	18.3093	15	340	8	97	346	14	82	0-00000
12	744	66.6976	18.3093	15	340	8	97	346	15	82	0-00000

YEARLY ANALYSIS OF RELATIVE HUMIDITY (%) OF YEAR 1979

- FREQ -	MEAN	STD	MIN	MINMONTH	MINDAY	MINHR	MAX	MAXMONTH	MAXDAY	MAXHR	RANGE	MISSING
8760	39.3132	24.761	0	10	302	21	100	1	19	23	100	0.251142
8760	39.3132	24.761	0	10	302	22	100	1	19	24	100	0.251142
8760	39.3132	24.761	0	10	302	22	100	1	20	19	100	0.251142
8760	39.3132	24.761	0	10	302	22	100	1	20	20	100	0.251142
8760	39.3132	24.761	0	10	302	22	100	1	20	21	100	0.251142
8760	39.3132	24.761	0	10	302	22	100	1	20	22	100	0.251142
8760	39.3132	24.761	0	10	302	22	100	1	21	1	100	0.251142
8760	39.3132	24.761	0	10	302	22	100	1	21	3	100	0.251142
8760	39.3132	24.761	0	10	302	22	100	1	21	4	100	0.251142
8760	39.3132	24.761	0	10	302	22	100	1	21	5	100	0.251142
8760	39.3132	24.761	0	10	302	22	100	11	321	4	100	0.251142
8760	39.3132	24.761	0	10	302	22	100	11	321	20	100	0.251142

SEASONAL ANALYSIS OF RELATIVE HUMIDITY (%) FOR 1978-1979

SEASON	_FREQ_	MEAN	STD	MIN	MINMONTH	MINDAY	MINHR	MAX	MAXMONTH	MAXDAY	MAXHR	RANGE	MISSING
WINTER	2160	63.9021	21.1333	11	2	54	10	100	12	336	1	89	0.740741
WINTER	2160	63.9021	21.1333	11	2	54	10	100	12	336	2	89	0.740741
WINTER	2160	63.9021	21.1333	11	2	54	10	100	12	336	3	89	0.740741
WINTER	2160	63.9021	21.1333	11	2	54	10	100	12	340	2	89	0.740741
WINTER	2160	63.9021	21.1333	11	2	54	10	100	12	340	3	89	0.740741
WINTER	2160	63.9021	21.1333	11	2	54	10	100	12	343	4	89	0.740741
WINTER	2160	63.9021	21.1333	11	2	54	10	100	12	358	3	99	0.740741
WINTER	2160	63.9021	21.1333	11	2	54	10	100	12	358	17	89	0.740741
WINTER	2160	63.9021	21.1333	11	2	54	10	100	12	358	18	89	0.740741
WINTER	2160	63.9021	21.1333	11	2	54	10	100	12	358	19	89	0.740741
WINTER	2160	63.9021	21.1333	11	2	54	10	100	12	358	20	49	0.740741
WINTER	2160	63.9021	21.1333	11	2	54	10	100	12	358	21	89	0.740741
WINTER	2160	63.9021	21.1333	11	2	54	10	100	12	358	22	89	0.740741
WINTER	2160	63.9021	21.1333	11	2	54	10	100	12	358	23	89	0.740741
WINTER	2160	63.9021	21.1333	11	2	54	10	100	12	358	24	89	0.740741
WINTER	2160	63.9021	21.1333	11	2	54	10	100	12	359	1	89	0.740741
WINTER	2160	63.9021	21.1333	11	2	54	10	100	12	359	2	89	0.740741
WINTER	2160	63.9021	21.1333	11	2	54	10	100	12	359	3	89	0.740741
WINTER	2160	63.9021	21.1333	11	2	54	10	100	12	359	4	89	0.740741
WINTER	2160	63.9021	21.1333	11	2	54	10	100	12	359	5	89	0.740741
WINTER	2160	63.9021	21.1333	11	2	54	10	100	1	19	23	89	0.740741
WINTER	2160	63.9021	21.1333	11	2	54	10	100	1	19	24	89	0.740741
WINTER	2160	63.9021	21.1333	11	2	54	10	100	1	20	19	89	0.740741
WINTER	2160	63.9021	21.1333	11	2	54	10	100	1	20	20	89	0.740741
WINTER	2160	63.9021	21.1333	11	2	54	10	100	1	20	21	89	0.740741
WINTER	2160	63.9021	21.1333	11	2	54	10	100	1	20	22	89	0.740741
WINTER	2160	63.9021	21.1333	11	2	54	10	100	1	21	1	89	0.740741
WINTER	2160	63.9021	21.1333	11	2	54	10	100	1	21	3	89	0.740741
WINTER	2160	63.9021	21.1333	11	2	54	10	100	1	21	4	89	0.740741
WINTER	2160	63.9021	21.1333	11	2	54	10	100	1	21	5	89	0.740741
WINTER	2160	63.9021	21.1333	11	2	54	10	100	5	122	1	91	0.000000
WINTER	2160	63.9021	21.1333	11	2	54	10	100	5	122	1	91	0.000000
WINTER	2160	63.9021	21.1333	11	2	54	10	100	5	122	1	91	0.000000
WINTER	2160	63.9021	21.1333	11	2	54	10	100	5	122	1	91	0.000000
WINTER	2160	63.9021	21.1333	11	2	54	10	100	8	243	1	91	0.000000
WINTER	2160	63.9021	21.1333	11	2	54	10	100	8	243	24	95	0.000000
WINTER	2160	63.9021	21.1333	11	2	54	10	100	8	243	24	95	0.000000
WINTER	2160	63.9021	21.1333	11	2	54	10	100	8	243	24	95	0.000000
WINTER	2160	63.9021	21.1333	11	2	54	10	100	8	243	24	95	0.000000
WINTER	2160	63.9021	21.1333	11	2	54	10	100	8	243	24	95	0.000000
WINTER	2160	63.9021	21.1333	11	2	54	10	100	8	243	24	95	0.000000
WINTER	2160	63.9021	21.1333	11	2	54	10	100	8	243	24	95	0.000000
WINTER	2160	63.9021	21.1333	11	2	54	10	100	10	321	4	100	0.457875
WINTER	2160	63.9021	21.1333	11	2	54	10	100	10	321	20	100	0.457875

SEASONAL DAILY CYCLE OF RELATIVE HUMIDITY (%) OF YEAR 78-79

SEASON	HOUE	_FREQ_	MEAN	STD	MIN	MAX	RANGE	MISSING
WINTER	1	90	75.5455	14.4905	33	100	67	2-22222
WINTER	2	90	75.9770	14.9059	30	100	70	3-33333
WINTER	3	90	77.2247	14.9718	29	100	71	1-11111
WINTER	4	90	73.6136	14.9861	29	100	71	2-22222
WINTER	5	90	66.8764	16.0693	27	100	73	1-11111
WINTER	6	90	58.2135	16.8506	26	93	67	1-11111
WINTER	7	90	51.7444	17.7483	21	98	77	0-00000
WINTER	8	90	46.2000	17.7734	12	93	81	0-00000
WINTER	9	90	43.5667	17.4717	16	98	82	0-00000
WINTER	10	90	42.6333	18.5433	11	93	82	0-00000
WINTER	11	90	44.1667	19.5817	13	94	81	0-00000
WINTER	12	90	46.4444	20.0741	15	94	79	0-00000
WINTER	13	90	51.7667	21.0553	15	94	79	0-00000
WINTER	14	90	59.2333	19.8789	24	96	72	0-00000
WINTER	15	89	63.9326	19.1992	23	98	75	0-00000
WINTER	16	91	66.3333	17.7137	24	98	74	1-09890
WINTER	17	90	69.8111	17.2202	28	100	72	0-00000
WINTER	18	90	72.1111	17.3674	36	100	64	0-00000
WINTER	19	90	73.5000	16.5055	36	100	64	0-00000
WINTER	20	90	74.0449	16.7738	25	100	75	1-11111
WINTER	21	90	75.5169	16.1844	25	100	75	1-11111
WINTER	22	90	75.6966	15.6353	34	100	66	1-11111
WINTER	23	90	75.5056	15.3616	37	100	63	1-11111
WINTER	24	90	75.6180	15.4423	37	100	63	1-11111
SPRING	1	92	44.0761	17.5482	16	94	78	0-00000
SPRING	2	92	44.9130	18.3385	13	93	80	0-00000
SPRING	3	92	42.5543	17.4604	13	88	75	0-00000
SPRING	4	92	36.2717	16.0447	6	81	75	0-00000
SPRING	5	92	29.8370	13.9467	3	80	77	0-00000
SPRING	6	92	24.6196	12.3428	3	78	75	0-00000
SPRING	7	92	22.1304	11.8926	3	76	73	0-00000
SPRING	8	92	21.0543	12.1830	3	75	72	0-00000
SPRING	9	92	20.0761	11.6885	4	73	69	0-00000
SPRING	10	92	20.0000	11.0999	4	67	63	0-00000
SPRING	11	92	21.0761	11.7840	4	59	55	0-00000
SPRING	12	92	22.7065	13.4046	7	68	61	0-00000
SPRING	13	92	24.9674	13.7181	6	68	62	0-00000
SPRING	14	92	28.5435	14.3300	10	74	64	0-00000
SPRING	15	92	32.5761	14.1966	13	70	57	0-00000
SPRING	16	92	34.0543	14.3553	9	75	66	0-00000
SPRING	17	92	35.5978	15.0414	9	80	71	0-00000
SPRING	18	92	38.3913	15.3028	12	88	76	0-00000
SPRING	19	92	39.6630	14.1579	13	80	67	0-00000
SPRING	20	92	42.1848	15.2199	15	81	66	0-00000
SPRING	21	92	43.2500	16.6051	13	89	76	0-00000
SPRING	22	92	43.8696	17.2182	14	89	75	0-00000
SPRING	23	92	43.6630	17.2959	17	86	69	0-00000
SPRING	24	92	44.2826	17.4282	16	92	76	0-00000
SUMMER	1	92	29.1413	18.9311	10	93	83	0-00000
SUMMER	2	92	28.7717	18.6330	9	94	85	0-00000
SUMMER	3	92	26.4130	17.6474	9	91	82	0-00000
SUMMER	4	92	21.4348	14.0855	8	79	71	0-00000

SEASONAL DAILY CYCLE OF RELATIVE HUMIDITY (%) OF YEAR 78-79

SEASON	HOUR	FREQ.	MEAN	STD	MIN	MAX	RANGE	MISSING
SUMMER	5	92	17.9239	11.5380	8	66	58	0.0000
SUMMER	6	92	15.0435	10.2849	4	54	50	0.0000
SUMMER	7	92	13.7065	10.5148	4	55	51	0.0000
SUMMER	8	92	12.6304	10.9692	2	58	56	0.0000
SUMMER	9	92	12.7065	11.9307	2	59	57	0.0000
SUMMER	10	92	12.0978	11.8943	2	57	55	0.0000
SUMMER	11	92	12.3478	11.8400	3	59	56	0.0000
SUMMER	12	92	12.9239	12.4125	2	58	56	0.0000
SUMMER	13	92	14.6630	13.5795	4	65	61	0.0000
SUMMER	14	92	16.5761	14.8044	4	69	65	0.0000
SUMMER	15	92	19.1522	15.9807	6	77	71	0.0000
SUMMER	16	92	20.9565	16.7496	7	83	76	0.0000
SUMMER	17	92	21.9130	16.2998	8	83	75	0.0000
SUMMER	18	92	23.5435	17.2928	8	89	81	0.0000
SUMMER	19	92	24.1957	18.2240	7	93	86	0.0000
SUMMER	20	92	25.6196	19.1276	8	90	82	0.0000
SUMMER	21	92	26.0326	18.9113	8	95	87	0.0000
SUMMER	22	92	27.2826	19.8452	9	96	87	0.0000
SUMMER	23	92	28.1196	19.6993	9	94	85	0.0000
SUMMER	24	92	28.7935	19.3888	9	97	88	0.0000
AUTUMN	1	91	53.2333	22.8055	18	97	79	1.0989
AUTUMN	2	91	52.4000	22.2043	16	97	81	1.0989
AUTUMN	3	91	51.4556	21.2873	17	97	80	1.0989
AUTUMN	4	91	46.1099	20.6841	14	100	86	0.0000
AUTUMN	5	91	37.7000	18.0862	9	82	73	1.0989
AUTUMN	6	91	31.6374	17.3567	8	95	87	0.0000
AUTUMN	7	91	26.5604	16.1550	6	86	80	0.0000
AUTUMN	8	91	23.6264	15.7900	6	75	69	0.0000
AUTUMN	9	91	21.9011	15.3457	5	74	69	0.0000
AUTUMN	10	91	22.6044	14.7157	5	73	68	0.0000
AUTUMN	11	91	23.8352	15.2973	5	66	61	0.0000
AUTUMN	12	91	26.9780	16.9588	5	72	67	0.0000
AUTUMN	13	91	33.6264	18.7478	5	80	75	0.0000
AUTUMN	14	91	39.5604	19.9907	8	89	81	0.0000
AUTUMN	15	91	44.3516	20.9016	9	89	80	0.0000
AUTUMN	16	91	46.9231	21.3787	13	93	80	0.0000
AUTUMN	17	91	48.7253	20.0206	14	92	78	0.0000
AUTUMN	18	91	54.1319	20.3820	14	95	81	0.0000
AUTUMN	19	91	52.7333	21.2929	14	98	84	1.0989
AUTUMN	20	91	53.6222	22.1530	17	100	83	1.0989
AUTUMN	21	91	52.5506	22.6791	0	94	94	2.1978
AUTUMN	22	91	53.4000	23.5767	0	98	98	1.0989
AUTUMN	23	91	53.9890	22.6890	17	98	81	0.0000
AUTUMN	24	91	53.2444	22.3528	18	95	77	1.0989

MONTHLY ANALYSIS OF RELATIVE HUMIDITY (%) OF YEAR 1980

MONTH	FREQ_	MEAN	STD	MIN	MINDAY	MINHR	MAX	MAXDAY	MAXHR	RANGE	MISSING
1	744	64.2799	19.8178	8	31	10	98	21	4	90	0.134409
2	656	63.6660	21.2940	12	33	11	100	48	22	88	0.287356
3	744	52.8925	18.7455	14	68	11	100	69	24	86	0.000000
3	744	52.8925	18.7455	14	68	11	100	70	1	86	0.000000
3	744	52.8925	18.7455	14	68	11	100	70	2	86	0.000000
3	744	52.8925	18.7455	14	68	11	100	70	3	86	0.000000
4	720	30.8222	14.8795	3	119	11	72	119	21	69	0.000000
5	744	20.9194	11.0789	3	146	12	61	126	17	58	0.000000
5	744	20.9194	11.0789	3	151	11	61	126	17	58	0.000000
6	720	13.4319	8.3007	3	156	11	69	168	23	66	0.000000
6	720	13.4319	8.3007	3	157	12	69	168	23	66	0.000000
6	720	13.4319	8.3007	3	171	11	69	168	23	66	0.000000
6	720	13.4319	8.3007	3	176	13	69	168	23	66	0.000000
6	720	13.4319	8.3007	3	179	9	69	168	23	66	0.000000
6	720	13.4319	8.3007	3	179	10	69	168	23	66	0.000000
6	720	13.4319	8.3007	3	179	11	69	168	23	66	0.000000
6	720	13.4319	8.3007	3	179	12	69	168	23	66	0.000000
6	720	13.4319	8.3007	3	175	13	69	168	23	66	0.000000
7	744	15.1626	8.1990	3	185	8	53	205	18	50	0.000000
7	744	15.1626	8.1990	3	185	9	53	205	18	50	0.000000
7	744	17.0578	10.0676	4	220	10	85	224	20	81	0.000000
8	744	17.0578	10.0676	4	222	8	85	224	20	81	0.000000
8	744	17.0578	10.0676	4	222	9	85	224	20	81	0.000000
8	744	17.0578	10.0676	4	222	10	85	224	20	81	0.000000
8	744	17.0578	10.0676	4	222	11	85	224	20	81	0.000000
8	744	17.0578	10.0676	4	222	12	85	224	20	81	0.000000
8	744	17.0578	10.0676	4	222	13	85	224	20	81	0.000000
8	744	17.0578	10.0676	4	244	11	85	224	20	81	0.000000
8	744	17.0578	10.0676	4	244	12	85	224	20	81	0.000000
9	720	25.3639	15.9898	5	247	10	93	270	22	88	0.000000
9	720	25.3639	15.9898	5	257	10	93	270	22	88	0.000000
9	720	25.3639	15.9898	5	257	11	93	270	22	88	0.000000
9	720	25.3639	15.9898	5	257	12	93	270	22	88	0.000000
10	744	29.2218	15.4160	4	262	9	81	277	18	77	0.000000
10	744	29.2218	15.4160	4	282	9	81	298	24	77	0.000000
11	720	57.0084	22.3474	9	327	8	100	316	1	91	0.555556
11	720	57.0084	22.3474	9	327	9	100	316	2	91	0.555556
11	720	57.0084	22.3474	9	327	9	100	316	3	91	0.555556
11	720	57.0084	22.3474	9	327	9	100	316	4	91	0.555556
11	720	57.0084	22.3474	9	327	9	100	316	5	91	0.555556
11	720	57.0084	22.3474	9	327	9	100	316	24	91	0.555556
11	720	57.0084	22.3474	9	327	9	100	317	1	91	0.555556
11	720	57.0084	22.3474	9	327	9	100	317	2	91	0.555556
11	720	57.0084	22.3474	9	327	9	100	317	3	91	0.555556
11	720	57.0084	22.3474	9	327	9	100	333	1	91	0.555556
12	744	64.9648	21.5076	16	342	10	100	352	6	84	0.672043
12	744	64.9648	21.5076	16	342	10	100	352	7	84	0.672043
12	744	64.9648	21.5076	16	342	10	100	352	8	84	0.672043
12	744	64.9648	21.5076	16	342	10	100	355	24	84	0.672043
12	744	64.9648	21.5076	16	342	10	100	356	1	84	0.672043

YEARLY ANALYSIS OF RELATIVE HUMIDITY (%) OF YEAR 1980

FREQ	MEAN	SID	MIN	MINMONTH	MINDAY	MINHR	MAX	MAXMONTH	MAXDAY	MAXHR	RANGE	MISSING
8784	37.8054	25.8874	3	4	119	11	100	2	48	22	97	0.136612
8784	37.8054	25.8874	3	5	146	12	100	3	69	24	97	0.136612
8784	37.8054	25.8874	3	5	151	11	100	3	70	1	97	0.136612
8784	37.8054	25.8874	3	6	156	11	100	3	70	2	97	0.136612
8784	37.8054	25.8874	3	6	156	12	100	3	70	3	97	0.136612
8784	37.8054	25.8874	3	6	157	12	100	11	316	1	97	0.136612
8784	37.8054	25.8874	3	6	171	11	100	11	316	2	97	0.136612
8784	37.8054	25.8874	3	6	176	13	100	11	316	3	97	0.136612
8784	37.8054	25.8874	3	6	175	9	100	11	316	4	97	0.136612
8784	37.8054	25.8874	3	6	179	10	100	11	316	5	97	0.136612
8784	37.8054	25.8874	3	6	179	11	100	11	316	24	97	0.136612
8784	37.8054	25.8874	3	6	179	12	100	11	317	1	97	0.136612
8784	37.8054	25.8874	3	6	179	13	100	11	317	2	97	0.136612
8784	37.8054	25.8874	3	7	185	8	100	11	317	3	97	0.136612
8784	37.8054	25.8874	3	7	185	9	100	11	333	1	97	0.136612
8784	37.8054	25.8874	3	7	185	10	100	12	352	6	97	0.136612
8784	37.8054	25.8874	3	7	185	10	100	12	352	7	97	0.136612
8784	37.8054	25.8874	3	7	185	10	100	12	352	8	97	0.136612
8784	37.8054	25.8874	3	7	185	10	100	12	355	24	97	0.136612
8784	37.8054	25.8874	3	7	185	10	100	12	355	24	97	0.136612
8784	37.8054	25.8874	3	7	185	10	100	12	356	1	97	0.136612

SEASONAL ANALYSIS OF RELATIVE HUMIDITY (%) FOR 1979-1980

SEASON	_FREQ_	MEAN	STD	MIN	MINMONIH	MINDAY	MINHR	MAX	MAXMONTH	MAXDAY	MAXHR	RANGE	MISSING
WINTER	2184	64.5661	15.8352	8	1	31	10	100	2	48	22	52	0.137363
SPRING	2208	34.9221	20.4543	3	4	119	11	100	3	69	24	97	0.000000
SPRING	2208	34.9221	20.4543	3	5	146	12	100	3	70	1	97	0.000000
SPRING	2208	34.9221	20.4543	3	5	151	11	100	3	70	2	97	0.000000
SPRING	2208	34.9221	20.4543	3	5	151	11	100	3	70	3	97	0.000000
SUMMER	2208	15.2369	9.0213	3	6	156	11	85	8	224	20	82	0.000000
SUMMER	2208	15.2369	9.0213	3	6	156	12	85	8	224	20	82	0.000000
SUMMER	2208	15.2369	9.0213	3	6	157	12	85	8	224	20	82	0.000000
SUMMER	2208	15.2369	9.0213	3	6	171	11	85	8	224	20	82	0.000000
SUMMER	2208	15.2369	9.0213	3	6	176	13	85	8	224	20	82	0.000000
SUMMER	2208	15.2369	9.0213	3	6	179	9	85	8	224	20	82	0.000000
SUMMER	2208	15.2369	9.0213	3	6	179	10	85	8	224	20	82	0.000000
SUMMER	2208	15.2369	9.0213	3	6	179	11	85	8	224	20	82	0.000000
SUMMER	2208	15.2369	9.0213	3	6	179	12	85	8	224	20	82	0.000000
SUMMER	2208	15.2369	9.0213	3	6	179	13	85	8	224	20	82	0.000000
SUMMER	2208	15.2369	9.0213	3	7	185	8	85	8	224	20	82	0.000000
SUMMER	2208	15.2369	9.0213	3	7	185	9	85	8	224	20	82	0.000000
SUMMER	2208	15.2369	9.0213	3	7	185	10	85	8	224	20	82	0.000000
AUTUMN	2184	37.0739	22.9392	4	10	282	9	100	11	316	1	96	0.000000
AUTUMN	2184	37.0739	22.9392	4	10	282	9	100	11	316	2	96	0.183150
AUTUMN	2184	37.0739	22.9392	4	10	282	9	100	11	316	3	96	0.183150
AUTUMN	2184	37.0739	22.9392	4	10	282	9	100	11	316	4	96	0.183150
AUTUMN	2184	37.0739	22.9392	4	10	282	9	100	11	316	5	96	0.183150
AUTUMN	2184	37.0739	22.9392	4	10	282	9	100	11	316	24	96	0.183150
AUTUMN	2184	37.0739	22.9392	4	10	282	9	100	11	317	1	96	0.183150
AUTUMN	2184	37.0739	22.9392	4	10	282	9	100	11	317	2	96	0.183150
AUTUMN	2184	37.0739	22.9392	4	10	282	9	100	11	317	3	96	0.183150
AUTUMN	2184	37.0739	22.9392	4	10	282	9	100	11	333	1	96	0.183150

SEASONAL DAILY CYCLE OF RELATIVE HUMIDITY (%) OF YEAR 79-80

SEASON	HOUR	_FREQ_	MEAN	STD	MIN	MAX	RANGE	MISSING
WINTER	1	92	77.5783	14.5753	36	98	62	0.0000
WINTER	2	91	78.9670	14.0716	34	97	63	0.0000
WINTER	3	91	78.4066	15.5458	33	97	64	0.0000
WINTER	4	91	75.0000	14.7121	29	98	69	0.0000
WINTER	5	91	69.3626	15.1236	23	96	73	0.0000
WINTER	6	91	61.6044	15.4531	18	94	76	0.0000
WINTER	7	91	55.2308	16.2946	14	96	82	0.0000
WINTER	8	91	49.8791	16.7841	13	97	84	0.0000
WINTER	9	90	47.9111	18.4894	9	95	86	0.0000
WINTER	10	91	45.8242	18.0982	8	97	89	0.0000
WINTER	11	91	45.5011	18.2343	10	97	87	0.0000
WINTER	12	91	45.8132	18.4155	9	97	88	0.0000
WINTER	13	91	49.6154	18.7603	10	95	85	0.0000
WINTER	14	91	56.7889	17.7438	5	97	88	1.0989
WINTER	15	91	62.3736	17.5611	15	97	82	0.0000
WINTER	16	91	65.1578	16.4406	20	95	75	0.0000
WINTER	17	91	67.5780	16.1994	25	94	69	0.0000
WINTER	18	91	70.5714	14.9754	27	94	67	0.0000
WINTER	19	91	72.5231	14.4232	25	95	66	0.0000
WINTER	20	91	74.5714	13.4686	32	98	61	0.0000
WINTER	21	91	75.6889	13.5287	32	96	64	1.0989
WINTER	22	91	76.7111	13.8038	31	100	69	1.0989
WINTER	23	91	77.2857	14.1416	33	97	64	0.0000
WINTER	24	91	77.4286	13.8437	35	97	62	0.0000
SPRING	1	92	47.3152	20.5934	16	100	84	0.0000
SPRING	2	92	48.0870	20.5157	17	100	83	0.0000
SPRING	3	92	46.2609	21.4440	15	100	85	0.0000
SPRING	4	92	40.1739	20.4443	12	92	80	0.0000
SPRING	5	92	33.7826	18.6653	10	81	71	0.0000
SPRING	6	92	28.9022	16.6463	7	74	67	0.0000
SPRING	7	92	25.9565	16.6317	5	72	67	0.0000
SPRING	8	92	23.3261	15.1832	5	64	59	0.0000
SPRING	9	92	21.6522	14.4195	4	66	62	0.0000
SPRING	10	92	21.7203	15.3974	4	70	66	0.0000
SPRING	11	92	22.3587	16.4955	3	77	74	0.0000
SPRING	12	92	23.4674	17.3651	3	78	75	0.0000
SPRING	13	92	25.3370	17.3739	4	78	74	0.0000
SPRING	14	92	29.3152	18.5561	5	80	75	0.0000
SPRING	15	92	32.9239	18.3178	8	84	76	0.0000
SPRING	16	92	34.4783	18.5842	9	89	80	0.0000
SPRING	17	92	36.3478	18.6314	12	91	79	0.0000
SPRING	18	92	38.2535	18.1602	12	93	81	0.0000
SPRING	19	92	39.7174	19.2818	14	94	80	0.0000
SPRING	20	92	41.4130	19.1656	14	94	80	0.0000
SPRING	21	92	42.7500	19.5001	11	93	82	0.0000
SPRING	22	92	43.8913	19.6348	12	93	81	0.0000
SPRING	23	92	44.6196	19.9476	10	96	86	0.0000
SPRING	24	92	46.0326	20.1142	16	100	84	0.0000
SUMMER	1	92	22.9022	8.6686	8	65	61	0.0000
SUMMER	2	92	23.0217	8.5111	8	70	62	0.0000
SUMMER	3	92	20.4565	7.4456	8	63	55	0.0000
SUMMER	4	92	16.7717	5.1466	8	38	30	0.0000

SEASONAL DAILY CYCLE OF RELATIVE HUMIDITY (%) OF YEAR 79-80

SEASON	HOUR	_FREQ_	MEAN	STD	MIN	MAX	RANGE	MISSING
SUMMER	5	92	13.6957	3.6093	7	23	16	0.0000
SUMMER	6	92	10.9348	2.6009	6	18	12	0.0000
SUMMER	7	92	5.3370	2.4327	4	17	13	0.0000
SUMMER	8	92	7.9348	2.4709	3	15	12	0.0000
SUMMER	9	92	7.2717	2.6483	3	16	13	0.0000
SUMMER	10	92	7.3043	3.4057	3	23	20	0.0000
SUMMER	11	92	7.4348	4.1861	3	25	22	0.0000
SUMMER	12	92	7.6848	4.4374	3	33	30	0.0000
SUMMER	13	92	9.0109	5.3953	3	37	34	0.0000
SUMMER	14	92	11.0109	6.0538	4	45	41	0.0000
SUMMER	15	92	13.6848	6.9439	4	56	52	0.0000
SUMMER	16	92	15.6957	7.3973	5	51	46	0.0000
SUMMER	17	92	17.4457	8.5335	5	59	54	0.0000
SUMMER	18	92	19.1630	9.2229	8	60	52	0.0000
SUMMER	19	92	19.9457	9.6594	9	69	60	0.0000
SUMMER	20	92	20.2283	10.4504	9	85	76	0.0000
SUMMER	21	92	19.9674	9.3884	8	73	65	0.0000
SUMMER	22	92	21.1304	9.5310	6	68	62	0.0000
SUMMER	23	92	21.4674	9.2480	6	69	60	0.0000
SUMMER	24	92	22.1848	9.0237	8	66	58	0.0000
AUTUMN	1	91	48.7143	22.9610	18	100	82	0.0000
AUTUMN	2	91	49.2747	22.4004	17	100	83	0.0000
AUTUMN	3	91	46.4505	23.1734	17	100	83	0.0000
AUTUMN	4	91	38.7582	22.0365	12	100	88	0.0000
AUTUMN	5	91	33.2418	15.8899	10	100	90	0.0000
AUTUMN	6	91	27.7473	17.7254	9	92	83	0.0000
AUTUMN	7	91	24.1538	16.0298	6	80	74	0.0000
AUTUMN	8	91	21.4505	14.8909	5	75	70	0.0000
AUTUMN	9	91	20.0659	14.1961	4	69	65	0.0000
AUTUMN	10	91	19.3626	14.3948	5	66	61	0.0000
AUTUMN	11	91	20.7363	15.4070	5	79	74	0.0000
AUTUMN	12	91	23.7692	17.5215	5	76	71	0.0000
AUTUMN	13	91	28.0110	19.0079	6	77	71	0.0000
AUTUMN	14	91	34.2088	19.9725	8	84	76	0.0000
AUTUMN	15	91	38.7802	20.4379	10	85	75	0.0000
AUTUMN	16	91	40.6264	21.1947	14	88	74	0.0000
AUTUMN	17	91	43.6763	21.4856	12	91	79	0.0000
AUTUMN	18	91	45.6923	21.9508	13	93	80	0.0000
AUTUMN	19	91	46.5385	22.1852	14	94	80	0.0000
AUTUMN	20	91	47.7582	22.9973	16	98	82	0.0000
AUTUMN	21	91	47.4725	23.4840	15	95	80	0.0000
AUTUMN	22	91	48.6813	23.4965	17	97	80	0.0000
AUTUMN	23	91	47.0341	21.9128	18	96	78	3.2967
AUTUMN	24	91	48.0222	23.2929	17	100	83	1.0989

MONTHLY ANALYSIS OF RELATIVE HUMIDITY (%) OF YEAR 1981

MONTH	_FREQ_	MEAN	STD	MIN	MINDAY	MINHR	MAX	MAXDAY	MAXHR	RANGE	MISSING
1	744	71.5210	20.1948	21	27	11	100	3	23	79	0.94086
1	744	71.5210	20.1948	21	27	13	100	3	24	79	0.94086
1	744	71.5210	20.1948	21	27	13	100	4	1	79	0.94086
1	744	71.5210	20.1948	21	27	13	100	4	2	79	0.94086
1	744	71.5210	20.1948	21	27	13	100	4	3	79	0.94086
1	744	71.5210	20.1948	21	27	13	100	4	24	79	0.94086
1	744	71.5210	20.1948	21	27	13	100	10	1	79	0.94086
1	744	71.5210	20.1948	21	27	13	100	25	3	79	0.94086
2	672	65.3219	21.1538	9	32	11	100	49	3	91	0.14881
3	744	51.3938	21.2370	14	79	10	98	66	21	84	0.00000
4	720	29.2958	16.5424	3	101	12	89	94	1	86	0.00000
4	720	29.2958	16.5424	3	101	13	89	94	1	86	0.00000
4	720	29.2958	16.5424	3	120	13	89	94	1	86	0.00000
4	720	29.2958	16.5424	3	120	14	89	94	1	86	0.00000
5	744	21.9919	11.1809	3	149	10	60	121	22	57	0.00000
5	744	21.9919	11.1809	3	149	11	60	121	23	57	0.00000
6	720	17.2542	8.6033	2	152	9	43	159	22	41	0.00000
7	744	17.2688	8.9132	4	196	12	70	208	1	66	0.00000
7	744	17.2688	8.9132	4	196	13	70	208	1	66	0.00000
8	744	17.2809	8.5919	4	220	12	50	215	22	46	0.00000
8	744	17.2809	8.5919	4	227	10	50	215	22	46	0.00000
8	744	17.2809	8.5919	4	227	11	50	215	22	46	0.00000
9	720	31.1917	23.7488	3	271	11	100	250	1	97	0.00000
9	720	31.1917	23.7488	3	271	11	100	268	1	97	0.00000
10	744	38.2245	20.6439	7	275	9	95	297	24	88	0.00000
10	744	38.2245	20.6439	7	275	10	95	297	24	88	0.00000
10	744	38.2245	20.6439	7	277	10	95	297	24	88	0.00000
10	744	38.2245	20.6439	7	281	11	95	297	24	88	0.00000
11	720	45.4819	21.6610	9	306	9	100	322	23	91	0.00000
11	720	45.4819	21.6610	9	307	8	100	322	24	91	0.00000
11	720	45.4819	21.6610	9	318	12	100	322	24	91	0.00000
11	720	45.4819	21.6610	9	319	10	100	322	24	91	0.00000
12	744	68.8327	21.3812	20	346	9	100	347	24	80	1.20968
12	744	68.8327	21.3812	20	346	9	100	348	2	80	1.20968
12	744	68.8327	21.3812	20	346	9	100	348	3	80	1.20968
12	744	68.8327	21.3812	20	346	9	100	348	19	80	1.20968
12	744	68.8327	21.3812	20	346	9	100	348	20	80	1.20968
12	744	68.8327	21.3812	20	346	9	100	348	22	80	1.20968
12	744	68.8327	21.3812	20	346	9	100	348	23	80	1.20968
12	744	68.8327	21.3812	20	346	9	100	348	24	80	1.20968
12	744	68.8327	21.3812	20	346	9	100	349	1	80	1.20968
12	744	68.8327	21.3812	20	346	9	100	349	2	80	1.20968
12	744	68.8327	21.3812	20	346	9	100	349	3	80	1.20968
12	744	68.8327	21.3812	20	346	9	100	349	4	80	1.20968
12	744	68.8327	21.3812	20	346	9	100	349	5	80	1.20968
12	744	68.8327	21.3812	20	346	9	100	349	6	80	1.20968
12	744	68.8327	21.3812	20	346	9	100	349	20	80	1.20968
12	744	68.8327	21.3812	20	346	9	100	349	21	80	1.20968
12	744	68.8327	21.3812	20	346	9	100	349	22	80	1.20968
12	744	68.8327	21.3812	20	346	9	100	349	23	80	1.20968
12	744	68.8327	21.3812	20	346	9	100	349	24	80	1.20968
12	744	68.8327	21.3812	20	346	9	100	350	1	80	1.20968

MONTHLY ANALYSIS OF RELATIVE HUMIDITY (%) OF YEAR 1981

MONTH	FREQ	MEAN	STD	MIN	MINDAY	MINHR	MAX	MAYDAY	MAYHR	RANGE	MISSING
12	744	68.8327	21.3812	20	346	9	100	350	2	80	1.20968
12	744	68.8327	21.3812	20	346	9	100	350	3	80	1.20968
12	744	68.8327	21.3812	20	346	9	100	350	4	80	1.20968
12	744	68.8327	21.3812	20	346	9	100	363	1	80	1.20968

YEARLY ANALYSIS OF RELATIVE HUMIDITY (%) OF YEAR 1981

FREQ	MEAN	STD	MIN	MINMONTH	MINDAY	MINHR	MAX	MAXMONTH	MAXDAY	MAXHR	RANGE	MISSING
8760	39.4142	26.6281	2	6	152	9	100	1	3	23	98	0-194064
8760	39.4142	26.6281	2	6	152	9	100	1	3	24	98	0-194064
8760	39.4142	26.6281	2	6	152	9	100	1	4	1	98	0-194064
8760	39.4142	26.6281	2	6	152	9	100	1	4	2	98	0-194064
8760	39.4142	26.6281	2	6	152	9	100	1	4	3	98	0-194064
8760	39.4142	26.6281	2	6	152	9	100	1	4	24	98	0-194064
8760	39.4142	26.6281	2	6	152	9	100	1	10	1	98	0-194064
8760	39.4142	26.6281	2	6	152	9	100	1	25	3	98	0-194064
8760	39.4142	26.6281	2	6	152	9	100	2	49	3	98	0-194064
8760	39.4142	26.6281	2	6	152	9	100	9	250	1	98	0-194064
8760	39.4142	26.6281	2	6	152	9	100	9	268	1	98	0-194064
8760	39.4142	26.6281	2	6	152	9	100	11	322	23	98	0-194064
8760	39.4142	26.6281	2	6	152	9	100	11	347	24	98	0-194064
8760	39.4142	26.6281	2	6	152	9	100	12	348	2	98	0-194064
8760	39.4142	26.6281	2	6	152	9	100	12	348	3	98	0-194064
8760	39.4142	26.6281	2	6	152	9	100	12	348	19	98	0-194064
8760	39.4142	26.6281	2	6	152	9	100	12	348	20	98	0-194064
8760	39.4142	26.6281	2	6	152	9	100	12	348	22	98	0-194064
8760	39.4142	26.6281	2	6	152	9	100	12	348	23	98	0-194064
8760	39.4142	26.6281	2	6	152	9	100	12	348	24	98	0-194064
8760	39.4142	26.6281	2	6	152	9	100	12	349	1	98	0-194064
8760	39.4142	26.6281	2	6	152	9	100	12	349	2	98	0-194064
8760	39.4142	26.6281	2	6	152	9	100	12	349	3	98	0-194064
8760	39.4142	26.6281	2	6	152	9	100	12	349	4	98	0-194064
8760	39.4142	26.6281	2	6	152	9	100	12	349	5	98	0-194064
8760	39.4142	26.6281	2	6	152	9	100	12	349	6	98	0-194064
8760	39.4142	26.6281	2	6	152	9	100	12	349	20	98	0-194064
8760	39.4142	26.6281	2	6	152	9	100	12	349	21	98	0-194064
8760	39.4142	26.6281	2	6	152	9	100	12	349	22	98	0-194064
8760	39.4142	26.6281	2	6	152	9	100	12	349	23	98	0-194064
8760	39.4142	26.6281	2	6	152	9	100	12	349	24	98	0-194064
8760	39.4142	26.6281	2	6	152	9	100	12	350	1	98	0-194064
8760	39.4142	26.6281	2	6	152	9	100	12	350	2	98	0-194064
8760	39.4142	26.6281	2	6	152	9	100	12	350	3	98	0-194064
8760	39.4142	26.6281	2	6	152	9	100	12	350	4	98	0-194064
8760	39.4142	26.6281	2	6	152	9	100	12	350	4	98	0-194064
8760	39.4142	26.6281	2	6	152	9	100	12	363	1	98	0-194064

SEASONAL ANALYSIS OF RELATIVE HUMIDITY (%) FOR 1980-1981

SEASON	FREQ.	MEAN	STD	MIN	MINMONTH	MINDAY	MINHR	MAX	MAXMONTH	MAXDAY	MAXHE	RANGE	MISSING
WINTER	2160	67.3680	21.1760	9	2	32	11	100	12	352	6	91	0-.601852
WINTER	2160	67.3680	21.1760	9	2	32	11	100	12	352	7	91	0-.601852
WINTER	2160	67.3680	21.1760	9	2	32	11	100	12	352	8	91	0-.601852
WINTER	2160	67.3680	21.1760	9	2	32	11	100	12	355	24	91	0-.601852
WINTER	2160	67.3680	21.1760	9	2	32	11	100	12	356	1	91	0-.601852
WINTER	2160	67.3680	21.1760	9	2	32	11	100	1	3	23	91	0-.601852
WINTER	2160	67.3680	21.1760	9	2	32	11	100	1	3	24	91	0-.601852
WINTER	2160	67.3680	21.1760	9	2	32	11	100	1	4	1	91	0-.601852
WINTER	2160	67.3680	21.1760	9	2	32	11	100	1	4	2	91	0-.601852
WINTER	2160	67.3680	21.1760	9	2	32	11	100	1	4	2	91	0-.601852
WINTER	2160	67.3680	21.1760	9	2	32	11	100	1	4	3	91	0-.601852
WINTER	2160	67.3680	21.1760	9	2	32	11	100	1	4	24	91	0-.601852
WINTER	2160	67.3680	21.1760	9	2	32	11	100	1	10	1	91	0-.601852
WINTER	2160	67.3680	21.1760	9	2	32	11	100	1	25	3	91	0-.601852
WINTER	2160	67.3680	21.1760	9	2	32	11	100	2	49	3	91	0-.601852
WINTER	2160	67.3680	21.1760	9	2	32	11	100	3	66	21	95	0-.000000
SPRING	2208	34.2808	20.9955	3	4	101	12	98	3	66	21	95	0-.000000
SPRING	2208	34.2808	20.9955	3	4	101	13	98	3	66	21	95	0-.000000
SPRING	2208	34.2808	20.9955	3	4	120	13	98	3	66	21	95	0-.000000
SPRING	2208	34.2808	20.9955	3	4	120	14	98	3	66	21	95	0-.000000
SPRING	2208	34.2808	20.9955	3	5	149	10	98	3	66	21	95	0-.000000
SPRING	2208	34.2808	20.9955	3	5	149	11	98	3	66	21	95	0-.000000
SUMMER	2208	17.2681	8.7012	2	6	152	9	70	7	208	1	68	0-.000000
AUTUMN	2184	38.2985	22.7822	3	9	271	11	100	9	250	1	97	0-.000000
AUTUMN	2184	38.2985	22.7822	3	9	271	11	100	9	268	1	97	0-.000000
AUTUMN	2184	38.2985	22.7822	3	9	271	11	100	11	322	23	97	0-.000000
AUTUMN	2184	38.2985	22.7822	3	9	271	11	100	11	322	24	97	0-.000000

SEASONAL DAILY CYCLE OF RELATIVE HUMIDITY (%) OF YEAR 80-81

SEASON	HOUR	_FREQ_	MEAN	SID	MIN	MAX	RANGE	MISSING
WINTER	1	90	83.7222	11.6812	54	100	46	0.00000
WINTER	2	90	83.6322	11.1628	47	100	53	3.33333
WINTER	3	90	84.0899	11.8087	51	100	49	1.11111
WINTER	4	90	79.1348	12.1320	44	98	54	1.11111
WINTER	5	90	69.2022	13.5966	37	97	60	1.11111
WINTER	6	90	61.1778	15.9589	24	100	76	0.00000
WINTER	7	90	53.5843	17.0686	20	100	80	1.11111
WINTER	8	90	49.3667	18.7948	16	100	84	0.00000
WINTER	9	90	46.7222	19.0257	15	97	82	0.00000
WINTER	10	90	44.0778	19.2676	13	98	85	0.00000
WINTER	11	90	42.9205	18.2997	9	96	87	2.22222
WINTER	12	90	45.1124	19.3035	12	96	84	1.11111
WINTER	13	90	51.4444	19.8783	14	98	84	0.00000
WINTER	14	90	58.6111	18.7471	25	98	73	0.00000
WINTER	15	90	65.1556	16.9996	29	97	68	0.00000
WINTER	16	90	69.4444	15.9106	31	98	67	0.00000
WINTER	17	90	72.5778	14.9636	30	96	66	0.00000
WINTER	18	90	76.2444	14.2184	32	98	66	0.00000
WINTER	19	90	78.0778	14.1344	45	98	53	0.00000
WINTER	20	90	79.4889	13.3157	46	98	52	0.00000
WINTER	21	90	79.9556	13.0831	37	98	61	0.00000
WINTER	22	90	80.3222	12.3869	39	98	59	0.00000
WINTER	23	90	81.0568	12.4885	46	100	54	2.22222
WINTER	24	90	82.1124	13.3096	51	100	49	1.11111
SPRING	1	92	50.5761	22.0086	10	93	83	0.00000
SPRING	2	92	51.2935	22.3531	8	96	88	0.00000
SPRING	3	92	46.4022	22.2410	15	94	79	0.00000
SPRING	4	92	38.7065	19.2283	13	84	71	0.00000
SPRING	5	92	30.8696	16.3211	8	75	67	0.00000
SPRING	6	92	26.3478	13.9665	9	66	57	0.00000
SPRING	7	92	23.2717	13.6680	7	88	81	0.00000
SPRING	8	92	20.4783	11.5449	6	60	54	0.00000
SPRING	9	92	19.0435	10.3126	4	50	46	0.00000
SPRING	10	92	17.9348	9.8648	3	47	44	0.00000
SPRING	11	92	18.3587	10.5805	3	47	44	0.00000
SPRING	12	92	19.6413	11.9537	3	54	51	0.00000
SPRING	13	92	21.6413	13.2595	3	59	56	0.00000
SPRING	14	92	25.4022	15.5097	3	69	66	0.00000
SPRING	15	92	30.9239	17.1696	5	71	66	0.00000
SPRING	16	92	34.4239	18.6608	7	77	70	0.00000
SPRING	17	92	36.6304	19.2164	8	84	76	0.00000
SPRING	18	92	38.9022	19.3823	10	90	80	0.00000
SPRING	19	92	41.6957	19.3281	10	91	81	0.00000
SPRING	20	92	43.6196	19.7922	11	95	84	0.00000
SPRING	21	92	45.3152	20.5934	10	98	88	0.00000
SPRING	22	92	46.5978	21.7675	10	97	87	0.00000
SPRING	23	92	47.0870	22.2808	12	96	84	0.00000
SPRING	24	92	47.5761	22.2746	8	95	87	0.00000
SUMMER	1	92	26.0326	7.5629	11	70	59	0.00000
SUMMER	2	92	24.8696	8.2957	10	68	58	0.00000
SUMMER	3	92	21.1848	8.3441	7	60	53	0.00000
SUMMER	4	92	17.2065	6.9859	6	57	51	0.00000

SEASONAL DAILY CYCLE OF RELATIVE HUMIDITY (%) OF YEAR 80-81

SEASON	HOUR	_FREQ_	MEAN	STD	MIN	MAX	RANGE	MISSING
SUMMER	5	92	14.6413	5.8396	5	43	38	0
SUMMER	6	92	12.8043	4.8477	4	34	30	0
SUMMER	7	92	11.2026	5.0172	4	42	38	0
SUMMER	8	92	9.9022	4.0412	5	35	30	0
SUMMER	9	92	9.0652	3.1477	2	22	20	0
SUMMER	10	92	8.6957	2.8001	4	25	21	0
SUMMER	11	92	8.8804	3.5544	4	30	26	0
SUMMER	12	92	9.7826	4.1558	4	29	25	0
SUMMER	13	92	10.6304	4.6921	4	33	29	0
SUMMER	14	92	12.6413	5.0916	5	33	28	0
SUMMER	15	92	15.1304	5.7765	5	36	31	0
SUMMER	16	92	18.4565	6.8443	8	40	32	0
SUMMER	17	92	20.0326	6.9889	9	42	33	0
SUMMER	18	92	21.0761	7.3309	10	44	34	0
SUMMER	19	92	21.9891	7.2741	11	40	29	0
SUMMER	20	92	22.5978	7.8517	10	44	34	0
SUMMER	21	92	23.7174	8.3262	9	53	44	0
SUMMER	22	92	24.3913	7.7827	11	52	41	0
SUMMER	23	92	24.3043	6.3588	12	43	31	0
SUMMER	24	92	25.1196	6.1570	11	42	31	0
AUTUMN	1	91	50.4725	22.4055	16	100	84	0
AUTUMN	2	91	50.8462	22.4504	16	98	82	0
AUTUMN	3	91	46.9231	22.0430	12	97	85	0
AUTUMN	4	91	38.7033	20.4562	11	90	79	0
AUTUMN	5	91	32.2637	17.8175	7	77	70	0
AUTUMN	6	91	25.8242	14.3547	5	63	58	0
AUTUMN	7	91	22.5165	14.0169	4	62	58	0
AUTUMN	8	91	20.3516	13.1895	5	66	61	0
AUTUMN	9	91	19.4066	12.7104	4	60	56	0
AUTUMN	10	91	19.1538	12.1572	4	51	47	0
AUTUMN	11	91	20.0000	13.0350	3	70	67	0
AUTUMN	12	91	22.6484	13.7569	4	72	68	0
AUTUMN	13	91	27.6703	16.4202	6	82	76	0
AUTUMN	14	91	34.6813	18.4336	10	83	73	0
AUTUMN	15	91	40.0330	19.4562	12	85	73	0
AUTUMN	16	91	43.6593	19.8898	13	94	81	0
AUTUMN	17	91	46.4835	20.2788	13	90	77	0
AUTUMN	18	91	49.0220	20.7830	12	91	79	0
AUTUMN	19	91	50.4945	21.9608	9	93	84	0
AUTUMN	20	91	51.3407	22.5582	9	96	87	0
AUTUMN	21	91	51.6813	22.3790	10	94	84	0
AUTUMN	22	91	51.5165	22.9097	12	97	85	0
AUTUMN	23	91	52.0110	22.5578	14	100	86	0
AUTUMN	24	91	51.4615	22.3901	15	100	85	0

MONTHLY ANALYSIS OF RELATIVE HUMIDITY (2) CF YEAR 1982

MONTH	MEAN	STD	MIN	MINDAY	MINHR	MAX	MAXDAY	MAXHR	RANGE	MISSING
1	70.2544	20.1048	21	26	10	100	7	23	79	0.672043
1	70.2544	20.1048	21	31	10	100	8	1	79	0.672043
1	70.2544	20.1048	21	31	11	100	26	20	79	0.672043
2	57.2634	20.4096	11	40	12	94	34	2	83	0.000000
2	57.2634	20.4096	11	40	12	94	34	22	83	0.000000
2	57.2634	20.4096	11	40	12	94	47	1	83	0.000000
3	51.2615	22.8161	6	68	9	100	70	1	94	0.268817
3	51.2615	22.8161	6	68	10	100	70	1	94	0.268817
3	51.2615	22.8161	6	68	10	100	70	1	94	0.268817
4	57.7542	19.1311	2	52	8	58	117	22	96	0.138889
4	57.7542	19.1311	2	52	11	58	118	1	96	0.138889
5	30.7715	14.6136	7	145	14	75	125	18	68	0.000000
5	30.7715	14.6136	7	145	5	75	125	24	68	0.000000
5	30.7715	14.6136	7	145	12	75	126	24	68	0.000000
6	14.3403	7.5026	3	167	11	37	165	23	34	0.000000
6	14.3403	7.5026	3	170	10	37	165	1	34	0.000000
6	14.3403	7.5026	3	170	11	37	165	1	34	0.000000
6	14.3403	7.5026	3	171	11	37	165	1	34	0.000000
6	14.3403	7.5026	3	175	10	37	165	1	34	0.000000
6	14.3403	7.5026	3	179	11	37	165	1	34	0.000000
6	14.3403	7.5026	3	180	11	37	165	1	34	0.000000
6	14.3403	7.5026	3	180	12	37	165	1	34	0.000000
7	16.4288	11.9941	2	150	8	85	204	22	83	0.060000
7	16.4288	11.9941	2	150	12	85	204	23	83	0.060000
7	16.4288	11.9941	2	159	10	85	204	23	83	0.060000
7	16.4288	11.9941	2	159	12	85	204	23	83	0.060000
8	15.3491	11.5192	3	210	10	95	243	22	92	0.268817
9	27.7931	17.0068	4	263	9	97	244	1	93	0.000000
9	27.7931	17.0068	4	264	8	97	244	1	93	0.000000
10	50.7527	22.1326	7	278	7	54	295	2	87	0.000000
10	50.7527	22.1326	7	278	8	54	302	1	87	0.000000
10	50.7527	22.1326	7	278	9	54	302	1	87	0.000000
10	50.7527	22.1326	7	278	10	54	302	1	87	0.000000
11	55.5458	18.2881	15	313	11	93	305	1	74	0.000000
11	55.5458	18.2881	15	313	10	93	305	1	74	0.000000
12	44.5269	18.8091	20	335	12	58	352	3	78	0.000000
12	44.5269	18.8091	20	335	12	58	352	4	78	0.000000

YEARLY ANALYSIS OF RELATIVE HUMIDITY (%) OF YEAR 1982

PLAK	SID	MIN	MINMONTH	RINDAY	MINHR	MAX	MAXMONTH	MAXDAY	MAXHR	RANGE	MISSING
8760	25.5807	2	4	92	8	100	1	7	23	98	0.114155
8760	25.5807	2	4	92	11	100	1	8	1	98	0.114155
8760	25.5807	2	7	190	8	100	1	26	20	98	0.114155
8760	25.5807	2	7	190	12	100	3	70	1	98	0.114155
8760	25.5807	2	7	195	10	100	3	70	1	98	0.114155
8760	25.5807	2	7	195	12	100	3	70	1	98	0.114155

SEASONAL DAILY CYCLE OF RELATIVE HUMIDITY (%) OF YEAR 81-82

SEASON	HOUR	-FREQ-	MEAN	STD	MIN	MAX	RANGE	MISSING
WINTER	1	90	82.6667	11.1637	50	100	50	1.11111
WINTER	2	90	82.5775	11.8360	51	100	49	1.11111
WINTER	3	90	83.4362	11.0669	47	100	53	1.11111
WINTER	4	90	79.6227	12.4226	45	100	55	2.22222
WINTER	5	90	69.2000	14.4650	44	100	56	0.00000
WINTER	6	90	59.5776	15.9803	32	100	68	0.00000
WINTER	7	90	52.1556	17.4921	22	97	75	0.00000
WINTER	8	90	46.6444	16.5583	20	94	74	0.00000
WINTER	9	90	42.1011	16.1598	18	91	73	1.11111
WINTER	10	90	40.6444	16.0947	14	90	76	0.00000
WINTER	11	90	41.5222	17.1374	13	91	78	0.00000
WINTER	12	90	43.7776	18.0130	11	93	82	0.00000
WINTER	13	90	46.7111	18.5207	12	93	81	0.00000
WINTER	14	90	56.5111	19.4455	18	97	79	0.00000
WINTER	15	90	61.5333	18.1066	17	98	81	0.00000
WINTER	16	90	66.6444	16.5416	27	97	70	0.00000
WINTER	17	90	76.6556	15.4040	33	97	64	0.00000
WINTER	18	90	76.4333	13.5581	38	98	60	0.00000
WINTER	19	90	78.0562	13.2411	49	100	60	0.00000
WINTER	20	90	78.5316	12.8150	47	100	53	1.11111
WINTER	21	90	80.7386	12.1158	49	100	51	2.22222
WINTER	22	90	81.3700	12.6534	30	100	70	1.11111
WINTER	23	90	82.0795	11.6098	50	100	50	2.22222
WINTER	24	90	55.5217	19.2288	25	100	75	0.00000
SPRING	1	92	56.5217	18.8816	27	98	71	0.00000
SPRING	2	92	52.5121	15.6127	21	94	73	1.08656
SPRING	3	92	45.5783	15.6521	13	95	83	0.00000
SPRING	4	92	39.0000	16.5946	8	95	87	0.00000
SPRING	5	92	33.6848	16.5223	5	80	75	0.00000
SPRING	6	92	30.4239	17.1402	3	78	75	0.00000
SPRING	7	92	27.1304	15.6740	2	73	71	0.00000
SPRING	8	92	25.5109	15.6840	4	83	79	0.00000
SPRING	9	92	24.9239	16.2766	6	81	75	0.00000
SPRING	10	92	24.5891	15.5500	2	76	74	0.00000
SPRING	11	92	25.6217	15.6668	5	83	78	0.00000
SPRING	12	92	26.4074	15.8443	5	85	80	0.00000
SPRING	13	92	29.5074	17.5214	7	85	78	0.00000
SPRING	14	92	34.4239	17.6854	10	87	77	0.00000
SPRING	15	92	37.6304	18.2273	9	89	80	0.00000
SPRING	16	92	40.5130	18.1154	13	89	76	0.00000
SPRING	17	92	43.5891	15.0773	17	90	73	0.00000
SPRING	18	92	46.5761	18.5284	22	91	69	0.00000
SPRING	19	92	48.8261	18.5501	15	97	78	0.00000
SPRING	20	92	51.7609	18.3467	23	96	73	0.00000
SPRING	21	92	51.6567	19.2425	22	98	76	0.00000
SPRING	22	92	52.5457	15.3756	21	96	75	0.00000
SPRING	23	92	53.4111	18.3443	21	93	72	2.17351
SPRING	24	92	24.1522	12.6343	11	91	80	0.00000
SUMMER	1	92	24.3987	11.4581	11	82	71	0.00000
SUMMER	2	92	26.7174	5.2823	11	73	62	0.00000
SUMMER	3	92	17.0761	5.1989	7	78	71	0.00000
SUMMER	4	92						

SEASONAL DAILY CYCLE OF RELATIVE HUMIDITY (%) OF YEAR 81-82

SEASON	HOUR	_FREQ_	MEAN	STD	MIN	MAX	RANGE	MISSING
SUMMER	5	92	13.5674	6.6323	5	53	48	C-00000
SUMMLK	6	92	11.7826	5.8023	4	46	42	C-00000
SUMMER	7	92	9.5326	3.8842	3	35	32	C-00000
SUMMER	8	92	8.2351	4.1148	2	39	37	C-00000
SUMMER	9	92	7.5435	4.2655	3	38	35	C-00000
SUMPLK	10	92	7.1898	3.9445	2	34	32	C-00000
SUMMLK	11	92	7.3696	4.7317	3	40	37	C-00000
SUMMER	12	92	8.6109	5.4642	2	40	38	C-00000
SUMMER	13	92	8.7717	5.1741	4	40	36	C-00000
SUMMER	14	92	10.7174	6.3839	4	50	46	C-00000
SUMMER	15	92	13.4674	7.5170	6	48	42	C-00000
SUMMLK	16	92	14.8696	7.9824	7	67	60	C-00000
SUMMLK	17	92	15.1826	8.8263	4	70	66	C-00000
SUMMER	18	92	17.2065	9.5060	6	73	67	C-00000
SUMMER	19	92	18.5130	10.6695	5	80	75	C-00000
SUMMER	20	92	19.5652	9.9816	6	80	74	C-00000
SUMMLK	21	92	21.3478	12.4127	6	90	84	C-00000
SUMMER	22	92	22.7285	14.1134	5	95	86	C-00000
SUMMLK	23	92	22.5604	12.1812	5	92	83	C-00000
SUMMER	24	92	23.9165	12.4654	10	93	83	C-00000
AUTUMN	1	91	58.5341	21.6251	16	97	81	C-00000
AUTUMN	2	91	55.3167	21.8250	15	94	79	C-00000
AUTUMN	3	91	58.6879	22.3008	18	92	74	C-00000
AUTUMN	4	91	45.5824	21.6739	11	89	78	C-00000
AUTUMN	5	91	41.3736	20.4563	9	89	80	C-00000
AUTUMN	6	91	34.0655	19.1571	7	52	85	C-00000
AUTUMN	7	91	29.2527	17.7636	5	91	86	C-00000
AUTUMN	8	91	27.4565	17.5286	4	87	83	C-00000
AUTUMN	9	91	26.2857	16.0563	4	81	77	C-00000
AUTUMN	10	91	25.8901	14.9015	5	69	64	C-00000
AUTUMN	11	91	26.7033	14.6657	5	71	66	C-00000
AUTUMN	12	91	25.0549	17.0850	5	83	78	C-00000
AUTUMN	13	91	32.8681	17.7909	6	80	74	C-00000
AUTUMN	14	91	36.6374	18.6426	8	83	75	C-00000
AUTUMN	15	91	43.2308	18.3158	12	84	72	C-00000
AUTUMN	16	91	46.7055	18.7560	14	91	77	C-00000
AUTUMN	17	91	45.6055	18.4753	17	86	69	C-00000
AUTUMN	18	91	53.5534	18.3751	17	87	70	C-00000
AUTUMN	19	91	55.3626	18.2458	20	90	70	C-00000
AUTUMN	20	91	56.4615	15.6084	15	85	70	C-00000
AUTUMN	21	91	58.4835	15.4156	15	92	73	C-00000
AUTUMN	22	91	57.5451	20.5228	16	52	76	C-00000
AUTUMN	23	91	56.5026	26.5674	17	92	75	C-00000
AUTUMN	24	91	57.6154	21.1428	15	53	78	C-00000

SECTION 13

This section is Mr. El-Karmi's report on the data base activities in Task 4 of EES-45.

A PROTOTYPE DATA BASE MANAGEMENT SYSTEM
FOR METEOROLOGICAL AND
AIR QUALITY DATA

Prepared by

A.O.EL-KARMI

TASK LEADER, EES-45

ENVIRONMENTAL AND EARTH SCIENCES DIVISION

KUWAIT INSTITUTE FOR SCIENTIFIC RESEARCH

P.O.BOX. 24885

SAFAT

KUWAIT

APRIL 1983

The increasing rate of information collection requires, in most application fields, the use of a data base management systems (DBMS). DBMS, originally confined to managerial and commercial applications, is now applied to scientific problems. In applying DBMS to scientific cases, however several new factors in addition to those related to the traditional DBMS requirements should be investigated. These factors stem from the fact that scientific applications are more user oriented than commercial and managerial applications, not to mention that the processing of scientific data is rather different from processing managerial or commercial data. This report is the conclusion of an effort to explore the adaptability of DBMS to air quality and meteorological data. Similar efforts were made, for example, by Runca et al. (1978).

This work is a part of the Air Pollution Dispersion and Prediction Model for Shuaiba Industrial Area (SIA) of Kuwait. The SIA is about 8.44 million m² (8.44 km²) occupied by different industrial companies ranging from petrochemical industries and power plants to fishing industries.

But what is a data base and a data base management system? Ullman (1980, page 1) defined the term data base as "a collection of data stored more or less permanently in a computer" and "the software that allows one or many person to use and/or modify this data" is termed a data base management system. DBMS deals with the data base in an abstract form. The smallest portion of distinguishable information existing in a data base is termed an entity. Each such datum has certain properties associated with it (called attributes). Such attributes constitute a set referred to as an entity set. The retrieval mechanism of each entity set is done via a key. Since each entity can be distinguished from another entity, a key uniquely represents each entity set.

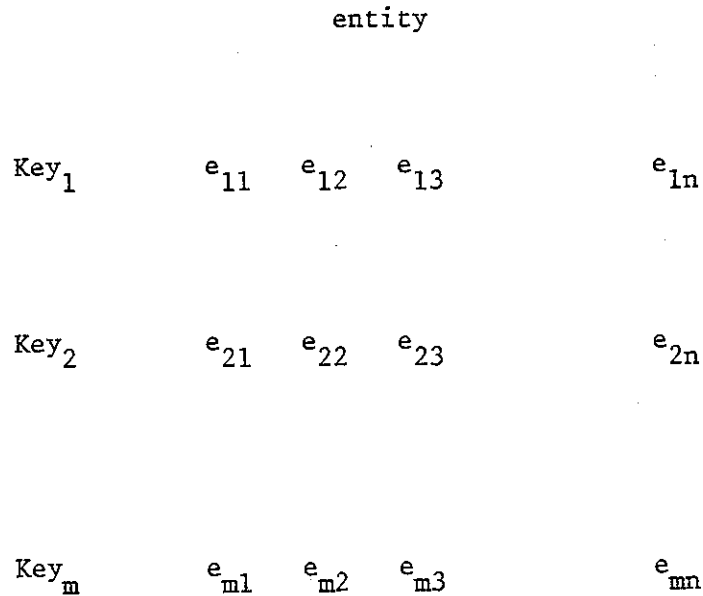


Fig. 1 Keys, entities and entity sets

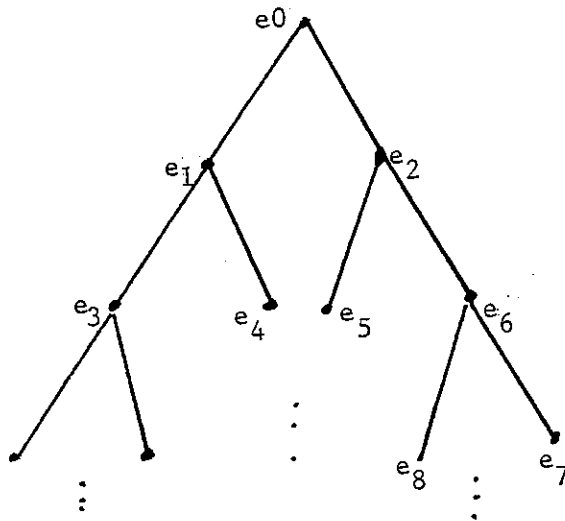
2. Data Base System Models

There are three different data base systems models, which differ in the logical organization of data. The three models are (Neimat, 1981):

- 1) hierarchical,
- 2) network, and
- 3) relational.

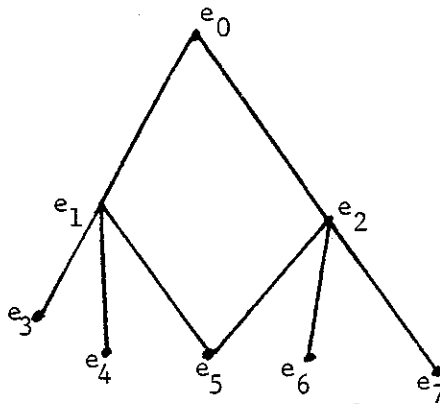
2.1 Hierarchal Model

The hierarchichal model views data or entities as a tree in which each entity ("Son") has a unique higher level ("Father") dominating it, as depicted below.



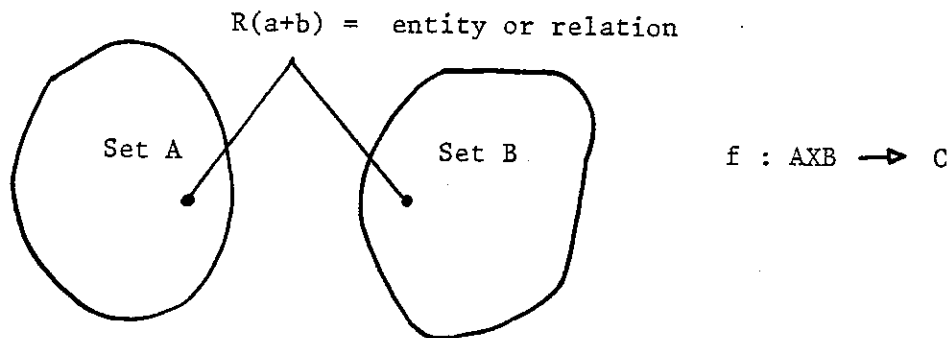
2.2 Network Model

In the network model, it is possible for one entity to be the son of two different entities as depicted below. Most network models still retain the constraint that no entity may be both father and son in the same relationship.



2.3 Relational Models

A relational model deals with entities with no explicit relationship between them. An entity is called a relation, and it consists of a set of ordered n-tuples drawn from n-domains defining the relation. An example with $n = 2$ is depicted below



3. Logical and Comparison Operations of the Proposed Prototype

In data base management systems, data processing depend heavily on logical operations and comparison operators. The known logical operations are AND OR, and NOT, in which NOT is a single argument function and OR and AND are double-argument functions.

The comparison operators are

NE	not equal
EQ	equal
GT	greater than
GE	greater than or equal
LT	less than
LE	less than or equal

It can be demonstrated that these logical operators form a complete set, i.e., can cover all possible logical operations. Moreover, it must be pointed out that AND and NOT can simulate OR' and OR and NOT can simulate AND, according to the following schemes:

$$(1) C_1 \text{ OR } C_2 = \text{NOT} (\text{NOT } C_1 \text{ AND NOT } C_2)$$

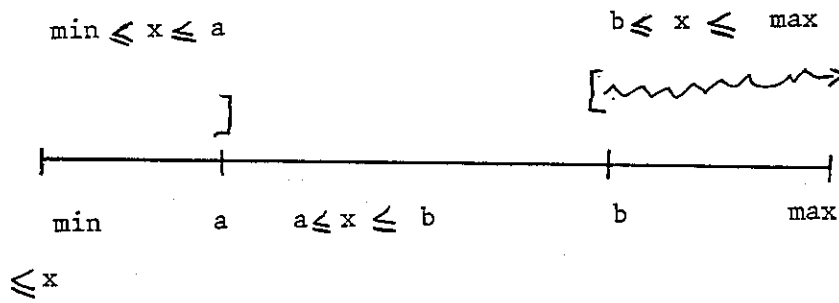
$$(2) C_1 \text{ AND } C_2 = \text{NOT} (\text{NOT } C_1 \text{ OR NOT } C_2)$$

C_1	C_2	NOT C_1	NOT C_2	C_1 AND C_2	C_1 OR C_2	R.H.S. of 1	R.H.S. of 2
T	T	F	F	T	T	T	T
F	T	T	F	F	T	T	F
T	F	F	T	F	T	T	F
F	F	T	T	F	F	F	F

The truth tables of both AND and OR are shown in the table below.

C_1	C_2	AND (C_1, C_2)	OR (C_1, C_2)
T	T	T	T
F	T	F	T
T	F	F	T
F	F	F	F

Practically, the DBMS user will communicate with the data base via certain conditions. It has been found that the range condition ("is the variable in a certain range?") can simulate all possible comparison conditions (see the figure below).



That is, by setting the upper and lower ranges of the condition, one can extract the data he desires. The proposed prototype of DBMS allows the processing of four conditions imposed on the data. Each condition corresponds to one parameter in which the DBMS will allow the user to specify a simple condition for each parameter. The processing is then carried out with the desired logical operands. (For more details about logical operators refer to Ref. 2). This argument can be illustrated by the following example.

Example: What are the records in which the temperature is in the range of 15-20°C while the wind speed was 27 miles per hour.

The DBMS will identify two conditions here connected with the logical operator AND (which corresponds to "while"), then the processing will be as follows:

- get all keys for records satisfying temperature range
- get all keys for records satisfying wind speed = 27
- perform the logical operation (AND) on them
- obtain a list of selected record keys satisfying both conditions

- extract the date and time of these selected records
- extract these records
- pilot these records to the specified device.

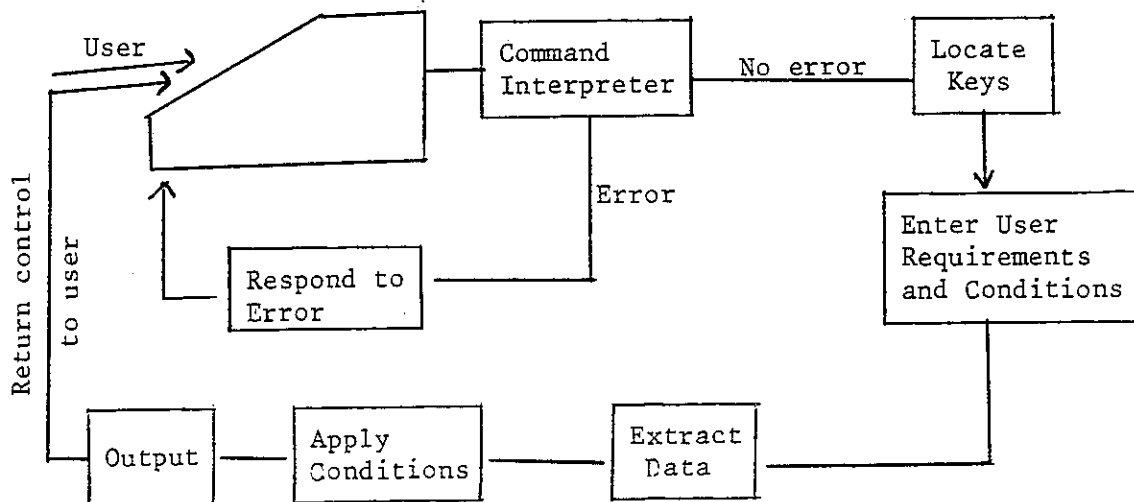
4. Prototype Basic Structure

The prototype data base management system for air quality and meteorological data can be subdivided into three basic structures:

- command interpreter and data retrieval,
- data processing, and
- data output.

4.1 Command Interpreter and Data Retrieval

Five legal commands have been identified, each with a unique function. These commands cover the three basic structures. The command analyzer and interpreter was designed in a flexible manner. This will be helpful for a DBMS user who has never been exposed to computers. The command interpreter has a section to analyze any error in the command line and respond accordingly. An overall description of the proposed prototype, showing the three structures, is depicted below.



The five legal commands of this prototype DBMS are:

1. Locate
2. Analyze
3. Print
4. Help
5. End

4.1.1 The "Locate" Command. This command has the following format (H: hour)

LOC, ^S_M , H_S, M_S, D_S, Y_S, H_E, M_E, D_E, Y_E,

H : hour
M : month
D : day
Y : year

where the subscripts are S for starting and E for ending.

The command must have the three ASCII (American Standard Code for Information Interchange) characters LOC. Any failure to supply these three characters will result in an error message by the command interpreter. A delimiter is to be put immediately after these three characters. This is either a comma or a blank. The next input is a character denoting the type of locate, i.e., either an S, to indicate a single parameter, or an M, for multiple parameters. After this, a set of numbers must be entered, separated by delimiters, indicating the starting and ending hours and date.

The command interpreter section will scan the input and analyze any entry error. As an example, the command interpreter can provide the DBMS user with an error message if the year (starting or ending) is not a leap year but the month and day entered happen to be February 29.

The DBMS is supported with an error selection section that will supply the user with a variety of error messages. The command interpreter error messages are listed in Section 6.

The locate command takes the prescribed input and translates it into two keys. The keys indicate the starting and ending records in which the investigation will occur. The keys are carried out to the next command in which the user specifies the desired parameters and ranges.

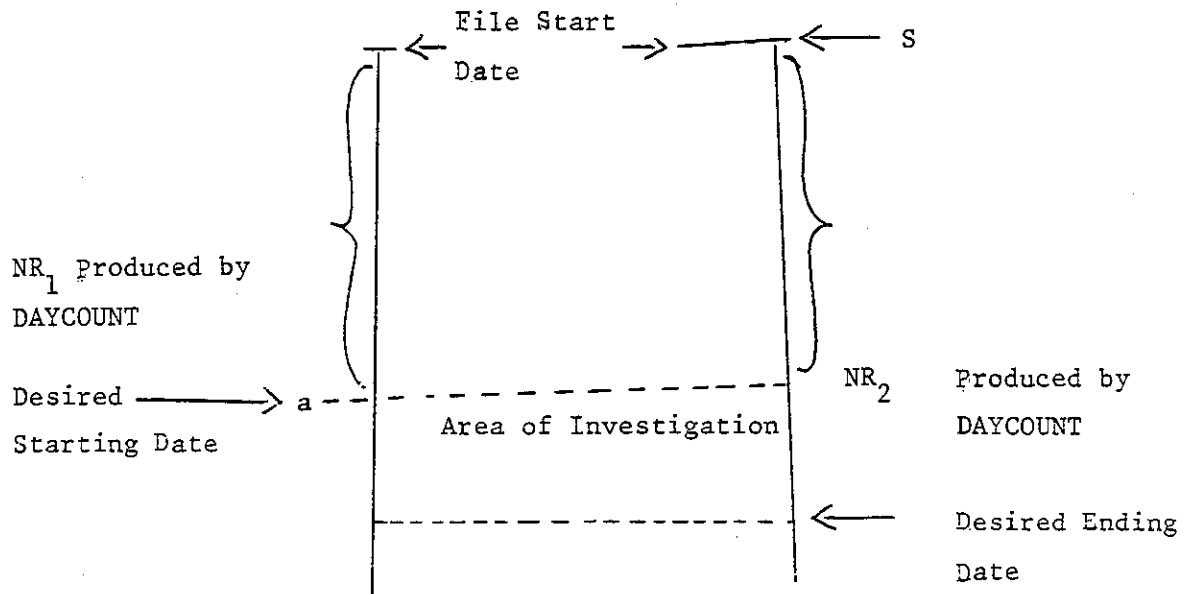
The calculation of the keys is based on the following information:

- the key uniquely identifies the record,
- the record has only one corresponding key, and
- the records are related to date and hour.

These points suggest the following formula for key calculation:

$$\text{Key} = 24 \times (\text{desired date} - \text{file start date}) + \text{hour}$$

Subroutine DAYCOUNT will take the date as an input and produce the number of days between that date and the file start date (see the figure below).



In this scheme, NR_1 indicates the position of the desired starting date in the date base, and NR_2 indicates the position of the desired ending date in the data base. The searching mechanism will start immediately from NR_1 to NR_2 . This means that the access to the Data Base is performed not in a sequential manner but in a random access mode.

Since the key-record relation is one-to-one, one can produce the key for a given date or produce the date from a given key. This is not an advantage as such, but it is built this way, so dates will not be stored, and hence storage will be minimized (see future enhancements and concluding remarks in Section 5). The algorithm of extracting the date out of a given key is described in the Section 4.2 (data processing).

4.1.2 Analyze Command. This command analyzes user requirements for the parameters to be processed. It has the following structure

ANL, $\begin{matrix} S \\ M \end{matrix}$, "PARM", Range_{min}, Range_{max}, etc.....

This command is scanned on the same principles as the locate command. In this formula, "PARM" stands for any one of the four parameters below:

"TEMP" : Temperature
"WINS" : Wind speed
"PRES" : Pressure
"HUMD" : Humidity

4.1.3 Print Command. This command puts the computed result on any desired device. The command structure is as follows:

PRT, device code where device code can be any of the following:

13 : printer
26 : movable disk file
27 : fixed disk file
28 : magnetic tape
10 : CRT
29 : plotter (under development)

4.1.4 Help Command. This command orients the user about the package. It gives the command structure, illustrating various commands with examples. Practically, what will be displayed to the user is a user's guide to the package. The structure for this command is HLP.

4.1.5 END Command. This command terminates the execution of the package, clears all parameters, and resets the data files.

4.2 Data Processing and Logic Flow of Package

When the user initiates the package, the display routine starts execution by displaying the package identification. If there is a recent update note written by the package maintenance section or the previous user, it will be displayed. Afterwards, the command interpreter starts its function awaiting the user's input. The actual processing of records is done on key bases. The key for each record satisfying user requirements is kept in its corresponding location in a two-dimensional array. User conditions on imposed requirements are performed on these keys (either using OR, AND, or NOT). Results are kept in the last entry of this array.

The user, by this, can issue another analysis command on another set of parameters with different ranges, but within the same time period. The analysis section will then carry out the new user conditions with the previously accumulated results (upon the end of each analysis, the date retrieval mechanism takes control and calculates dates and hours for the next command).

The mechanism of extracting the date out of the keys is very simple and is illustrated by this logic sequence:

1. get start and end dates
2. check for leap year and adjust accordingly
3. for all result keys, perform steps 4 to 11
4. get the remainder of key value over 24 and store result in hour
5. then, for month 1 to month 11, perform steps 6 to 11
6. subtract number of days in month from extracted number of days and put result back in number of days

7. if number of days less than or equal to the days of the next month go to 9
8. otherwise go to 6
9. month is extracted and number of days will be the day number
10. extract the data and print it
11. go to 4
12. exit

5. Future Enhancements and Concluding Remarks

This DBMS System is still under development and various aspects are not yet completed. The following suggestions can be taken into consideration for future enhancements:

1. Selection of the Data Base: The package should be flexible enough to cover any other data base present on the system, provided it is stored in a similar format. A simple query such as, "DB?" should give a list of all data bases that can be accessed.
2. A section should be added to the package to access a routing for writing any recent analysis performed on the data base, for possible other users. Also as mentioned before calculation of date and time out of each record is done upon and of analyses command. This is very time consuming. It is suggested that future enhancement date and time be stored within the data record.
3. The DBMS should optionally print the content of the screen on the printer.
4. The print command should have an option for suppressing part of the output (i.e., if average, max, min, and st. dev. are not needed).

5. Automatic problem-oriented check of stored data (e.g., data range, continuity, data consistency, extremes, etc). In conclusion, the discussed prototype represents a substantial improvement in data handling capabilities. The package will be further developed in the near future and will probably be installed in a larger computer (e.g., KISR's IBM 4341 system) to fully exploit its unique data manipulation power.

6.

Command Interpreter Error Messages

- Starting hour is wrong, hours should be between 1 and 24 only
- Ending hour is wrong, hours should be between 1 and 24 only
- Starting month is wrong check command again
- Ending month is wrong check command again
- Error in number of days of the starting month
- Error in number of days of the ending month
- The starting year is not a leap year
- The ending year is not a leap year
- Command line structure is wrong

References

- Runca Eli, P. Melli and P. Zannetti. 1978. A COMPUTER-ORIENTED EMISSIONS inventory procedure for urban and industrial sources. APCA Journal 6: 584-588.
- Enderton "Introduction to Mathematical Logic"
- Herbert B. Enderton. 1972. A Mathematical Introduction to Logic. Academic Press 1972.
- Ullman, Jeffrey D. 1980. Principles of data base systems. Computer Science page 1.
- Neimat M.K. 1981. UMI Research Press, Ann Arbor, Michigan. Search Mechanisms for Large Files.

SECTION 14

This section contains Mr. Al-Sudairawi's report of tether sonde measurement (Task 2 of EES-45).

TETHERSONDE MEASUREMENTS IN SHUAIBA

Prepared by

MANE AL-SUDAIRAWI

TASK LEADER, EES-45

ENVIRONMENTAL AND EARTH SCIENCES DIVISION

KUWAIT INSTITUTE FOR SCIENTIFIC RESEARCH

P. O. BOX 24885

SAFAT

KUWAIT

APRIL 1983

Introduction

For air pollution modeling three types of data need to be collected: emission data to estimate the amount of pollutants emitted, meteorological data to predict the dispersion of the pollutant, and air quality data for calibrating the model.

There are two types of meteorological measurements: surface and aloft (direct or by remote sensing). Some instruments that can be used to measure the upper atmospheric data are radiosondes and tether sondes (direct measurements) and acoustic sounders (remote sensing).

The radiosonde is a balloon inflated by helium gas to lift a meteorological sensors package, which transmits the data by an electric signal to a ground station. This balloon can be traced by a theodolite or a radar to estimate the wind speed and wind direction at different altitudes. The tether sonde balloon is similar to the radiosonde, but is attached to a tetherline and, therefore, can be recovered. Moreover, tether sonde balloons have an aerodynamic shape allowing them to measure wind direction. The tether sonde can fly up to 1000 meters whereas the radiosonde can reach up to 30,000 meters.

Atmospheric acoustic sounding is a remote sensing technique developed in the last 10 years, which has been particularly successful in air pollution studies. Using this technique, an acoustic pulse is transmitted through the atmosphere and, by analyzing its echo, important information on vertical turbulence structure can be inferred (e.g., multiple layers, inversions, mixing height, etc.). Moreover, using Doppler techniques (Doppler Acoustic Sounders) the semi-instantaneous wind vector can be evaluated at different altitudes.

The first kilometer above the ground is the most important atmospheric layer for air pollution studies. In comparing the upper air instruments, we see that the radiosonde transmits a set of data every 100-300 m meters, whereas the tether sonde transmits the data at any height chosen by the operator. Moreover, the radiosonde would be lost after each flight but the tether sonde can be recovered and used again. Acoustic sounding provides

excellent continuous data, but is still difficult to interpret. Doppler acoustic sounding is probably the best instrumentation for air pollution studies, but it was not considered to be a cost-effective choice at this stage of the project. The tethered sonde balloon was selected as the most suitable instrumentation for the air pollution research purposes in Kuwait.

Two persons representing KISR and SAA were sent to the U.S. to visit the tethered sonde manufacturer (Atmospheric Instrumentation Research Incorporation), to examine the instruments, and to receive proper training on the hardware.

2. Tethered Sonde Balloon Description and Specifications

The tethered sonde balloon instrument consists of four major parts-- plastic balloon, airborne package, winch and receiver.

2.1 Balloon (2.25 m³ size)

The balloon should be filled with 2.4 m³ of helium; hydrogen, however, can be used with the necessary precautions. It has an aerodynamic shape that stabilizes it in line with the wind, thus enabling a magnetic sensor to measure wind direction. It is made of a strong and rugged plastic material that can stand very high temperatures.

The ground station can display, print or record all the different variables with the desired units. These variables are:

- 1.....Time of day (hhmmss)
- 2.....Elapsed time (hhmmss)
- 3.....Date (yyymmdd)
- 4.....Sonde status (6 independent digits)
- 5.....Spare
- 6.....Dry-bulb temperature (°C)
- 7.....Wet-bulb temperature (°C)
- 8.....Pressure (mb)
- 9.....Wind speed (m/s), 16 channel sonde
- 10.....Wind direction (deg), 16 channel sonde

- 11.....Dry-bulb temperature ($^{\circ}\text{F}$)
- 12.....Wet-bulb temperature ($^{\circ}\text{F}$)
- 13.....Internal temperature ($^{\circ}\text{C}$)
- 14.....Depression, T-TW ($^{\circ}\text{C}$)
- 15.....Depression, T-TW ($^{\circ}\text{F}$)
- 16.....Pressure (in. HG)
- 17.....Pressure (mm HG)
- 18.....Pressure (psi)
- 19.....Pressure (KPa)
- 20.....Saturation vapor pressure (mb) at:
dry bulb temperature
- 21.....wet bulb temperature
- 22.....Vapor pressure (mb)
- 23.....Dew point temperature ($^{\circ}\text{C}$)
- 24.....Dew point temperature (deg F)
- 25.....Mixing ratio (Gm/Kg)
- 26.....Relative humidity (%)
- 27.....Altitude (m) of sonde
- 28.....Altitude (m) above MSL, using
NACA Standard Atmosphere
- 29.....Theodolite azimuth angle (deg)
- 30.....Theodolite elevation angle (deg)
- 31.....Theodolite's: wind speed (m/sec)
- 32.....direction (deg)
- 33.....16 ch sonde's: wind speed (mph)
- 34.....wind speed (knots)
- 35.....Theodolite's: wind speed (mph)
- 36.....wind speed (knots)
- 37.....Altitude (ft) of sonde
- 38.....Altitude (ft) above MSL, using
NACA Standard Atmosphere
- 39.....Refractivity
- 40.....Potential temperature (K @ 1000 mb)
- 41.....Potential temperature (F @ 1000 mb)
- 42.....Enthalpy (KJ/Kg)

The tethersonde system has been used in the Shuaiba Industrial Area for the KISR/SAA Project (Air Pollution Dispersion and Prediction Model, EES-45). Between December, 1982 and February, 1983 an average of three experiments per week at different times of the day have been performed by SAA and KISR staff. This data will be used for the air pollution model, and will provide better information about the atmospheric turbulence in Shuaiba.

A better understanding of the variation in the atmospheric profile between the Kuwait International Airport and the Shuaiba area has been achieved by comparing the tethersonde data and the airport radiosonde data collected twice a day by the Kuwait Meteorological Department.

3. Tethersonde Operation

Usually, two technicians are required to fly the balloon, and one person to observe the ground station. The calibration procedure is done by running a punched tape through the ground station (ADAS TS-3A), and should be done only once for each new sensor package. The information is stored in the system memory, but the time of the day and the date must be entered every time before operating the system.

The basic operation of the tethersonde consists of initially performing a few readings (about five at the surface 4-5 above the ground). Then the balloon is lifted to different elevations, with typical increments of 30. At each elevation, the balloon is kept steady and a few readings (about four) are performed to obtain representative information on the meteorological parameters at that level. Most of the time data are collected on both the ascending and the descending movement of the balloon. The maximum height reached by the balloon depends very much on wind speed. So far, the average height reached by the balloon was about 300 and the maximum height was 400.

4.

Tethersonde Field Experiments

The following is a brief description of some of the tethersonde experiments during December, January and February and a comparison with the airport upper air data.

The data indicate that there was no inversion in the layer. Since the airport is 56 meters above the mean sea level, this difference must be taken into account in comparing the two flights. The Shuaiba surface temperature was 2°C lower than the airport surface temperature at different times during the experiment, but the temperatures were similar above 160 meters. The pressure was also very close, with the humidity slightly higher at the surface in Shuaiba due to the effects of the sea. There was a 10° difference in wind direction and the wind speeds were very similar.

The surface temperature at the airport during the time of the tethersonde experiment was 0.27°C higher than the Shuaiba Area temperature. The pressure corrected to sea level at the airport was 5 mb higher, the wind direction was the same, and the wind speed was 2 m/s higher.

4.1 1st Flight

Date: 13/12/83

Time: 11 05 AM

Tethersonde data

TIME	HEIGHT m ABOVE SEA LEVEL	PT °K	DTDC	PEMB	RH%	WD°	WS m/s
1113 AM	00	289.61	17.73	1016.4	57.5	150	4.5
1117 AM	41	288.85	16.64	1011.4	58.6	140	6.7
1121 AM	62	288.93	16.52	1009.0	58.3	143	8.6
1123 AM	119	289.78	16.50	1002.2	56.6	145	7.5
1136 AM	131	290.1	17.01	1000.8	56.8	140	7.5
1138 AM	144	289.99	16.77	999.2	56.5	120	8.7
1134 AM	164	290.61	17.21	996.9	56.2	132	7.9
1140 AM	202	290.19	16.40	992.4	60.0	142	7.4

There was an elevated inversion between 119 and 164 meters. There was about 1°C increase in the temperature. (The 164 meter height observation was made before the 131 meter observation.)

Airport Sounding Data 13/12/1982

TIME	GPH	PRES	TEMP	HUM	DD	FF	WEATHER	CLOUDS
200	PM 56	1011.0	19.7	47	120	8.0		4
200	PM 119	1003.8	18.6	52	119	7.9		
200	PM 182	996.5	17.5	56	125	8.9		
200	PM 242	989.4	16.5	58	128	9.8	NIL	4
1113	PM 000	1021.4	18.0	49	150	6.5		

4.2 2nd Flight

Date: 18/12/1982

Time: From 10 24 AM to 1101 AM

It was overcast during the experiment. Rain started at 1050 AM.

Tethersonde Data

TM/DAY	PT=DC	PH=M	DT=DC	PR=MB	RH=PC	WD=PY	WS=MS
AM							
1037	283.62	00	11.95	1018.6	95.9	91	1.3
1039	283.44	56	11.29	1012.5	98.7	297	1.9
1041	283.46	82	11.00	1009.3	100.0	309	2.5
1042	283.53	122	10.75	1004.5	100.0	335	3.0
1047	283.71	156	10.59	1000.3	100.0	342	3.5
1048	283.73	177	10.40	997.8	100.0	346	3.1
1049	282.24	202	8.5	994.9	100.0	350	3.0
1050	281.76	230	7.92	991.5	100.0	350	2.6
1052	281.75	251	7.71	989.0	100.0	012	3.4
105311	283.18	254	9.10	988.5	100.0	014	2.5
105321	283.19	262	9.03	987.6	100.0	103	3.4
105332	281.98	287	7.58	984.7	100.0	104	3.0
1054	283.36	310	8.74	981.9	100.0	54	0.5
1055	283.74	315	9.06	981.2	100.0	121	1.4
1057	281.17	137	8.24	1002.7	100.0	340	2.2
1058	280.97	102	8.39	1007.0	100.0	313	1.8
1058	280.95	64	8.73	1011.6	100.0	334	1.3
1059	280.94	28	9.08	1016.1	100.0	279	1.2
1100	281.90	00	10.33	1019.7	100.0	-	1.0

The Shuaiba tethersonde data shows an elevated inversion between 251 and 313 meters. There was 1.39°C increase in temperature between 251 m and 254 m, and 1.52°C decrease between 254 m and 287 m and 315 m. The surface temperature dropped 1.62°C during the 30 minutes of the experiments; there was a similar decrease of temperature at all levels. The wind shifted 130° in direction, between 230 m and 315 m (the inversion layer)

Airport Sounding Data (18/12/1982)

TIME	GPH=M	DT=DC	PR=MB	WRH=PC	WD=DG	WS=MS	CLOUDS
0200 PM	56	11.1	1014.0	92	30	1.5	
0200 "	107	9.4	1008.0	91	31	1.3	
0200 "	156	9.8	1002.1	89	88	2.0	
0200 "	202	10.1	996.5	86	105	3.4	
0200 "	251	10.4	990.8	83	111	4.6	
0200 "	304	10.1	984.4	80	116	5.6	
0200 "	354	9.8	977.9	78	117	6.4	
0200 "	414	9.5	971.5	77	118	7.0	
0200 "	467	9.1	965.4	78	120	7.5	
1037 AM	000	11.5	1022.4*	85	320	2.5	8

The airport data show an elevated inversion between 107 and 251 meters of height and a 1°C increase in temperature. The inversion over Shuaiba was about 150 higher than the airport inversion. The depth of the inversion layer over the Shuaiba area was 74 and over the airport was 144.

* Pressure corrected to sealevel.

4.3 3rd Flight

Date: 20/12/198

Time: 1035 to 1135 AM

Tethersonde Data

TMDAY=LST	PT=DC	PHT=M	DT=DC	PR=MB	RH=PC	WD=DG	WS=MS
1038	284.18	0	12.38	1016.6	73.2	252	2.6
1039	283.50	34	11.36	1012.5	73.2	290	4.0
1042	283.53	77	10.97	1007.3	73.2	305	4.2
1047	283.78	122	10.78	1001.9	69.9	304	4.9
1048	283.95	158	10.61	997.5	70.4	319	4.4
1051	284.09	180	10.52	994.8	71.2	307	5.0
1052	284.69	205	10.88	991.9	65.0	322	5.3
1059	284.67	233	10.58	988.5	66.8	322	4.8
1102	284.81	267	10.39	984.5	68.3	316	4.5
1102	285.34	302	10.58	980.4	61.2	10	4.8
1103	285.05	279	10.51	983.1	64.0	350	6.2
1107	284.67	242	10.50	987.5	68.7	317	5.8
1113	284.56	210	10.70	991.3	69.8	352	7.0
1123	284.85	183	11.29	994.4	68.3	319	5.1
1129	285.04	158	11.64	997.4	64.9	311	4.9
1131	284.98	117	12.02	1002.4	64.2	308	5.5
1133	284.90	64	12.46	1008.7	61.2	312	5.7
1135	284.85	44	12.61	1011.2	63.4	319	5.8
Missing		00					

The surface temperature observed by the tether sonde was 0.8°C higher than the surface temperature observed by the radiosonde. (Temperatures were observed at different times). The surface temperature observed at 1030 a.m. at Shuaiba was 0.4°C higher than the temperature observed at the same time at the airport.

The temperature observed at different heights was slightly higher over the Shuaiba area up to 156m. Above that height the temperature was about 2°C higher over the airport.

The tethersonde data showed no inversion over the Shuaiba area at the time of the experiment. The atmosphere was in a stable condition, however, as indicated by the increase in the potential temperature between 80 and 300 m high.

The surface temperature and the sounding temperature were 1°C higher during the descent of the balloon than they were during the ascent (40 minutes to one hour difference).

Airport Sounding Data (20/12/1982)

TMDAY=LST	PHT=M	DT=DC	PR=MB	RH=PC	WD=DG	WS=MS
0200 PM	56	16.9	1013.8	44	330	5.5
0200 PM	122	15.2	1006.0	45	330	5.4
0200 PM	190	14.6	998.0	46	328	5.7
0200 PM	258	14.0	989.9	48	327	6.0
0200 PM	326	13.3	482.1	49	327	6.1
0200 PM	396	12.6	974.0	50	326	6.2
0200 PM	464	11.9	966.1	51	325	6.3
1038 AM	00	13.5	1022.4	61	320	3.5

The airport sounding data do not indicate an inversion. The airport surface temperature during the sounding experiment (0300 PM) was 4.5°C higher than the Shuaiba Area surface temperature at the time of the tethersonde experiment (1038 AM), where the airport surface temperature at 1038 AM was 1.1°C higher than the Shuaiba surface temperature at the same time.

4.4 4th Flight

Date: 22/12/1982

Time: From 0535 AM to 0622 AM

Tethersonde Data

TMDY	PT=DC	PHT=M	DT=DC	PR=MB	RH=PC	WD=DG	WS=MS
0535	282.0	2	9.98	1014.2	100	193	1.9
0538	282.58	39	10.21	1009.7	100	170	7.0
0540	283.06	61	10.47	1007.0	100	152	8.6
0540	284.13	90	11.27	1003.0	100	160	11.1
0555	285.44	125	12.23	999.3	100	240	12.5
0559	285.57	139	12.23	997.6	100	147	13.0
0607	285.21	125	12.00	999.2	100	285	12.6
0612	283.78	90	10.91	1003.5	100	294	10.5
0617	283.26	64	10.64	1006.6	100	275	9.1
0619	282.85	38	10.48	1009.7	100	165	8.0
0621	282.31	00	10.47	1016.3	100	186	3.3

The tethersonde data showed a strong surface inversion over the Shuaiba area. The temperature was increasing up to 139 (maximum height reached) meters, so the top of the inversion cannot be estimated. The surface pressure had increased 2 mb between the beginning and the end of the experiment. That caused an error in the physical height calculation. There was also an increase in the surface temperature between the beginning and the end of the experiment.

Airport Radiosonde Data (22/12/1982)

TMDAY=LST	CLOUD	PHT=M	PR=MB	DT=DC	RH=PC	WD=DG	WS=MS
0200 AM		56	1011.9	8.0	93	180	2.5
0200 AM		113	1005.1	10.9	81	180	2.5
0200 AM		172	998.0	13.8	69	167	4.2
0200 AM		234	990.8	13.7	71	163	5.9
0200 AM		296	983.4	13.5	74	160	7.3
0200 AM		357	967.3	13.1	78	159	8.4
0200 AM		417	969.4	12.6	81	158	9.3
0535 AM	3	00	1018.0	10.3	93	160	4.5

The airport radiosonde data showed a surface inversion extended up to 200 m close to the depth of the Shuaiba inversion. The surface temperature at the airport at 0200 AM was 2°C lower than the surface temperature at the Shuaiba area at 1535 AM, but the surface temperature at the airport at 0535 AM was higher than the Shuaiba surface temperature at 0535 AM. The surface pressure at the airport at 0535 AM was 4 mb higher than the Shuaiba surface pressure at the same time. The wind speed and wind direction were similar at the two locations.

4.5 5th Flight

Date: 25/12/1982

Time: a) from 1000 AM to 1100 AM

b) from 1100 AM to 1135 AM

Tethersonde Data

a) First Experiment:

TMDAY	PT=DC	PHT=M	DT=DC	PR=MB	RH=PC	WD=DG	WS=MS
1010 AM	283.14	0	11.66	1020.2	82.1	263	3.6
1006 AM	282.64	30	10.82	1016.6	85.4	298	6.2
1009 AM	282.82	48	10.82	1014.3	84.8	304	5.6
1011 AM	282.74	67	10.56	1012.1	85.9	305	6.0
1011 AM	282.73	91	10.31	1009.1	86.2	307	6.2
1012 AM	282.85	121	10.15	1005.5	86.8	350	5.4
1019 AM	283.19	161	10.10	1000.6	86.4	308	7.1
1020 AM	283.10	194	9.67	996.6	88.6	301	5.7
1030 AM	283.28	220	9.60	993.5	88.5	113	6.1
1033 AM	283.36	190	9.97	997.1	87.4	125	6.3
1034 AM	283.39	163	10.26	1000.3	85.4	345	7.9
1043 AM	283.17	134	10.34	1003.9	85.8	296	7.9
1045 AM	283.06	102	10.53	1007.7	84.7	298	6.3
1049 AM	283.37	68	11.18	1011.9	81.1	292	5.1
1051 AM	283.32	42	11.38	1014.8	80.2	297	4.0
1052 AM	283.90	0	12.41	1020.4	78.1	279	4.9

b) Second Experiment:

TMDAY	PT=DC	PHT=M	DT=DC	PR=MB	RH=PC	WD=DG	WS=MS
1053	284.61	4	13.09	1020.1	74.3	71	2.2
1054	283.39	43	11.48	1015.4	80.8	288	5.0
1059	284.19	104	11.68	1008.0	79.6	311	5.9
1101	284.06	136	11.24	1004.1	81.6	311	5.2
1103	284.62	198	11.19	996.6	81.2	299	5.0
1106	284.33	229	10.60	992.9	82.0	312	5.6
1113	284.63	253	10.67	990.0	81.7	321	5.2
1113	284.58	284	10.31	986.4	83.7	312	4.7
1113	284.68	314	10.12	982.8	84.3	330	4.0
1113	284.62	330	9.90	980.9	85.0	345	5.0
1114	285.38	376	10.21	975.4	83.6	319	5.4
1115	284.67	340	9.85	979.7	84.6	320	5.2
1116	284.50	298	10.09	984.7	83.6	340	4.7
1117	284.46	250	10.52	990.3	80.8	294	7.5
1118	284.34	224	10.67	993.5	80.2	314	5.9
1118	284.24	193	10.86	997.2	79.3	314	5.9
1121	284.36	160	11.31	1001.2	77.9	316	5.9
1123	284.52	133	11.73	1004.4	75.8	125	7.7
1133	284.59	103	12.09	1008.0	73.2	331	5.8
1133	284.50	86	12.16	1010.0	73.2	311	8.1
1134	284.39	55	12.36	1013.8	71.1	336	7.1
1136	284.85	17	13.19	1018.4	68.1	332	6.2
1137	284.89	04	13.36	1020.0	67.5	333	5.4

The first experiment showed no inversion and a 0.8°C increase in surface temperature between the beginning and end of the experiment; the second experiment showed a 0.3°C increase in temperature between 330 and 376 m of height, but since we did not obtain any information for heights more than 376 m, such increase is not enough to substantiate the existence of an inversion in that layer.

Airport Radiosonde Data (25/12/1982)

TMDAY	CLOUD	PHT=M	DT=DC	PR=MB	RH=DG	WD=DG	WS=MS
0200 PM		56	16.2	1014.4	43	330	7.0
0200 PM		164	14.8	1001.7	49	329	6.9
0200 PM		267	13.4	989.4	53	326	7.6
0200 PM		361	12.3	278.4	55	323	8.2
0200 PM		447	11.2	968.4	57	322	8.6
0200 PM		530	10.3	958.8	59	320	8.8
1010 AM	2	00	12.6	1024.3	70	320	5.5

The radiosonde data does not indicate an inversion. The surface temperature at the airport at the time of the radiosonde experiment was 4.5°C higher than the Shuaiba area surface temperature during tetherosonde experiment (a) and 3.0°C during tetherosonde experiment (b). The wind speed and direction were slightly higher at the airport and the surface pressure was 4 mb higher at the airport at 1010 AM.

4.6 6th Flight

Date: 29/12/1982

Time: a) from 0911 AM to 1000 AM

b) from 1000 AM to 1032 AM

Tethersonde Data

a) First Experiment:

TMDAY	PT=DC	PHT=M	DT=DC	PR=MB	RH=PC	WD=DG	WS=MS
0911 AM	286.42	3	14.30	1012.6	86.4	192	0.9
0913 AM	286.30	40	13.82	1008.1	86.5	124	1.0
0916 AM	286.67	104	13.56	1000.5	86.9	100	2.7
0917 AM	286.74	140	13.28	996.2	89.1	123	3.3
0918 AM	288.25	160	14.59	993.9	80.2	121	4.4
0920 AM	289.71	198	15.67	989.3	70.7	99	4.8
0922 AM	289.41	235	15.00	985.0	76.2	94	4.8
0922 AM	290.67	263	15.99	981.7	68.7	88	4.1
0923 AM	291.25	299	16.22	977.6	63.0	88	3.9
0925 AM	293.04	324	17.76	974.7	54.6	135	3.7
0927 AM	293.52	354	17.93	971.3	53.5	143	3.0
0930 AM	294.29	375	18.49	968.8	53.3	150	4.3
0931 AM	294.43	344	18.93	972.4	53.7	155	5.3
0932 AM	294.34	376	18.53	968.7	53.2	157	5.0
0933 AM	295.05	352	19.46	971.5	51.2	158	5.7
0933 AM	294.42	330	19.06	973.9	53.6	156	5.3
0936 AM	293.17	311	18.01	976.2	55.1	143	5.0
0937 AM	293.06	293	18.07	978.2	54.5	140	5.6
0940 AM	292.50	263	17.8	981.6	54.9	127	5.5
0948 AM	291.20	236	16.78	984.8	62.7	103	5.8

TMDAY		PT=DC	PHT=M	DT=DC	PR=MB	RH=PC	WD=DG	WS=MS
0949	AM	291.73	191	17.74	990.0	60.6	132	6.6
0952	AM	288.65	161	14.96	993.5	79.2	128	5.1
0953	AM	288.17	143	14.65	995.6	80.5	125	4.3
0954	AM	287.57	105	14.43	1000.2	85.0	119	4.5
0957	AM	287.23	75	14.39	1003.7	83.8	120	3.9
0958	AM	287.29	42	14.76	1007.6	82.1	121	3.7
1000	AM	287.29	0	15.23	1013.3	81.1	58	2.7

b) Second Experiment:

TMDAY		PT=DC	PHT=M	DT=DC	PR=MB	RH=PC	WD=DG	WS=MS
1001	AM	287.83	0	15.79	1013.6	79.3	172	1.7
1002	AM	287.91	25	15.63	1610.6	80.3	78	4.0
1002	AM	287.69	55	15.12	1007.6	82.7	98	3.9
1002	AM	287.59	87	14.70	1003.2	83.5	189	4.7
1002	AM	287.7	117	14.51	999.5	83.9	161	4.2
1002	AM	287.97	144	14.51	996.4	82.6	85	4.4
1002	AM	288.76	171	15.04	993.2	-	110	4.3
1003	AM	289.63	195	15.69	990.4	71.3	114	3.9
1003	AM	290.38	218	16.21	987.7	66.6	113	3.5
1003	AM	291.08	239	16.69	985.2	60.5	107	3.2
1003	AM	291.62	263	17.0	982.5	57.2	108	3.5
1003	AM	292.11	285	17.28	980.0	55.2	92	3.1
1003	AM	292.62	305	17.59	977.7	53.9	124	3.4

TMDAY		PT=DC	PHT=M	DT=DC	PR=MB	RH=PC	WD=DG	WS=MS
1004	AM	293.14	319	17.97	976.1	52.7	139	3.3
1004	AM	293.54	373	18.23	974.5	52.0	142	3.3
1006	AM	294.06	371	18.37	970.1	54.3	147	4.6
1007	AM	294.26	375	18.53	969.7	53.8	148	4.6
1007	AM	294.24	377	18.49	969.4	54.1	155	6.2
1007	AM	294.22	379	18.45	969.2	54.2	150	4.7
1008	AM	295.85	333	18.53	974.4	54.8	156	5.9
1009	AM	293.62	303	18.59	977.8	55.3	156	7.1
1009	AM	293.13	268	18.45	981.9	55.7	144	6.6
1011	AM	291.96	239	17.57	985.3	56.2	132	6.2
1019	AM	293.04	201	19.01	989.6	51.8	117	4.6
1020	AM	291.78	174	18.03	992.7	57.9	112	4.7
1022	AM	290.57	135	17.20	997.3	67.3	127	4.9
1023	AM	288.77	103	15.70	1001.0	78.1	148	4.3
1026	AM	288.29	88	15.37	1008.8	79.4	147	3.2
1027	AM	288.12	41	15.66	1008.4	79.3	135	3.9
1029	AM	288.25	10	16.18	1013.2	76.8	179	2.3

Tethersonde experiments (a) and (b) showed an elevated inversion between 144 and 370 m. In experiment (a), there was about a 1°C increase in the temperature at all levels between the time of ascension and descension of the balloon. In experiment (b), there was about a 0.5°C increase.

Airport Radiosonde Data (29/12/1982)

TMDAY	CLOUD	PHT=M	DT=DG	PR=MB	RH=PC	WD=DG	WS=MS
0200	PM	56	22.4	1006.2	45	130	6.5
0200	PM	120	21.1	999.0	48	129	6.3
0200	PM	183	19.9	991.6	50	144	7.1
0200	PM	246	18.6	984.4	51	154	8.0
0200	PM	313	18.4	976.8	51	161	8.9
0200	PM	384	18.2	968.7	49	166	9.6
0200	PM	453	19.0	960.9	45	169	10.2
0200	PM	518	19.8	953.7	41	172	10.6
0200	PM	579	20.3	947.0	36	174	10.9
0200	PM	642	20.6	940.0	34	176	11.2
0200	PM	710	20.6	932.7	33	177	11.2
0200	PM	777	20.4	925.5	34	178	11.3
0200	PM	844	20.0	918.3	33	179	11.2
0911	PM	6	00	1017.0	-	Calm	Calm

The data showed an inversion layer between 384 and 710 m, which was 240 m higher than the inversion over the Shuaiba area. The surface temperature at the airport was 8°C higher than the surface temperature during experiment (a) and 7°C higher during experiment (b).

4.7 7th Flight Date: 5/1/1983 Time: From 1240 PM to 1248 PM

The experiment was not completed due to a power failure. The maximum height reached was 160 m.

Tethersonde Data

TMDAY	PT=DC	PHT=M	DT=DC	PR=MB	RH=PC	WD=DG	WS=MS
124002	285.66	3	13.89	1017.0	43.8	84	4.0
124103	284.43	31	12.37	1013.5	45.9	355	4.4
124246	284.55	52	12.29	1011.1	44.5	345	4.9
124358	284.58	80	12.06	1007.7	45.9	65	4.6
124704	284.43	120	11.52	1002.9	47.5	357	4.4
124826	284.54	160	11.24	998.1	47.5	356	3.7

These data does not indicate any inversion in the layer observed.

Airport Radiosonde Data (5/1/1983)

TIME	HEIGHT	PRESSURE	TEMP.	R.H.	WIND DIRECTION	SPEED M.P.S.
0200 PM	56	1015.3	15.0	30%	330	4.0
-	103	1009.7	13.6	34	329	3.9
-	148	1004.3	12.2	37	333	4.0
-	195	998.7	11.8	38	336	4.3
-	244	992.9	11.2	39	340	4.4
-	297	986.6	10.7	40	341	4.6
-	352	980.1	10.3	40	343	4.5
1240 PM	000	1022.4	14.5	-	330	5

The airport radiosonde data does not indicate any inversion. The airport surface temperature was 0.5°C higher than the Shuaiba surface temperature at 1240 PM. Wind speed and direction were similar.

4.8 8th Flight Date: 3/1/1983 Time: From 12 PM to 1248 PM

Tetherosome Data

TMDAY	PT=DC	PHT=M	DT=DC	PR=MB	RH=PC	WD=DG	WS=MS
120725	281.82	3	10.33	1020.7	63.9	334	2.9
120806	281.49	29	9.74	1017.5	64.3	317	2.8
121020	281.69	58	9.66	1014.0	64.1	350	1.4
121153	281.67	80	9.42	1011.2	60.5	331	2.4
121315	281.84	110	9.30	1007.6	61.7	339	2.9
121508	281.56	132	8.81	1004.9	60.3	333	3.1
121559	281.61	163	8.55	1001.1	60.3	342	2.6
121712	281.82	194	8.45	997.3	61.2	332	3.9
122037	281.96	224	8.30	993.8	58.9	337	2.7
122200	282.03	265	7.97	988.8	61.6	313	3.3
122444	281.95	286	7.69	986.3	62.5	341	3.5
122658	282.09	301	7.69	984.5	61.3	332	1.7
122800	282.37	282	8.15	986.8	60.4	340	3.5
122841	281.91	261	7.89	989.2	61.5	319	3.2
123105	281.92	232	8.18	992.8	59.9	344	4.5
123248	282.16	198	8.75	996.8	59.7	321	5.3
123452	281.80	162	8.74	1001.2	62.9	331	4.5
123747	281.65	134	8.88	1004.6	62.6	328	4.3
124327	281.45	101	8.99	1008.6	62.2	351	5.2
124347	281.41	83	9.13	1010.8	61.6	343	4.0
124449	281.29	42	9.41	1015.8	60.8	348	5.0
124653	281.49	3	9.99	1020.6	58.8	349	4.0

Data show a slight increase in the potential temperature between 163 and 256 m, which indicates a neutral to stable condition. There was a 0.5°C decrease in the surface temperature between the beginning and the end of the experiment.

Airport Radiosonde Data (8/1/1983)

TIME	HT=M	PR=MB	DT=DC	RH=PC	CLOUD	WD=DG	WS=MS
0200 PM	56	1017.1	9.4	64		320	6.0
0200 PM	109	1010.7	8.2	59		319	5.8
0200 PM	161	1004.3	6.9	54		315	4.8
0200 PM	217	997.5	7.0	48		307	3.9
0200 PM	275	990.4	7.4	40		299	3.0
0200 PM	334	983.4	7.9	49		285	2.5
0200 PM	392	976.5	8.5	53		272	2.2
0200 PM	453	969.4	8.9	54		256	2.0
0200 PM	514	962.3	9.2	55		240	1.9
0200 PM	574	955.4	9.4	53		227	2.0
0200 PM	633	948.6	9.2	51		218	2.1
0200 PM	692	941.9	9.0	48		213	2.2
0200 PM	750	935.2	8.8	46		207	2.2
0200 PM	811	928.4	8.7	45		206	2.3
0200 PM	930	915.2	8.5	40		199	3.1
0200 PM	992	908.2	8.4	37		196	3.6
0200 PM	1055	901.3	8.3	42		195	4.1
1000 PM	00	1025.2	10.5	52	5	360	0.3

4.9 9th Flight Date: 10/1/1983 Time: From 0909 AM to 0950 AM

Tethersonde Data

TMDAY	PT=DC	PHT=M	DT=DC	PR=MB	RH=PC	WD= DG	WS=MS
091355	276.75	5	5.74	1027.3	81.9	305	3.6
091508	276.61	31	5.35	1024.1	82.6	296	5.0
091651	276.70	54	5.21	1021.1	82.6	337	5.1
091957	276.91	83	5.14	1017.5	83.2	299	4.7
092048	277.23	111	5.19	1014.1	79.8	313	5.3
092334	277.62	149	5.21	1009.4	75.9	316	4.9
092537	278.30	173	5.66	1006.4	70.6	90	5.0
092650	278.63	201	5.71	1003.0	70.7	332	4.7
093047	279.06	242	5.74	997.9	70.6	81	5.7
093241	279.48	272	5.87	994.2	66.4	341	5.2
093322	279.31	240	6.01	998.1	68.8	331	5.9
093424	278.88	205	5.92	1002.4	68.9	97	7.1
093618	278.55	176	5.87	1006.0	70.6	105	6.9
094331	278.05	166	5.46	1007.2	76.1	334	4.8
094504	278.02	130	5.79	1011.6	74.7	332	5.2
094606	277.75	101	5.81	1015.2	77.6	334	4.8
094718	277.53	54	6.04	1021.1	77.2	322	4.0
094810	277.35	3	6.35	1027.5	76.5	316	4.1

The data show an elevated inversion above the airport in the layer 161 to 574 m. The wind speed was decreasing with height. There was also an increase in the cloud amount, which could indicate that the inversion was a frontal inversion, approaching the area after the performance of the tether sonde experiment.

Since the potential temperature increased with height, these data indicate a stable condition up to the maximum height observed (272 m). There was about a 0.7°C increase in the surface temperature between the beginning and the end of the experiment.

Airport Radiosonde Data (10/1/1983)

TIME	HT=M	PR=MB	DT=DC	RH=PC	CLOUD	WD=DG	WS= MS
0200 PM	56	1022.0	11.0	62		330	4.5
0200 PM	117	1014.7	9.8	61		329	4.3
0200 PM	184	1006.5	8.4	62		327	5.5
0200 PM	252	998.2	7.8	63		325	6.6
0200 PM	321	989.9	7.2	65		323	7.5
0200 PM	387	982.1	6.7	67		322	8.2
0915 AM	000	1030.0	6.0	77	-	300	2.5

The data did not indicate inversion at 0200 PM over the airport. The surface temperature at the airport at 0915 AM was 0.3°C higher than in the Shuaiba area. The surface temperature at the airport increased 5.0°C between 0915 AM (the time of the tetheredsonde experiment) and 0200 PM (the time of the radiosonde experiment).

4.10 10th Flight Date: 26/1/1983 Time: From 1234 PM to 1312 PM

Tethersonde Data

TMDAY	PT=DC	PHT=M	DT=DC	PR=MB	RH=PC	WD=DG	WS=MS
123443	286.14	8	14.31	1016.2	63.9	65	2.8
124115	285.62	32	13.55	1013.3	63.4	68	4.9
124410	284.84	61	12.48	1009.7	64.7	14	5.7
124603	284.82	119	11.89	1002.7	63.9	31	3.9
124655	285.06	151	11.81	998.9	64.9	5	4.5
124818	285.24	172	11.80	996.4	66.5	48	4.7
125001	285.04	198	11.34	993.3	65.5	21	4.0
125052	285.04	239	10.93	988.3	66.4	35	3.9
125225	285.03	264	10.68	985.3	66.6	352	4.9
125307	285.20	297	10.53	981.5	65.8	4	3.4
125500	285.18	329	10.19	977.7	67.2	91	3.6
125521	285.19	360	9.90	974.0	68.9	8	3.0
125612	285.21	409	9.44	968.4	71.1	306	1.3
125654	285.11	378	9.66	972.0	69.5	347	2.4
130224	285.06	342	9.95	976.2	67.2	334	3.4
130316	285.08	311	10.27	979.8	65.9	31	3.8
130347	285.33	284	10.78	983.0	64.4	345	4.6
130428	285.26	259	10.96	986.0	65.8	6	4.9
130520	285.32	228	11.32	989.6	63.9	5	5.1
130601	285.02	193	11.36	993.8	64.6	35	5.1
130653	284.84	168	11.42	996.7	63.7	22	5.0

4.11 11th Flight Date: 26/1/1983 Time: From 1036 AM to 1116 AM

Tethersonde Data

TMDAY	PT=DC	PHT=M	DT=DC	PR=MB	RH=PC	WD=DG	WS=MS
AM							
103639	286.33	5	14.42	1015.2	95.9	351	2.8
103720	285.45	35	13.24	1011.6	88.0	302	6.6
103741	285.43	52	13.06	1009.6	80.5	missing	
104148	285.02	121	11.96	1001.2	59.5	305	6.8
104239	285.53	146	12.23	998.2	59.1	307	6.9
104402	285.50	172	11.95	995.1	58.4	331	5.7
104433	285.61	209	11.71	990.8	60.9	313	5.4
104504	285.66	226	11.58	988.7	60.3	308	7.4
104535	285.60	192	11.86	992.8	59.4	116	7.9
104555	285.09	146	11.79	998.2	59.7	353	9.7
104718	284.91	110	11.97	1002.6	59.1	270	10.1
104759	284.90	81	12.24	1006.0	57.3	278	10.2
104932	285.07	58	12.64	1008.8	57.7	301	9.2
105013	285.03	30	12.87	1012.2	56.0	300	9.1
105858	285.46	108	12.54	1002.8	56.2	297	7.4
110010	285.57	140	12.34	999.0	54.7	316	5.8
110204	285.68	185	12.01	993.6	56.7	353	6.2
110214	285.96	210	12.04	990.6	56.8	313	6.8
110245	285.88	247	11.60	986.3	58.5	308	5.7
110326	286.17	272	11.64	983.3	58.3	338	5.0
110407	286.39	301	11.58	979.9	58.9	2	6.8
110519	285.93	270	11.42	983.5	58.9	306	6.8

TMDAY	PT=DC	PHT=M	DT=DC	PR-MB	RH=PC	WD=DG	WS=MS
131050	284.85	131	11.80	1001.3	61.6	5	6.4
131111	284.70	101	11.95	1004.9	61.3	21	5.8
131132	284.66	76	12.14	1007.8	61.2	85	7.7
131202	284.60	43	12.42	1011.9	61.5	28	6.6
131233	284.59	9	12.73	1016.0	61.2	5	4.0

The potential temperature in these data indicate a stable layer between 119 and 172 m of height and neutral up to 400 m. There was a 2°C decrease in the surface temperature between the beginning and the end of the experiment.

Airport Radiosonde Data (26/1/1983)

TIME	GHP=M	PRES	TEMP	HUM	CLOUD	WD=DG	WS=MS
0200 PM	56	1014.1	14.5	47		330	4.0
0200 PM	126	1005.8	13.5	47		329	3.9
0200 PM	200	997.0	12.5	48		323	4.0
0200 PM	275	988.1	11.6	50		319	4.3
0200 PM	349	979.4	10.8	52		317	4.4
1200 PM	000	1021.4	14.5	-	6	340	0.8

No inversion was indicated in the data. There was no change in the surface temperature between the Shuaiba area at the time of the tetheredsonde experiment and the airport at the time of the radiosonde experiment.

TMDAY	PT=DC	PHT=M	DT=DC	PR=MB	RH=PC	WD=DG	WS=MS
110550	285.68	236	11.51	987.6	59.1	333	7.6
110621	285.50	195	11.73	992.3	58.7	339	10.4
111028	285.71	169	12.19	995.5	56.8	252	9.2
111324	286.00	135	12.81	999.6	54.3	301	8.8
111344	285.64	106	12.74	1003.0	54.8	296	9.6
111446	285.86	85	13.16	1005.5	53.7	333	9.1
111517	286.11	65	13.62	1008.0	52.4	357	8.1
111538	285.78	34	13.58	1011.6	52.5	122	8.4
111608	285.73	0	13.86	1015.7	52.0	339	6.9

The tethersonde data indicate neutral conditions.

Airport Radiosonde Data (26/1/1983)

TIME	GHP=M	PRES	TEMP	HUM	CLOUD	WD=DG	WS=MS
0200 PM	56	1010.6	17.3	29		300	3.5
0200 PM	112	1004.1	16.4	31		299	3.4
0200 PM	168	997.5	15.5	33		317	3.6
0200 PM	226	990.8	14.7	34		330	4.2
0200 PM	281	984.2	14.0	35		338	4.7
0200 PM	337	977.8	13.2	36		344	5.1
0200 PM	390	971.5	12.5	37		348	5.6
1030 PM	000	1020.2	13.0	47		316	5.0

The radiosonde data does not indicate an inversion. There was a 3.0°C increase in the surface temperature between the two experiments. The wind speed observed by the tetheredsonde over Shuaiba was slightly higher than the wind speed observed by the radiosonde over the airport.

4.12 12th Flight Date: 14/2/1983 Time: from 0600 AM to 0642 AM

Tethersonde Data

TMDAY	PT=DC	PHT=M	DT=DC	PR=MB	RH=PC	WD=DG	WS=MS
060012	281.20	2	8.99	1011.8	42.4	248	2.7
060124	283.80	39	11.23	1007.2	33.1	285	5.6
060205	285.61	71	12.74	1003.4	29.5	32	4.4
060500	287.13	113	13.85	998.4	33.8	331	4.8
060541	287.62	151	13.96	993.8	32.8	336	4.0
060704	287.72	183	13.75	990.1	33.5	346	3.8
060846	287.77	214	13.49	986.4	34.5	19	3.7
060959	288.0	248	13.40	982.4	33.9	340	3.4
061141	288.24	276	13.36	979.2	34.3	335	3.0
061457	288.32	295	13.26	977.0	33.0	320	3.4
061609	288.57	320	13.25	974.0	32.7	359	2.5
061955	288.12	295	13.05	976.9	34.9	18	4.2
062016	287.37	264	12.60	980.5	40.7	51	4.8
062047	287.53	247	12.93	982.6	38.2	34	4.4
062138	286.76	214	12.49	986.4	42.0	43	5.7
062606	286.75	183	12.78	990.1	41.6	56	6.2
063104	287.27	151	13.62	993.9	35.4	63	5.3
063206	286.19	113	12.91	998.4	41.6	318	6.8

TMDAY	PT=DC	PHT=M	DT=DC	PR=MB	RH=PC	WD=DG	WS=MS
063521	285.72	95	12.61	1000.5	39.2	306	5.6
063612	283.96	50	11.29	1005.9	43.3	88	7.0
063714	283.27	34	10.76	1008.0	41.4	272	8.3
064233	280.78	4	8.56	1011.6	45.0	90	7.0

The tethersonde data indicate a surface inversion extending up to 151 m and stable conditions extending up to 320 m over the maximum height reached by the balloon.

Airport Radiosonde Data (14/2/1983)

TIME	GHP=M	PRES	TEMP	HUM	CLOUD	WD=DG	WS=MS
0200 AM	56	1009.6	7.4	49		CALM	
0200 AM	107	1003.6	14.6	26		CALM	
0200 AM	158	997.5	14.6	27		315	0.7
0200 AM	208	991.6	14.5	28		315	1.2
0200 AM	259	985.6	14.3	28		315	1.8
0200 AM	313	979.4	14.1	29		315	2.2
0200 AM	364	973.5	13.8	29		315	2.5
0600 AM	00	1016.4	5.6	55	5	180	1.5

The radiosonde data indicate a surface inversion up to 259 m. The radiosonde surface temperature is 1.5^oC lower than that measured by the tethersonde. The wind speed measured by the tethersonde was higher than that measured by the radiosonde but the wind direction was the same.

4.13 13th Flight

Date: 16/2/1983

Time: from 1050 AM to 1116 AM

from 1116 AM to 1145 AM

The wind speed was not measured because the cup anemometer was out of order.

Tethersonde Data

TMDAY	PT=DC	PHT=M	DT=DC	PR=MB	RH=PC	WD=DG	WS=MS
105431	293.42	8	21.19	1011.0	25.9	92	
105441	293.02	33	20.54	1008.0	27.2	247	
105510	293.03	76	20.12	1003.0	24.8	252	
105530	292.92	110	19.69	999.0	24.7	244	
105550	292.96	147	19.37	994.7	24.3	251	
105629	293.09	177	19.20	991.2	24.7	245	
105649	293.20	211	18.98	987.3	25.0	244	
105718	293.17	247	18.60	983.1	25.5	245	
105817	293.17	288	18.20	978.5	26.4	245	
105827	293.19	298	18.12	977.3	26.8	246	
105837	293.31	310	18.12	975.9	26.1	253	
110044	293.49	341	18.00	972.4	26.7	247	
110114	294.07	379	18.20	968.0	22.8	248	
110143	293.83	402	17.74	965.5	24.4	260	
110213	294.07	430	17.70	962.2	22.6	254	
110312	294.30	476	17.48	957.1	26.7	272	
110351	294.60	445	18.07	960.6	27.8	256	
110440	294.86	412	18.65	964.2	27.0	251	

TMDAY	PT=DC	PHT=M	DT=DC	PR=MB	RH=PC	WD=DG	WS=MS
110500	294.60	380	18.71	967.9	28.6	249	
110519	294.48	347	18.91	971.6	28.2	250	
110539	294.20	319	18.92	974.9	29.0	242	
110608	294.00	284	19.05	978.8	28.7	73	
110707	293.56	248	18.97	983.0	28.0	241	
111113	294.36	218	20.06	986.4	27.1	236	
111152	294.00	189	19.99	989.8	26.1	46	
111222	293.49	159	19.76	993.2	27.0	36	
111350	293.84	131	20.39	996.4	26.6	79	
111558	293.96	108	20.74	999.1	27.6	250	
111617	293.68	76	20.76	1002.8	28.8	250	
111637	293.83	43	21.25	1006.7	27.5	232	
111707	293.78	6	21.67	1012.5	26.8	88	
111845	293.78	48	21.14	1006.1	27.0	245	
111855	293.84	70	20.99	1003.5	26.6	249	
111914	293.92	109	20.68	998.9	26.8	219	
112058	294.33	146	20.74	994.7	28.8	215	
112141	293.92	180	19.99	990.8	26.8	227	
112211	293.99	210	19.76	987.3	27.6	226	
112300	294.05	244	19.50	983.4	27.9	64	
112359	294.29	278	19.40	979.5	29.1	180	
112428	294.54	317	19.27	975.1	29.0	224	
112616	294.27	341	18.77	972.3	27.3	103	

TMDAY	PT=DC	PHT=M	DT=DC	PR=MB	RH=PC	WD=DG	WS=MS
112646	294.86	374	19.03	986.6	29.1	227	
112725	294.83	417	18.59	963.7	31.5	233	
112844	294.49	370	18.70	969.0	28.2	230	
112923	294.50	338	19.03	972.7	29.1	95	
113051	294.58	302	19.45	976.7	28.4	55	
113111	294.47	276	19.60	979.7	28.7	49	
113210	294.15	246	19.58	983.2	27.5	95	
113408	294.02	218	19.72	986.4	27.9	233	
114100	294.39	155	20.70	993.6	25.0	18	
114139	294.69	128	21.26	996.8	24.9	100	
114159	294.61	92	21.54	1000.9	25.1	231	
114248	294.23	15	21.90	1009.8	25.4	239	
114318	295.04	3	22.84	1011.2	23.5	200	

The first flight indicated a weak inversion between 341 and 379 m. The second flight indicated an inversion between 341 and 374 m. Conditions were stable in both flights. There was a 1°C increase in the atmospheric temperature up to 450 m between the first and second flight.

Airport Radiosonde Data (16/2/1983)

TIME	GPH=M	PRES	TEMP	HUM	CLOUD	WD=DG	WS=MS
0200 PM	56	1004.3	24.0	21		230	4.5
0200 PM	118	997.5	22.7	22		231	4.4
0200 PM	179	990.4	21.4	23		230	4.4
0200 PM	238	983.7	21.7	24		229	4.6
0200 PM	297	977.0	20.7	25		228	4.7
0200 PM	356	970.4	19.8	26		227	4.8
0200 PM	413	964.0	18.9	27		226	4.7
1000 AM	000	1014.3	17.8	33	4	320	12.0
1100 AM	000	1013.6	21.6	23	3	270	12.0

The data indicate an elevated inversion between 179 and 238 m, which correlated with the inversion indicated by the two tethersonde flights. The airport surface temperature at 0200 PM was 3°C higher than the Shuaiba surface temperature, but there was no difference in the surface temperature observed at the same time (1050). There was a 2 mb difference in the pressures observed at the same time at the two locations.

4.14 14th Flight Date: 19/2/1983

Time: From 0610 AM to 0650 AM

Tethersonde Data

TMDAY	PT=DC	PHT=M	DT=DC	PR=MB	RH=PC	WD=DG	WS=MS
061000	284.08	7	11.79	1010.6	78.0	40	
061209	284.17	32	11.57	1006.8	78.1	270	
061308	284.68	63	11.78	1003.1	77.3	190	
062430	285.46	92	12.28	999.6	68.5	312	
062727	286.93	121	13.47	996.2	55.8	40	
063105	287.71	151	13.96	992.7	51.4	222	
063154	287.99	161	14.14	991.5	50.5	246	
063502	287.64	151	13.88	992.6	53.8	52	
063839	287.36	127	13.84	995.5	55.2	241	
064444	286.74	90	13.57	999.9	59.7	356	
064841	285.49	61	12.61	1003.3	68.9	232	
065110	284.65	38	11.99	1006.1	74.3	20	

These data indicate a low level inversion started at 32 m and extended up to 161 m (the maximum height observed by the balloon).

Radiosonde Data (19/2/1983)

TIME	GPH=M	PRES	TEMP	HUM	CLOUD	WD=DG	WS=MS
0200 AM	56	1005.2	12.4	82		150	3.0
0200 AM	118	998.0	14.6	32		149	2.9
0200 AM	178	990.9	16.7	32		153	6.0
0200 AM	236	984.2	17.6	30		154	8.6
0200 AM	294	977.4	18.4	29		154	10.9
0200 AM	357	970.4	18.2	29		154	12.7
0200 AM	420	963.3	17.8	29		155	14.2
0600 AM	000	1011.6	12.4	88		140	0.5

The radiosonde data indicate a surface inversion up to 294 m. The surface temperature observed by the radiosonde was 1°C higher than the surface temperature observed by the tethersonde. The temperature at 170 m was 2°C lower over the Shuaiba area. The surface temperature at 0600 AM was similar at the two places.

4.15 15th Flight Date: 21/2/1983 Time: from 0615 AM to 0704 AM

Tethersonde Data

TMDAY	PT=DC	PHT=M	DT=DC	PR=MB	RH=PC	WD=DG	WS=MS
061543	283.15	5	11.42	1017.6	43.0	294	
061701	285.40	26	13.47	1015.1	34.6	317	
061741	285.82	58	13.58	1011.2	34.3	324	
062019	286.07	83	13.58	1008.2	35.4	313	
062138	286.44	110	13.69	1004.9	35.2	291	
062217	286.81	143	13.75	1001.0	34.4	337	
062703	287.38	178	13.96	996.8	34.3	321	
062901	287.94	199	14.32	994.3	32.6	315	
063149	288.54	223	14.69	991.5	32.2	300	
063734	288.68	237	14.69	989.9	32.3	297	
064150	288.23	200	14.60	994.2	32.8	294	
065043	287.41	171	14.07	997.7	35.3	293	
065657	287.15	144	14.07	1000.9	36.3	54	
070004	286.48	110	13.73	1004.9	38.4	318	
070054	285.98	81	13.51	1008.3	39.7	303	
070213	285.71	55	13.49	1011.5	40.8	339	
070302	285.29	31	13.31	1014.4	42.3	310	
070411	284.08	00	12.58	1020.4	46.2	297	

The data observed by the tethersonde indicate a surface inversion up to 237 m (the maximum height observed). There was a 1.3°C increase in the surface temperature between the beginning and the end of the experiment.

Radiosonde Data (21/2/1983)

TIME	GHP=M	PRES	TEMP	HUM	CLOUD	WD=DG	WS=MS
0200 AM	56	1013.3	12.5	89		CALM	
0200 AM	114	1003.6	16.6	36		CALM	
0200 AM	172	996.8	16.6	34		311	1.2
0200 AM	232	989.8	16.6	30		313	2.3
0200 AM	292	982.7	16.7	25		313	3.1
0200 AM	355	975.6	16.6	22		312	3.9
0200 AM	417	968.4	16.3	20		313	4.5
0600 AM	000	1018.4	12.3	45		320	3.5
0700 AM	000	1019.2	11.8	56		330	3.5

These data indicates a surface inversion up to 292 m, which correlates with the tethersonde inversion. The surface temperature at the airport at the beginning of the radiosonde experiment was 1°C higher than the surface temperature observed at the Shuaiba area at the beginning of the tethersonde experiment. The pressure was 1 mb higher at the airport.

The summary table that follows presents the results of the 15 flights of the tethersonde ballon in Shuaiba and of the radiosonde balloon at the airport. One of the two daily radiosonde experiments was chosen for comparison according to the time of the tethersonde balloon experiment (e.g., if the tethersonde experiment was performed before sunrise, we present the 2.00 AM radiosonde experiment, and, if the tethersonde experiment was performed after sunrise, we present the 0200 PM radiosonde experiment). The second table presents the differences between the radiosonde and tethersonde data.

In this second table, the average time difference between the beginning of the tethersonde experiment and radiosonde experiment was 3 h 20 min. The average difference in surface temperatures observed at the beginning of each experiment was 2.7°C whereas the average difference of the surface temperature observed at the same at the two locations was only 1.3°C . There was an average of 5 mb difference in the surface pressure measured at the two locations; it was always higher at the Shuaiba area because of its lower elevation. The pressure measured at the airport and corrected to sea level was, on the average, 3.8 mb higher than the pressure measured at the Shuaiba area at the same time. This difference may be related to the different instrumentation used.

Only one tethersonde experiment indicated an inversion not measured by the radiosonde experiment performed in the same day. Moreover, only one radiosonde experiment indicated the existence of an inversion not measured by the tethersonde experiment during the same day. The other 13 experiments correlate well. These two uncorrelated cases are probably caused by the time difference between the two experiments.

Among these 13 experiments, seven indicated the presence of inversions, and six did not indicate their presence. The average difference of the top of the inversions was 108.5 m and the average difference of the bottom was 159 m. The average difference of the two temperature increases between the bottom and the top of the inversion was 1.7°C .

This information indicates a strong correlation between the occurrence of the inversions over the airport and the Shuaiba area. The difference in the depth of the inversion and the height of the top and bottom is probably entirely due to the time lag between the two experiments.

The number of experiments performed was not large enough to provide conclusive answers. More experiments should be performed in the region for a more accurate evaluation of the three-dimensional variation of the major meteorological parameters.

SUMMARY TABLE

LIGHT DATE	TIME		MH	SURFACE TEMPERATURE (°C)				SURFACE PRESSURE (mb)		INVERT IONS									
	T.S.			R.S.	T.S.		R.S.	T.S.		Base (m)	T.S.		Base (m)	DT (°C)	R.S.				
	FROM	TO			BEG.	END		BEG.	END		Top (m)	Top (m)			Top (m)	Top (m)			
1	13/12/1982	1113 AM	1140 AM	0200 PM	202	17.73	-	19.7	18.0	1016.4	-	1011.0	1021.4	120	164	1.01	-	-	-
2	18/12/1982	1037 AM	1100 AM	0200 PM	315	11.95	10.33	11.1	11.5	1018.6	1019.7	1014.0	1022.4	251	315	1.39	107	251	1.0
3	20/12/1982	1038 AM	1135 AM	0200 PM	302	12.38	12.61	16.9	13.5	1016.6	1011.2	1013.0	1022.4	-	-	-	-	-	-
4	22/12/1982	0535 AM	0621 AM	0200 AM	139	9.98	10.47	8.0	10.3	1014.2	1016.3	1011.9	1018.0	00	139	2.2	00	200	5.7
5	25/12/1982	1010 AM	1052 AM	0200 PM	220	11.66	12.41	16.2	12.6	1020.2	1020.4	1014.4	1024.3	-	-	-	-	-	-
6a	29/12/1982	0911 AM	1000 AM	0200 PM	376	14.30	15.23	22.4	11.8	1012.6	1013.3	1006.2	1017.0	144	370	4.9	384	710	2.4
6b	29/12/1982	1000 AM	1029 AM	0200 PM	379	15.79	16.18	22.4	11.8	1013.6	1013.2	1006.2	1017.0	144	370	4.0	384	710	2.4
7	5/01/1983	1240 PM	1248 PM	0200 PM	160	13.89	-	15.0	14.5	1017.0	-	1015.3	1022.4	-	-	-	-	-	-
8	8/01/1983	1107 PM	1246 PM	0200 PM	301	10.33	9.99	9.4	10.5	1020.7	1020.6	1017.1	1025.2	-	-	-	161	574	2.5
9	10/01/1983	0913 AM	0948 AM	0200 PM	272	5.74	6.35	11.0	6.0	1027.3	1027.5	1022.0	1030.9	-	-	-	-	-	-
10	26/01/1983	1234 PM	1312 PM	0200 PM	409	14.31	12.73	14.5	14.5	1016.2	1016.0	1014.1	1021.4	-	-	-	-	-	-
11	9/02/1983	1036 AM	1116 AM	0200 PM	301	14.42	13.86	17.3	13.0	1015.2	1015.7	1010.6	1020.2	-	-	-	-	-	-
12	14/02/1983	0600 AM	0642 AM	0200 AM	320	8.49	8.56	7.4	5.6	1011.8	1011.6	1009.6	1016.4	00	151	5.0	00	259	7.0
13a	16/02/1983	1050 AM	1116 AM	0200 PM	476	21.19	21.67	24.0	18.9	1011.0	1012.5	1004.3	1014.3	341	379	0.2	179	238	0.3
13b	16/02/1983	1116 AM	1145 AM	0200 PM	417	21.67	22.84	24.0	18.9	1012.5	1011.2	1004.3	1014.3	341	374	0.3	179	238	0.3
14	19/02/1983	0610 AM	0650 AM	0200 AM	161	11.79	11.99	12.4	12.4	1010.6	1006.1	1005.2	1011.6	32	161	2.35	00	294	6.0
15	21/02/1983	0615 AM	0704 AM	0200 AM	237	11.42	12.58	12.5	12.3	1017.6	1020.4	1010.3	1018.4	00	237	3.2	00	292	4.2

List of Abbreviation (Summary Table)

- T.S. - Tethersonde Balloon measurements
R.S. - Radiosonde measurements
MH - Maximum height
T.S. time - Observation made at the beginning of the tethersonde
experiment
R.S. time - Observation made at the beginning of the radiosonde
experiment
Base - Height of the bottom of the inversion
Top - Height of the top of the inversion
DT - Difference in the temperature between the top and the bottom
of the inversion
R.S. 56 m - Data observed at the time of radiosonde experiment
T.S. S.L. - Data observed at the time of tethersonde experiment
corrected to sea level
Beg. - Observation made at the beginning of the experiment
End - Observation made at the end of the experiment

DIFFERENCES BETWEEN THE TETHERSONDE DATA AND THE RADIOSONDE DATA

Flight No	Date	TIME		SURFACE TEMP. (°C)			SURFACE PRESSURE (mb)			INVERSIONS			
		Beg.	End	Beg.	End	Same Time	Beg.	End	Same Time	Consistent	Base	Top	D.T.
1	13/12	2:45	2:20	2.0	-	0.3	-5.4	-	4.6	No	-	-	-
2	18/12	3:30	3:00	-0.8	0.8	-0.4	-4.6	-5.7	3.8	Yes	-144	-64	-3.9
3	20/12	3:30	2:30	4.52	4.3	1.12	-3.6	1.8	5.8	Yes	-	-	-
4	22/12	3:35	4:20	-2.0	-2.5	0.32	-2.3	-4.4	3.8	Yes	00	61	3.5
5	25/12	3:50	3:10	4.54	3.8	0.94	-5.8	-6.0	4.1	Yes	-	-	-
6a	29/12	4:50	4:00	8.1	7.2	-2.5	-6.6	-7.1	4.4	Yes	240	<370	> 2.5
6b	29/12	4:00	3:30	6.6	6.2	-4.0	-7.4	-7	3.4	Yes	240	<370	>-1.6
7	5/1	1:20	1:10	1.1	-	0.6	-1.7	-	5.4	Yes	-	-	-
8	8/1	1:50	1:10	-0.3	-0.6	0.17	-3.6	-3.5	4.5	No	-	-	-
9	10/1	4:45	4:10	5.3	4.7	0.3	-5.3	-5.5	3.6	Yes	-	-	-
10	26/1	1:30	00:50	0.2	1.8	0.2	-2.1	-1.9	5.2	Yes	-	-	-
11	9/2	3:30	2:45	2.9	3.4	-1.42	-4.6	-5.1	5	Yes	-	-	-
12	14/2	4:00	3:10	-1.1	-1.16	-2.9	-2.2	-2.0	4.8	Yes	00	108	2
13a	16/2	3:10	2:45	2.81	2.33	-2.29	-6.7	-8.2	3.3	Yes	-162	-141	0.1
13b	16/2	2:45	2:15	2.33	1.16	-3.27	-8.3	-6.9	1.8	Yes	-162	-136	0
14	19/2	4:10	4:50	0.61	0.41	0.61	-5.4	-0.9	1	Yes	-32	133	<3.65
15	21/2	4:15	5:00	1.08	1.08	0.9	-7.3	-10.1	0.8	Yes	00	<55	<1
Absolute Total		57:00	50:20	46.3	41.3	22.24	82.9	76.1	65.3	15 Yes	980	1438	13.74
Average Total		3:20	3:00	2.7	2.8	1.3	4.9	5.1	3.8		108.5	<159.7	1.7

List of Abbreviation (Difference between the tethersonde data and radiosonde data)

Column

1. Flight No.
2. Date
3. Time (beg.) : The time difference between the beginning of the tethersonde experiment and radiosonde experiment
4. Time (end) : The time difference between the end of the tethersonde experiment and the radiosonde experiment

Surface temperature

5. Beg. : Difference in surface temperature between the beginning of the tethersonde experiment and the radiosonde experiment
6. End. : Difference in surface temperature at the end of the tethersonde experiment and radiosonde experiment
7. Same time: The difference between the Shuaiba area and the airport surface temperature observed at the same time (i.e., at the beginning of the tethersonde experiment)

Surface pressure

8. Beg. : The difference between the surface pressure observed at the beginning of the tethersonde experiment and radiosonde experiment
9. End : The difference between the surface pressure observed at the end of the tethersonde experiment and the surface pressure observed at the radiosonde experiment
10. Same time(SL) : The difference between the pressure observed at the beginning of the radiosonde experiment and the airport surface pressure observed at the same time and corrected to sea level

Inversions

11. Consistent : Yes indicates the existence or non-existence of an inversion is consistent between the tethersonde experiment and the radiosonde experiment
12. Base : Difference between the height of the base of the inversion observed over the airport and over the Shuaiba area
13. Top : The difference between the height of the top of the inversion observed over the airport and over the Shuaiba area
14. DT : The difference in the temperature increase of the inversion observed over the airport and over the Shuaiba area

The (-) sign indicates that the Shuaiba area observation was higher.
All totals and averages are absolute values.



DISTRIBUTION LIST

Check Appropriate Security Classification

DISTRIBUTION : KISR	NUMBER OF COPIES				COPY NOS.
	GENERAL	<u>RESTRICTED</u>	CONFIDENTIAL	OTHER	
Director General	1	1	1		1
DDG/Research	1	1	1 COPY TO APPLICABLE DDG ONLY		2
DDG/Research	1	1			3
DDG/Planning & Development	1	1			
DDG/AF & SS	1	1			
Senior Advisors' Office	1	1			4
Policy and Planning Director	1	1			5
Division Director	5	1	1		6
Department Manager	5	1			7
Project Leader	5	1			8
NSTIC	2	2	1*		9-10
Project Management Office	1	Original + 1	Original + 1		11
Publications & Public Information	Original				
Board of Trustees	13*				
Finance Division	1**	1**	1**		
DISTRIBUTION: OUTSIDE KISR					
Kuwait University	5*				
Client . SAA		3			12-14

* Reports only

** Proposals and Extensions/Amendments only



Kuwait Institute for Scientific Research
P. O. Box 1638, Salmiya
State of Kuwait